Coccolithophore response to modern and past ocean acidification events

Dissertation

zur Erlangung des Doktorgrades
der Mathematisch-Naturwissenschaftlichen Fakultät
der Christian-Albrechts-Universität
zu Kiel

vorgelegt von
Christine Berger geb. Bauke
Kiel, 2013

Erste Gutachterin: Prof. Dr. Priska Schäfer
Zweite Gutachterin: Prof. Dr. Birgit Schneider
Tag der Disputation: 15.01.2014
Zum Druck genehmigt: 15.01.2014
gez. Prof. Dr. Wolfgang J. Duschl, Dekan

EIDESSTATTLICHE ERKLÄRUNG

Hiermit erkläre ich an Eides statt, dass die vorliegende Dissertation mit dem Titel ‘Coccolithophore response to modern and past ocean acidification events’, abgesehen von der Beratung durch meine akademischen Lehrer, in Inhalt und Form meine eigene Arbeit darstellt. Des Weiteren versichere ich, dass die vorliegende Dissertation weder im Ganzen noch zum Teil einer anderen Stelle im Rahmen eines Prüfungsverfahrens vorgelegen hat und unter Einhaltung der Regeln guter wissenschaftlicher Praxis der Deutschen Forschungsgemeinschaft entstanden ist.

Kiel, November 2013

_____

Christine Berger geb. Bauke

Summary

The absorption of the recent rising atmospheric CO_2 alters the oceans carbonate system and affects the living conditions for marine calcifiers. Coccolithophores as major calcifying phytoplankton largely contribute to the modern carbonate production and play an important role in the global carbon cycle. Thus, changes in the calcite production of the coccolithophores have an impact on the carbon cycle. The effect of ocean acidification on coccolithophore calcification has been observed in several types of experimental, field, and sediment studies, even in combination with other environmental factors, but most studies base on short-term laboratory experiments with single species or strains. Despite various results with species and strain specific response, the most frequent finding in recently conducted experiments is a decrease in coccolithophore calcification under future CO_2 levels. In contrast to monospecific laboratory experiments, natural coccolithophore assemblages consist of a heterogenous composition with diverse species and morphotypes, adapted to various environmental conditions. In a natural assemblage changing seawater conditions can lead to a dominance shift to better adapted species or morphotypes with different coccolith weight or size. To gain insights into the possible impact on the carbon cycle due to changing coccolithophore calcification, the response of the entire assemblage to changing environmental conditions in recent and past oceans should be taken into account.

The main objective of this thesis was to investigate coccolithophore calcification of the dominant coccolithophore family Noelaerhabdaceae in different past atmospheric CO_2 scenarios to obtain the influence of the changing seawater carbonate chemistry and to untangle the response from other environmental factors. Coccolith weight estimates are suggested as a possible indicator to reconstruct calcification rates and were obtained with the automatic recognition system SYRACO.

To examine the variability of Noelaerhabdaceae mean coccolith weights during times of predominantly stable atmospheric CO_2 conditions, coccolith weights from the pre-industrial Holocene were measured on 3 sediment cores from the North Atlantic. The results show opposing trends in different regions in an amplitude of weight variability which is similar to the previously reported weight change of the last glacial/interglacial change that was associated to ocean acidification. The changes in the Noelaerhabdaceae mean coccolith weight from the Holocene are referable to variations in the coccolithophore assemblage (shifts in species and morphotypes) but also to changing calcification. Apparently, these changes are induced by differences in nutrient or productivity settings between the studied sites.

To assess the response of Noelaerhabdaceae mean coccolith weights to a natural increase in atmospheric CO_2, two sediment cores from different locations in the North Atlantic were selected which cover the atmospheric CO_2 increase of the penultimate deglaciation (Termi-

nation II). At the temperate Rockall Plateau with its changing environmental conditions due to a shift in the oceanic frontal system, mean coccolith weight shows positive variances around the Heinrich event 11 which is in close connection to a shift within the assemblage. In the Florida Strait, which is far from influences of frontal zones, mean coccolith weight doubles during Termination II, primarily due to more heavily calcified coccoliths. This increase in calcification at the Florida Strait is simultaneous to the rise in atmospheric CO_2 and an increase in seawater HCO_3^- concentration accompanied by a high total alkalinity, DIC, CO_3^{2-} and calcite saturation state, which indicates favourable conditions for calcification in the ocean. A comparison of the weight record from the Florida Strait with earlier studies from the CO_2 increase of Termination I in tropical regions shows opposing weight trends under similar changes of the seawater carbonate system. In the tropics, different carbonate systems in both Terminations indicate better ion concentrations conditions for calcification during Termination II. The results illustrate that the total $CaCO_3$ production of a coccolithophore assemblage under increasing CO_2 depends on regional seawater characteristics and the local assemblage composition. But despite rising atmospheric CO_2 the conditions of the seawater carbonate system can be favourable for coccolithophore calcification.

Noelaerhabdaceae mean coccolith weight from a sediment core in the Gulf of Taranto in the central Mediterranean Sea was studied to investigate the response to the rising ocean acidification of the past 200 years. The study area is under influence of enhanced anthropogenic nutrient load from the Po River which is known to affect the coastal ecosystems. So far, the results reveal no negative influence of the ocean acidification on coccolith weight or the assemblage composition. Noelaerhabdaceae mean coccolith weight is positively influenced during times of negative North Atlantic Oscillation which strengthens the Po River discharge and leads to enhanced nutrient transport to the coring site via Adriatic Surface Water. The higher nutrient concentration extends the coccolithophore productivity season from winter until late spring and raises the mean Noelaerhabdaceae coccolith weight. The results suggest that a possible negative effect of the rising acidification of the ocean on coccolith calcification can be outcompeted by enhanced nutrient content.

The results of this thesis point out the importance of understanding the response of natural coccolithophore assemblages to changing seawater carbonate chemistry and other environmental conditions. The high variability of the Noelaerhabdaceae mean coccolith weight under stable and rising atmospheric CO_2 conditions indicates an assemblage specific response, which is further able to mask possible negative effects of rising atmospheric CO_2 conditions when other environmental factors, i.e. productivity are favourable.

Zusammenfassung

Der Anstieg des atmosphärischen CO_2 führt durch den Gasaustausch zwischen der Luft und dem Meerwasser zu einer Veränderung der Karbonatchemie im Ozean, der sogenannten Ozeanversauerung. Diese kann die Lebensbedingungen mariner Kalkproduzenten massiv beeinträchtigen. Eine der bedeutendsten kalkbildenden Phytoplanktonarten im Ozean sind Coccolithophoriden. Sie tragen einen wesentlichen Anteil zur Karbonatproduktion im Ozean bei und stellen dadurch für den Kohlenstoffkreislauf einen entscheidenden Faktor dar. Änderungen in der Karbonatproduktion der Coccolithophoriden haben dementsprechend einen großen Einfluss auf den Kohlenstoffkreislauf. Der Einfluss der Ozeanversauerung auf die Karbonatproduktion von Coccolithophoriden wurde in unterschiedlichen experimentellen, Feld- und Sedimentstudien untersucht, auch in Verbindung mit anderen Umweltfaktoren. Hauptsächlich basieren die Untersuchungen jedoch auf kurzzeitigen Laborexperimenten mit einzelnen Arten oder monoklonalen Kulturen. Trotz der zwischen Arten und Kulturstämmen unterschiedlichen Reaktionen ist am häufigsten eine geringere Kalkproduktion der Coccolithophoriden unter zukünftigen CO_2 Gehalten festgestellt worden. Im Gegensatz zu den monospezifischen Laborexperimenten bestehen natürliche Vergesellschaftungen von Coccolithophoriden aus einer heterogenen Zusammensetzung verschiedener Arten und Morphotypen, die an unterschiedliche Umweltbedingungen angepasst sind. In solchen natürlichen Vergesellschaftungen können Veränderungen der Meerwasserbedingungen zu einer Verschiebung zu anderen, z.B. besser angepassten Arten oder Morphotypen führen, die sich in Gewicht und Größe ihrer Coccolithen, und somit in ihrem Karbonatgehalt, unterscheiden. Für ein besseres Verständnis wie sich eine veränderte Karbonatproduktion von Coccolithophoriden auf den Kohlenstoffkreislauf auswirken kann, ist es von Bedeutung die Kalkproduktion einer gesamten Coccolithophoriden Vergesellschaftung und deren Reaktion auf wechselnde Umweltbedingungen zu berücksichtigen. Hilfreich sind hierbei Untersuchungen an rezenten sowie an Paläo-Vergesellschaftungen unter verschiedenen Umweltbedingungen.

Das Hauptziel dieser Arbeit ist die Untersuchung der Kalzifizierung von Coccolithen der dominanten Coccolithophoriden-Familie Noelaerhabdaceae zu Zeiten verschiedener atmosphärischer CO_2 Konzentrationen in der Vergangenheit. Sowohl der Einfluss der ozeanischen Karbonatchemie als auch der Einfluss anderer Umweltfaktoren soll untersucht werden. Mit dem automatischen Erkennungssystem SYRACO werden Gewichte von einzelnen Coccolithen gemessen, und diese können als Indikator für die Rekonstruktion der Kalzifizierung von Coccolithen genutzt werden.

Zur Bestimmung der Variabilität des Durchschnittsgewichts der Coccolithen der Familie Noelaerhabdaceae während überwiegend stabiler atmosphärischer CO_2 Bedingungen, wurden

Coccolithengewichte aus dem vorindustriellen Holozän an drei Sedimentkernen aus dem Nord-Atlantik gemessen. Die Ergebnisse zeigen gegensätzliche Trends in den drei unterschiedlichen Regionen. Zudem variiert das Gewicht in einem ähnlichen Ausmaß wie zu Zeiten des natürlichen CO_2 Anstiegs und des daraus resultierenden schwachen Ozeanversauerungseffekts während der letzten Deglaziation, welche in früheren Studien aufgezeigt wurden. Die Veränderungen des durchschnittlichen Noelaerhabdaceae Coccolithengewichts während des Holozän lassen sich sowohl auf wechselnde Häufigkeiten von Arten und Morphotypen innerhalb der Coccolithophoriden Vergesellschaftung, als auch auf veränderte Kalzifizierung zurückführen. Offenbar werden diese Veränderungen durch Unterschiede im Nährstoffgehalt oder der Produktivität der Coccolithophoriden in den Untersuchungsgebieten verursacht.

Um die Auswirkungen eines natürlichen atmosphärischen CO_2 Anstiegs auf das durchschnittliche Noelaerhabdaceae Coccolithengewicht zu beurteilen, wurde der CO_2 Anstieg der vorletzten Deglaziation (Termination II) ausgewählt und anhand von zwei Sedimentkernen aus verschiedenen Regionen im Nord-Atlantik untersucht. Das in gemäßigten Breiten liegende Rockall Plateau stand während der Termination II unter Einfluss einer Verschiebung des ozeanischen Frontensystems. Während des Heinrich 11 Ereignisses zeigen die Noelaerhabdaceae Coccolithengewichte am Rockall Plateau einen starken Anstieg welcher in engem Zusammenhang mit einer Häufigkeitsverschiebung der Arten innerhalb der Vergesellschaftung steht. Die tropische Florida Strait befindet sich hingegen weit entfernt von Einflüssen der Frontensysteme. Hier verdoppelt sich das durchschnittliche Coccolithengewicht während der Termination II, überwiegend aufgrund einer Zunahme von stärker kalzifizierten Coccolithen. Die Zunahme der Kalzifizierung in der Florida Strait findet zeitgleich mit dem Anstieg des atmosphärischen CO_2 und der Konzentration von HCO_3^- im Meerwasser statt. Zusätzlich scheinen hohe Alkalinität, DIC, CO_3^{2-} und Calcitsättigungsgrad die Kalzifizierung zu fördern. Ein Vergleich der Ergebnisse aus der Florida Strait mit früheren Studien an Coccolithengewichten aus der Termination I in den Tropen zeigt entgegengesetzte Gewichtstrends und lässt auf bessere Bedingungen für die Kalkproduktion während Termination II schließen. Diese Ergebnisse zeigen, dass die absolute $CaCO_3$ Produktion der Coccolithophoriden Vergesellschaftung unter ansteigenden CO_2 Bedingungen von den regionalen Meerwassereigenschaften sowie der Zusammensetzung der lokalen Vergesellschaftung abhängt. Die Bedingungen der Karbonatchemie im Meerwasser können offenbar trotz zunehmendem atmosphärischen CO_2 Gehalts förderlich für die Kalzifizierung der Coccolithophoriden sein.

Anhand eines Sedimentkerns aus dem Golf von Taranto im zentralen Mittelmeer konnte die Auswirkung des ansteigenden CO_2 Gehalts der letzten 200 Jahre auf die Durchschnittsgewichte der Noelaerhabdaceae Coccolithen bestimmt werden. Das Untersuchungsgebiet steht

unter dem Einfluss von steigenden anthropogenen Nährstoffgehalten aus dem Po-Fluss, welcher sich auf das ökologische System der Küste auswirkt. Bis jetzt lassen sich keine nachteiligen Auswirkungen der ansteigenden Ozeanversauerung auf die Coccolithengewichte oder die Zusammensetzung der Vergesellschaftung feststellen. Das durchschnittliche Gewicht der Noelaerhabdaceae Coccolithen wird während einem negativen Index der Nord Atlantik Oszillation positiv beeinflusst, da dieser den Abtransport über den Po-Fluss intensiviert und zu einem verstärkten Nährstoffzustrom über das Adriatische Oberflächenwasser in den Golf von Taranto führt. Der erhöhte Nährstoffgehalt verlängert die Phase der Coccolithenproduktivität von Winter bis in den späten Frühling hinein, was einen positiven Einfluss auf das durchschnittliche Noelaerhabdaceae Coccolithengewicht hat. Die Ergebnisse weisen darauf hin, dass ein möglicher negativer Effekt der zunehmenden Ozeanversauerung auf die Kalzifizierung der Coccolithophoriden von einem erhöhten Nährstoffgehalt ausgeglichen wird.

Die Ergebnisse der vorliegenden Arbeit verdeutlichen die Notwendigkeit eines besseren Verständnisses der Reaktion von natürlichen Coccolithophoriden Vergesellschaftungen auf sowohl veränderte Meerwasser-Karbonatchemie als auch auf andere Umweltbedingungen. Die hohe Variabilität des Noelaerhabdaceae Coccolithengewichts unter stabilen sowie ansteigenden atmosphärischen CO_2 Bedingungen, deutet auf eine spezifische Reaktion der verschiedenen Vergesellschaftung hin, die zudem bewirken kann, dass mögliche negative Effekte eines zunehmenden CO_2 Gehalts maskiert werden, wenn andere Umweltfaktoren, wie zum Beispiel Produktivität, vorteilhaft sind.

Table of contents

1. Introduction

1.1 Motivation

The atmospheric CO_2 concentration of the last 800000 years varied between 180 parts per million by volume (ppmv) during glacial and 300 ppmv during interglacial periods (Archer et al., 2000; Siegenthaler et al., 2005; Lüthi et al., 2008). From 1750, i.e. with the beginning of the industrial era, atmospheric CO_2 concentrations started increasing to a current concentration of around 390.5 ppmv (IPCC, 2013) (Fig. 1.1). The average rate of atmospheric CO_2 increase of the past century is at least an order of magnitude higher than that of the last millions of years in earth history (Doney et al., 2009).

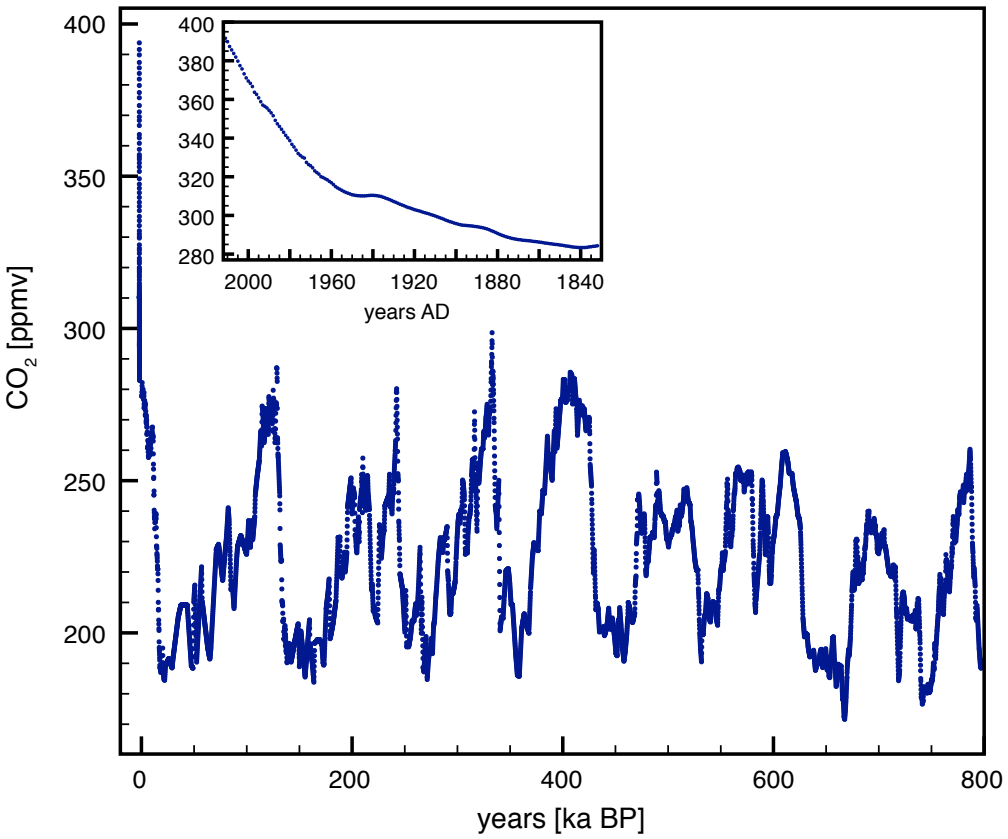

Figure 1.1. Atmospheric CO_2 concentration of the past 800000 years (EPICA Dome C from Lüthi et al., 2008) and from 1832 - 2012 AD (combined data: Law Dome DE08 and DSS ice cores from Etheridge et al., 1998; Mauna Loa from Tans and Keeling, 2012).

The ocean is the largest sink for atmospheric CO_2, since the beginning of the industrial era the ocean has absorbed approximately one third of the anthropogenic CO_2 emissions. Without this absorption the atmospheric CO_2 concentration would have been much higher (Sabine et al., 2004). However, the uptake of CO_2 results in alterations of the marine carbonate chemistry, including a reduction of the surface seawater pH which termed the process as

"ocean acidification" (Feely et al., 2004; Raven et al., 2005, IPCC 2007). The changing seawater chemistry is suspected to have serious consequences for the marine life (e.g. Fabry et al., 2008), such as a reduction of sea urchin larval growth (e.g. Doo et al., 2012) or lower calcification rates of corals and pteropods (e.g. Gattuso et al., 1998; Comeau et al., 2009). Particularly for calcifying organisms the process of acidification will make it more difficult to form calcium carbonate (Orr et al., 2005). Coccolithophores are a key group of marine calcifying nannoplankton, they play a fundamental role in the global carbon cycles by combining photosynthetic carbon fixation and calcification (Rost and Riebesell, 2004). Their calcite scales, the coccoliths, export inorganic carbon to the deep sea and further act as ballast for the transport of organic carbon (Klaas and Archer, 2002; Rost and Riebesell, 2004). In the present oceans, coccolithophores are the dominant planktic calcifiers, responsible for around half of the modern $CaCO_3$ precipitation (Milliman, 1993). Therefore, variations in the calcite production of coccoliths influence the carbon export and hence affect the global carbon cycle (Zondervan, 2007). The effects of ocean acidification on coccolithophores and their calcification have been extensively studied in culture experiments, mesocosms and in field studies, revealing various response within species and strains (Langer et al., 2006, 2009; Iglesias-Rodriguez et al., 2008; Shi et al., 2009; Doney et al., 2009). Still, the most common observation is a reduction of coccolithophore calcification in response to increasing CO_2 (Zondervan et al., 2002; De Bodt et al., 2010; Bach et al., 2012). The combined effect of ocean acidification and other environmental parameters (e.g. temperature, nutrients) on coccolithophore calcification is even more complicated (e.g. De Bodt et al., 2010; Matthiessen et al., 2012; Fiorini et al., 2011). Most of these studies base on experimental work and neglect the possible adaptation potential or long-term effects on coccolithophore assemblages in their natural environment. Strong changes in the total amount of calcite produced within a coccolith assemblage are not solely caused by the varying calcification of a single species, but also by abundance shifts to better adapted species or morphotypes (e.g. Triantaphyllou et al., 2010; Flores et al., 2010; Beaufort et al., 2011). These shifts can compensate possible negative effects on the calcification of other species or morphotypes from the assemblage. Moreover the scale of variability in coccolith calcification during times of rather stable atmospheric CO_2 is still unknown, as well as the consequences for the average calcite mass of the coccolithophore assemblage. Further the question arises if other environmental factors (e.g. temperature or nutrient supply) can compensate a possible negative effect of changing carbonate chemistry conditions on coccolithophore calcification. With respect to the ongoing changes in seawater carbonate chemistry, a better understanding of how these changes influence the entire calcification of a coccolithophore assemblage is fundamental. The coccolithophore family Noelaerhabdaceae has dominated most assemblages for more than 20 million years (Beaufort et al., 2011) and is therefore suitable for palaeo-perspectives on changes in cocco-

lithophore calcification during episodes with stable and elevated atmospheric CO_2 which can give indications for the possible response to the current rising CO_2 conditions.

1.2 Structure of the thesis

1.2.1 Aims and Objectives

This study was performed within the framework of the Biological Impacts of Ocean Acidification (BIOACID) project, funded by the Federal Ministry of Education and Research (Bundesministerium für Bildung und Forschung; 03F0608A). The project focuses on the effects of ocean acidification on marine organisms and their habitats. Main objectives of the project are to obtain the underlying mechanisms of response and possible adaptations of marine key species and the possible consequences for the marine ecosystem, ocean biogeochemical cycles and the climate system.

As part of the BIOACID project the overall objective of this thesis is to advance the understanding of the fossil calcification response of the dominant coccolithophore family Noelaerhabdaceae to different atmospheric CO_2 conditions and other environmental factors (e.g. temperature, nutrient supply). The thesis focuses on the following questions:

1) What is the intrinsic weight variability of Noelaerhabdaceae coccoliths during times of relatively stable atmospheric CO_2?
2) What is the response of Noelaerhabdaceae coccolith weight to the naturally occurring CO_2 increase at glacial/interglacial transitions?
3) How strong is the coccolith weight response to the very fast atmospheric CO_2 increase over the past 200 years?
4) Is there a general response pattern of the coccolithophore family Noelaerhabdaceae to ocean acidification events?
5) Are changes in mean Noelaerhabdaceae coccolith weight driven by ecological or evolutionary shifts within the assemblage or by changes in calcification?
6) Do other environmental factors weaken or strengthen the response to increasing atmospheric CO_2?

In order to answer the main questions of this thesis, the following set of investigations was carried out, covering a variety of different settings:

1) Noelaerhabdaceae weight variability of the Holocene (last 10000 years) in the North Atlantic Ocean was studied from three locations spanning different climatic and biogeographic

zones. This time period is characterised by relatively stable atmospheric CO_2 (~20 ppmv range, between ~260 to ~280 ppmv), but with considerable environmental differences between locations with different assemblage composition. The intrinsic variability that is not related to CO_2 changes but rather to other environmental parameters and assemblage composition was investigated.

2) Changes of Noelaerhabdaceae weight during a moderate CO_2 increase (~100 ppmv, from ~190 to ~290 ppmv) of the penultimate glacial/interglacial transition (Termination II) over a long time episode (10000 years) from the tropical and subpolar/temperate North Atlantic was investigated. The tropical setting is characterised by relatively small environmental change, but a moderate assemblage and evolutionary shift, while the temperate setting shows strong environmental changes and assemblage shifts.
3) The variability of Noelaerhabdaceae weight was studied during the moderate CO_2 increase (~100 ppmv, from ~280 to ~390 ppmv) over a very short time span (last 200 years) from a sediment record in the Mediterranean Sea. This site is characterised by a stable coccolithophore assemblage and no indications of evolutionary driven variations within the coccolithophores, but reveals a strong nutrient increase whilst other environmental conditions remain relatively stable.

1.2.2 Outline

The thesis is structured in 7 Chapters. The remaining Chapter 1 contains an introduction into coccolithophores and the seawater carbonate system in respect to ocean acidification.

Chapter 2 focusses on the study area and the methods, including oceanographic settings, sample material and preparation, the automated coccolith recognition system SYRACO and SEM studies as well as on the reconstruction of palaeo-seawater conditions.

Chapter 3 presents the mean weight changes of the coccolithophore family Noelaerhabdaceae in 3 locations of the North Atlantic over the Holocene. The study reflects the influence of environmental factors as temperature and productivity in times of ocean carbonate system stability due to small changes in atmospheric CO_2. This chapter is under review for *Biogeosciensces*: “Changes in coccolith calcification under stable atmospheric CO_2“ by C. Bauke, K.J.S. Meier H. Kinkel and K-H. Baumann. A previous discussion manuscript has been published in *Biogeosciences Discussions* (Bauke et al. 2013). I wrote the manuscript, conducted the coccolith measurements, and the calculations of the carbonate chemistry parameters. All authors contributed to the discussion of the results. K-H. Baumann provided coccolith assemblage data.

In Chapter 4 Noelaerhabdaceae coccolith mean weight is studied in the tropic and the temperate zone of the North Atlantic during the atmospheric CO_2 increase of Termination II. This chapter has been submitted to *Marine Micropaleontology*: “Increasing coccolith calcification

during CO_2 rise of the penultimate deglaciation (Termination II)“ by C. Bauke, K.J.S. Meier and H. Kinkel. I wrote the manuscript, conducted the coccolith measurements, and the calculations of the carbonate chemistry parameters. The co-authors of the manuscript contributed to the discussion of the results.

Chapter 5 focusses on Noelaerhabdaceae coccolith mean weight during the CO_2 increase over the last 200 years in a sediment core from the Gulf of Taranto, central Mediterranean Sea. This manuscript is in preparation for submission to *Ocean Acidification*: “Ocean fertilisation versus acidification: anthropogenic influence on coccolithophore calcification over the last 200 years in the Gulf of Taranto“ by C. Bauke, K.J.S. Meier and H. Kinkel. I wrote the manuscript, conducted the coccolith measurements, and the calculations of the carbonate chemistry parameters. The co-authors of the manuscript contributed to the discussion and the SEM counts.

Additionally, a study on laboratory results of *E. huxleyi* is presented in Chapter 6. This chapter results from a cooperation with Lennart Bach from the BIOACID subproject 3.1.1. which is published in *Biogeosciences*: “Influence of changing carbonate chemistry on morphology and weight of coccoliths formed by *Emiliania huxleyi*“ by L.T. Bach, C. Bauke, K.J.S. Meier, U. Riebesell and K.G. Schulz. I conducted the coccolith weight measurements of this study and contributed to the discussion.

Chapter 7 presents the conclusions of the thesis and an outlook.

The Appendix provides a compilation of supplementary data which were generated in the framework of this thesis.

1.3 Seawater carbonate system

With its large storage capacity of carbon the ocean plays a fundamental part in the carbon cycle. Due to the exchange of carbon from ocean and atmosphere, atmospheric CO_2 concentrations are strongly coupled to the oceanic reservoir (Raven et al., 2005; Zeebe et al., 2011).

The seawater carbonate system is a highly complex system including numerous parameters, thus it should be noted that the following description of the carbonate system is set in the context of ocean acidification.

1.3.1 Parameters describing the seawater Carbonate system

In typical surface seawater of pH ~8,1, ~86,5 % of DIC is HCO_3^-, ~13 % is CO_3^{2-} and ~0.5 % is CO_2, the concentration of H_2CO_3 is very small and can be neglected (Zeebe, 2007; Zeebe and Wolf-Gladrow, 2001). In chemical equilibrium most of the parameters are interdependent, i.e. a change in one parameter leads to a proportional change in the others (Kleypas and

Langdon, 2006). Mathematically the carbonates system consists of six parameters, and can be described by four equations (Table 1). Therefore it is possible to calculate all parameters if any two of them are known with the given equilibrium constants (Fig. 1.2), which depend on salinity, temperature and pressure (Zeebe and Wolf-Gladrow, 2001). This also allows to calculate estimates of the carbonate system for the past (see Chapter 2).

Table 1.1. Parameters and formulas describing the carbonate system

Parameter	Formula
dissolved carbon dioxide [CO_2]	$CO_2 + H_2O = HCO_3^- + H^+$ **(1)**
bicarbonate ions [HCO_3]	
carbonate ions [CO_3^2]	$HCO_3^- + H^+ = CO_3^{2-} + 2H^+$ **(2)**
pH	-log [H^+]
dissolved inorganic carbon (DIC)	[HCO_3^-] + [CO_3^{2-}] + [CO_2] **(3)**
Total alkalinity (TA)	[HCO_3^-] + 2 [CO_3^{2-}] + [OH^-] - [H^+] + minor components **(4)**

The exchange of CO_2 between the ocean and the atmosphere alters the seawater chemistry conditions. When atmospheric CO_2 enters the surface, it reacts with water and forms H_2CO_3 which dissociates into HCO_3^-, CO_3^{2-} and H^+ (Fig. 1.2) (Zeebe, 2007; Zeebe and Wolf-Gladrow, 2001).

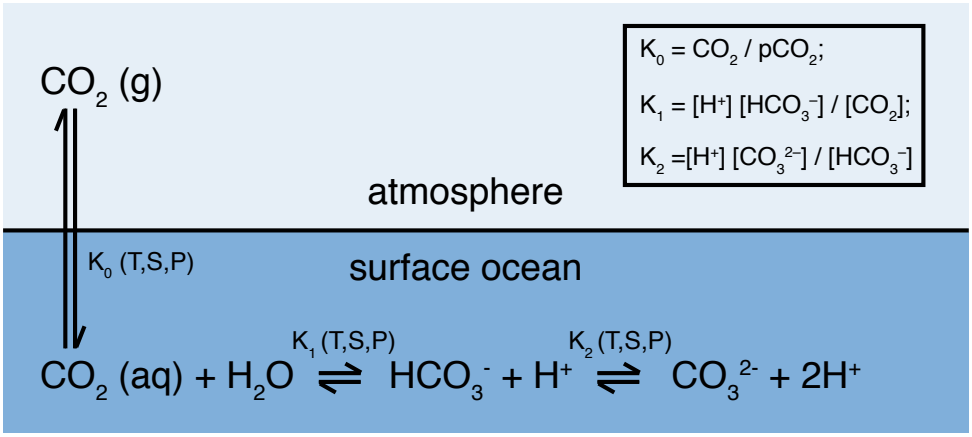

Figure 1.2. CO_2 exchange between atmosphere and ocean. K_0 is the solubility constant of CO_2 in seawater, K_1 and K_2 are equilibrium constants, all constants are functions of temperature (T), salinity (S) and pressure (P). Modified after Zeebe and Wolf-Gladrow (2001).

The generation of H^+ ions during the dissociation steps leads to rising seawater acidity and decreasing seawater pH levels. The term pH describes the acidity of a liquid and is defined as the negative common logarithm of the concentration of hydrogen ions (pH = -log [H^+]).

The seawater pH is buffered by the total alkalinity (TA) which represents the balance of the acid-base system of seawater defined by the sum of weak bases and describes the ability to accept H^+ ions and therefore to neutralise acids (Dickson, 1981; Zeebe and Wolf-Gladrow, 2001).

1.3.2 Processes affecting the carbonate system

Various processes affect the carbonate system in the ocean, including physicochemical (e.g. temperature, salinity and depth) and biological (e.g. photosynthesis and respiration, $CaCO_3$ formation, nutrient uptake and dissolution) processes. Consequently, the seawater carbonate system differs regionally, seasonally as well as between surface and deep ocean (Zeebe and Wolf-Gladrow, 2001; Feely et al., 2001).

Physicochemical processes

The Bjerrum plot **(Fig. 1.3)** illustrates the equilibrium relationships between the DIC parameters CO_2, HCO_3^-, and CO_3^{2-} in relation to pH and further the dependence of the inorganic carbon concentrations on physicochemical parameters (temperature, salinity, pressure). The plot shows shifts of CO_2, HCO_3^-, and CO_3^{2-} concentrations, induced by various temperature, salinity and pressure combinations (Zeebe and Wolf-Gladrow, 2001).

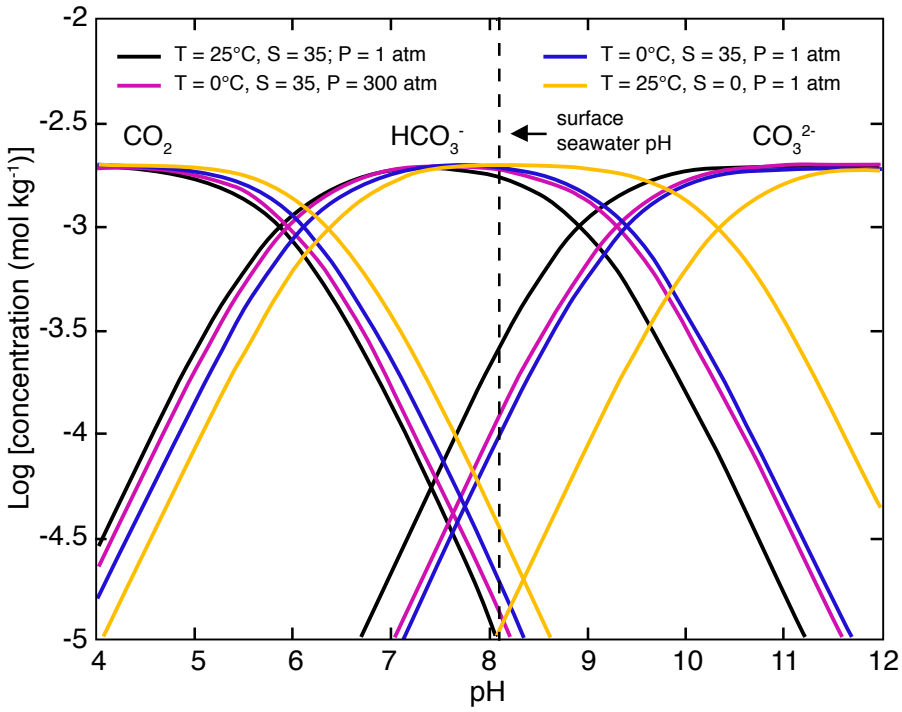

Figure 1.3. Bjerrum plot describing the carbonate system and the effect of temperature, pressure and salinity on the relative distribution of the carbon species as a function of pH. In all cases the reference is T = 25°C, S = 35 and P = 1. The dashed line marks the present day mean surface pH. Modified after Zeebe and Wolf-Gladrow (2001).

When e.g. temperature decreases at the same pH, the equilibrium shifts towards higher CO_2 and lower CO_3^{2-} concentration due to the higher CO_2 solubility in colder waters. Vice versa, in warmer regions the surface seawater tends to outgas CO_2, has a higher CO_3^{2-} concentration and is more saturated with respect to calcite. (Zeebe et al., 2012).

Biological Processes

The activities of phytoplankton as e.g. coccolithophores can have distinct effects on the oceanic carbonate system (Rost and Riebesell, 2004). Their biological processes can influence either DIC and/or TA by changing the concentration of carbonate chemistry parameters (Fig 1.4). Photosynthesis decreases DIC due to the consumption of CO_2, but slightly increases TA which is a result of a simultaneous consumption of nutrients, shifting the system to higher pH and lower CO_2 levels.

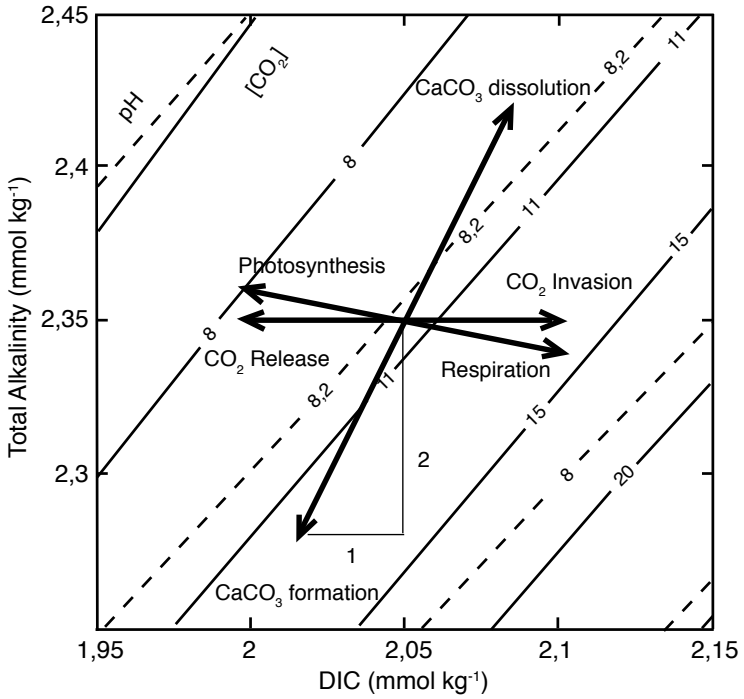

Figure 1.4. Processes affecting DIC and TA (arrows). Solid and dashed background isoclines indicate CO2 (in μmol kg^{-1}) and pH as function of DIC and TA. Redrawn after Zeebe and Wolf-Gladrow (2001).

The production and dissolution of $CaCO_3$ can decrease or increase both DIC and TA in a 1:2 ratio. The production of 1 mole $CaCO_3$ reduces TA by 2 moles due to the removal of 2 charges from solution by only requiring 1 mole of carbon and one mole of double positively charged Ca^{2+} ions:

$$Ca^{2+} + 2HCO_3^- \leftrightarrow CaCO_3 + H_2O + CO_2 \qquad (1.1)$$

As a result the carbonate system shifts to higher CO_2 and lower pH levels. When $CaCO_3$ dissolves in seawater it has the opposite effect (Zeebe and Wolf-Gladrow, 2001).

1.3.3 Ocean acidification

The surface of the oceans and the atmosphere are in a continuous CO_2 exchange by absorbing and releasing CO_2 to maintain an equilibrium (Raven et al., 2005; IPCC 2007). With increasing anthropogenic emissions over the past 250 years, the atmospheric CO_2 concentration has risen from 280 ppmv to 390.5 ppmv (Doney et al., 2009; IPCC 2013). This concentration exceeds any level of the past 800000 years (IPCC 2013). By the year 2100 worst-case estimations predict an increase of atmospheric CO_2 levels to more than 1000 ppmv, which is higher than it has been for several million years (IPCC 2013).

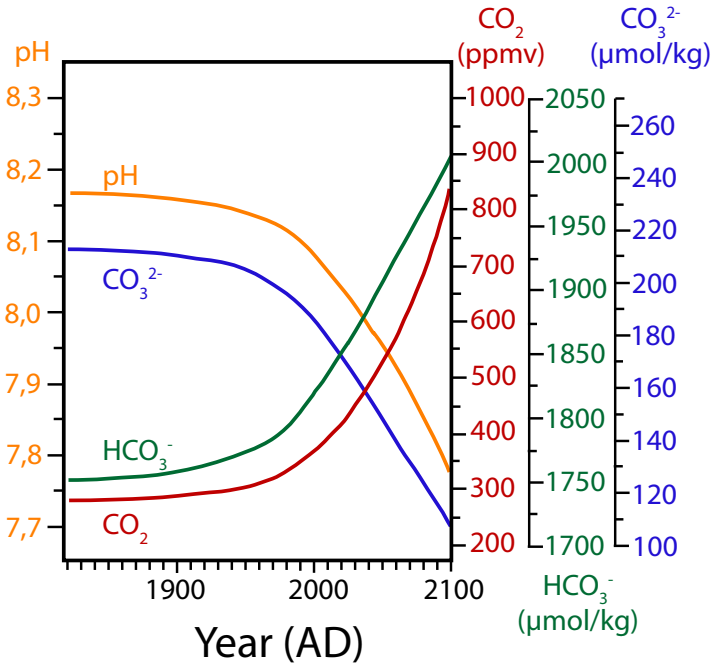

Figure 1.5. Predicted changes in CO_2 and ocean chemistry. Redrawn after Pelejero et al. (2010).

Up to now, the oceans have absorbed nearly 30 % of the anthropogenic CO_2 emissions from the combustion of fossil fuels, cement production, and agricultural activities (Sabine et al., 2004). The net result of the CO_2 uptake is a decrease in CO_3^{2-} and an increase in HCO_3^- and H^+ ions, which leads to a reduction of the seawater pH (Zeebe and Wolf-Gladrow, 2001). This ongoing process is known as ocean acidification (Caldeira and Wickett, 2003).

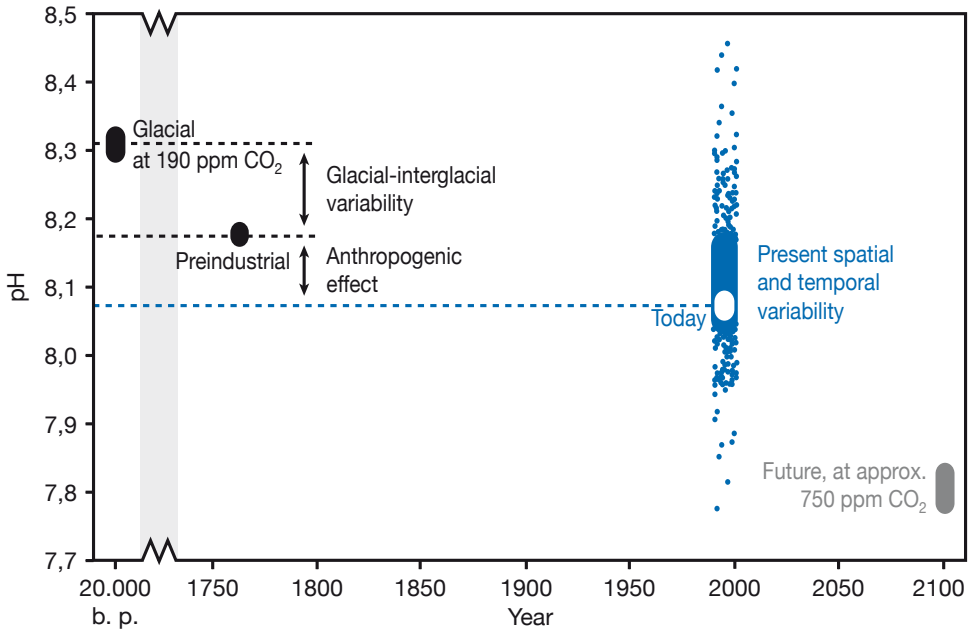

Figure 1.6. Variations of average seawater pH levels at past, present and predicted (750 ppmv) CO_2 concentrations. Modified after WBGU Special Report (2006) from IMBER (2005).

Natural fluctuations of the average pH have never exceeded a range of slightly more than 0,1 over the past 23 million years (WBGU 2006). The anthropogenic CO_2 increase has already led to a decrease in the global average surface pH of the oceans by 0.1 units over the last 250 years (Fig. 1.6) (Caldeira & Wicket, 2003). Modelling studies of the surface seawater pH under the IS92a scenario predicted a decrease by 0.3 - 0.4 units until 2100, which is equivalent to an increase of H^+ ions of 100 - 150 % (Orr et al., 2005).

A consequence of the decrease in CO_3^{2-} is the lowering of the $CaCO_3$ saturation state (Feely et al., 2009). The $CaCO_3$ saturation state (Ω) is a function of CO_3^{2-}, defined by:

$$\Omega = [Ca^{2+}]\,[CO_3^{2-}] / K^*_{sp} \qquad (1.2)$$

The solubility product K^*_{sp} depends on local conditions of temperature, salinity and pressure and is written as: $K^*_{sp} = [Ca^{2+}]_{sat}\,[CO_3^{2-}]_{sat}$, whereas $[Ca^{2+}]_{sat}$ and $[CO_3^{2-}]_{sat}$ define the equilibrium of calcium and carbonate ion concentrations in a seawater solution saturated with $CaCO_3$. Where Ω is > 1, seawater is supersaturated with respect to aragonite and calcite, where Ω is < 1, seawater is undersaturated and corrosive to $CaCO_3$. In cold latitudes and in high water depths, the saturation state is lowest, whereas it is highest in shallow, warm and tropical waters (Feely et al., 2004). The location where Ω = 1 is called the saturation horizon which is positioned in shallower depths for aragonite than for calcite due to the higher solubility of aragonite. The saturation horizons of aragonite and calcite are found in shallower depth in the Pacific than in the Atlantic Ocean, due to the older age of the Pacific bottom waters

which have taken up more CO_2 than the Atlantic Ocean bottom waters (Zeebe and Wolf-Gladrow, 2001). In the North Pacific the calcite saturation horizon is approximately in a water depth of 750 m, in contrast to the calcite saturation horizon depth of 4300 m in the North Atlantic. (Gianguzza et al., 2000). Below the saturation horizon follows the lysocline, where dissolution of $CaCO_3$ starts and intensifies with increasing depth. Subjacent, where the dissolution of $CaCO_3$ equals its rate of accumulation, is the location of the calcite compensation depth (CCD) (Summerhayes et al., 1996). The uptake of anthropogenic CO_2 over the last 250 years has already shallowed the aragonite saturation horizon in all oceans. Under the IS92a scenario, the entire water column of the Southern Ocean will become undersaturated, with respect to aragonite, during the twenty-first century (Feely et al., 2004; Orr et al., 2005).

1.3.4 Palaeo-ocean acidification

Measurements of Antarctic ice cores show periodic variations in atmospheric CO_2 with the glacial-interglacial cycles. Over the past 800000 years of earth history, atmospheric CO_2 concentrations have fluctuated between ~180 and ~280 ppmv (Siegenthaler et al., 2005; Lüthi et al., 2008). Over longer timescales (million years) proxies indicate periods of much higher CO_2 concentrations as e.g. during the Cretaceous with concentrations between three and ten times higher than present (Raven et al., 2005, 2005; Doney et al., 2009). There is evidence that large CO_2 releases during earth history changed the carbonate chemistry of the seawater and theoretically had the potential for an ocean acidification event. But due to the large time scales, compared to the recent increase in CO_2, the ocean-atmosphere system was able to reduce atmospheric CO_2 and balance the carbonate chemistry. An important factor on long term scales >10000 years is the rise of terrestrial weathering of carbonate and silicate rocks induced by high atmospheric CO_2 and increasing temperature (Kump et al., 2009; Zeebe et al., 2012). Enhanced weathering provides alkalinity in the form of HCO_3^- to the ocean and therefore draws down CO_2. As a result, this process balances the oceans carbonate chemistry and decouples atmospheric CO_2 and ocean pH from $CaCO_3$ saturation state (Kump et al., 2009; Hönisch et al., 2012). On shorter time scales or during times of faster CO_2 increase as the current rate of > 45 ppmv per 100 years, the buffer capacity of weathering is not fast enough to balance sea water carbonate chemistry (Zeebe et al., 2012; Hönisch et al., 2012).

Despite different periods in earth history with rapid CO_2 increase as the deglaciations, the Paleocene-Eocene thermal maximum (PETM), Mesozoic ocean anoxic events (OAEs), the Triassic-Jurassic (T/J) boundary or the Permian-Triassic boundary (P/T), it is difficult to find an event which is analogue to the present rapid increase in CO_2 (Hönisch et al., 2012). Well-known examples are the CO_2 rises of around 100 ppmv during the last and the penultimate deglaciation (Termination I and II) (Monnin et al., 2001; Petit et al. 1999). The amplitudes are

rather comparable to the recent increase in CO_2, but take place over a large time interval of around 10 ka (Kukla et al., 2002), and they therefore had very slow rates of around 0.8 ppmv CO_2 per 100 years (Monnin et al., 2001; Hönisch et al., 2012). Surface seawater pH and saturation state declined during deglaciations, but due to the large timescale, they are slow and moderate acidification events where the deep sea pH remained rather stable (Zeebe and Marchitto, 2010; Hönisch et al., 2012; Zeebe et al., 2012). However, there is no event in the past, related to an increase in CO_2, which is comparable to the recent rate of environmental change, which is therefore driving to unpredictable changes in the oceans chemistry (Kump et al., 2009; Pelejero, 2010). As it is rather difficult to establish natural conditions in the laboratory, past events in Earth`s history with a notable increase in CO_2 help to clarify the possible response of marine calcifiers in the future. Palaeo-studies on coccolithophore communities during rising atmospheric CO_2 conditions give indications about the ecological response (e.g. assemblage shifts, adaptation) from the entire assemblage in their natural environment. Another advantage is the possibility to study the effects of the changing carbonate chemistry in combination with accompanied environmental changes.

1.4 Coccolithophores

1.4.1 Biology and ecology

Coccolithophores are unicellular marine nannoplankton, belonging to the phylum Haptophyta, subclass Prymnesiophycidae (Edvardsen et al., 2000). They are photoautotrophic and one of the major primary producers (Cortés et al., 2001). Since their first appearance during the Triassic, around 220 Ma ago (Edvardsen and Medlin, 2007), coccolithophores evolved around 4000 morphologically different species (De Vargas et al., 2007). Nowadays they are represented by 280 extant species, with numerous morphological variants (morphotypes) (Young et al., 2003; Young et al., 2005). They have a complex life cycle with alternating haploid and diploid generations, during which they reproduce by asexual mitotic division (Billard and Inouye, 2004).

Coccolithophores produce an exoskeleton of small calcite plates, the coccoliths, which cover their cell in single or multiple layers and form the coccosphere. The taxonomy of coccolithophores is based on the morphological differences of the coccoliths (Billard and Inouye, 2004). Depending on their life cycle stage, two different types of coccoliths can be produced by the same organism: The most common, intracellulary produced heterococcoliths (Brownlee and Taylor, 2004) and the extracellulary produced holococcoliths (Rowson et al., 1986). Heterococcoliths are produced during the diploid stage, formed by interlocked crystal units of variable shape whereas holococcoliths, produced during the haploid stage, are formed of

identical, non-interlocked crystal units (Young et al., 1992). Some species as e.g. *E. huxleyi* and *Gephyrocapsa* calcify only during the diploid phase (Young and Henriksen, 2003).
The function of coccoliths is still under debate, diverse hypotheses have been proposed: protection of the cell wall against mechanical damage, grazers or bacterial infestation; regulating light reflection; buoyancy or protection from osmotic changes (Young, 1994). Calcification and photosynthesis are most probably not coupled and therefore calcification is not a source for CO_2 in coccolithophores (Herfort et al., 2004; Trimborn et al., 2007; Leonardos et al., 2009). There is strong evidence that coccolithophores generally use external CO_2 for photosynthesis (Sikes et al., 1980; Rost et al., 2003; Schulz et al., 2007), as e.g. photosynthesis in non-calcifying cells is as possible as in calcifying-cells, or even more efficient (Rost and Riebesell, 2004).
The internal production of coccoliths occurs in a Golgi-derived intracellular vesicle and requires the uptake of calcium (Ca^{2+}) and inorganic carbon (C) from the external medium (Brownlee and Taylor, 2004). There is strong evidence that HCO_3^- is the primary carbon source for calcification in coccolithophores (e.g. Sikes et al., 1980; Nimer and Merrett, 1992, 1996; Buitenhuis et al., 1999; Bach et al., 2013). The production of calcite in the coccolith vesicles is isolated from the surrounding seawater. Within the vesicles, the $CaCO_3$ concentration is tightly controlled (Jones et al., 2013) in order to provide a supersaturated solution during calcite nucleation and growth (Marsh et al., 2003). Calcite formation produces H^+ ions ($Ca^{2+} + HCO_3^- \leftrightarrow CaCO_3 + H^+$), the increase in H^+ decreases the pH in the cell and leads to an activation of H^+ ion channels which releases the ions from the cell to maintain a constant pH (Taylor et al., 2011; Decoursey et al., 2013).

1.4.2 Coccolithophore biogeography

Modern coccolithophores are widespread in all marine environments, their biogeographical distribution, growth and calcification is controlled by parameters as temperature, nutrient availability, light, salinity, trace elements and vitamins (Winter et al., 1994; Bown and Young, 1998). Individual species are adapted to a different range of environmental conditions, their biogeographical distribution roughly follows broad latitudinal belts or zones, separated by frontal systems (McIntyre and Bé, 1967; Winter et al., 1994; Brand, 1994). McIntyre and Bé (1967) divided the Atlantic and the Pacific Ocean into nannofloral assemblage zones, characterised by specific coccolithophore communities. In the Atlantic Ocean the authors identified five nannofloral assemblage zones: tropical, subtropical, transitional, subarctic and subantarctic (McIntyre and Bé, 1967).

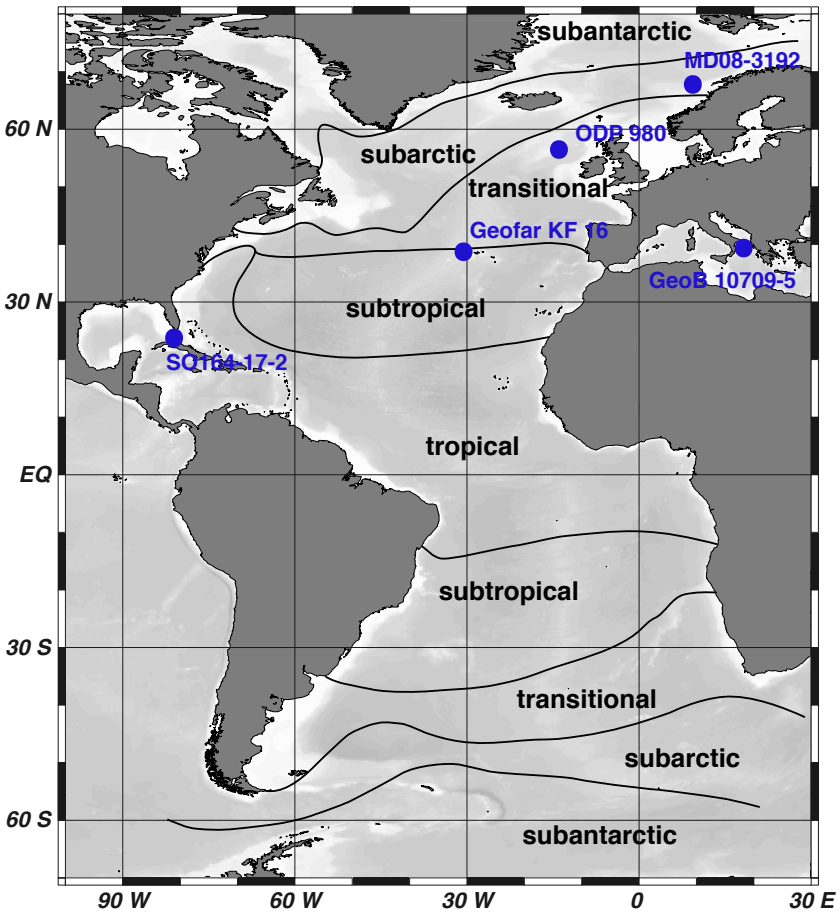

Figure 1.7. Coccolith assemblage zones and site locations. Redrawn after McIntyre and Bé (1967).

Today, most coccolithophores are K-selected species, they grow slowly and flourish in nutrient pour waters (Brand et al., 1994; Young, 1994). Therefore the highest coccolithophore diversity, but lowest coccolithophore production, is in warm oligotrophic stable environments such as subtropical gyres (Hulburt, 1963), whereas the diversity is much lower in polar waters (McIntyre, 1967). Some species as e.g. *E. huxleyi* and to a lesser extent *G. oceanica* are r-selected opportunistic species with wide ecological tolerances and able to build monospecific assemblages with enhanced coccolithophore productivity in highly eutrophic and instable systems (McIntyre and Bé, 1967; Brand et al., 1994; Young, 1994).

1.4.3 Coccolithophore response (growth and calcification) to environmental conditions

In general, coccolithophores are adapted to a wide range of sea surface temperatures, they are distributed from tropical to temperate waters. Each species or even morphotype has its individual, and often narrow temperature tolerance (e.g. Baumann et al., 2005; Langer et al., 2007; de Bodt et al., 2010; Flores et al., 2010). Studies on correlations between temperature and calcification rates showed different results, Beaufort et al. (2007) concluded that there is no global relationship between sea surface temperature (SST) and the degree of calcifica-

tion, especially in *E. huxleyi* due to its high morphologic and genetic diversity with different temperature tolerances (Young et al., 2003; Hagino et al., 2011).

In the open ocean, coccolithophores are adapted to salinity fluctuations of 32 - 37 ppt, but several species have wider salinity tolerances (Brand, 1994 and references therein). Bollmann et al. (2009) as well as Fielding et al. (2009) found morphological changes in *E. huxleyi* over a large salinity gradient, with a linear increase in coccolith numbers and size with increasing salinity. However, there is no strong correlation between the calcification of coccolithophores and salinity (Beaufort et al., 2011).

Growth and calcification of coccolithophores are highly responsive to nutrient concentrations. Under phosphate limited conditions cells can maintain the production of biomass and calcite but are unable to divide due to the lack of phosphate for nucleic acid synthesis (Raven et al. 2012). This can result in enhanced calcite content per coccolith or coccolith production in some species (Nimer and Merrett, 1993; Paasche, 1998; Shiraiwa, 2003). Nitrate limitation inhibits the synthesis of proteins which leads to less biomass production but calcification continues, resulting in higher calcite content per cell (Müller et al., 2008, 2012; Raven et al., 2012). In general, nutrient limitation leads to increasing particular inorganic carbon (PIC): particular organic carbon (POC) ratio (Raven et al., 2012).

Also enhanced nutrient supply can have a positive influence on coccolith weight (e.g. Engel et al., 2005; Beaufort et al., 2007; Rouco et al., 2013). The weight of *E. huxleyi* and *G. oceanica* increased during the nutrient rich conditions of two upwelling induced blooms and accordingly during times with high coccolithophore production, which suggests a link between the degree of calcification and primary production. *E. huxleyi* coccoliths formed the major part of all coccolithophore calcite during the bloom (Beaufort et al., 2007). In addition Engel et al. (2005) observed an increase in *E. huxleyi* coccolith weight by 25 to 50 % during blooms in mesocosm experiments after adding nutrients. Rouco et al. (2013) reported about an increase in both, cellular particulate inorganic and organic carbon under nutrient replete conditions at high CO_2, accompanied by a slight increase in coccosphere volume and coccolith size.

Coccolithophores are photosynthetic organisms which generally live in the photic zone where light levels are sufficient to carry out photosynthesis (Winter et al., 1994). The calcification of coccoliths requires energy and is thus a light-dependent process (Anning et al., 1996; Zondervan, 2007). In comparison to other phytoplankton groups (e.g. diatoms and dinoflagellates), some coccolithophore species as *E. huxleyi* are not photoinhibited by high light intensities and able to maintain photosynthesis and calcification (Nimer and Merret, 1993; Nanninga and Tyrrell, 1996). In contrast, at low irradiance the particular organic carbonate production of *E. huxleyi* is more sensitive to light than the calcification which saturates at lower light intensities. Therefore the ratio of calcite to particular organic carbon increases with de-

creasing irradiance. However, this trend reverses when the irradiance is severely limited (Zondervan, 2007).

1.4.4 Coccolithophores and their importance for palaeostudies

Coccolithophores are sensitive indicators of surface water conditions, their organic and inorganic remains can be used in palaeoceanographic reconstructions. Their biogeographical distribution, assemblage composition, elemental and isotopic composition of their carbonate, alkenone data, morphology and weight of their coccoliths provide information about past environmental and biological conditions such as calcification rates, sea surface temperature or palaeoproductivity (Stoll and Ziveri, 2004).

In this study, reconstructions on past environmental conditions from coccolithophores base on the analysis of coccolith weights, coccolithophore accumulation rates for palaeoproductivity reconstructions, and include alkenone sea surface temperature data from other studies. These proxies are briefly introduced in the following.

Coccolithophore calcification can be expressed in different ways: in the coccolith exocytosis rate, in the size of coccoliths and in the weight per coccolith. Culture studies on *E. huxleyi* showed a correlation between calcification rates and coccolith weight, expressed in a simultaneous change in exocytosis rate and coccolith weight. This suggests the use of single coccolith weights as a potential indicator for coccolithophore calcification rates (Bach et al., 2012).

Coccolithophores are significant contributors to the oceanic primary production, their accumulation rates can be used as an indicator for palaeoproductivity dynamics (Lotoskaya et al., 1998; Stolz and Baumann, 2010; Schwab et al., 2012). Main factors which control the primary productivity of phytoplankton are nutrients, light and temperature (Winter and Siesser, 1994). Despite the optimum development of coccolithophorids in nutrient limited mesotrophic/oligotrophic environments, which is reflected in a high diversity, the abundance of coccolithophores is rather low in this areas. The highest abundance (but lowest diversity) of coccolithophores in present day and fossil records is represented in nutrient rich eutrophic areas as equatorial upwelling zones or along continental margins. Thus coccolith accumulation rates in the sediment can be linked to nutrient availability (Baumann et al., 1999; Flores et al., 2013), if factors as dilution, dissolution or alteration are considered (Lototskaya et al., 1998; Flores et al., 2013).

A further well established proxy from coccolithophores is the alkenone undersaturation ratio of alkenone biomarkers (U_{37}^{K}). Alkenones are long-chain ketones, produced by species of the family Noelaerhabdaceae, and are used to reconstruct sea surface temperatures (e.g. Marlowe et al., 1990; Müller et al., 1997, Prahl et al., 2000).

1.4.5 Coccolithophore family Noelaerhabdaceae

This thesis focuses on the coccolithophore family Noelaerhabdaceae from the order Isochrysidales which has dominated most assemblages over the past 20 Ma (Beaufort et al., 2011). In their dominant diploid life cycle phase they are usually heterococcolith-bearing (non motile) while during their alternate, haploid phase they are non-calcifying (motile). Therefore, Noelaerhabdaceae have no holococcolith stage (Young et al., 2003). Modern Noelaerhabdaceae include the genera *Emiliania*, *Gephyrocapsa* and *Reticulofenestra* (more common in the Pacific Ocean) which are the dominant coccolithophores in most assemblages (Young et al., 2003). An overview of the ecology of selected coccolithophore species from the family Noelaerhabdaceae which are used in this study are described in the following.

Emiliania huxleyi

E. huxleyi evolved from the gephyrocapsids around 250 ka BP and has been the most abundant coccolithophore for the last 70 ka (Tyrrell and Young, 2009). Usually, *E. huxleyi* cells are surrounded by 12 - 15 coccoliths per organism, with this number rising or falling under changing environmental conditions (Balch et al., 1993). Typical *E. huxleyi* coccolith length is between 2.5 - 5 μm (Young and Ziveri 2000; Young et al., 2003), and the mean weight per coccolith is between 1.2 - 5.3 pg (Young and Ziveri, 2000; Beaufort et al., 2005), variations are also known from culture data (e.g. Bach et al., 2012).

E. huxleyi is an r-selected, opportunistic species with a high cell division rate up to 2.8 per day (Brand and Guillard, 1981; Paasche, 2002). Nowadays it accounts for 30 - 50 % of the total coccolithophore assemblage in most regions and up to 100% in sub-polar waters (Winter and Siesser, 1994; Mohan et al., 2008). *E. huxleyi* has an extensive genetic and morphologic diversity with diverse environmental tolerances (Medlin et al., 1996; Young et al., 2003). Based on distinct morphologic features of the coccoliths, *E. huxleyi* can be divided into different morphotypes, termed type A, B, C and the additional morphotypes B/C, R and var. corona (Young and Westbroek, 1991; Young et al., 2003), of which at least three are genetically distinct (Schroeder et al., 2005; Cook et al., 2011). Coccoliths of morphotype A are very common in the oceanic population, globally widespread and bloom forming (Young and Westbroek, 1991; Paasche et al., 1996). Morphotype B is primarily is found in the North Sea, (van Bleijswijk et al., 1991) and type B/C in the Southern Hemisphere (Findlay and Giraudeau, 2000; Cubillos et al., 2007; Cook et al., 2011). The heavily calcified morphotype R is similar to type A but with heavily calcified shield elements and often closed slits. It has been found in the SW Pacific (Young et al., 2003) and the Southern Ocean (Burns, 1977; Nishida, 1979).

Figure 1.8. SEM pictures of Noelaerhabdaceae coccoliths and coccospheres. a) - b) *E. huxleyi* coccoliths (site MD08-3192, Vøring Plateau, Holocene), c) Overcalcified *E. huxleyi* coccolith (site MD08-3192, Vøring Plateau, Holocene), d) *E. huxleyi* coccolith (site SO164-17-2, Florida Strait, Termination II), e) *E. huxleyi* coccosphaere (GeoB10709-5, Gulf of Taranto, past 200 years), f) - g) *G. muellerae* coccolith (site MD08-3192, Vøring Plateau, Holocene), h) - i) *G. oceanica* coccoliths (site SO164-17-2, Florida Strait, Termination II), j) - k) *G. ericsonii* coccoliths (site SO164-17-2, Florida Strait, Termination II), l) *G. protohuxleyi* coccolith (site SO164-17-2, Florida Strait, Termination II), m) cluster of small *Gephyrocapsa* coccoliths (site SO164-17-2, Florida Strait, Termination II), n) *G. oceanica* and *G. ericsonii* coccoliths (site SO164-17-2, Florida Strait, Termination II), o) *E. huxleyi*, *G. oceanica*, *G. ericsonii* and small *Gephyrocapsa* coccoliths (site SO164-17-2, Florida Strait, Termination II).

Recently, Smith et al. (2012) reported on dominance of a heavily calcified *E. huxleyi* morphotype in the North Atlantic (Bay of Biscay) during winter, when pH and $CaCO_3$ saturation are lowest. Further, Beaufort et al. (2011) observed a highly calcified *E. huxleyi* morphotype in Patagonian-shelf and Chilean upwelling waters that is able to calcify heavily in waters characterised by low carbonate ion concentrations. These findings indicate that this morphotype may be adapted to a lower pH calcification optimum. Adaptations of other *E. huxleyi* morphotypes to specific environmental conditions are e.g. the large, cold water preferring morphotype *E. huxleyi* > 4 *μ*m, which corresponds to Type B (Colmenero-Hidalgo et al., 2002; Hagino et al., 2005; Flores et al., 2010).

Due to the large intraspecific diversity, *E. huxleyi* has a large ecological tolerance with a wide temperature (1 - 31°C) and salinity (11 - 41 ppt) range (McIntyre et al., 1970; Hajo and Honjo, 1989; Brand, 1994; Winter et al., 1994). It occurs under eutrophic and oligotrophic conditions but with higher abundances in nutrient rich subpolar waters, in equatorial and coastal upwelling regions, outer shelf areas and along borders of subtropical gyres (Flores et al., 2010). Moreover, one freshwater form is documented (Bown, 1998). *E. huxleyi* tolerates high irradiance, which does not inhibit growth, but rather seems to induce blooms of this species (Paasche, 2002). Extensive blooms of *E. huxleyi* are formed during summer and early autumn and can cover up to 8 million km^2, with cell densities larger than a million cells per litre (Brown and Yoder, 1994; Moore et al., 2012).

Gephyrocapsa oceanica

The first appearance of the genus *Gephyrocapsa* was observed in the Middle Miocene, 15 Ma BP (Pujos, 1987), a frequent occurrence was reported in the Early Pliocene, 3.5 Ma BP (Bollmann and references therein). The large species *G. oceanica* evolved at the base of the Pleistocene through *G. caribbeanica* (Samtleben, 1980). As all *Gephyrocapsa* species, *G. oceanica* is characterised by a single bar (bridge) across the central area (Bollmann et al., 1997). Its coccospheres consist of 9 - 14 coccoliths with a single coccolith length of 3.5 - 6 *μ*m and mean coccolith weights between 12.3 - 53 pg (Okada and McIntyre, 1977; Young and Ziveri, 2000; Young et al., 2003, Beaufort et al., 2005).

G. oceanica is abundant in tropical waters of 12 - 30°C (Okada and McIntyre, 1979), with highest growth rates at 27°C (Klaas et al., 1999). It has a high salinity tolerance and an affinity for warm and nutrient rich waters (Kleijne et al., 1989; Houghton and Guptha, 1991; Giraudeau et al., 1993; Ziveri and Thunell, 2000; Broerse et al., 2000) and is therefore reported to be abundant in temperate and tropical waters as well as equatorial and upwelling areas (Bollmann, 1997; Okabe, 1997; Ziveri et al., 2004). Like *E. huxleyi*, *G. oceanica* is able to form massive blooms (e.g. Blackburn and Cresswell, 1993; Rhodes et al.,1995).

Gephyrocapsa muellerae

G. muellerae evolved in the late Pleistocene, around 240 - 220 ka BP from *G. margeli*. The coccosphere of *G. muellerae* consists of 14 - 24 coccoliths, which are 3 - 4,5 *µ*m long and have a mean coccolith weight around 8 pg (Young and Ziveri, 2000).

This species has an affinity for moderate productive cool surface waters (Winter et al., 1994) where it occurs in high abundances or even as dominant taxon (Bollmann, 1997; Findlay and Giraudeau, 2002) and is thus often used as a cold water indicator (Weaver and Pujol, 1988). It is highly abundant in the eastern North Atlantic, in a preferred temperature range of 12 - 18°C, and an optimum temperature of 14°C (Giraudeau et al., 2010).

Gephyrocapsa ericsonii

The first appearance of *G. ericsonii* was documented in the late Pleistocene around 300 ka BP. This species is characterised by its small size and a strong bridge. The coccosphere is covered with 20 - 34 coccoliths with a length of around 1.4 - 2.7 *µ*m per coccolith and a mean coccolith weight around 3.6 pg (Samtleben, 1980; Young and Ziveri, 2000). *G.ericsonii* can be classified into three groups regarding morphological variability: (1) *G. ericsonii*: without slits between distal shield elements, (2) *G. protohuxleyi*: with slits between distal shield elements, (3) *"with thorn"*: well developed slits and a slender thorn (Cros and Fortuño, 2002).

G. ericsonii has a preference for high nutrient contents and less saline surface water conditions (Boeckel et al., 2006). It tolerates temperature ranges from 12 - 27 °C and thus has a wide biogeographical distribution from tropical to temperate oceans (Okada and Honjo, 1973; Bollmann, 1997; Ziveri et al., 2004).

1.4.6 Coccolithophores and ocean acidification

Coccolithophores are one of the most important pelagic calcifying organism, about half of the modern $CaCO_3$ precipitation is estimated to be produced by coccolithophores (Milliman, 1993). They play an important role in the marine carbon cycle by participating in both carbon pumps, in the organic carbon pump via photosynthesis and in the carbonate counter pump via calcification of coccoliths (Purdie and Finch, 1994). Photosynthesis of coccolithophores consumes CO_2 but calcification of coccoliths counteracts the CO_2 uptake by producing CO_2 (Rost and Riebesell, 2004; Harlay et al., 2010). In comparison to non-calcifying phytoplankton, coccolithophores can be a smaller sink for CO_2, during coccolithophore blooms they can become a source for CO_2 (Robertson et al., 1994; Rost and Riebesell, 2004).

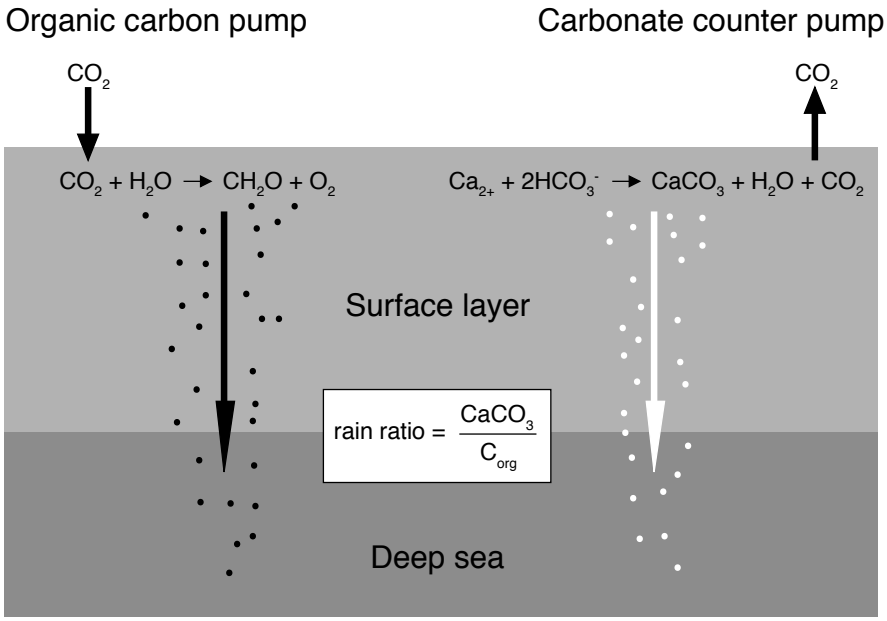

Figure 1.9. The biological carbon pumps: The organic carbon pump is a CO_2 sink in the ocean: CO_2 is taken up during photosynthetic carbon fixation and transported to depth. The carbonate counter pump releases CO_2 by producing calcium carbonate and counteracts the organic carbon pump. The relative strength of both pumps is described by the rain ratio. Redrawn after Rost and Riebesell (2004).

However, on geological timescales, the production of coccolithophore carbonate and organic carbon and sedimentation act as sink for atmospheric CO_2 (Buitenhuis et al., 2001). Further, their coccoliths act as ballast in sinking organic aggregates as marine snow or faecal matter when they sink from the surface to the deep ocean (McIntyre and Bé, 1967; Klaas and Archer, 2002). Calcite enriched particles enhance the vertical mass transfer of organic carbon and thus increase the strength of the organic carbon pump (McIntyre and Bé, 1967; Ploug et al., 2008). Thus, variations in coccolithophore calcite production via changing cell abundance or coccolith calcification affect the sinking velocity of the aggregates and consequently the organic carbon export to depth (Beaufort et al., 2007; Ziveri et al., 2007; Zondervan et al., 2011).

The response of coccolithophores to the ongoing uptake of anthropogenic CO_2 and the concomitant changes in the oceans carbonate chemistry has gained increasing attention in recent years. Numerous laboratory, field and sediment studies were conducted in the last years, beginning with the initial paper of Riebesell et al. (2000), who reported about reduced calcite production of monospecific *E. huxleyi* and *G. oceanica* cultures at high CO_2. Subsequent laboratory experiments revealed similar negative feedbacks, decreasing calcification or malformation with increasing CO_2 and decreasing pH (Zondervan et al., 2001, 2002; Feng et al., 2008). In contradiction to these results are findings of enhanced calcification under elevated CO_2 (Iglesias-Rodriguez et al., 2008a; Shi et al., 2009), which led to discussions about realistic manipulations of the carbonate system in the laboratory (Iglesias-Rodriguez et al., 2008a, 2008b), and the introduction of a guideline for best practice in OA experiments (Rie-

besell et al., 2010) Further studies have shown that the nonuniform response of different coccolithophore taxa is due to species specific and strain specific calcification optima with respect to changing carbonate chemistry (Langer et al., 2006, 2009; Krug et al., 2011). In the following, laboratory and mesocosm experiments with a combination of rising CO_2 and parameters as e.g. temperature, nutrient and light conditions were conducted and indicated even more variances in the response (e.g. Sciandra et al., 2003; Engel et al., 2005; De Bodt et al., 2010; Borchard et al., 2011; Fiorini et al., 2011; Matthiessen et al., 2012; Rouco et al., 2013). Nevertheless, laboratory studies are useful to isolate impacts of different factors but have to be considered very carefully as it is impossible to establish natural seawater conditions in the laboratory. Further, most of the laboratory studies are short term experiments on monospecific cultures which neglect a possible evolutionary adaptation (Riebesell et al., 2009; Ridgwell et al., 2009). Exceptional is the recently conducted long term study of Lohbeck et al. (2012) which revealed an adaptation of *E. huxleyi* calcification to enhanced CO_2 due to genotypic selection as well as mutations within the population. This study emphasises the important role of the evolutionary adaptation in changing environmental conditions.

Studies on natural heterogenous coccolithophore assemblages showed dominance shifts to better adapted morphotypes of the same species as response to varying seawater carbonate chemistry (e.g. Triantaphyllou et al., 2010; Beaufort et al., 2011, Smith et al., 2012). Field and sediment studies offer insights from the natural habitat of coccolithophores to which they are evolutionary adapted (Smith et al., 2012), as e.g. the recently conducted study on sediment samples from different ocean basins which presented a correlation between decreasing coccolith weight and declining carbonate ion concentration during the CO_2 increase of the last deglaciation (Beaufort et al., 2011). Data sets on the coccolithophore response to the recent rising atmospheric CO_2 conditions reported an increase in coccolith mass of 40 % over last 220 years (Iglesias-Rodriguez et al., 2008), which were later attributed by Halloran et al. (2008) to a coccolith size increase of the large coccolithophores (as *Calcidiscus leptoporus, Coccolithus pelagigus*) while smaller species (*E. huxleyi, G. oceanica, G. muellerae*) showed more lightly calcified coccoliths. In the findings of Grelaud et al. (2009), coccolith mass of exact these smaller species increased between 1917 and 2004, but concomitant with rising sea surface temperature and decreasing iron and phosphate nutrient availability which enhanced the difficulty to disentangle the main controlling factor of the increasing coccolith mass.

Considering these previous studies from laboratory, mesocosm and sediment studies it is difficult to make a general statement on coccolithophore calcification. Species and strain specific response and adaptation to both changing carbonate chemistry and other environmental factors in the ocean enhance the difficulty to predict the future responses of coccolithophores to changing carbonate chemistry (Raven et al., 2012).

2. Study area and methods

2.1 Site selection

In order to meet the afore mentioned objectives, 5 sediment cores covering 3 time intervals were selected (Fig. 2.1). The Holocene, i.e. the last 10000 years, was selected for studies on coccolith weights during times of minimum variability in the carbonate system. Three sediment cores from the North Atlantic Ocean covering different biogeographic areas were chosen (MD08-3192, ODP Site 980, Geofar KF 16). To investigate the response of coccolith calcification to a natural atmospheric CO_2 rise, 2 sediment cores were picked (ODP Site 980, SO164-17-2) which cover the penultimate deglaciation from MIS 6 to MIS 5 (Termination II, 125 - 135 ka BP). Investigations on coccolith weight changes of the recent atmospheric CO_2 increase were carried out on a sediment core covering the past 200 years (GeoB10709-5).

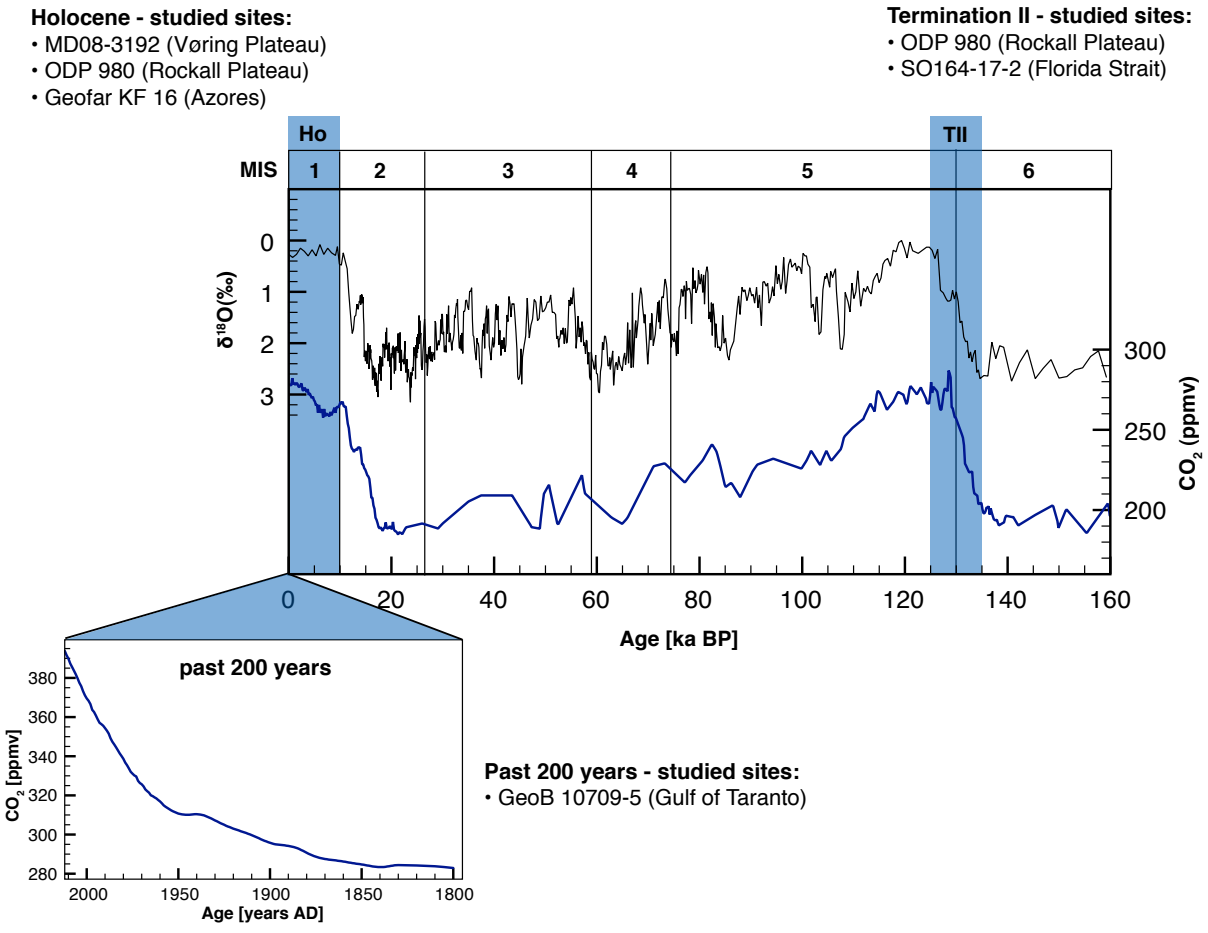

Figure 2.1 Atmospheric CO_2 concentrations of the last 160 ka (blue line, CO_2 data from EPICA Dome C from Lüthi et al., 2008) and planktic foraminiferal $\delta^{18}O$ record (black line, sediment core MD95-2042, from Shackleton et al., 2000). Chosen time intervals are marked in light blue Abbreviations: Marine Isotope Stages (MIS), Holocene (Ho), Termination II (TII).

2.2 Study area and (palaeo-)oceanographic settings

The selected sediment cores for this study are located in the North Atlantic and the Mediterranean Sea. Different climatic zones are covered (transitional, subtropical and tropical areas) with various productivity regimes, SST and carbonate systems.

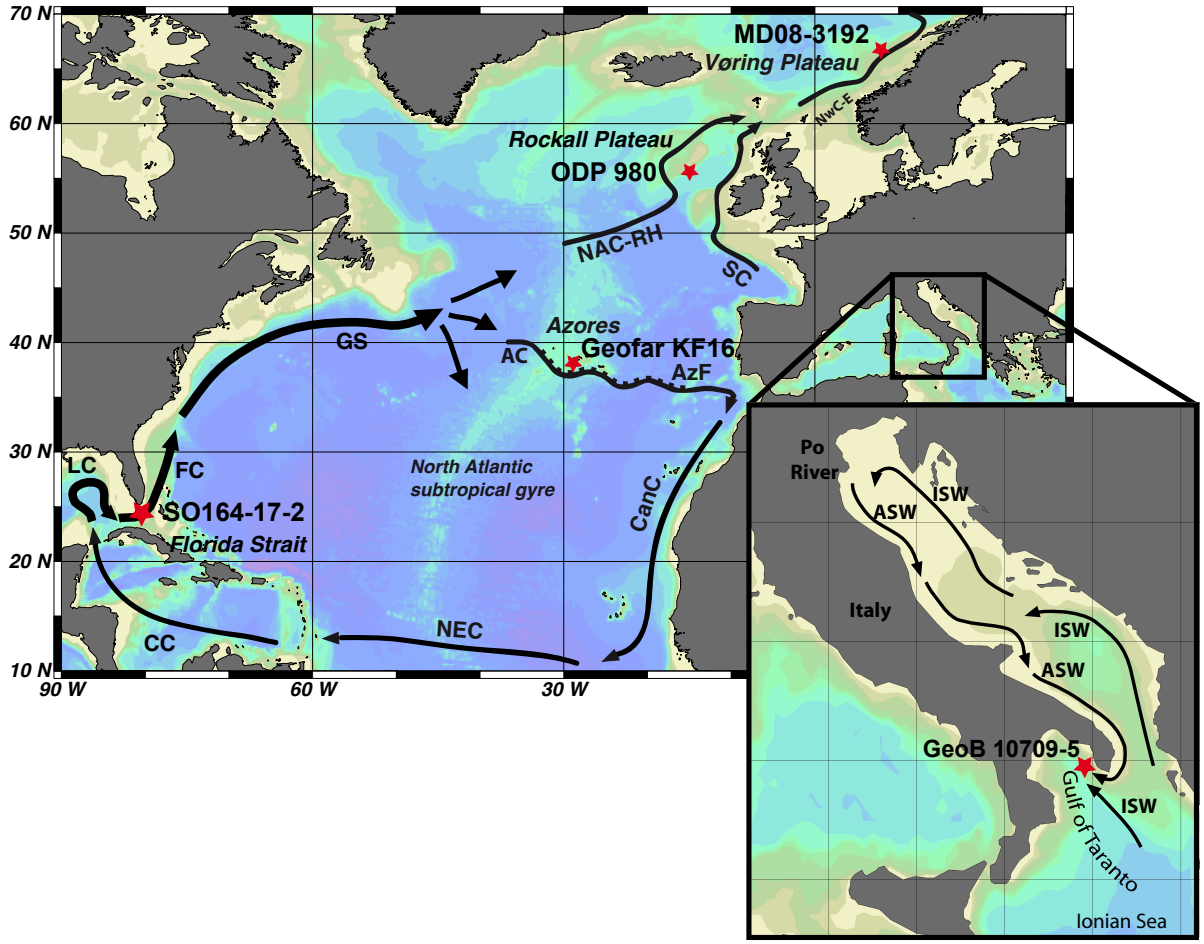

Figure 2.2. Map of the North Atlantic and parts of the Mediterranean Sea with core positions and main oceanographic features: Red stars mark the location of the studied sediment cores. Black arrows show major ocean surface currents: Caribbean Current (CC), Loop Current (LC), Florida Current (FC), Gulf Stream (GS), North Atlantic Current Rockall-Hatton branch (NAC-RH), Slope Current (SC), eastern branch of the Norwegian Current (NwC-E), Azores Current (AC) with the corresponding Azores Front (AzF) figured as black dashed line, Canary Current (CanC), North Equatorial Current (NEC), Adriatic Surface Water (ASW), Ionian Surface Water (ISW). The map was designed with the ODV software by R. Schlitzer (Ocean Data View software, 2010, http//odv.awi.de).

MD08-3192 (Holocene)

The Calypso Square Core MD08-3192 (66°55.86'N, 007°33.92'E; Fig. 2.2) was taken from the Vøring Plateau in the eastern Norwegian Sea from 1010 m water depth (Kissel et al. 2009). The location is influenced by the eastern branch of the Norwegian Atlantic Current, an extension of the North Atlantic Current (Andersson et al., 2010). Most of this water inflow

originates from the slope current, carrying warm and saline water into higher latitudes (Blindheim and Østerhus, 2005). During the early Holocene, the North Atlantic current increased in strength (Birks and Koç, 2002), and warmest sea surface conditions occurred from the early Holocene until approximately 6 ka BP (Berner et al., 2011). During the middle and late Holocene SST decreased to present-day conditions, synchronous to decreasing summer insolation (Calvo et al., 2002). Coccolithophore productivity rates at the Vøring Plateau increased during the entire Holocene and reached a maximum peak between 3 and 4 ka BP (Giraudeau et al., 2010).

ODP Site 980 (Holocene and Termination II)

ODP Site 980 (55°12.90'N, 14°14.20'W; Fig. 2.2) was taken during ODP Leg 162 (Jansen et al., 1996) from a water depth of 2179 m. The site is located in the eastern North Atlantic at the Rockall Plateau, in the high accumulation area of the Feni Drift, which is deposited along the northwestern flank of the Rockall Trough (Jansen et al., 1996). The Rockall Plateau is mainly influenced by Western North Atlantic water of the North Atlantic Current and its local northerly flowing Rockall-Hatton Branch, carrying relatively warm and salty water. Eastward of the Rockall Plateau, the warmer, more saline and less stratified Slope Current flows into the Rockall Trough (Hansen and Østerhus, 2000; Pollard et al., 2004). This current belongs to East North Atlantic Water and originates in the Bay of Biscay (Read, 2001). SST at ODP Site 980 ranges around 9.8 °C in winter and around 12.1 °C in summer (Antonov et al., 2006; Locarnini et al., 2006).

ODP Site 980 is located southwards of the Arctic front which separates the warm Atlantic from the cold Arctic waters (Swift, 1986**)**. The transition from the penultimate glacial (Marine Isotope Stage 6) to the penultimate interglacial (Marine Isotope Stage 5), called Termination II, in the North Atlantic is characterised by changes in the palaeoceanographic conditions. The activity of the NAC was reduced during Termination II and the position of the Arctic front migrated southwards, close to ODP Site 980. This resulted in harsh sea water conditions with sea ice and low sea surface temperature. Lowest SST combined with reduced coccolith numbers and diversity denote the Heinrich event 11. During MIS 5 the increasing influence of the NAC resulted in ameliorate climate conditions, with enhanced growth conditions for coccolithophores characterised by increasing coccolith numbers and taxa (Stolz and Baumann, 2010).

During the Holocene, between 7 and 5.4 ka BP, a decreasing summer insolation and the end of meltwater influence caused the reorganisation of surface circulation patterns resulting in a weaker North Atlantic current and a stronger influence of the Slope Current after 5 - 6 ka BP (Solignac et al., 2008). These regional changes are reflected in an increase of alkenone SST

at ODP Site 980 between 3.5 ka and 2 ka and a following decrease (J. Holtvoeth, unpublished data, pers. comm.). The coccolithophore productivity at ODP Site 980 is relatively stable over the entire Holocene with highest rates in the early and late Holocene.

Geofar KF 16 (Holocene)

Piston core Geofar KF 16 was retrieved southwest of the Azores islands (37°99.90'N, 31°12.83'W; Fig. 2.2), at the northern rim of the subtropical gyre (Richter, 1998) from a water depth of 3050 m (GEOFAR cruise; Richter, 1998). Additionally, a surface sediment sample from the same location (boxcore GEOFAR KG 14) was analysed. The northeastern boundary of the subtropical gyre is defined by the Azores Current System with the corresponding Azores Front (Klein and Siedler, 1989; Rogerson et al., 2004). The Azores Front separates two different productivity regimes: low primary production in the subtropical gyre in the south, and nutrient rich conditions in the north (Schwab et al., 2012). At the coring site, enhanced productivity during the early Holocene is followed by a shift to modern oligotrophic conditions around 6 ka BP. The productivity changes due to a northward shift of the Azores Front in the late Holocene (Schwab et al., 2012). Sea surface temperature at the coring site is around 20º C in the early Holocene, decreases to 17.8º C at 8.2 ka BP and stabilises after 8 ka BP to modern conditions of 18.5 - 19.5º C (Schwab et al., 2012).

SO164-17-2 (Termination II)

Piston core SO164-17-2 (24°04.99′N; 80°53.00′W; Fig. 2.2) is located at the southern Florida Strait and was recovered during R/V Sonne Cruise SO164 from 954 m water depth (Nürnberg et al., 2003). Through the Florida Strait, the strong Florida Current flows between Florida and the Bahamas into the North Atlantic (Richardson et al., 1969). It is considered as the major source of the Gulf Stream and carries warm tropical waters to higher latitudes (Wennekens, 1959). The Florida Current derives from water masses of the Loop Current which is the extension of the Caribbean Current (Gordon, 1967; Molinari and Morrison, 1988). According to the results of Lynch Stieglitz et al. (1999) who reported about a reduced Gulf Stream in the Florida Strait during the last glacial maximum, Bahr et al. (2011) found similar indications that suspect a lowered Florida Current strength (and thus reduced Gulf stream) during MIS 6, and an enhancement during early MIS 5.5. The resulting stronger transport of warm water masses explain the strong SST increase at the end of Termination II (Bahr et al., 2011).

GeoB 10709-5 (past 200 years)

Sediment core GeoB 10709-5 (39°45.39´N; 17°53.57´E; fig. 2.2) was retrieved with a multicoring device during the POSEIDON cruise "CAPPUCCINO" from 172.3 m water depth (Zonneveld et al., 2008 a, b). Core GeoB 10709-5 is located in the Gulf of Taranto in the southern Adriatic Sea. Its hydrography is influenced by the ocean circulation of the Adriatic Sea and the Ionian Sea. In the Adriatic Sea the surface waters are strongly influenced by the discharges of the Po-river, the so called "Po-discharge plume", which is the primary source of nutrients to the Adriatic Sea (Penna et al., 2004; Milligan and Cattaneo, 2007). An anticlockwise surface water circulation transports the fresh, nutrient rich and low salinity waters along the southwest Adriatic coast and in the Gulf of Taranto (Lee et al., 2007). These waters, called Adriatic Surface Water (ASW), lead to a nutrient rich belt with enhanced productivity along the western Italian coast (Turchetto et al., 2007). Within the Gulf of Taranto, water masses of the ASW mix with the warmer and more saline Ionian Surface Water (ISW), coming from the Eastern Mediterranean (Socal et al., 1999; Poulain, 2001; Turchetto et al., 2007). SST in the Gulf of Taranto vary between 13 °C in winter and 26 °C in summer (Boldrin et al., 2002, Zonneveld et al., 2009).

2.3 Age models

The age models of the coring sites base on previously published studies (see table 2.1), for site MD08-3192 an own age model was established (see table 2.1 and Appendix III).

Table 2.1. Sediment sites and applied age models

Site	Age model	Reference/Source
Geofar KF 16	Holocene part: accelerator mass spectrometer (AMS) data of planktonic foraminifera (*Globigerina bulloides*, *Globigerinoides ruber*). Additionally: alkenone SST record and planktonic oxygen isotope record were correlated with the NGRIP oxygen isotope record.	Schwab et al. (2012)
ODP 980	Holocene and Termination II: Epifaunal benthic foraminiferal $\delta^{18}O$ measurements	Oppo et al. (2006)

Site	Age model	Reference/Source
MD08-3192	Graphically tuning (Analyseries, Paillard et al., 1996) of red-green colour-scan data to core MD95-2011. Tie points: significant peaks from the end of the Younger Dryas, during the Mid-Holocene and Late Holocene. The age model of core MD95-2011 bases on AMS ^{14}C dates of the foraminifera *Neogloboquadrina pachyderma* (Risebrobakken et al., 2003).	This study (Appendix III)
SO164-17-2	Based on calcareous nannofossils and *Globorotalia menardii* biozones, a detailed age model of MIS 5 is based on the tuning of the benthic isotope record of *Cibicidoides wuellerstorfi* to the global benthic isotope stack LR04	Bahr et al. (2011)
GeoB 10709-5	$^{210}Pb/^{137}Cs$-dating via gamma spectroscopy from 9 sediment slices in depth between 0.5 - 34.75 cm	Elshanawany (2010)

2.4 Methods

2.4.1 Scanning electron microscope (SEM)

For scanning electron microscopy 35 samples from site SO164-17-2, 6 samples from GeoB Site 10709-5 and 1 sample from site MD08-3192 were prepared with a combined dilution/ filtration technique after Andruleit (1996). A small amount of dry bulk sediment (approximately 0.07 g) was suspended in tap water, ultrasonicated (ca. 15 - 30 sec.) and wet-splitted with a rotary sample divider (™Fritsch Laborette 27) by a factor of 100. The splitted aliquot was filtered on a polycarbonate filter with a pore size of 0.4 μm and dried in the oven with 40°C for 24 hours. Small pieces were cut out of each filter, mounted onto SEM-stubs and sputtered with gold/palladium. Coccoliths were counted at a magnification of 5000x, using a ™Cam-Scan 44 SEM. The species were counted on measured transects by using the taxonomy from Young et al. (2003). Absolute abundances, total coccolith concentrations and species concentrations were calculated according to Andruleit (1996):

$$\text{Coccoliths [number/ g sediment]} = (F \times C \times S) / (A \times W) \qquad (2.1)$$

F = filter area [mm^2]
C = number of counted coccoliths
S = split factor
A = investigated filter area [mm^2]
W = weight of sample [g]

2.4.2 Weight estimates of coccoliths with SYRACO

Smear slides and images

A few grains of sediment were taken with a toothpick, mixed with a drop of water on a glass microscope slide and smeared homogeneously on the slide. After drying quickly on a hot plate the sediment was embedded in 3 - 4 drops of the resin EUKITT and a cover slip. For scanning the smear slides a polarised light microscope (Leica DM6000B) with 1000x magnification and immersion oil (Leica, type N, refraction index n=1.512) was used. The microscope was equipped with a SPOT Insight black and white camera. Between 200 and 400 pictures of every sample were taken. The light of the microscope bulb was continuously controlled to avoid a decrease in light intensity over time. Therefore 200 images of two control slides were taken after the imaging of 10 smear slides. The brightness of the control images was checked with the program ImageJ and compared with the previous results. Additionally, a weekly control with the highest possible light conditions of the microscope was conducted. Both methods revealed brightness changes of less than 2 % and are therefore negligible (Appendix IV).

Weight estimates

Coccoliths are too small to weigh them directly, therefore the automated recognition software for coccolithophores SYRACO (Systeme de Reconnaissance Automatique de Coccolithes) was used to detect single coccoliths and estimate their weight (Beaufort and Dollfus, 2004). SYRACO bases on an Artificial Neural Network (ANN) and is trained to identify and classify coccoliths in cross polarised light. SYRACO makes use of the fact that calcite objects such as coccoliths are birefringent and therefore illuminated in cross polarised light. The software identifies and classifies coccoliths in the image files and returns output files containing coccoliths of a single species. In the output files, coccolith length and the grey level of every component pixel were measured. The sum of grey levels of a coccolith image was used to estimate coccolith weight. The brightness of coccolith calcite is proportional to its thickness in the range between 0 - 1.5 μm (Beaufort, 2005). After calibration to a known calcite standard (see chapter "*Calibration of weight and grey level with $CaCO_3$*") the summation of grey level of every single coccolith can be converted with an equation (2.2) into the estimated weight of the coccolith in picogram (Beaufort and Dollfus, 2004; Beaufort, 2005):

$$\text{coccolith weight} = \text{grey level} * 0.0016 \qquad (2.2)$$

Coccolith identification

Main focus of this study was the observation of coccolith weights of the Noelaerhabdaceae, i.e. *Emiliania* and *Gephyrocapsa* species (Fig. 2.3). In total 183,824 single Noelaerhabdaceae coccoliths were measured. A problem of SYRACO are invaders such as non coccoliths or wrong species in the output files. This is mostly due to missing bridges of *Gephyrocapsa* species, which may then be classified as *E. huxleyi*. *Gephyrocapsa* species may differ considerably in weight from *E. huxleyi*, and therefore all *Gephyrocapsa* and *Emiliania* species, i.e. the family Noelaerhabdaceae, were investigated together, in order to avoid mistakes due to misidentification. To minimise errors we removed non-Noelaerhabdaceae by manual checking of the output frames of all *Gephyrocapsa* species. The output frames of *E. huxleyi* were used in their original form, as they contain neglectable amounts of non Noelaerhabdaceae

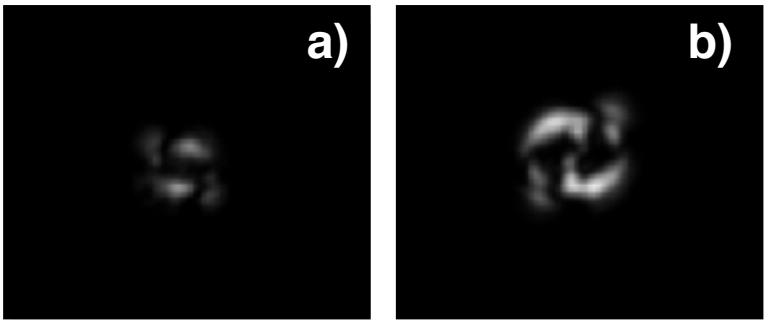

Figure 2.3. Classified coccoliths from SYRACO in cross polarised light (not to scale), a) *E. huxleyi*, b) *G. oceanica*

Calibration of weight and grey level with $CaCO_3$ (method after Beaufort, 2005)

In the range of 0 - 1.5 μm, the brightness of a calcite object in cross polarised light increases proportional to its thickness, displaying interference colours of first order grey, which change to light yellow above 1.5 μm (Beaufort, 2005). To convert the grey level into calcite mass, a transfer function is required. Therefore calibration-slides with increasing amounts of calcite powder were prepared following the method of Beaufort 2005. An amount of 16.55 mg fine ground (1 - 2 μm) $CaCO_3$ was added into 20 ml of water. Using a micropipette, 10 slides with volumes from 0.2 - 2.0 ml of the mixture were filtered on cellulose nitrate filters. After drying and embedding a part of the filter between slide and cover slip, 50 images were taken of every sample. In each of the images, the mean grey level value was measured with the image processing program ImageJ and the mean grey level per pixel was calculated. With the known size of the filter area, the image size and the number of pixel per frame, the mass of $CaCO_3$ per pixel could be calculated. A linear regression of the grey level per pixel versus the mass of $CaCO_3$ per pixel results in a linear correlation with a slope of 0.0016 (Fig. 2.4). There

is an error due to sample preparation that may result in a patchy distribution of the calcite particles on the filter, but the method is highly reproducible, resulting in an estimated uncertainty of +- 0.13 pg in this study. For a more detailed description of SYRACO see Beaufort and Dollfus (2004) and Beaufort (2005).

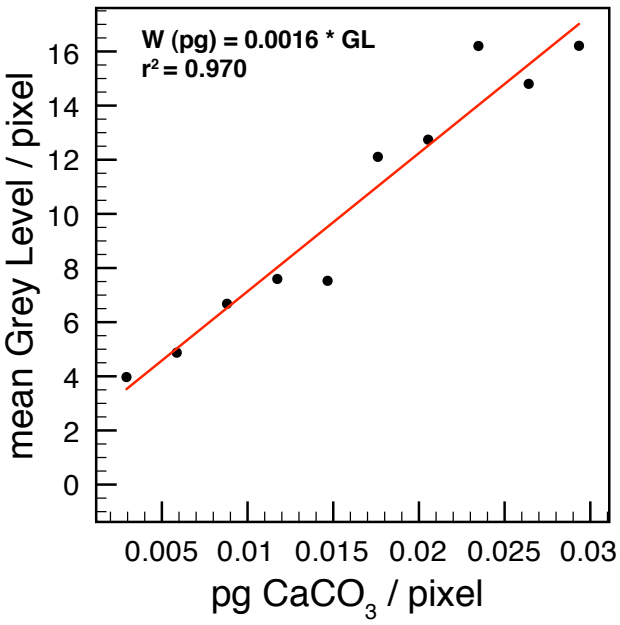

Figure 2.4. Transfer function to transform grey levels into calcite weight. The x-axis represents the calcite weight per pixel, the y-axis shows the mean of the measured Grey Level per pixel. The line presents the linear regression of the data points.

2.5 Reconstructions of coccolithophore productivity, carbonate chemistry and salinity

Coccolithophore accumulation rates have been successfully used to reconstruct coccolithophore palaeoproductivity dynamics (Lototskaya et al., 1998; Stolz and Baumann, 2010; Schwab et al., 2012). Therefore, coccolith concentrations were calculated into coccolith accumulation rates by using the bulk density and the sedimentation rate with the equation of Van Kreveld et al. (1996):

$$cocAR = ANC \times SR \times BD \qquad (2.3)$$

cocAR	total coccolith accumulation rate [number of coccoliths/cm² ka]
ANC	absolute numbers of coccoliths [number of coccoliths/g dry sediment]
SR	sedimentation rate [cm/ka]
BD	bulk density [g/cm³]

Parameters of the surface ocean carbonate system were reconstructed with the program CO2Sys (Lewis and Wallace, 1998). As input parameters salinity, temperature, total alkalinity and pCO_2 are required. Atmospheric CO_2 data are available from Vostok ice core measurements (Petit et al., 1999), Taylor Dome Ice Core data (Indermühle et al., 1999), Law Dome DE08 and DSS ice core measurements (Etheridge et al., 1998). For the calculation of the salinity $\Delta\delta^{18}O$ is required, which is calculated from $\delta^{18}O_{sw}$ by correcting with $\delta^{18}O_{ice\ volume}$ for the global sea level effect (Waelbroeck et al. 2002; Bemis et al. 1998) (eq. 2.4):

$$\Delta\delta^{18}O = \delta^{18}O_{sw} - \delta^{18}O_{ice\ volume} \quad (2.4)$$

$\delta^{18}O_{sw}$ is calculated with eq. 2.5) after Bemis et al. (1998):

$$\delta^{18}O_{sw} = (SST - 14.9) / -4.8 + \delta^{18}O\ -0.27 \quad (2.5)$$

$\delta^{18}O_{ice\ volume}$ is calculated using sea level data of Lea et al. (2003) and Jevrejeva et al. (2008):

$$\delta^{18}O_{ice\ volume} = sea\ level\ x\ 1,1\ /\ 130 \quad (2.6)$$

Total Salinity was derived from $\Delta\delta^{18}O$, using the equation of Duplessy et al. (1991):

$$SSS_{past} = SSS_{modern} + \delta\ SSS_{global} + (2 * \Delta\delta^{18}O) \quad (2.7)$$

where

$$\delta\ SSS_{global} = SSS_{modern} * (\text{sea level}) / (\text{present mean ocean water depth} - \Delta\ \delta^{18}O) \quad (2.8)$$

with

SSS_{modern} = 34,7 (Duplessy et al., 1991)

present mean ocean water depth = 3900m

Total alkalinity (TA) was calculated using the equations of Lee et al. (2006) for the North Atlantic (eq. 2.9) or (sub)tropics (eq. 2.10):

North Atlantic:

$$TA = 2305 + 53,97 * (SSS - 35) + 2,74 * (SSS - 35)^2 - 1,16 * (SST - 20) - 0,04 * (SST - 20)^2 \quad (2.9)$$

(sub) tropics:

$$TA = 2305 + 58{,}66^{*} (SSS - 35) + 2{,}32 * (SSS - 35)^2 - 1{,}41 * (SST - 20) - 0{,}04 * (SST - 20)^2 \quad (2.10)$$

The present reconstruction of the carbonate system consists of several parameters which may include different uncertainties, nonetheless the overall trends of the reconstructions seem to be reliable.

3. Changes in coccolith calcification under stable atmospheric CO_2

C. Bauke[1], K.J.S. Meier[1], H. Kinkel[2], K-H. Baumann[3]

[1]Christian-Albrechts-Universität zu Kiel, Institute of Geosciences, Ludewig-Meyn-Str. 10, 24118 Kiel, Germany

[2]University of Southern Denmark, Campusvej 55, 5230 Odense, Denmark

[3]Universität Bremen, Department of Geosciences, 28334 Bremen, Germany

Under review for Biogeosciences

3.1 Abstract

Coccolith calcification is known to respond to ocean acidification in culture experiments as well as in present and past oceans. The response, however, is different between species and strains, and for the relatively small changes observed in natural environments a uniform response of the entire coccolithophore community has not been documented so far. Moreover, previous studies basically focus on changes in coccolith weight due to increasing CO_2 and the resulting changes in the carbonate system, and only few studies focus on the influence of other environmental factors. In order to untangle changes in coccolithophore calcification due to environmental factors such as temperature and/or productivity from changes caused by increasing pCO_2 and decreasing carbonate ion concentration we here present a study on coccolith calcification from the Holocene North Atlantic Ocean. The pre-industrial Holocene with its predominantly stable atmospheric CO_2 provides the conditions for such a comprehensive analysis. For an analysis on changes in major components of Holocene coccolithophores under natural conditions, the family Noelaerhabdaceae was selected, which constitutes the main part of the assemblage in the North Atlantic.

Records of average coccolith weights from three Holocene sediment cores along a North-South transect in the North Atlantic were analysed. During the Holocene mean weight (and therefore calcification) of Noelaerhabdaceae (*E. huxleyi* and *Gephyrocapsa*) coccoliths decreases at the Azores (Geofar KF 16) from around 7 to 6 pg, but increases at the Rockall Plateau (ODP Site 980) from around 6 to 8 pg and at the Vøring Plateau (MD08-3192) from 7 to 10 pg. This amplitude of average weight variability is within the range of glacial/interglacial changes that were interpreted to be an effect of decreasing carbonate ion concentration. By comparison with SEM assemblage counts, we show that weight changes are partly due to variations in the coccolithophore assemblage, but also an effect of a change in calcification and/or morphotype variability within single species. Our results indicate that there is no single

key factor responsible for the observed changes in coccolith weight. A major increase in coccolith weight occurs during a slight decrease in carbonate ion concentration in the Late Holocene at the Rockall Plateau and Vøring Plateau. Here, more favourable productivity conditions apparently lead to an increase in coccolith weight, either due to the capability of coccolithophore species, especially *E. huxleyi*, to adapt to decreasing carbonate ion concentration, or due to a shift towards heavier calcifying morphotypes.

3.2 Introduction

With the increasing anthropogenic influence on the carbon cycle by CO_2 emissions into the atmosphere over the past 250 years, seawater carbonate chemistry changed due to the uptake of atmospheric CO_2 into the ocean (Doney et al., 2009). One result of the uptake is a decrease in seawater pH, a process known as ocean acidification (Feely et al., 2004; Raven et al., 2005; IPCC 2007). The impact of ocean acidification on calcifying organisms e.g. corals, molluscs and calcifying plankton, is one of the most actively followed marine research topics in recent years (e.g.: Gattuso et al., 1998; Riebesell et al., 2000; Fabry et al., 2008). A special focus lies on organisms that interact with the global carbon cycle. Among other calcifying plankton groups, particularly interesting are coccolithophores, which are one of the main producers of calcite in the oceans. Their small calcite scales, the coccoliths, form a large part of the carbonate flux from the surface to the deep ocean (Westbroek et al., 1993). As they can act as ballast in sinking organic aggregates, coccoliths enhance the vertical mass transfer of organic carbon and therefore have an influence on the biological carbon pump (Klaas and Archer, 2002; Ploug et al., 2008). Thus, variations in coccolith calcification affect the sinking velocity of the aggregates and consequently the organic carbon export to depth (Beaufort et al., 2007; Ziveri et al., 2007; Zondervan et al., 2001). The degree of coccolith calcification can be reflected in the exocytosis rate, in the size of coccoliths and in the weight per coccolith (Bach et al., 2012). Bach et al. (2012) showed a correlation between calcification rates and coccolith weight in *E. huxleyi*, expressed in a simultaneous change in coccolith weight and exocytosis rate and suggested the use of single coccolith weights as a potential indicator for calcification rates.

It is known that changing seawater carbonate chemistry influences coccolith calcification (Riebesell et al., 2000; Beaufort et al., 2011). Previous culture studies on different coccolithophore taxa reveal both species specific and strain specific optimum curve responses to changing carbonate chemistry (Langer et al., 2006; Krug et al., 2011). However, the most frequent response in recently conducted experiments is a decrease in coccolith calcification under future pCO_2 levels (Zondervan et al., 2002; De Bodt et al., 2010; Bach et al., 2012). A recently conducted study on sediment samples in different ocean basins presented a correla-

tion between decreasing coccolith weight and declining carbonate ion concentration during the CO_2 increase of the last deglaciation (Beaufort et al., 2011). Interestingly in the same study, the authors observed a morphotype of the extant species *E. huxleyi* in Patagonian-shelf and Chilean upwelling waters that is able to calcify heavily in waters characterised by low carbonate ion concentrations. These findings were recently supported by the findings of Smith et al. (2012), who detected a seasonal dominance of a heavily calcified *E. huxleyi* morphotype in the Bay of Biscay under elevated CO_2 conditions. As calcification in coccolithophore species and even strains shows an optimum response with respect to various carbonate chemistry parameters (Krug et al., 2011; Bach et al., 2011), these results may indicate that this morphotype has its calcification optimum at a relatively low pH. Apart from seawater carbonate chemistry, other factors also have an effect on coccolithophore calcification. Environmental factors such as temperature (Grelaud et al., 2009), coccolithophore productivity (Beaufort et al., 2007; Flores et al., 2012) and salinity (Bollmann and Herrle, 2007) are suggested to have an influence on coccolith weight and size too. However, according to Beaufort et al. (2011) these factors play a minor role for coccolith calcification when the carbonate chemistry changes notably. Thus it can be expected, that during times of rather stable atmospheric CO_2 the influence of other environmental factors will be more prominent than the carbonate chemistry of the sea water. The scale of variability in coccolith calcification in an environment with only minor changes in the carbonate system is still unknown, as well as the consequences for the mean calcite mass of a coccolithophore community. For reliable predictions of future coccolith calcification under elevated CO_2 conditions predicted for the end of the century (Raven et al., 2005; IPCC 2007) it is necessary to study them in a natural environment with relatively constant CO_2 conditions. The probably relatively minor changes in the carbonate system over the last 10,000 years allow testing the influence of environmental conditions (temperature, coccolithophore productivity) on coccolithophore calcification. In our study, we focus on the coccolithophore family Noelaerhabdaceae as it dominates the coccolithophore assemblage in the Holocene North Atlantic and represents up to 84 % of the assemblage (e.g. Andruleit, 1995; Andruleit & Baumann, 1998; Schwab et al., 2012). The variability of single Noelaerhabdaceae coccolith weight was measured in three Holocene sediment cores along a North-South transect in the North Atlantic. The diverse trends and gradients of temperature, carbonate ion concentration and coccolithophore productivity in the three studied cores allow to gain insights which of the factors are reflected in coccolith weight and therefore in their calcification.

3.3 Material and Methods

3.3.1 Material

Holocene sediment samples from three sediment cores from the North Atlantic areas were analysed. Piston core GEOFAR KF 16 was retrieved southwest of the Azores islands (37°99.90'N, 31°12.83'W) from a water depth of 3050 m (GEOFAR cruise; Richter, 1998). Additionally, a surface sediment sample from the same location (boxcore GEOFAR KG 14) was analysed. ODP Site 980 (55°12.90'N, 14°14.20'W, 2179 m water depth) is located in the eastern North Atlantic at the Rockall Plateau and was taken during ODP Leg 162 (Jansen et al., 1996). The Calypso Square Core MD08-3192 was taken at 66°55.86'N, 007°33.92'E in 1010 m water depth in the eastern Norwegian Sea (Kissel et al. 2009) (Fig. 3.1).

3.3.2 Age models

The age model for core GEOFAR KF 16 was published by Schwab et al. (2012). The Holocene part of the age model of this core is based on accelerator mass spectrometer (AMS) data of planktonic foraminifera (*Globigerina bulloides*, *Globigerinoides ruber*). In addition, an alkenone SST record and a planktonic oxygen isotope record were correlated with the NGRIP oxygen isotope record. The age model for ODP Site 980 relies on AMS measurements of the benthic foraminifera *C. wuellerstorfi* (Oppo et al., 2006). We established an age model for MD08-3192 by graphically tuning red-green colour-scan data to the nearby core MD95-2011, using the software package Analyseries (Paillard et al., 1996). Significant peaks in the colorscan data at the end of the Younger Dryas, during the Mid-Holocene and Late Holocene were used as tie points. The age model of core MD95-2011 is based on AMS ^{14}C dates of the foraminifera *Neogloboquadrina pachyderma* (Risebrobakken et al., 2003).

3.3.3 Methods

3.3.3.1 Sample preparation (Smear slides), imaging and SYRACO weight measurements

A few milligram of sediment were taken with a toothpick, mixed with a drop of water on a glass microscope slide and smeared homogeneously on the slide. After drying quickly on a hot plate the sediment was fixed with 3 - 4 drops of the resin EUKITT and a cover slip. For scanning the smear slides a polarised light microscope (Leica DM6000B) with 1000x magnification was used. The microscope was equipped with a SPOT Insight black and white camera. Between 200 and 400 pictures of every sample were taken. The light of the Microscope bulb was continuously controlled to avoid a decrease in light intensity over time. Every 10

smear slides, 200 images of two control-slides were taken and the brightness was checked with the program ImageJ and compared with the previous results. In addition a weekly control with the highest possible light conditions of the microscope was conducted. Both methods revealed brightness changes of less than 2 % and are therefore negligible.
The automated recognition software for coccolithophores SYRACO (Beaufort and Dollfus, 2004) was used to identify and measure coccoliths. The software identifies and classifies coccoliths in the image files and returns output files containing coccoliths of a single species. In the output files, coccolith length and the grey level of every component pixel were measured. The sum of grey levels of a coccolith image was used to estimate coccolith weight. The brightness of coccolith calcite depends on its thickness, which can be expressed in an equation. After calibration to a known calcite standard (method after Beaufort et al., 2005, with a calcite particle size of 1-2 μm) the summation of grey level of every single coccolith can be converted with an equation (weight = grey level * 0.0016) into the estimated weight of the coccolith in picogram. Depending on coccolith content in the sediment sample and the preparation of the smear slide, roughly between 100 and 3500 Noelaerhabdaceae coccoliths were measured in each sample, in total 89,160 single coccoliths (see supplementary information). Error bars with 95% confidence intervals are shown in Fig. 3.2 and 3.5 - 3.10 to assess the statistical significance of each data point. For a more detailed description of SYRACO see Beaufort et al. (2004 and 2005).

3.3.3.2 Carbonate chemistry, salinity, temperature and coccolithophore productivity

Alkenone Sea Surface Temperature data at the Azores is available from Schwab et al. (2012) and Repschläger et al. (in prep.). At the Rockall Plateau no published SST data were available for ODP Site 980, instead alkenone temperature data from site MD95-2015 (Marchal et al., 2002) were used as an indication. The SST data of MD95-2015 were compared to SST data from ODP Site 980 (Holtvoeth, unpublished) which confirm the general trend (with a difference of around 3° C upwards) but slightly differ after 4 ka BP. Furthermore no SST data were obtainable for core MD08-3192, alkenone temperature from nearby site MD95-2011 were used (Calvo et al., 2002).

Coccolith accumulation rate has been successfully used to trace palaeoproductivity dynamics (Lototskaya et al., 1998; Stolz and Baumann, 2010; Schwab et al., 2012). Coccolith accumulation rates are available for the Azores from Schwab et al. (2012). Rockall Plateau coccolith concentrations base on SEM counts and were calculated into coccolith accumulation rates by using the bulk density (Jansen et al., 2005) and sedimentation rate of ODP Site 980 using the equation of Van Kreveld et al. (1996). Vøring Plateau coccolith concentrations were provided by Giraudeau (MD95-2011, unpublished) and calculated into coccolith accu-

mulation rates by using the sedimentation rate and bulk density of sediment core MD95-2011 (Bassinot and Labeyrie, 1996). Carbonate ion concentrations at the coring sites were calculated with the program CO2Sys (Lewis and Wallace 1998). Salinity, temperature, total alkalinity and pCO_2 were used as input parameters. Taylor Dome Ice Core data were used for atmospheric CO_2 (Indermühle et al., 1999), total alkalinity was calculated using the equation of Lee et al. (2006). Salinity was reconstructed from $\Delta\delta^{18}O$, using the equation of Duplessy et al. (1991). For the calculation of $\Delta\delta^{18}O$, $\Delta\delta^{18}O_{seawater}$ was derived to correct the global sea level effect, and $\delta^{18}O_{ice\ volume}$ was calculated after Waelbroeck et al. (2002). At the Rockall Plateau, salinity estimates from the adjacent core NA87-22 (Duplessy et al., 2005) were used. At the Azores and the Vøring Plateau salinity was calculated from $\Delta\delta^{18}O$, which bases on the data Geofar KF 16 from Schwab et al. (2012) and Repschläger et al. (in prep.) and MD95-2011 from Risebrobakken et al. (2003).

3.4 Palaeoceanographic changes during the Holocene

Sediment core Geofar KF 16 is positioned southwest of the Azores Islands, at the northern rim of the subtropical gyre (Richter, 1998). The northeastern boundary of the subtropical gyre is defined by the Azores Current System with the corresponding Azores Front (Klein and Siedler, 1989; Rogerson et al., 2004). The Azores Front separates two different productivity regimes: low primary production in the subtropical gyre in the south, and nutrient rich conditions in the north (Schwab et al., 2012). At the coring site, enhanced productivity during the early Holocene is followed by a shift to modern oligotrophic conditions around 6 ka BP. The productivity changes due to a northward shift of the Azores Front in the late Holocene (Schwab et al., 2012). Sea surface temperature (SST) at the coring site is around 20° C in the early Holocene, decreases to 17.8° C at 8.2 ka BP and stabilises after 8 ka BP to modern conditions of 18.5 - 19.5° C.

ODP Site 980 is located in the North Atlantic at the eastern edge of Rockall Plateau, in the high accumulation area of the Feni Drift, which is deposited along the northwestern flank of the Rockall Trough (Jansen et al., 1996). The Rockall Plateau is mainly influenced by Western North Atlantic water of the North Atlantic Current and its local northerly flowing Rockall-Hatton Branch, carrying warm and salty water. Eastward of the Rockall Plateau, the warmer, more saline and less stratified Slope Current flows into the Rockall Trough (Hansen and Østerhus, 2000; Pollard et al., 2004). This current belongs to East North Atlantic Water and origins in the Bay of Biscay (Read, 2001). Between 7 and 5.4 ka BP, a reorganisation of surface circulation patterns in the north-eastern North Atlantic occurred due to decreasing summer insolation and the end of meltwater influence.

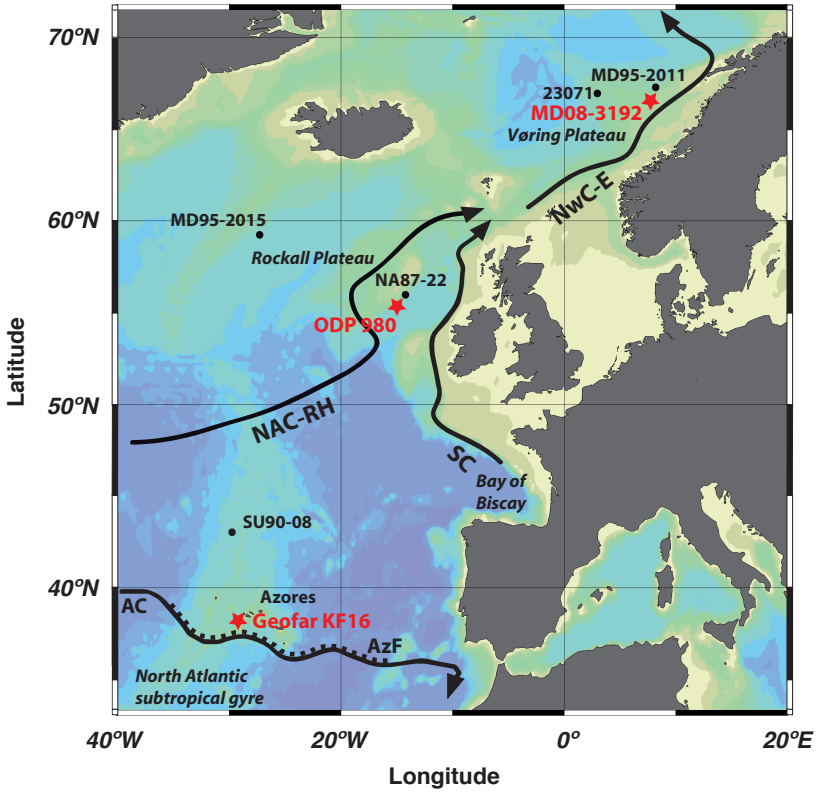

Figure 3.1. Core position and main oceanographic features: Red stars mark the location of the studied sediment cores, black dots mark the position of other locations providing data for calculations of the carbonate system or coccolith counts discussed in the text. Black arrows show major ocean surface currents: North Atlantic Current Rockall-Hatton branch (NAC-RH), Slope Current (SC), eastern branch of the Norwegian Current (NwC-E), Azores Current (AC) with the corresponding Azores Front (AzF) figured as black dashed line. The map was designed with the ODV software by R. Schlitzer (Ocean Data View software, 2010, http//odv.awi.de).

The reorganisation resulted in a weaker North Atlantic current and a stronger influence of the Slope Current after 5 - 6 ka BP (Solignac et al., 2008). These regional changes are reflected in an increase of alkenone SST at ODP Site 980 between 3.5 ka and 2 ka and a following decrease (J. Holtvoeth, unpublished data, personal communication, 2013) and explain the opposing SST trend to site MD95-2015 after 3.5 ka BP. The coccolithophore productivity at ODP Site 980 is highly fluctuating over the entire Holocene with highest rates in the early and late Holocene.

Core MD08-3192, taken from the Vøring Plateau in the eastern Norwegian Sea is influenced by the Norwegian Atlantic Current, an extension of the North Atlantic Current (Andersson et al., 2010). Most of this water inflow originates from the slope current, carrying warm and saline water into higher latitudes (Blindheim and Østerhus, 2005). During the early Holocene, the North Atlantic current increased in strength (Birks and Koç, 2002), warmest sea surface conditions during the Holocene occurred in the early Holocene until approximately 6 ka BP (Berner et al., 2011). During the middle and late Holocene SST decreased to present-day

conditions, synchronous to decreasing summer insolation (Calvo et al., 2002). Coccolithophore productivity rates at the Vøring Plateau increased during the entire Holocene and reached a maximum peak between 3 and 4 ka BP (Giraudeau et al., 2010).

3.5 Coccolithophore family Noelaerhabdaceae

In our examined sites the coccolithophore family Noelaerhabdaceae includes *Emiliania huxleyi* and *Gephyrocapsa*. Both coccolithophore taxa in our study can be classified into different morphotypes and species. The Holocene *Gephyrocapsa* complex consists of a number of different species with frequencies dependent on the location. *Gephyrocapsa muellerae* is highly abundant in the North Atlantic, in a preferred temperature range of 12 - 18°C (Giraudeau et al., 2010) and often used as a cold water indicator (Weaver and Pujol, 1988).

The small species *Gephyrocapsa ericsonii* and *Gephyrocapsa ornata* have a preference for high nutrient contents and less saline surface water conditions (Boeckel et al., 2006), but are less abundant in our examined sites, especially in the two northernmost. *Gephyrocapsa oceanica* favours high nutrient concentrations and warmer waters (Kleijne et al., 1989; Bollmann et al., 1997). It is a minor taxa in our sites due to its distribution in lower latitudes (Ziveri et al., 2004).

The cosmopolitan coccolithophore species *E. huxleyi* has an extensive genetic and morphologic diversity with diverse environmental tolerances (Medlin et al., 1996; Young, 2003) and dominates the assemblage in our examined sites. In the Holocene North Atlantic, *E. huxleyi* can be separated into different types, regarding coccolith size and weight. Coccoliths < 4 μm are highly abundant in Holocene samples while coccoliths > 4 μm, which serve as a cold water indicator, are more common in glacial sediments and decrease during the deglaciation (Termination I) (Colmenero-Hidalgo et al., 2002; Flores et al., 2010). Recently, Smith et al. (2012) reported on increasing abundance of a heavily calcified *E. huxleyi* morphotype in the North Atlantic (Bay of Biscay) during winter, when pH and $CaCO_3$ saturation are lowest. These findings support the results of Beaufort et al. (2011), who observed a highly calcified *E. huxleyi* morphotype (R-type), adapted to waters with low pH.

Regarding the mean coccolith weight of Noelaerhabdaceae, the different response of coccolithophore species and their morphotypes to environmental factors should be taken into account. A major abundance shift of one species or morphotypes can have an influence on the mean weight of Noelaerhabdaceae coccoliths.

3.6 Results

3.6.1 Holocene Noelaerhabdaceae weight trends

Mean Noelaerhabdaceae coccolith weight in sediment core Geofar KF 16 (Azores) shows a two-part trend during the Holocene (Fig. 3.2a). Characterised by significant oscillations over the entire Holocene, the mean coccolith weight record fluctuates around 7 pg in the early and middle Holocene until 6 ka BP, and subsequently decreases to values of less than 6 pg in the late Holocene. The same change can be observed in the relative abundance of Noelaerhabdaceae coccolith weight classes (Fig. 3.2a). During the early and middle Holocene a relatively broad weight range reaches high relative abundance. In the late Holocene the range narrows and a distinct maximum between 2 and 3 pg is observed.

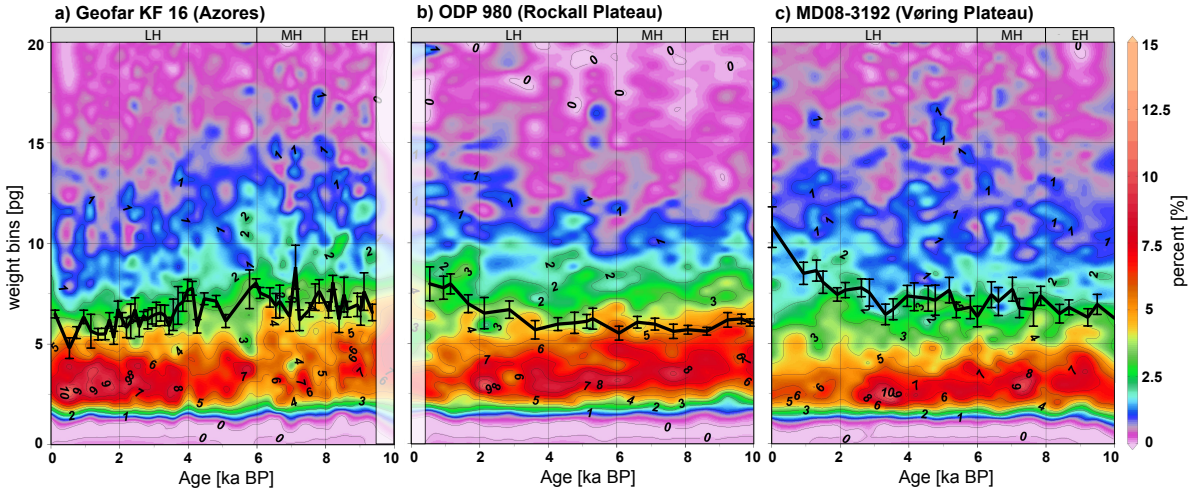

Figure 3.2. a) Azores, core Geofar KF 16 b) Rockall Plateau, ODP Site 980 c) Vøring Plateau, core MD08-3192. Abundance of Noelaerhabdaceae coccoliths within weight bins (colours) and Noelaerhabdaceae mean coccolith weight (black line). Abundance of Noelaerhabdaceae coccoliths within weight bins (colours) and Noelaerhabdaceae mean coccolith weight (black line). For the weight bins the data set has been divided into classes (bins) with a step of 0.4 pg, each bin contains the frequency of data points in % of each sample from the Holocene data set. Error bars indicate 95 % confidence intervals of the mean weight. Abbreviations: early Holocene (EH), middle Holocene (MH), late Holocene (LH)

At the Rockall Plateau mean Noelaerhabdaceae coccolith weight fluctuates around 6 pg during the early, middle and the beginning of the late Holocene, followed by an increase to 8 pg after 3.5 ka BP in the late Holocene (Fig. 3.2b). The relative abundance of Noelaerhabdaceae coccolith weight classes shows a maximum of light coccoliths between 3 and 5 pg in the early and middle Holocene (Fig. 3.2b). In the late Holocene the maximum of light coccoliths is less pronounced and narrows to 2.5 and 4 pg, paralleled by an increase in the abundance of heavier weight classes. From 1 ka BP onwards, the maximum of light coccoliths further flattens, and simultaneously the weight classes extend to heavier values.

At the Vøring Plateau mean Noelaerhabdaceae coccolith weight increases with a range of fluctuations during the entire Holocene from around 7 to more than 10 pg. The weight increase is rather slight until 3 ka BP and notably stronger afterwards (Fig. 3.2c). The relative abundance of Noelaerhabdaceae weight classes shows a narrowing maximum of light coccoliths from 2 - 4.5 pg in the early Holocene to 2 - 3.5 pg in the late Holocene (Fig. 3.2c). From 1.2 ka BP onwards, the maximum of light coccoliths is less pronounced. The relative abundance of heavier weight classes is high over the entire Holocene.

3.6.2 Carbonate ion concentration

Despite the rather stable atmospheric CO_2 conditions, the reconstructed carbonate ion concentration in all studied cores decreases over the Holocene (Fig. 3.3). At the Azores carbonate ion concentration is highest. It decreases by about 30 μmol/kg SW over the Holocene, from more than 260 to 230 μmol/kg SW. At the Rockall Plateau the carbonate ion concentration is strikingly lower and decreases by 15 μmol/kg SW from 200 to 185 μmol/kg SW. The carbonate ion concentration at the Vøring Plateau represents the highest decrease of 45 μmol/kg SW from 225 to 180 μmol/kg SW from the early to the late Holocene, with a slight increase from 2.5 ka BP onwards to 190 μmol/kg SW.

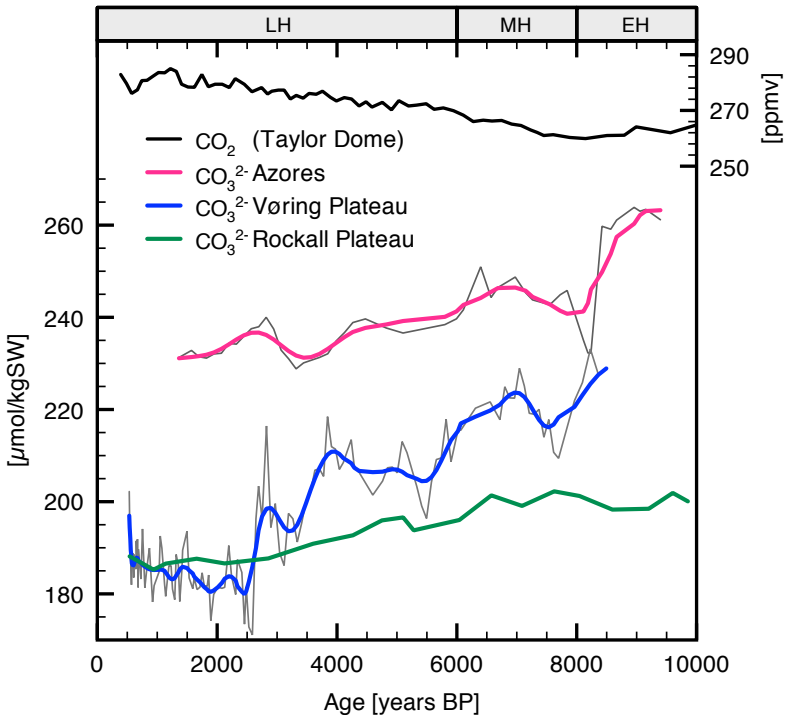

Figure 3.3. Holocene carbon dioxide concentration (black line), Holocene carbonate ion concentration of Azores (red line), Rockall Plateau (green line) and Vøring Plateau (blue line). Bold lines are smoothed (by factor 4), grey thin lines original data.

3.7 Discussion

3.7.1 Comparison with previous studies

The decreasing coccolith weight trend of Noelaerhabdaceae observed at the Azores is in line with results from previous studies (Beaufort et al., 2011), see Fig. 3.4. In one site of the data set of Beaufort et al. (2011, supplementary information), the authors studied a core near the Azores (SU90-08) covering the Holocene, and recognised a decrease in coccolith mass of the family Noelaerhabdaceae of around 0.5 pg. Our own data from the Azores (Geofar KF 16) confirms this trend and shows a decrease of about 1 pg for Noelaerhabdaceae coccolith mean weight (Fig. 3.4). It should be mentioned that the Noelaerhabdaceae weight of Beaufort et al. (2011) is represented by five data points and is therefore able to reflect the mean trend but not the short-term changes of coccolith weight. Therefore the mean coccolith weights of sediment core SU90-08 and Geofar KF 16 are not exactly the same but reflect the same decreasing trend.

The studied sites from Rockall and Vøring Plateau show some different developments of Noelaerhabdaceae coccolith weights (Fig. 3.4). At both sites the weight and the general variation in weight is rather comparable in the early and middle Holocene and increases during the late Holocene.

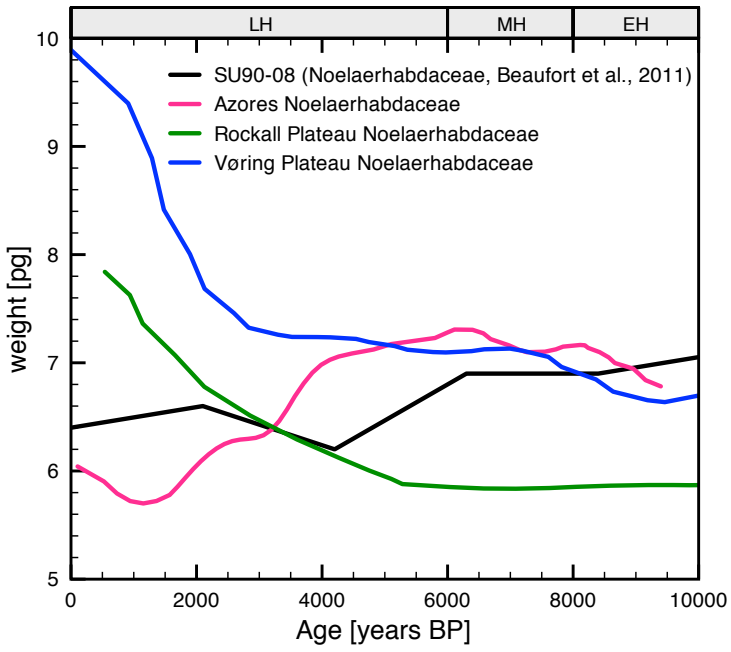

Figure 3.4. Noelaerhabdaceae coccolith weights from core SU90-08 (black line, Beaufort et al., 2011) in comparison to Noelaerhabdaceae smoothed mean weight record from the Azores (red line), Rockall Plateau (green line) and Vøring Plateau (blue line).

According to Beaufort et al. (2011) decreasing carbonate ion concentration affects coccolithophore calcification and explains the decrease in coccolith weight in their results. In our studied sites and in the results of Beaufort et al. (2011) the carbonate ion concentration decreases between 10 and 45 μmol/kg sea water (Fig. 3.3). Despite the decreasing trend in all sites, the coccolith weight reacts differently and leads to the assumption that other factors have a stronger influence on mean Noelaerhabdaceae coccolith weight in our studied sites of the Holocene North Atlantic. Possible factors that have an influence on the mean weight are other environmental factors as the sea surface temperature and coccolithophore productivity or changes within the assemblage of Noelaerhabdaceae.

3.7.2 The influence of assemblage shifts within the Noelaerhabdaceae

Weight changes of Noelaerhabdaceae due to assemblage shifts could be either result from changes in the relative abundance of differently calcifying species and/or their individual morphotypes within Noelaerhabdaceae or changes in the weight of species and/or their morphotypes within the Noelaerhabdaceae.

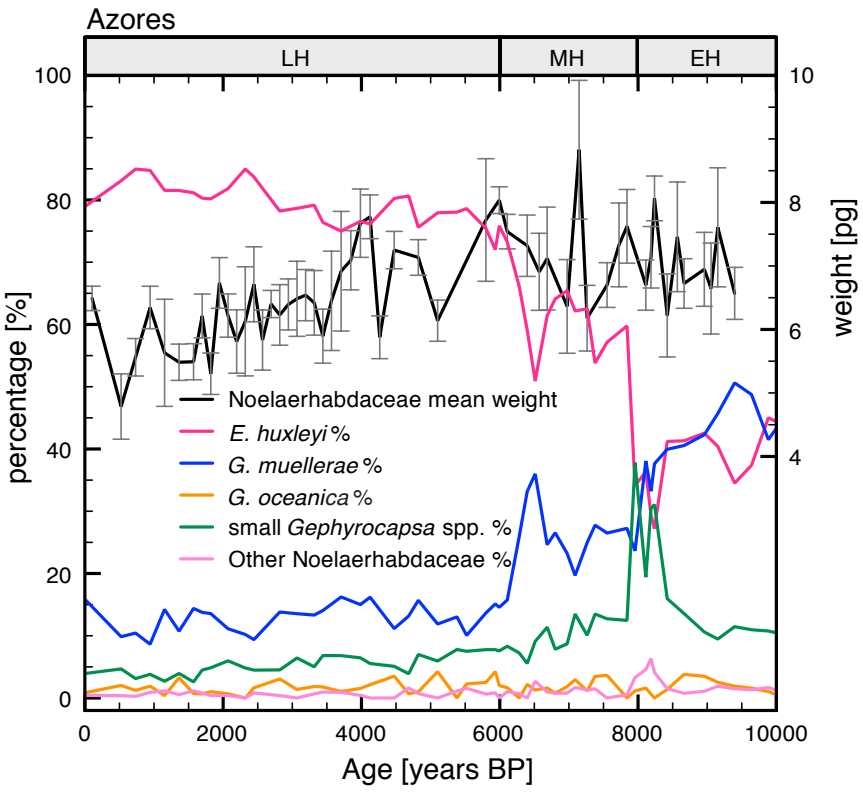

Figure 3.5. Relative abundance of Noelaerhabdaceae species at the Azores from sediment core Geofar KF 16 over the Holocene (Schwab et al., 2012): *E. huxleyi* (red line), *G. muellerae* (blue line), *G. oceanica* (orange line), small *Gephyrocapsa* (green line) and other Noelaerhabdaceae (light red line) in comparison to the Noelaerhabdaceae mean coccolith weight (black line).

To improve the identification and quantification of our results we compared the Noelaerhabdaceae mean weights to given SEM counts of our studied cores or nearby cores. According to SEM counts of Schwab et al. (2012), the family Noelaerhabdaceae at the Azores consists of coccoliths from the species *E. huxleyi*, *G. muellerae*, few *G. ericsonii* and *G. ornata* and a very small number of *G. oceanica* (Fig. 3.5). At the Rockall Plateau, Noelaerhabdaceae counts from ODP Site 980 include primarily *E. huxleyi* and *G. muellerae* and few *G. oceanica* and *G. ericsonii* (Fig. 3.6). At the Vøring Plateau, no SEM counts for the entire Holocene were available for MD08-3192, therefore a comparison to coccolith counts of Andruleit (1995) from a nearby core (GIK 23071) is used as an indication (Fig. 3.7). At this site the family Noelaerhabdaceae consist of *E. huxleyi* and *G. muellerae,* other coccolithophores of this family are not mentioned, and in all probability their number is less than 1 % and not worth considering.

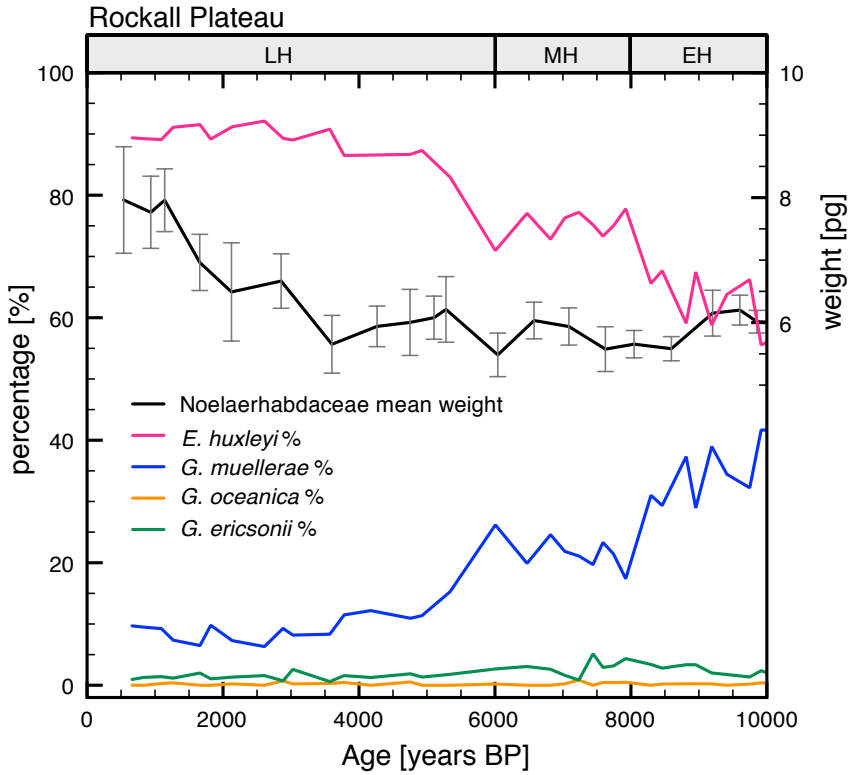

Figure 3.6. Relative abundance of Noelaerhabdaceae species at Rockall Plateau from ODP Site 980 over the Holocene (Baumann, previously unpublished): *E. huxleyi* (red line), *G. muellerae* (blue line), *G. oceanica* (orange line), *G. ericsonii* (green line) in comparison to the Noelaerhabdaceae mean coccolith weight (black line).

In all three SEM counts of Noelaerhabdaceae, the assemblage considerably changes over the Holocene. In general, related to the main part of the assemblage, the relative abundance of the lighter species *E. huxleyi* increases by around 30 %, while the heavier *G. muellerae* decreases in the same order. Interestingly, these changes are not reflected in the mean

weight of the studied sites, not even the strong decrease of *G. muellerae* at the Vøring Plateau between 7 - 8 ka BP. Therefore it seems very likely that the species itself change their weight. This could be caused by changes in the weight of *E. huxleyi* or *G. muellerae* or both. Another explanation is a shift in the abundance of e.g. a heavily calcifying morphotype of *E. huxleyi* or *G. muellerae* or both.

As verification we examined the uppermost sediment sample of the Vøring Plateau, with the highest Noelaerhabdaceae mean weight of all cores, under the SEM. Almost all coccoliths belong to the species *E. huxleyi* and a considerable number is heavily calcified. At this site it is very likely that the heavily calcifying morphotype increases the mean Noelaerhabdaceae weight. Our results do not support the high number of *G. muellerae* reported in light-microscopic counts of Giraudeau et al. (2010), which show an increase of *G. muellerae* at the Vøring Plateau after 2 ka BP. In our SEM counts we detected a very low abundance of around 1 % *G. muellerae*.

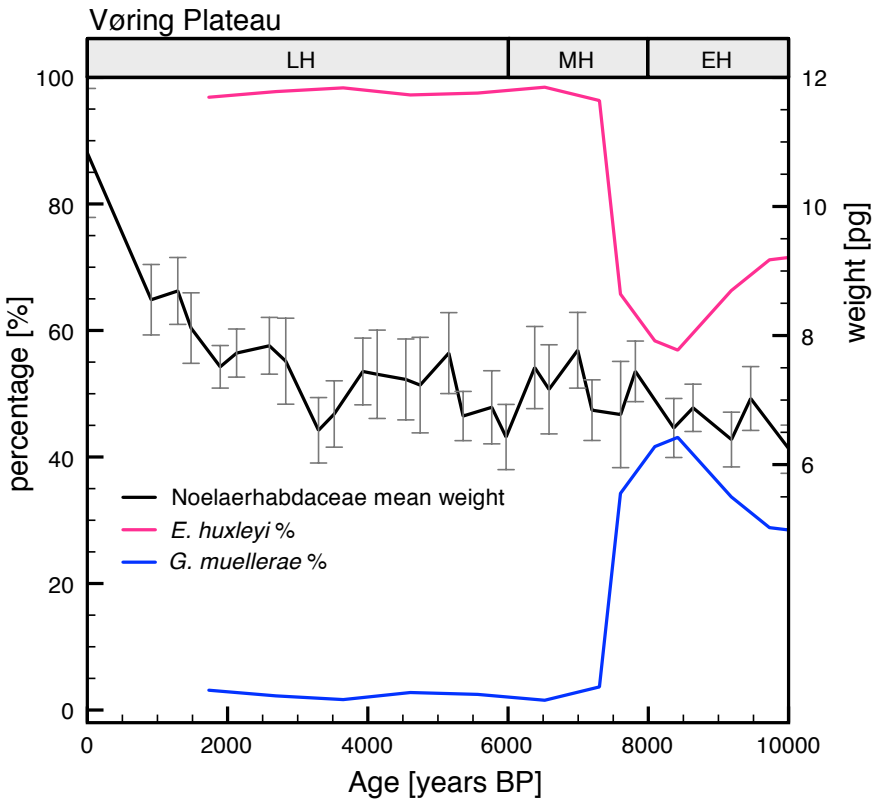

Figure 3.7. Relative abundance of Noelaerhabdaceae species at Vøring Plateau from sediment core GIK 23071 over the Holocene (Andruleit, 1995): *E. huxleyi* (red line), *G. muellerae* (blue line), in comparison to the Noelaerhabdaceae mean coccolith weight (black line).

3.7.3 Environmental factors

Based on our results, the individual response of single coccolithophore species and most likely their morphotypes is primarily responsible for changes in Noelaerhabdaceae weight. Hence, it is necessary to consider the factors that have an influence on species weight or changes in the abundance of their morphotypes. It is known that different coccolithophore species or morphotypes are adapted to individual environmental conditions (Bollmann, 1997; Henderiks et al., 2012). This might explain the implication of Beaufort et al. (2011) that coccolith weight in the North Atlantic and South Indian Ocean differ from tropical settings, especially during the Last Glacial Maximum, where coccolith weight displays a broad weight range but is not in line with the trend of coccolith weight from the tropical stack. Therefore it is not as simple as proposed to consider one main factor as for instance the carbonate system as the key factor for changes in coccolith weight especially not for the North Atlantic that deviates from the tropical or global trend. In the data set of Beaufort et al. (2011), temperature, productivity and salinity are also correlated to coccolith calcification, but weaker than CO_2 or carbonate ion concentration. This already indicates that other factors than carbonate ion concentration are important for coccolith calcification.

3.7.3.1 Temperature

Sea surface temperature (SST) in our examined sites decreases over the entire Holocene less than 2 ºC (Fig. 3.8c, 3.9c, 3.10c) and is unlikely to have a strong influence on Noelaerhabdaceae mean coccolith weight. Previous studies present indications for an influence on changes in SST on the abundance of coccolithophore species and their morphotypes or on their calcification, but with considerably higher temperature gradients (Hagino et al., 2005; Henderiks et al., 2012; Bach et al., 2012). In addition, studies on correlations between temperature and calcification rates of *E. huxleyi* showed different results (Langer et al., 2007; de Bodt et al., 2010). Beaufort et al. (2007) concluded that there is no global relationship between SST and the degree of *E. huxleyi* calcification. The influence of SST on *E. huxleyi* morphotypes is even more confusing due to its high morphologic and genetic diversity with different temperature tolerances (Young et al., 2003; Hagino et al., 2011) and it seems that the same morphotype can react differently. A heavily calcified *E. huxleyi* morphotype is reported to increase in abundance when SST is higher (Beaufort and Heussner, 2001; Grelaud et al., 2009), contrary to the results of Smith et al. (2012) where this morphotype increases during winter in the Bay of Biscay. For *Gephyrocapsa* only little is known about changes in calcification rate induced by temperature variability. The distribution of *Gephyrocapsa* species in the Holocene correlates with environmental gradients (Bollmann, 1997), e.g. *G. muellerae* occurs in moderate productive cool surface waters (Winter et al., 1994) and is thus of-

ten used as a cold water indicator (Weaver and Pujol, 1988), whereas *G. oceanica* has an affinity to warm and nutrient rich waters (Kleijne et al., 1989; Giraudeau et al., 1993; Ziveri and Thunell, 2000) and is therefore reported to be abundant in temperate and tropical waters as well as equatorial and upwelling areas (Okada and McIntyre, 1979; Bollmann, 1997; Ziveri et al., 2004). Due to the different response of species and morphotypes to SST, it is difficult to make a general statement for the coccolithophore family Noelaerhabdaceae to changes in SST. The slight decrease in temperature in our sites over the Holocene is unlikely to influence the calcification of coccoliths. More likely is the influence of morphotypes, which are adapted to different temperature conditions and therefore occur in different abundances in our sites. As detected by Flores et al. (2010), the abundance of the *E. huxleyi* cold water type with coccoliths > 4 μm increases with higher latitudes and reaches a number of 1 - 5 % at Vøring Plateau. The opposite trend is found in the distribution of *G. oceanica* of our studied sites. The abundance record decreases from less than 5 % at the Azores to around 1 % at Rockall Plateau and is probably absent at Vøring Plateau. Both coccolithophores could have an influence on the mean Noelaerhabdaceae coccolith weight, but the low number of 1 - 5 % might be too small to have significant effects on the average weight.

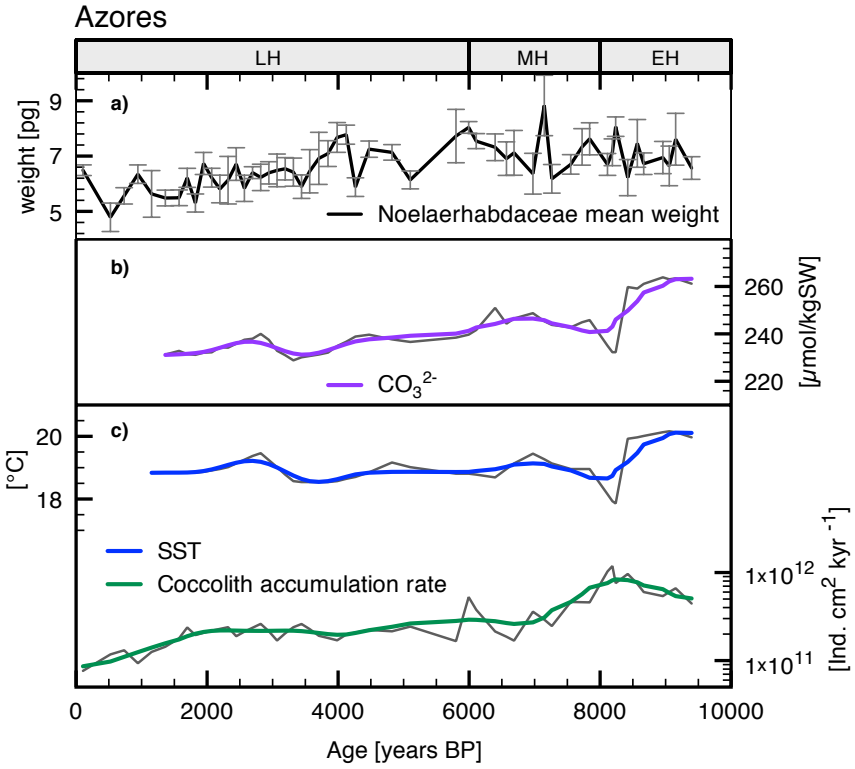

Figure 3.8. Azores, core Geofar KF 16. (a) Noelaerhabdaceae mean coccolith weight (black line), error bars indicate 95 % confidence intervals of the mean weight. (b) carbonate ion concentration (purple line) (c) SST (blue line) and coccolith accumulation rate (green line). Bold lines are smoothed (by factor 4), grey thin lines original data.

3.7.3.2 Salinity

Reconstructed palaeo-salinity changes at our coring sites are rather small at the Rockall Plateau (35.9 - 36.2), slightly higher at the Azores (35.9 - 37.4) and show high fluctuations at the Vøring Plateau (34.6 - 38.2). Despite some studies showed correlations between size and weight of *E. huxleyi* in plankton and culture studies with salinity (Bollmann et al., 2009; Fielding et al., 2009), there is no correlation between Noelaerhabdaceae mean coccolith weight in our results and the reconstructed paleo-salinity (not shown).

3.7.3.3 Carbonate ion concentration

Different factors of the oceans' carbonate system are discussed to affect calcification rates of coccolithophores such as pH levels, carbonate ion or bicarbonate ion concentration (Bach et al.,2012). During the Holocene the atmospheric CO_2 concentration changes only minor and consequently the reconstructed carbonate system of the ocean as well. As we focused more on environmental factors than on the oceans' carbonate system, we decided to show the parameter of the carbonate system which attracted attention in the study of Beaufort et al. (2011) to compare our results with the large data set of the authors.

Despite the minor changes of the atmospheric CO_2 concentration in the Holocene, the CO_2 solubility in the ocean changes geographically and seasonally due to the dependence on parameters such as SST, salinity, alkalinity and productivity (Feely et al., 2001; Zeebe & Wolf-Gladrow, 2001). Nowadays, the average CO_2 uptake of the ocean is smaller in the Azores region than at the Rockall or Vøring Plateau (see map of Takahashi et al., 2002). Our reconstructions of the Holocene carbonate system show a regional difference, e.g. the decrease of the carbonate ion concentration over the Holocene at the Vøring Plateau is stronger than at the Azores or the Rockall Plateau. The influence of the biological productivity, which strengthens the biological pump and leads to a decrease in CO_2 of the surface ocean and thus to changes in the oceans' carbonate system (Sigman and Haug, 2003), are not included in the reconstructions. It is therefore likely that the rising productivity at the Vøring Plateau enhanced the biological pump and led to a decrease in CO_2 of the surface ocean. Possibly, the decrease in carbonate ion concentration is weaker than in our reconstructions. Vice versa, the decreasing productivity at the Azores could lead to a stronger decrease in carbonate ion concentration than reconstructed. But despite these uncertainties, the Holocene changes in the oceans' carbonate system still are much smaller in comparison to e.g. the glacial/interglacial variability of the carbonate system.

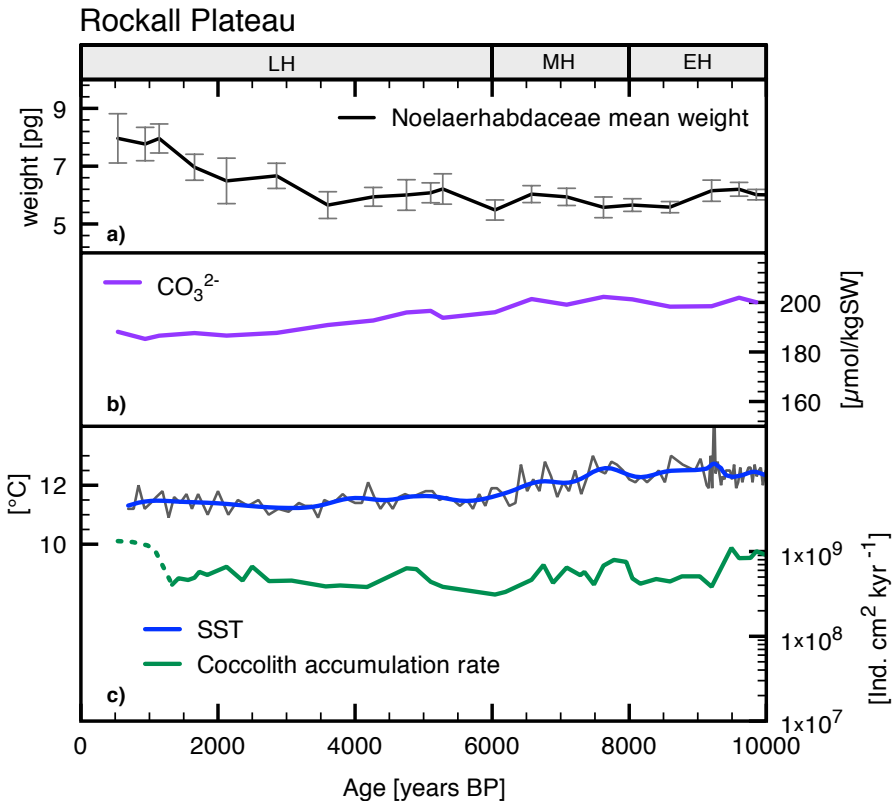

Figure 3.9. Rockall Plateau, ODP Site 980. (a) Noelaerhabdaceae mean coccolith weight (black line). Error bars indicate 95 % confidence intervals of the mean weight. (b) carbonate ion concentration (purple line) (c) SST (blue line) and coccolith accumulation rate (green line). Bold lines are smoothed (by factor 4), grey thin lines original data.

Further, it should be mentioned that our selected sites are located in areas affected by seasonal variations as productivity, temperature and pCO_2 (Nilsen, 2003; Rios et al., 2005; Tans and Conway, 2005; Schwab et al., 2012). If coccolithophore weight would be e.g. influenced by a seasonal change in the oceans carbonate chemistry (Smith et al., 2012), which differs from the overall mean trend over the Holocene, these seasonal signals in coccolithophore weight would not be comparable to the Holocene mean trend of the carbonate system. But as we consider multi-annual Noelaerhabdaceae mean weights, seasonal responses are averaged and can be neglected.

The decrease in carbonate ion concentration of around 30 μmol/kg in our results at the Azores might have an influence on coccolith mean weight (Fig. 3.8b), but here the carbonate ion concentration presents the highest values of all three studied sites, therefore the basic conditions for coccolithophores should be more favourable than at the Rockall or Vøring Plateau. At the Rockall Plateau the decreasing trend in carbonate ion concentration of around 10 μmol/kg sea water over the Holocene might be too small to have a large influence on coccolith calcification (Fig. 3.9b). At the Vøring Plateau, the decrease in Holocene carbonate

ion concentration is relatively prominent (about 45 μmol, Fig. 3.10b) and is even stronger than at the Azores, but the increasing coccolith weight does not confirm the negative influence of carbonate ion concentration on the weight. Therefore there is no uniform trend of Noelaerhabdaceae weight at the three different sites, and a general influence of decreasing carbonate ion concentration in the range of 10 - 45 μmol on coccolith weight cannot be observed. This indicates that the carbonate system can not be the main factor having influence on the mean coccolith weight in the Holocene North Atlantic.

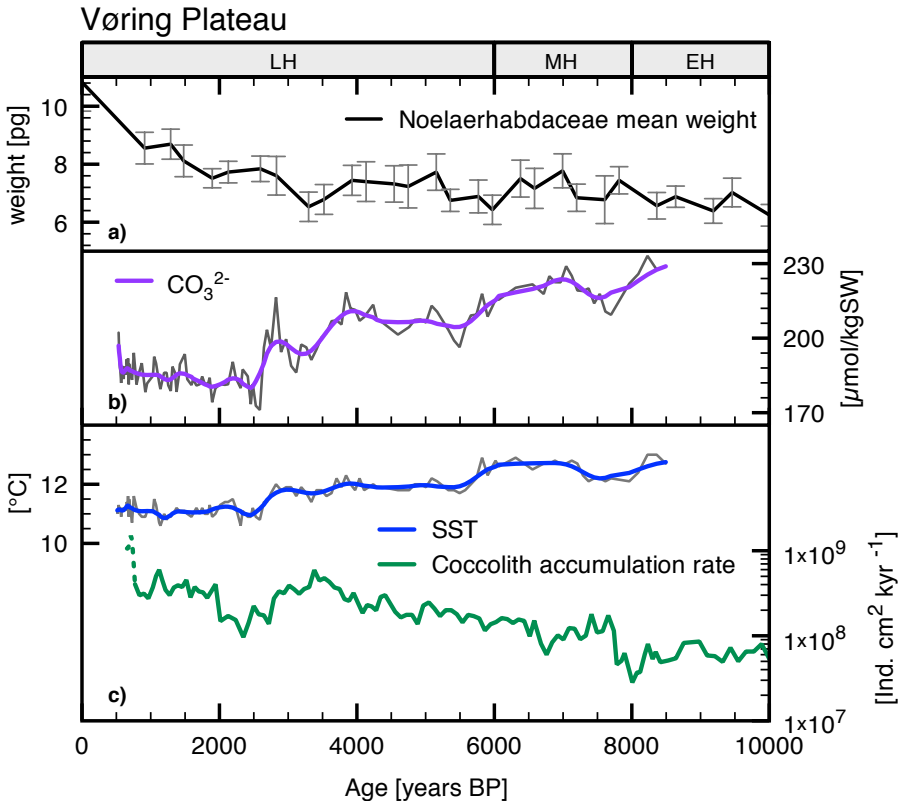

Figure 3.10. Vøring Plateau, core MD08-3192. (a) Noelaerhabdaceae mean coccolith weight (black line). Error bars indicate 95 % confidence intervals of the mean weight. (b) carbonate ion concentration (purple line) (c) SST (blue line) and coccolith accumulation rate (green line). Bold lines are smoothed (by factor 4), grey thin lines original data.

3.7.3.4 Coccolithophore productivity

The coccolithophore productivity decreases northwards in our examined sites in absolute numbers. The relative trends are different between the sites over the Holocene (Fig. 3.8c, 3.9c, 3.10c). At the Azores, coccolithophore productivity is highest. Beginning with the onset of a northward shift of the Azores Front and the following oligotrophic conditions after 6 ka BP (Schwab et al., 2012) the mean coccolith weight starts decreasing, suggesting a possible coupling between coccolithophore productivity and coccolith calcification. Similarly, at the

Vøring Plateau, where absolute coccolithophore productivity is 2 to 3 orders of magnitude lower, an overall increase in coccolithophore productivity over the entire Holocene is paralleled by the increasing Noelaerhabdaceae coccolith weight. At the Rockall Plateau the coccolithophore productivity is on the same level as at the Vøring Plateau, but relatively stable. Here, only a slight increase in coccolith productivity is observed during the Late Holocene when coccolith weight is increasing markedly, and coccolithophore productivity peaks are only slightly reflected in the mean weight. This may be caused by undersampling of the mean coccolith weight data, which could exclude short-term fluctuations from being detected.

Previous studies have shown the influence of enhanced coccolithophore productivity on coccolith weight. The weight of *E. huxleyi* increased during blooms and accordingly during times with high coccolithophore production (Beaufort et al., 2007). In addition Engel et al. (2005) observed an increase in *E. huxleyi* coccolith weight by 25 to 50 % during blooms in mesocosm experiments after adding nutrients. Therefore, productivity plays a major role in coccolith calcification and is probably rather prominent in our study because CO_2 variability is low during the Holocene. Considering the environmental factors in all three sites, the main trends of temperature and carbonate ion concentration are rather similar. The only distinct difference of the studied environmental factors is the coccolithophore productivity, which seems to have an influence on mean Noelaerhabdaceae coccolith weight. As the absolute values in coccolithophore productivity are extremely different between the Azores and the two northern sites, it is unlikely that productivity as such is responsible for the observed changes in coccolith weight. A more likely explanation would be abundance changes of morphotypes within the Noelaerhabdaceae, which might be also caused by different nutrient or primary productivity regimes. This may be due to oceanographic features such as the position of the subtropical gyre and the frontal system at the Azores (Schwab et al., 2012), or the reorganisation of the surface circulation patterns in the northern North Atlantic with a stronger influence of the Slope Current after 5 - 6 ka BP (Solignac et al., 2008; J. Holtvoeth, unpublished data, personal communication, 2013) at the Rockall Plateau and Vøring Plateau.

At the Vøring Plateau, Noelaerhabdaceae mean coccolith weight is controlled by two species, *E. huxleyi* and *G. muellerae.* Interestingly, and as previously mentioned, the shift in the relative abundance of the species between 7 - 8 ka BP is not reflected in the mean weight as well as the increase in weight in the late Holocene. This leads to the assumption of changing calcification of the species or abundance shifts of morphotypes. Compared to *G. muellerae*, *E. huxleyi* is a tough competitor and able to adapt more quickly to environmental changes (Okada and Wells, 1997; Schwab et al., 2012). A recently conducted long term study of Lohbeck et al. (2012) revealed an adaptation of *E. huxleyi* calcification to enhanced CO_2 due to genotypic selection as well as mutations within the population. The presence of a morphotype of *E. huxleyi* that is able to calcify heavily in waters characterised by low carbonate ion

concentrations supports this theory (Beaufort et al., 2011; Smith et al., 2012). Interestingly, in the findings of Beaufort et al. (2011) this morphotype appears in relatively cold coastal or frontal upwelling waters with enhanced productivity. Additionally, laboratory experiments of Müller et al., (2012) documented an increase of *E. huxleyi* coccolith volume with elevated pCO_2 and nutrient replete conditions. Therefore it is not unlikely to assume that the heavily calcifying *E. huxleyi* morphotype in the uppermost sediment sample at the Vøring Plateau is an adaptation to decreasing carbonate ion concentration, while other environmental factors as productivity are rather favourable. In contrast to the Azores where the decreasing productivity conditions are likely to impair the conditions for coccolithophore species or morphotypes. This might be a tentative indication that on a global scale, a part of the coccolith weight decrease expected to occur due to ocean acidification in the future could be compensated by increased productivity of heavily calcifying coccolithophore species or morphotypes (e.g. growing in frontal or upwelling regimes) adapted to calcify heavily at low carbonate ion concentrations. The same is true especially for other heavily calcifying coccolithophore species, such as *Coccolithus pelagicus* or *Calcidiscus leptoporus* that may reach considerable abundance in parts of the oceans and have a large influence on the total coccolithophore carbonate production. Therefore, future studies should focus on assemblage and morphotype response to carbonate system changes.

3.8 Conclusion

The dominant coccolithophore family Noelaerhabdaceae shows a strong variability in mean coccolith weight during rather stable CO_2 conditions of the pre-industrial Holocene in the North Atlantic. The recently debated negative influence of decreasing carbonate ion concentration on coccolithophore calcification could not be detected for a small decrease of 10 to 45 μmol/kgSW. Our results show weight changes during the Holocene of the same amplitude than previously reported for the CO_2 increase of the last glacial to interglacial change, but with opposing trends in different regions. Variability in Holocene Noelaerhabdaceae coccolith weight in a natural system of the North Atlantic is hardly driven by the carbonate system as a main reason. We show that in the absence of strong CO_2 variability in the North Atlantic coccolithophore productivity has a substantial influence on Noelaerhabdaceae coccolith weight. Favourable environmental conditions such as high coccolithophore productivity lead to increasing weight, either due to increasing calcification or an abundance shift to heavily calcifying morphotypes, even during times of decreasing carbonate ion concentration of 45 μmol/kgSW over the Holocene. Differences in nutrient or productivity settings between the sites are likely influencing the response of Noelaerhabdaceae coccolith weight. The high natural variability of coccolith weight during the Holocene raises the question, whether future

changes in the carbonate system of the oceans will have a positive or negative effect on coccolithophore calcification.

Acknowledgements

The authors thank J. Giraudeau for providing the coccolithophore data of site MD95-2011, J. Holtvoeth for discussions on temperature and surface currents of the Rockall Plateau and K. Kleiven for providing the sediment samples of site MD08-3192. B. Dannielou and IFREMER are acknowledged for providing samples of core GEOFAR KF 16. T. Oberließen and S. Häuser are thanked for their help in preparing the samples and images. Funds for this study were provided by the Federal Ministry of Education and Research (Bundesministerium für Bildung und Forschung; 03F0608A) in the framework of the Biological Impacts of Ocean Acidification (BIOACID) project.

4. Increasing coccolith calcification during CO_2 rise of the penultimate deglaciation (Termination II)

C. Bauke[1], K.J.S. Meier[1], H. Kinkel[2,]

[1]Christian-Albrechts-Universität zu Kiel, Institute of Geosciences, Ludewig-Meyn-Str. 10, 24118 Kiel, Germany

[2]University of Southern Denmark, Campusvej 55, 5230 Odense, Denmark

Submitted to Marine Micropaleontology

4.1 Abstract

Glacial to interglacial environmental changes have a strong impact on coccolithophore assemblage composition. At the same time, glacial terminations are characterised by an increase in atmospheric CO_2 concentration. In order to determine how these two processes influence the calcite production of coccolithophores, we compared coccolith weight estimates obtained with the automated coccolith recognition system SYRACO with SEM assemblage counts covering the penultimate glacial termination (T II) from two sediment cores in the North Atlantic Ocean. At the temperate Rockall Plateau (ODP Site 980), mean coccolith weight shows positive excursions around the Heinrich event 11. This is paralleled by a shift within the coccolith assemblage caused by the changes of the oceanic frontal system during Termination II. In the tropical Florida Strait, far from influences of frontal zones, mean Noelaerhabdaceae coccolith weight doubles during Termination II. This is only partly due to an assemblage shift towards larger and heavier calcifying morphotypes, but mainly an effect of increasing coccolithophore calcification. This increase is exactly mirroring the rise in atmospheric CO_2, contradicting previous findings from Termination I. Reconstructions of DIC, alkalinity and calcite supersaturation at the Florida Strait during Termination II exceed all previous settings for which coccolith weight estimates are available, and therefore are the most likely cause for the coccolithophore calcification increase during atmospheric CO_2 rise. Our results illustrate that even during rising atmospheric CO_2 the conditions of the seawater carbonate system can be favourable for coccolithophore calcification. The total $CaCO_3$ production of a coccolithophore assemblage under increasing CO_2 therefore depends on regional seawater carbonate system characteristics and the local assemblage composition.

Highlights: Noelaerhabdaceae mean coccolith weight increases during rising atmospheric CO_2 concentration; Increasing weight is induced by different factors at each site; Noelaerhabdaceae mean weight is strongly dependent on regional seawater conditions and assem-

blage composition; Assemblage shifts and changes in calcification strongly influence mean weight.

Keywords: Coccolith weight, Termination II, North Atlantic

4.2 Introduction

Coccolithophores, a group of marine calcifying phytoplankton, are known as major oceanic $CaCO_3$ producers (Milliman, 1993). They play a significant role in the marine carbonate system by combining photosynthetic carbon fixation and calcification (Rost and Riebesell 2004). Their small calcite scales, the coccoliths, export inorganic carbon to the deep sea and further act as ballast for the transport of organic carbon (Klaas and Archer, 2002; Rost and Riebesell, 2004). Changes in the calcite production of coccoliths therefore influence the carbon export and hence affect the global carbon cycle (Zondervan, 2007).

The uptake of atmospheric CO_2 by the oceans leads to increasing surface seawater CO_2 and HCO_3^- and decreasing pH and CO_3^{2-} concentrations, a process termed ocean acidification (Feely et al., 2004; Raven et al., 2005). Laboratory experiments on coccolithophore calcification under elevated CO_2 led to varying response patterns even within the same species or strain and revealed the sensitivity of these organisms to changing ocean chemistry (Riebesell et al., 2000; Iglesias-Rodriguez et al., 2008; Langer et al., 2009). Furthermore, experiments with a combination of rising CO_2 and parameters as e.g. different temperature and nutrient supply influenced coccolithophore calcification, and even improved or impaired the effects of changing carbonate chemistry (e.g. De Bodt et al., 2010; Matthiessen et al., 2012; Fiorini et al., 2011). Still, the most common observation is a reduction of coccolithophore calcification in response to increasing CO_2 (Zondervan et al., 2002; De Bodt et al., 2010; Bach et al., 2012).

In natural assemblages it has been shown that varying seawater carbonate chemistry and environmental factors can influence both coccolithophore calcification and shifts within the coccolithophore assemblage. *E. huxleyi* developed morphotypes with different weight or size adapted to diverse environmental conditions (Beaufort et al., 2011; Flores et al., 2010). In natural assemblages changing seawater conditions can lead to a dominance shift to better adapted morphotypes of the same species (e.g. Triantaphyllou et al., 2010; Flores et al., 2010; Beaufort et al., 2011). Therefore, besides varying calcification of a species, abundance shifts of morphotypes can lead to changes in the total amount of calcite produced from one species. Similarly, abundance changes of species within an assemblage can change the total amount of $CaCO_3$ produced by coccolithophores (Beaufort et al., 2007). The heterogenous composition of a coccolithophore assemblage within their natural environment is difficult to

establish in the laboratory. As a result most laboratory studies on coccolithophores focus on monospecific cultures with single strains of one species (Ridgwell et al., 2009). For investigating the responses of an entire coccolithophore assemblages and possible changes in its total calcite accumulation under increasing CO_2, field and sediment studies provide supporting information from the natural habitat of coccolithophores to which they are evolutionary adapted (Smith et al., 2012). Past events in Earth`s history with a notable increase in CO_2 help to clarify the possible response of coccolithophore assemblages in the future. During glacial to interglacial changes (deglaciations), atmospheric CO_2 increased and surface-ocean pH as well as the saturation state declined. Because of the relatively large timescale in the order of 10.000 years, deglaciations are a slow and moderate acidification event. Therefore they cannot be seen as an analogue to the current fast increase in CO_2 (Zeebe et al., 2012), but still they offer the opportunity for studies under increasing CO_2 in a natural system. A lately conducted study on the calcification of the dominant coccolithophore family Noelaerhabdaceae has shown a decrease in coccolith weight (and therefore calcification) during the CO_2 increase of the last deglaciation (Termination I, 19 - 10 ka BP, Beaufort et al., 2011). In the tropics, Noelaerhabdaceae mean coccolith weight decreased with declining CO_3^{2-}, which is attributed to a shift within the assemblage composition as well as a decrease in calcification (Beaufort et al., 2011). Aside from these results, few palaeo-studies on coccolith weight of natural assemblages under rising CO_2 are available. A recent study from the temperate zone of the North Atlantic examined the variability of coccolithophore calcification from different assemblages during the rather stable CO_2 conditions of the Holocene (Bauke et al., 2013). Even without strong changes in the carbonate system, Noelaerhabdaceae mean coccolith weight displays a strong intrinsic variability with opposing trends at different locations. Major causes for the weight changes are shifts within the assemblage as i.e. in the abundance of species and heavily calcifying morphotypes. The varying response of the different assemblages within the North Atlantic reveals the large influence of the assemblage compositions which varies regionally in the Holocene (Bauke et al., 2013). This raises the question if the response of an assemblage-driven coccolithophore community from the temperate zone of the North Atlantic is comparable to results of a community from the tropics, especially under rising CO_2 conditions. To examine the individual response of coccolithophore communities from different areas, we focused on two sediment cores from the tropical (Florida Strait, SO 164-17-2) and from the temperate zone (Rockall Plateau, ODP Site 980) of the North Atlantic during Termination II (135 - 125 ka BP). Termination II is the most rapid and abrupt termination of the late Quaternary (Jouzel et al., 2007), and the accompanying CO_2 increase is used here to test he response of coccolithophore calcification under a natural CO_2 rise. As coccolith weight is an indicator for coccolithophore calcification (Bach et al., 2012), we measured coccolith weights from the dominant coccolithophore family Noelaerhabdaceae

(*E. huxleyi* and *Gephyrocapsa* spp.) to investigate if weight changes are induced by assemblage shifts or by factors which can have an influence on the calcification (carbonate system, temperature and coccolithophore productivity) (Raven et al., 2012). The selected sediment cores are also influenced by different environmental conditions during Termination II. ODP Site 980 from the temperate zone is under influence of oceanic front migrations, which has a strong effect on the coccolithophore community and productivity (Stolz and Baumann, 2010). SO164-17-2 from the tropics is far from the influence of oceanic frontal zones with comparably stable environmental conditions (Bahr et al., 2011). We show that the mean coccolith weight of the Noelaerhabdaceae increases during rising atmospheric CO_2 in Termination II in the North Atlantic due to different mechanisms at each location.

4.3 Material and Methods

4.3.1 Material and age models

ODP Site 980 (55°12.90'N, 14°14.20'W; 2179 m water depth) was retrieved during ODP Leg 162 (Jansen et al., 1996) from the Rockall Plateau in the eastern North Atlantic (Fig. 4.1). The age model for ODP Site 980 has been published by Oppo et al. (2006) and relies on epifaunal benthic foraminiferal $\delta^{18}O$ measurements.

Piston core SO164-17-2 (24°04.99′N; 80°53.00′W; 954 m water depth) is located at the southern Florida Strait (Fig. 4.1) and was recovered during R/V Sonne Cruise SO164 (Nürnberg et al., 2003). The age model for SO164-17-2 was established by Bahr et al. (2011), using calcareous nannofossils and *Globorotalia menardii* biozones, a detailed age model of MIS 5 bases on the tuning of the benthic isotope record of *Cibicidoides wuellerstorfi* to the global benthic isotope stack LR04 (Bahr et al., 2011).

4.3.2 Sample preparation (Smear slides, SEM samples) and weight measurements

Smear slide samples were prepared from sediment samples and scanned with a polarised light microscope (Leica DM6000B, 1000x magnification). By using a SPOT Insight black and white camera, connected to the microscope, 200 - 400 pictures of every sample were randomly taken. The pictures were analysed with the automated recognition software for coccolithophores SYRACO (Beaufort and Dollfus, 2004), which identifies and measures coccoliths. SYRACO creates output files containing coccoliths from the same morphogroups, which were automatically measured in size and weight. The weighing relies on measuring the brightness (grey level) of calcite particles which is proportional to their thickness in cross-polarised light. The total brightness of a coccolith can be converted into the weight with an equation (weight = grey level * 0.0016) after calibration to a known calcite standard (method

after Beaufort et al., 2005, with a calcite particle size of 1-2 μm). In total 21302 single coccoliths at site SO164-17-2 and 32158 coccoliths at ODP Site 980 were measured. To control the light of the Microscope bulb and avoid a decrease in light intensity over time, 200 images of two control slides were taken after the imaging of 10 smear slides. The brightness of the control images was checked with the program ImageJ and compared with the previous results. Additionally, a weekly control with the highest possible light conditions of the microscope was conducted. Both methods revealed brightness changes of less than 2 % and are therefore negligible.

From site SO164-17-2, 28 samples for scanning electron microscope (SEM) were prepared with a combined dilution/filtration technique after Andruleit (1996). A small amount of dry bulk sediment (approximately 0.07 g) was suspended in tap water, ultrasonicated and wet-splitted with a rotary sampler divider (™Fritsch Laborette 27) by a factor of 100. The splitted aliquot was filtered on a polycarbonate filter with a pore size of 0.4 μm and dried in the oven with 40°C for 24 hours. Small pieces were cut out of each filter, mounted onto SEM-stubs and sputtered with gold/palladium. Coccoliths were counted using a CamScan 44 SEM, at a magnification of 5000x.

4.3.3 Temperature, coccolithophore productivity and carbonate chemistry

Sea surface temperature (SST) estimations from ODP Site 980 are available from Oppo et al. (2006) and base on planktonic foraminiferal assemblage changes, at site SO164-17-2, SST from Bahr et al. (2011) base on Mg/Ca reconstructions from the planktic foraminifera *G. ruber*.

Coccolithophore accumulation rates can be used to reconstruct coccolithophore palaeoproductivity (Lototskaya et al., 1998; Stolz and Baumann, 2010; Schwab et al., 2012). Coccolith concentrations from Site SO164-17-2 base on our SEM counts and were calculated into coccolith accumulation rates by using the bulk density (Nürnberg et al., 2003) and sedimentation rate of Site SO164-17-2 using the equation of Van Kreveld et al. (1996). At ODP Site 980 coccolith accumulation rates are available from Stolz and Baumann (2010).

Parameters of the surface ocean carbonate system were reconstructed with the program CO2Sys (Lewis and Wallace, 1998). As input parameters temperature (see above), pCO_2, total alkalinity and salinity are required. Atmospheric CO_2 data are available from Vostok ice core measurements (Petit et al., 1999), total alkalinity was calculated from salinity after Lee et al. (2006), using the equation for the North Atlantic for ODP Site 980 and the equation for the (sub)tropics for site SO164-17-2. Salinity was derived from $\Delta\delta^{18}O$, using the equation of Duplessy et al. (1991). For the calculation of $\Delta\delta^{18}O$, $\Delta\delta^{18}O_{seawater}$ was calculated after Bemis et al. (1998) and corrected with the global sea level effect ($\delta^{18}O_{ice\ volume}$) after Waelbroeck et

al. (2002) using sea level data of Lea et al. (2003). At ODP Site 980 and SO164-17-2, $\delta^{18}O$ is available from Oppo et al. (2006) and Bahr et al. (2011).

4.4 Oceanographic settings

ODP Site 980 is located at the eastern edge of the Rockall Plateau in the North Atlantic (Fig. 4.1), within the high accumulation area of the Feni Drift (Jansen et al., 1996). The Rockall Plateau is influenced from a branch of the North Atlantic Current (NAC), the Rockall-Hatton branch (NAC-RH), a northward flowing extension of the Gulf Stream, which carries warm and salty water. ODP Site 980 is located southwards of the Arctic front which separates the temperate Atlantic from the cold Arctic waters (Swift, 1986). The transition from the penultimate glacial (Marine Isotope Stage 6) to the penultimate interglacial (Marine Isotope Stage 5), called Termination II, in the North

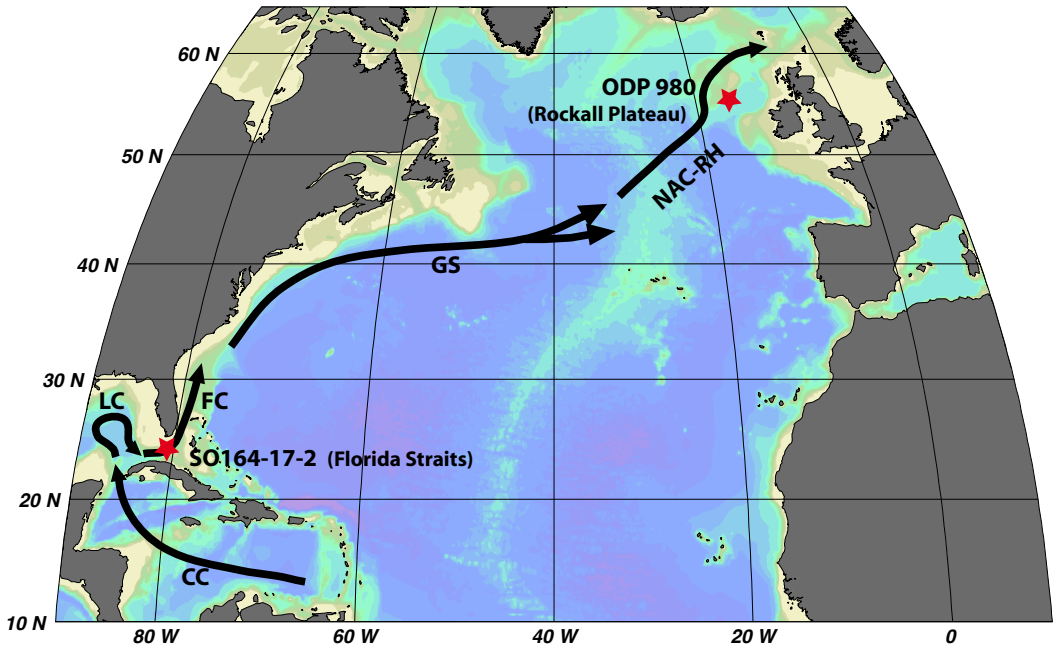

Figure 4.1. Locations of ODP Site 980 and SO164-17-2 and the main oceanographic features of the North Atlantic. Red stars mark the location of the studied sites, black arrows show major ocean surface currents: Caribbean Current (CC), Loop Current (LC), Florida Current (FC), Gulf Stream (GS), North Atlantic Current Rockall-Hatton branch (NAC-RH). The map was designed with the ODV software by R. Schlitzer (Ocean Data View software, 2010, http//odv.awi.de).

Atlantic is characterised by changes in the palaeoceanographic conditions. The activity of the NAC was reduced during Termination II and the position of the Arctic front migrated southwards, close to ODP Site 980. This resulted in harsh seawater conditions with sea ice and low sea surface temperature. Lowest SST combined with reduced coccolith numbers and diversity denote the Heinrich event 11 (H11). During MIS 5 the increasing influence of the NAC resulted in ameliorate climate conditions, with enhanced growth conditions for cocco-

lithophores characterised by increasing coccolith numbers and taxa (Stolz and Baumann, 2010).

Site SO164-17-2 is located in the region of the Florida Strait (Fig. 4.1), which is highly saturated with respect to calcite (Schwarz and Rendle-Bühring 2005). Through the Florida Strait, the strong Florida Current flows between Florida and the Bahamas into the North Atlantic (Richardson et al., 1969). It is considered as the major source of the Gulf Stream and carries warm tropical waters to higher latitudes (Wennekens, 1959). The Florida Current derives from water masses of the Caribbean Current, which flows from the Caribbean Sea into the Gulf of Mexico, known as the Loop Current (Gordon, 1967; Molinari and Morrison, 1988). According to the results of Lynch-Stieglitz et al. (1999) who reported about a reduced Gulf Stream in the Florida Strait during the last glacial maximum, Bahr et al. (2011) found similar indications for a lowered Florida Current strength (and thus reduced Gulf stream) during MIS 6, and an enhancement during early MIS 5.5. The resulting stronger transport of warm water masses explain the strong SST increase at the end of Termination II (Bahr et al., 2011).

4.5 Results and Discussion

4.5.1 Noelaerhabdaceae weight trends

At ODP Site 980 mean Noelaerhabdaceae coccolith weight increases towards the end of MIS 6, between 133 ka BP and 130 ka BP, from 5 pg to 6 pg (Fig. 4.2a). Three significant weight peaks mark the early MIS 5.5, one at its onset, two during H11, where the weight reaches around 7 - 7.7 pg. During the late Termination II, from around 128 ka BP onwards, the weight decreases and reaches approximately 5 pg after the end of Termination II. Mean Noelaerhabdaceae coccolith weight at SO164-17-2 is rather constant between 5 and 6 pg during MIS 6, from 143 until 135 ka BP (Fig. 4.3a). With the beginning of Termination II at 135 ka BP the weight strongly increases to around 12 pg until the end of Termination II at 125 ka BP. From 125 ka BP until 112 ka BP, during MIS 5.5, the weight remains on a high level and shows a slight increase characterised by fluctuations between 9.5 and 13 pg.

At both studied sites Noelaerhabdaceae mean weight strongly increases during the CO_2 rise and the concomitant changes in the oceans carbonate system of Termination II, which implicates that coccolithophore calcification was not negatively affected. This is in contrast to the recently reported decrease of Noelaerhabdaceae mean coccolith weight during the CO_2 increase of Termination I of Beaufort et al. (2011) (Fig. 4.4).

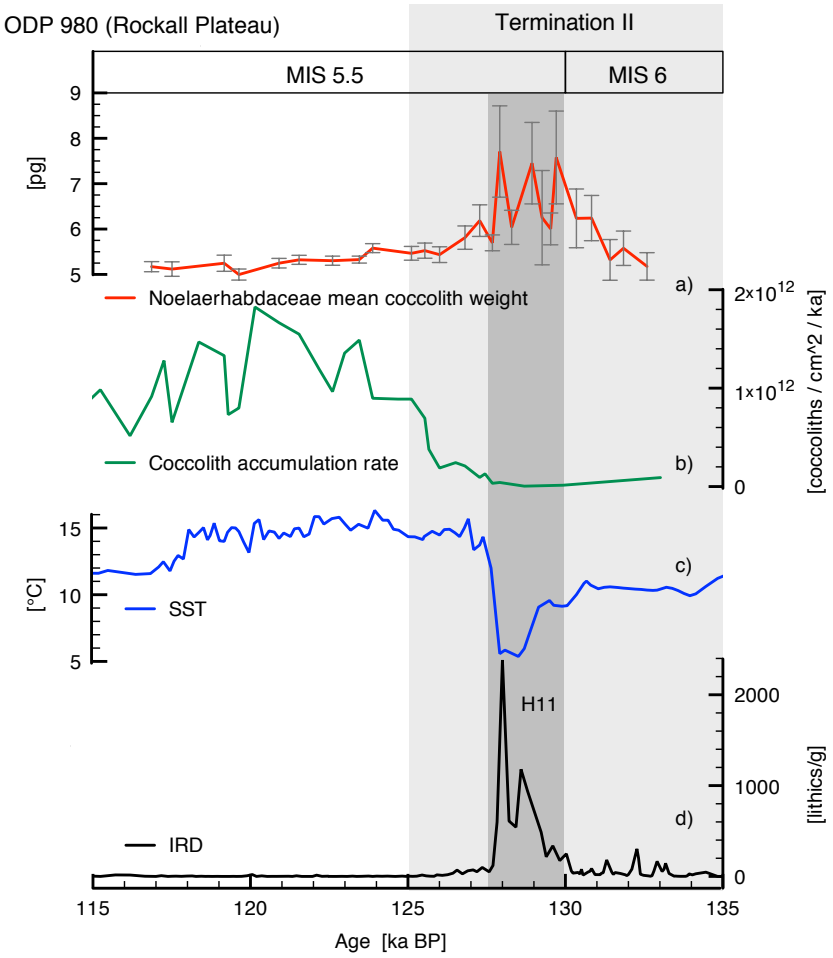

Figure 4.2. ODP Site 980, a) Noelaerhabdaceae mean coccolith weight. Error bars denote 95 % confidence intervals of the mean weight; b) Coccolith accumulation rate; c) SST; d) IRD abundances. Abbreviations: Marine Isotope Stage 6 (MIS 6), Marine Isotope Stage 5.5 (MIS 5.5), Heinrich event 11 (H11). Vertical light grey bar marks Termination II, vertical dark grey bar marks H11 (deduced from IRD abundances), MIS 5.5 and MIS 6 are labelled on top.

Obviously, Noelaerhabdaceae mean coccolith weight during Termination II at our sites is driven by other factors than during Termination I in the study of Beaufort et al. (2011). To assess the factors influencing coccolith weight of the Noelaerhabdaceae assemblage it is important to disentangle the underlying mechanisms of the weight changes.

The mean weight of the Noelaerhabdaceae assemblage changes when the composition of the assemblage changes, e.g. by a relative increase of a stronger calcifying species or morphotype, or if calcification is enhanced due to a physiological response to environmental processes. Both processes may be interlinked, as the environmental factors influencing calcification may also lead to an assemblage shift.

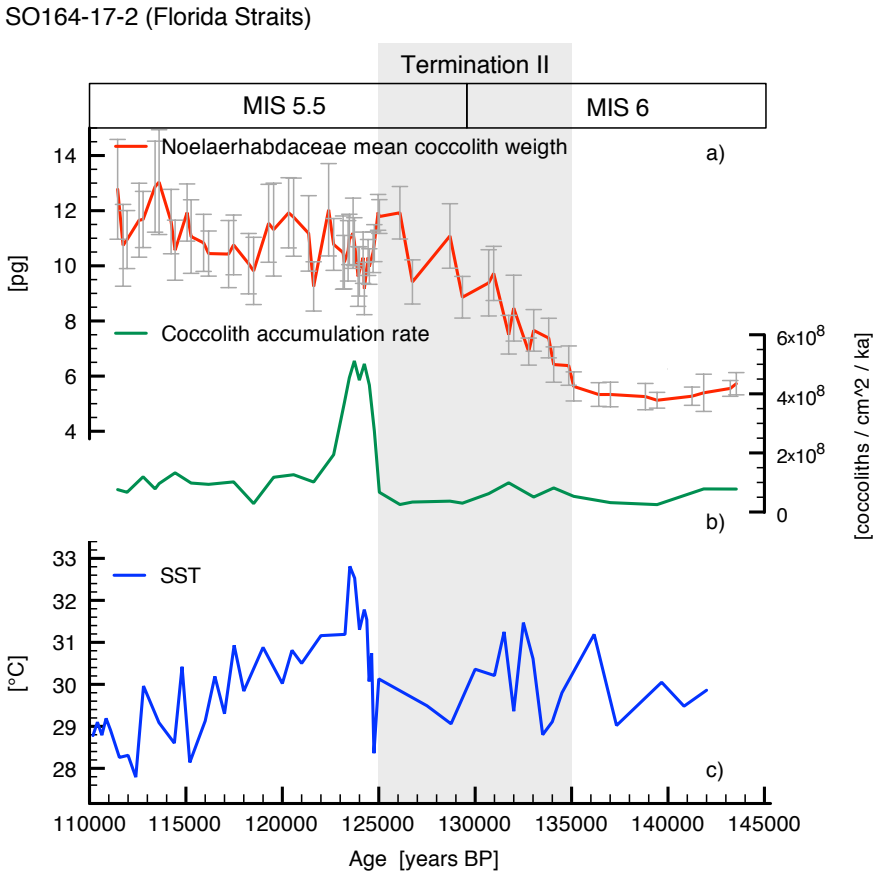

Figure 4.3. Site SO164-17-2, a) Noelaerhabdaceae mean coccolith weight. Error bars denote 95 % confidence intervals of the mean weight; b) Coccolith accumulation rate; c) SST. Abbreviations: Marine Isotope Stage 6 (MIS 6), Marine Isotope Stage 5.5 (MIS 5.5). Vertical light grey bar marks Termination II, MIS 5.5 and MIS 6 are labelled on top.

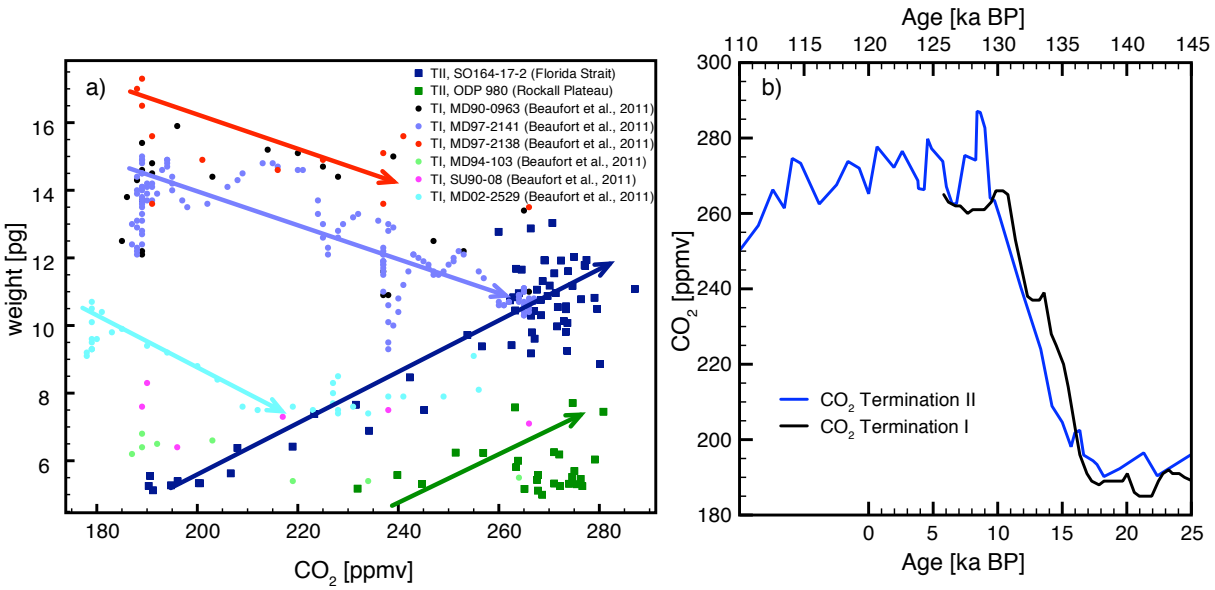

Figure 4.4. a) Relationship between Noelaerhabdaceae coccolith mean weight and atmospheric CO_2 from Termination I (Beaufort et al., 2011) and Termination II. Arrows indicate the rough trends of selected sediment cores. b) Atmospheric CO_2 concentration during Termination I (black line) and Termination II (blue line).

4.5.2 ODP Site 980 - Rockall Plateau

4.5.2.1 SEM counts and assemblage variations deduced from length and weight measurements

At the Rockall Plateau, SEM coccolith counts of Stolz and Baumann (2010) from ODP Site 980 were compared to our results (Fig. 4.5). The coccolithophore family Noelaerhabdaceae at this site consists of *E. huxleyi*, *G. muellerae* and *G. ericsonii*. In the first part of the record *G. muellerae* dominates the Noelaerhabdaceae assemblage with a relative abundance up to 85 %. Between 130 - 124 ka BP, the composition of the assemblage changes and *E. huxleyi* reaches a relative abundance up to 70 %, whereas *G. muellerae* decreases to around 30 %. The abundance of *G. ericsonii* is rather low and never exceeds 10 % of the assemblage.

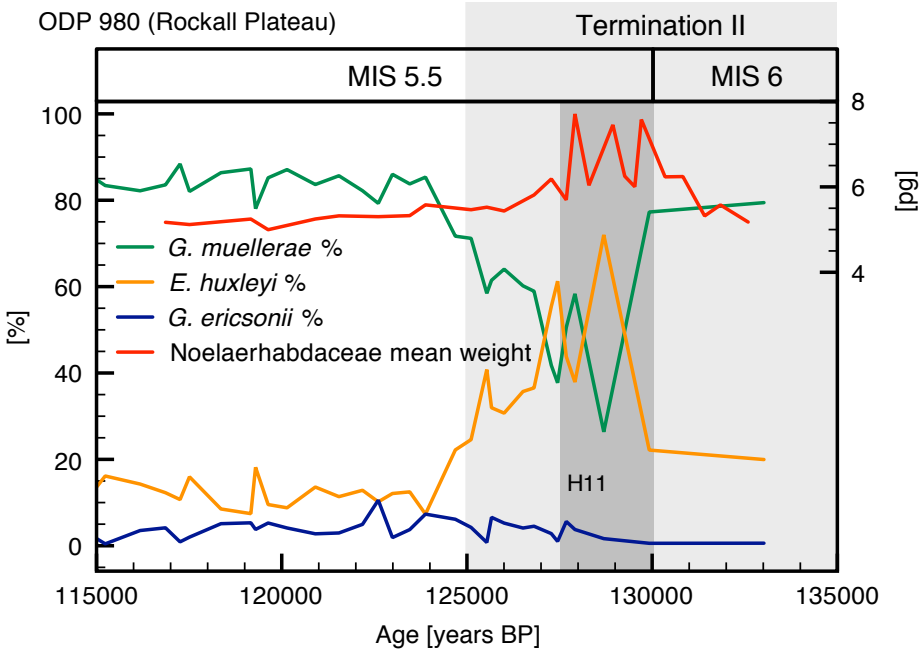

Figure 4.5. ODP Site 980, Relative abundance of coccolith species from the coccolithophore family Noelaerhabdaceae: *Gephyrocapsa muellerae* (green line), *Gephyrocapsa ericsonii* (blue line), *E. huxleyi* (yellow line), compared to Noelaerhabdaceae mean coccolith weight (red line).

The shift in the composition of the assemblage largely coincides with the increase in weight from 131 - 127 ka BP, but the increase in weight starts and ends earlier than the assemblage change and indicates an additional influence of other factors. Interestingly, Noelaerhabdaceae weight is highest when the abundance of *G. muellerae*, the heaviest species in the assemblage, is lowest (Fig. 4.5). Therefore, the observed assemblage shift can not account for the positive weight excursions. For a more detailed analysis of the measurements from SYRACO, coccoliths length and weight from H11 and surrounding H11 were separated (Fig. 4.6a, b). During H11 the average weight and the abundance of coccoliths larger 3 μm

increases (Fig. 4.6a, b), whereas the abundance of the length class 2.3 - 3 μm decreases (Fig. 4.6a). The Noelaerhabdaceae mean coccolith weight increase is therefore mainly caused by the increase in abundance and calcification of coccoliths > 3 μm which can be both *E. huxleyi* and *G. muellerae*. Due to the increasing abundance of *E. huxleyi* coccoliths, however, it is more likely that this species is mainly contributing to the weight shift. This will be discussed in the following chapters.

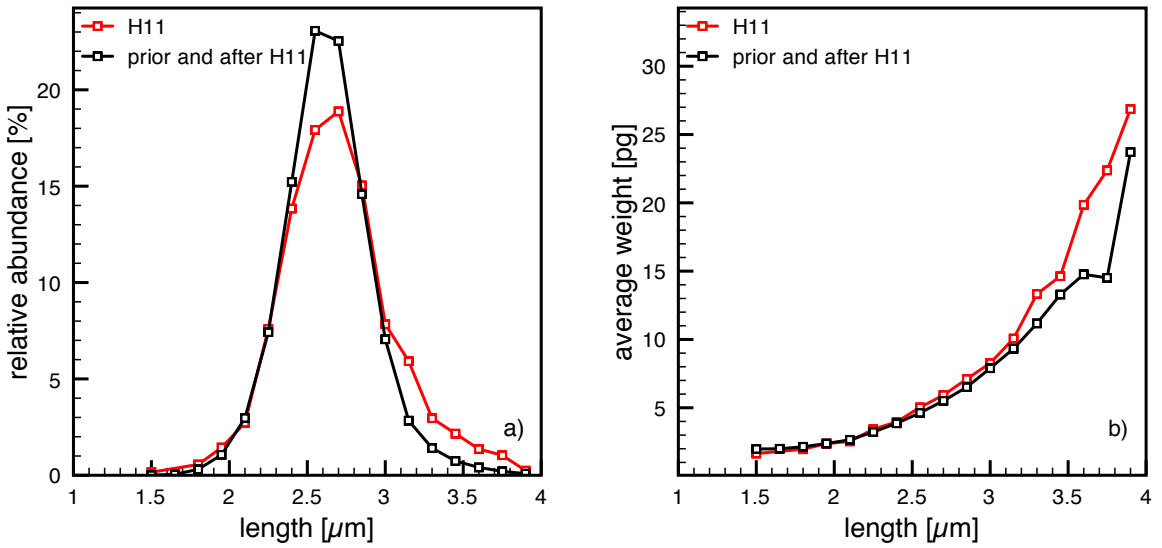

Figure 4.6. ODP Site 980, a) Relative abundance of coccolith length classes prior to and after H11 (black line) and during H11 (red line); b) Noelaerhabdaceae mean coccolith weight of different coccolith length classes prior to and after H11 (black line) and during H11 (red line).

4.5.2.2 SST and coccolithophore productivity

Coccolithophores are known to be sensitive to changing seawater conditions (as nutrient or primary productivity, SST and the oceans carbonate system) and respond with changes within the assemblage and their calcification (e.g.: Riebesell et al., 2000; Beaufort et al., 2007; Grelaud et al., 2009). During Termination II, coccolithophore accumulation rates are rather low and suggest diminished coccolithophore productivity due to unfavourable seawater conditions. Close to the end of Termination II at 126 ka BP, the accumulation rates and therefore the coccolithophore productivity start to increase (Stolz and Baumann, 2010) (Fig. 4.2b). During Termination II, neither the assemblage shift nor the increase in coccolithophore productivity is reflected in the mean coccolith weight, other factors seem to have a stronger influence.

Both, the assemblage shift and the increase in weight, coincide in main parts with the decrease in sea surface temperature induced by the Heinrich event 11 (H11), which is marked by enhanced ice-rafted detritus (IRD) layers (Oppo et al., 2006) between approximately 130 -

127,5 ka BP (Fig. 4.2c, d). The abundance of IRD in ODP Site 980 reflects the massive discharge of detrital material from icebergs (Oppo et al., 2006). The arctic seawater conditions with reduced sea surface temperature and salinity during H11 (Stolz and Baumann, 2010) seem to have a notable influence on the assemblage as well as on Noelaerhabdaceae mean weight. Stolz and Baumann (2010) noticed a higher number of reworked coccoliths around 130 ka BP but these are no Noelaerhabdaceae or Reticulofenestrid taxa (K. Stolz, pers. comm. 2013) that could be misidentified by SYRACO. Therefore the observed increase in weight is also not due to reworked coccoliths.

4.5.2.3 Carbonate system

A comparison to the carbonate system shows some correlations to the Noelaerhabdaceae mean weight and the assemblage shift during H11 as well. With the rising atmospheric CO_2 concentration during Termination II, CO_3^{2-}, pH and the calcite saturation state decrease and show lowest values at highest CO_2 concentrations between 128 - 129 ka BP (Fig. 4.7). At around 127 ka BP CO_3^{2-} and the calcite saturation state return to initial values whereas pH increases just slightly and levels off during MIS 5.5, CO_3^{2-} and calcite saturation state show a decreasing trend until 115 ka BP.

Dissolved inorganic carbon (DIC), HCO_3^- and total alkalinity (TA) increase with rising atmospheric CO_2 concentration and reach a maximum peak at 130 ka BP. At 130 ka BP HCO_3^-, TA and DIC start decreasing whereas TA and DIC show lowest values between 128 -129 ka BP, HCO_3^- at 127.5 ka BP. Until 115 ka BP HCO_3^- shows a slightly increasing trend, TA and DIC increases until 123.5 ka BP where the trend of TA starts decreasing and DIC displays a fluctuating but in mean rather constant trend. Noelaerhabdaceae mean weight is slightly correlated to HCO_3^-, atmospheric CO_2 and DIC (Fig. 4.7b, c, d) and in varying degrees anticorrelated to CO_3^-, pH, TA and the calcite saturation state (Fig. 4.7e, f, g,h).

This indicates a combined influence of the assemblage shift, the oceanic carbonate system and the SST on Noelaerhabdaceae mean coccolith weight. As previously mentioned, the weight is highest when *G. muellerae*, the heaviest species of the Noelaerhabdaceae assemblage, decreases. As *E. huxleyi* and *G. muellerae* represent the main part of the Noelaerhabdaceae assemblage and its mean weight, it is highly probable that either *G. muellerae* or *E. huxleyi* or both species increase their weight during the assemblage change. Due to the similar size of *E. huxleyi* and *G. muellerae* coccoliths it is difficult to disentangle shifts in size and weight of different species within the results of Noelaerhabdaceae measurements from SYRACO. Therefore, different explanations for the shift within the assemblage and the increase in weight are possible: (I) The southward migration of the arctic front during Termination II resulted in arctic seawater conditions (Stolz and Baumann, 2010). This might have enhanced the number of a large cold water preferring *E. huxleyi* morphotype as *E. huxleyi* >

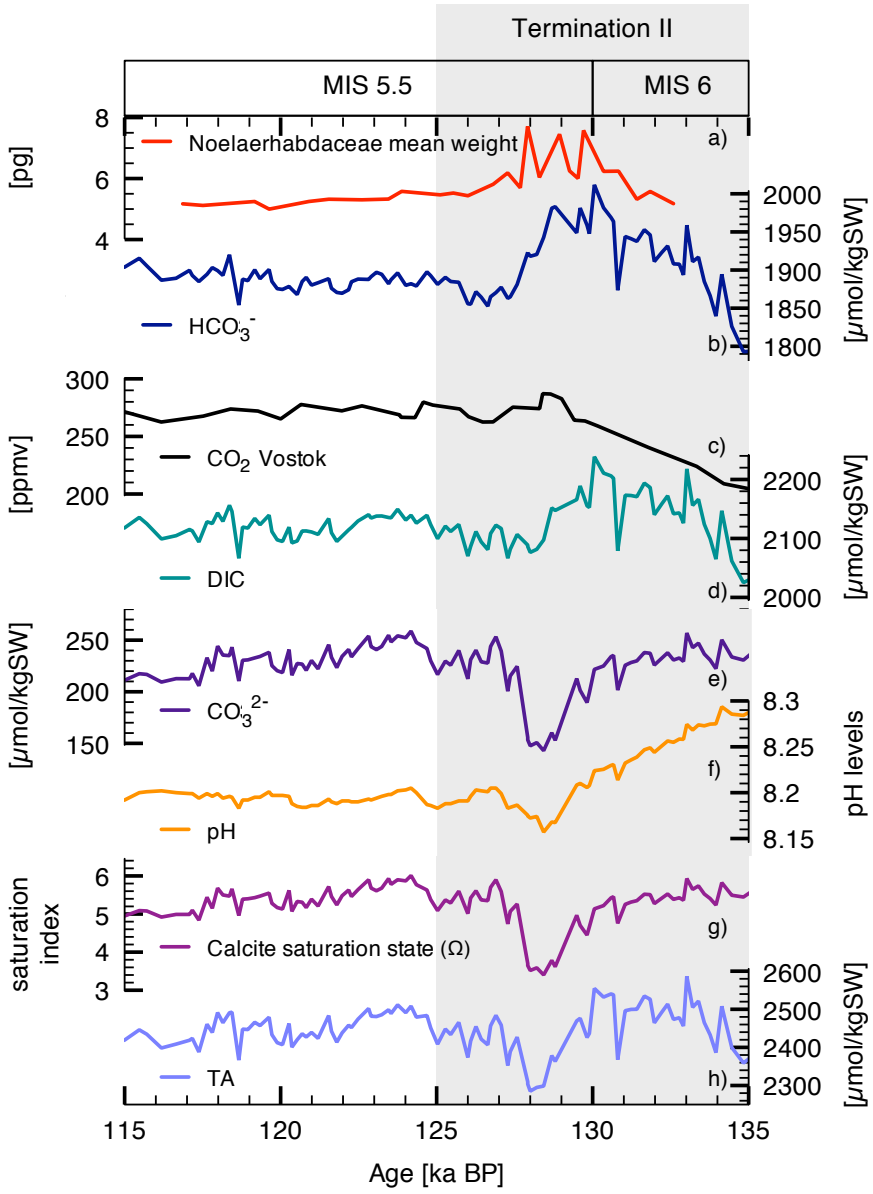

Figure 4.7. ODP Site 980, carbonate system compared to Noelaerhabdaceae mean weight: a) Noelaerhabdaceae mean weight; b) HCO_3^- concentration; c) atmospheric CO_2 concentration; d) dissolved inorganic carbon (DIC); e) CO_3^{2-} concentration; f) seawater pH; g) calcite saturation state (Ω); h) Total Alkalinity (TA).

4 µm (Colmenero-Hidalgo et al., 2002; Flores et al., 2010), which increases Noelaerhabdaceae mean weight. (II) The decrease in pH, CO_3^{2-} and TA increased the number of a heavily calcifying *E. huxleyi* morphotype, which is adapted to lower pH (Beaufort et al., 2011; Smith et al., 2012). (III) *G. muellerae* growth rate decreases due to unfavourable environmental conditions. Many laboratory studies have shown that during an inhibition of cell division the calcification rate is maintained constant, which leads to an increase in cellular calcification resulting in heavier coccoliths, especially under high concentrations of HCO_3^-. (Shiraiwa et al., 2003; Raven et al., 2012; Jones et al., 2013). But even if HCO_3^- concentrations

increase and *G. muellerae* abundance decrease at the same time it is not verifiable if the laboratory results can be compared to the assemblage response of the Rockall Plateau. At the Rockall Plateau the increase in Noelaerhabdaceae mean weight is induced by several factors and stands in close connection to the shift within the assemblage. Due to the low abundance of coccoliths during H11, only few measurements are possible, leading to large error bars of the Noelaerhabdaceae mean coccolith weight, which are however, mostly not overlapping with the surrounding lower values (Fig. 4.2a). It can not be ruled out that the strong increase in weight during H11 is biased by the lower number of measurements, but due to the coincidental change of the assemblage shift, the harsh seawater conditions and the coccolith weight we are confident that the increase in weight during H11 is not a statistical error. Therefore, according to our results, the main reason for the assemblage and weight change seem to be the harsh seawater conditions during H11, which altered the living conditions of Noelaerhabdaceae.

Further factors which should be taken into consideration are the higher concentrations of HCO_3^- and DIC during most of Termination II. There is substantial evidence that HCO_3^- is the principal inorganic carbon source for the calcification of coccoliths (Sikes et al., 1980; Herfort et al., 2002; Bach et al., 2013). In the studies of Bach et al. (2013, 2012), calcification rates of *E. huxleyi* increased with increasing HCO_3^- concentration, resulting in larger and heavier coccoliths, while low DIC results in decreasing calcification rates. The rising HCO_3^- and DIC concentration at the beginning of Termination II therefore possibly facilitates the precipitation of calcite and could lead to an increase in coccolith weight.

4.5.3 SO164-17-2 - Florida Strait

4.5.3.1 SEM counts and assemblage variations deduced from length and weight measurements

An SEM analysis of 28 sediment samples from Site SO164-17-2 showed that coccoliths were well-preserved, no effects of dissolution or calcite overgrowth were observed. The Noelaerhabdaceae family at this site predominantly consists of gephyrocapsids with a diverse morphological variability (compare Samtleben et al., 1980), and few *E. huxleyi*, together representing up to 65 % of the total assemblage. In this study gephyrocapsids were divided into small gephyrocapsids (mainly *G. ericsonii* and small *G. protohuxleyi*) and large gephyrocapsids (*G. oceanica* and large *G. protohuxleyi*) (Fig. 4.8).

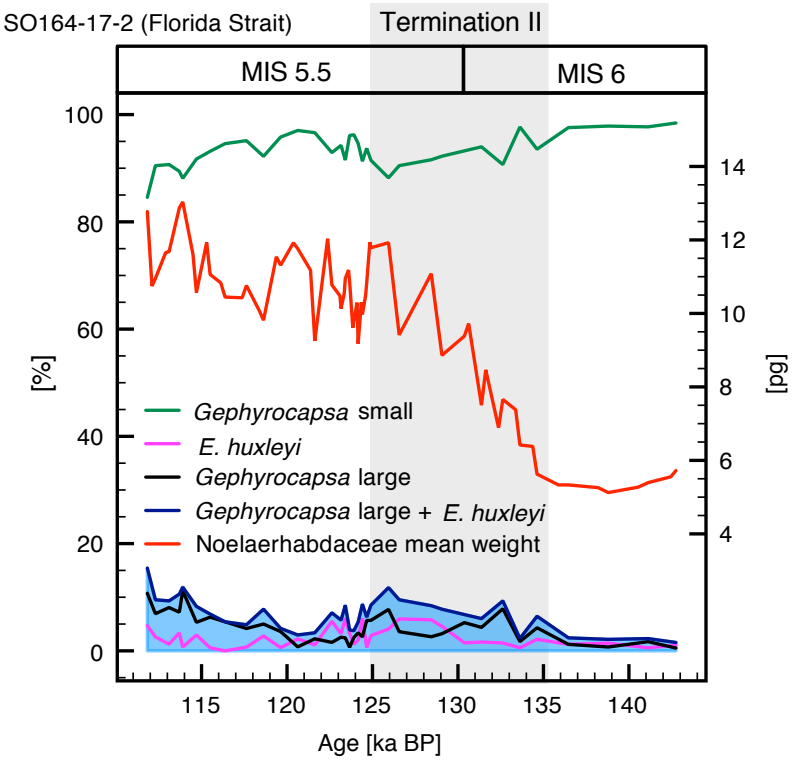

Figure 4.8. Site SO164-17-2, Relative abundance of coccolith species from the coccolithophore family Noelaerhabdaceae: *Gephyrocapsa* small (green line), *Gephyrocapsa* large (black line), *E. huxleyi* (pink line), *Gephyrocapsa* large + *E. huxleyi* (blue shaded area) compared to Noelaerhabdaceae mean coccolith weight (red line).

The relative abundance of the species within Noelaerhabdaceae is rather constant during MIS 6, with small gephyrocapsids dominating the assemblage. At around 136.5 ka BP, close to the beginning of Termination II, small gephyrocapsids decrease from 98 % to around 88 % at the end of Termination II, while *E. huxleyi* and large gephyrocapsids increase. During Termination II, large gephyrocapsids reach two peaks of around 8 % at 132.5 ka BP and 126 ka BP while *E. huxleyi* increases to up to 6 % in between these peaks. Towards the end of Termination II at 126 ka BP, the abundance of small gephyrocapsids increase up to 95 %, concomitant to a decrease of *E. huxleyi* and large gephyrocapsids. At around 121 ka BP, small gephyrocapsids start decreasing to around 84 % at 112 ka BP while large gephyrocapsids increase up to 10 % and *E. huxleyi* up to 6 %.

Our SEM counts of SO164-17-2 show increasing abundances of larger coccoliths (*Gephyrocapsa* large and *E. huxleyi*) during Termination II. This has an influence on Noelaerhabdaceae mean weight but the increase of from 2 % before Termination II to 12 % close to the end of Termination II does not explain the doubling of the weight (Fig. 4.8). Further, the decrease in abundance of the larger coccoliths after Termination II is not reflected in the mean weight. To disentangle the composition of the Noelaerhabdaceae assemblage from our measurements, mean weight and length before, during and after Termination II were separated (Fig. 4.9a, b).

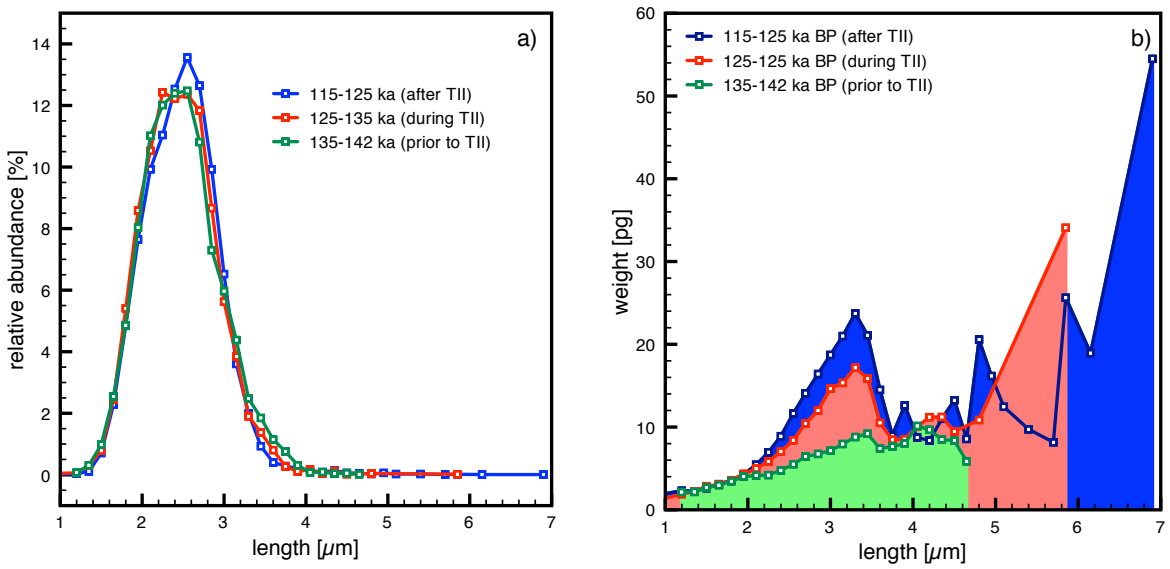

Figure 4.9. Site SO164-17-2, a) Relative abundance of coccolith length classes prior to TII (green line), during TII (red line) and after TII (blue line); b) Noelaerhabdaceae mean coccolith weight of different coccolith length classes prior to Termination II (green shaded area), during Termination II (red shaded area) and after Termination II (blue shaded area).

Prior to Termination II, mean Noelaerhabdaceae coccolith weight is less than 10 pg with mean lengths smaller than 5 μm (Fig. 4.9b). During and after Termination II, mean lengths up to almost 6 μm and 7 μm, respectively, are encountered, certainly reflecting the rising number of large *Gephyrocapsa*. However, the bulk of length classes lies between 1.8 and 3.3 μm for all intervals (Fig. 4.9a). Within these length classes, mean coccolith weight increases during and after Termination II (Fig. 4.9b), in combination with a slight shift to a higher abundance of larger coccoliths (Fig. 4.9a). The increase in weight and length of this class could result from increasing coccolith calcification or from an abundance shift within the morphologically highly variably gephyrocapsids to a more calcified species or morphotype (e.g. lighter/stronger calcified bridges or open/closed slits between the elements). Apparently, the increase in Noelaerhabdaceae mean coccolith weight during Termination II and the consistent enhanced weight after Termination II originates mainly from the enhanced calcification within the smaller size classes and partly from the appearance of a larger coccolith size classes through Termination II. However, it is highly likely that the shifts in the assemblage and the calcification are connected to changes in the seawater conditions which will be discussed in the following chapters.

4.5.3.2 SST and coccolithophore productivity

Coccolith accumulation rates at SO164-17-2 were used as an indicator for coccolithophore productivity. Coccolith accumulation rates are comparably low during MIS 6 and Termination

II, indication low coccolithophore productivity (Fig. 4.3b). With the end of Termination II at 125 ka BP, coccolith accumulation rates strongly increase to a maximum at around 124 ka BP and subsequently decrease to initial values at around 118.5 ka BP and remain at this level until 112 ka BP. The rather low coccolithophore accumulation rates during MIS 6 and Termination II indicate low coccolithophore productivity. The rising coccolithophore productivity at the end of Termination II might favour the conditions for coccolith calcification and maintain a high coccolith weight even when the number of heavier coccoliths decreases. But there is no overall correlation between coccolithophore productivity and Noelaerhabdaceae mean weight, indicating a minor influence of productivity on coccolith weight at the Florida Strait (Fig. 4.3b).

SST at the Florida Strait fluctuates between 29 and 31°C during late MIS 6 and Termination II, from 142 - 125 ka PB (Fig. 4.3c). With the end of Termination II SST increases to around 33°C at 123 ka BP and subsequently decreases during MIS 5.5. to 29°C. There is no correlation between Noelaerhabdaceae mean weight or the assemblage and SST.

4.5.3.3 Carbonate system

During MIS 6 TA, DIC and HCO_3^- decrease until around 140 ka BP and start rising with the increasing atmospheric CO_2 conditions, whereas highest levels are reached between 132 - 130 ka BP, before atmospheric CO_2 reaches maximum values at around 128.5 ka BP (Fig. 4.10). Subsequently TA, DIC and HCO_3^- decrease and display minimum levels at highest CO_2 concentrations, followed by an increase to a maximum at the end of Termination II. TA and DIC decrease again and level off between 124 - 123 ka BP whereas HCO_3^- slightly increases until 115 ka BP. The trend of seawater pH is opposite to the atmospheric CO_2 concentration, it decreases with rising atmospheric CO_2 and levels at around 128.5 ka BP. The trends of CO_3^{2-} and the calcite saturation state are identical and decrease until 140 ka BP, followed by an increase from 140 ka BP until 131 ka BP, which is interrupted by a minimum at 133.5 ka BP. A strong decrease between 131 and 128.5 ka BP is followed by an increase until the end of Termination II. A comparison of Noelaerhabdaceae mean weight and the carbonate system shows some correlations. There is positive correlation between the increasing weight and the rising trends of HCO_3^-, atmospheric CO_2, DIC and TA at the beginning of Termination II (Fig. 4.10b, c, d, h) and a negative correlation to the pH level as well as minor negative correlations to the trends of CO_3^{2-} and the calcite saturation state (Fig. 4.10e, f, g). The decrease in the concentration of most carbonate system parameters between around 130 and 125 ka BP is not reflected in the mean weight. There might be at least two explanations for the increase in weight: As HCO_3^- is the main carbonate source for coccolithophores

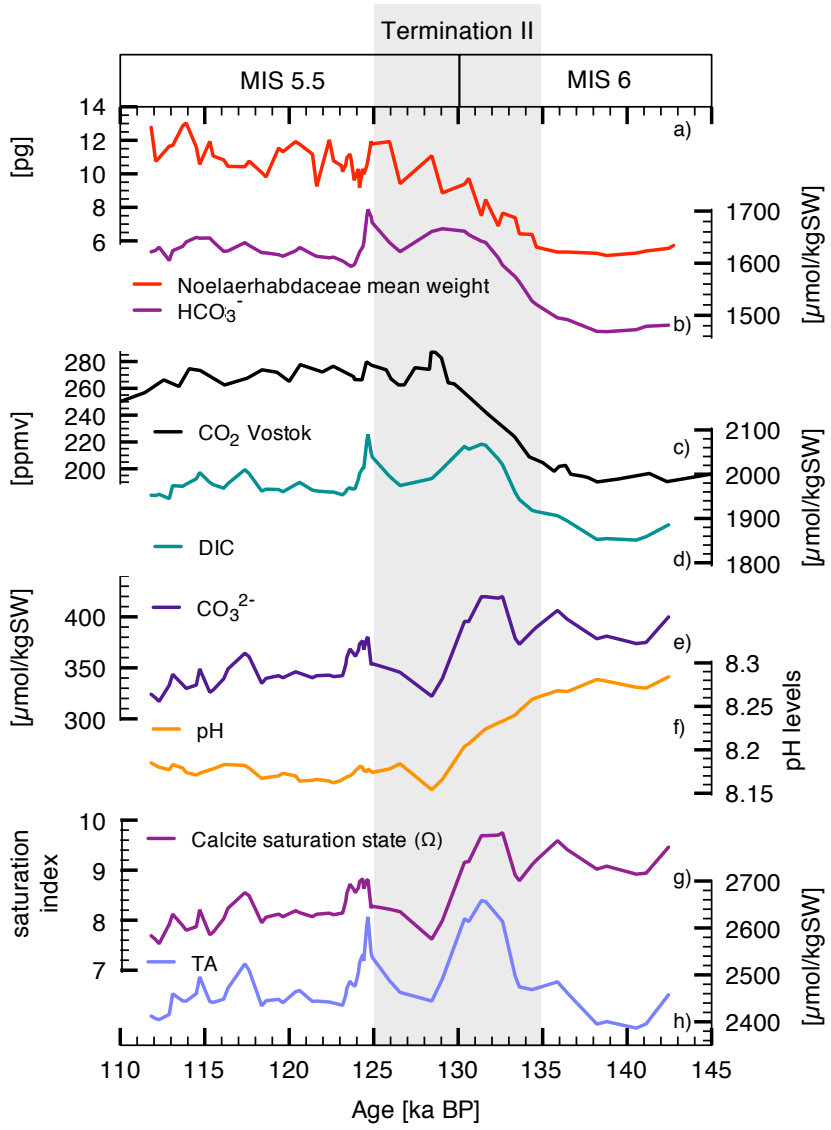

Figure 4.10. Site SO164-17-2, carbonate system compared to Noelaerhabdaceae mean weight: a) Noelaerhabdaceae mean weight; b) HCO_3^- concentration; c) atmospheric CO_2 concentration; d) dissolved inorganic carbon (DIC); e) CO_3^{2-} concentration; f) seawater pH; g) calcite saturation state (Ω); h) Total Alkalinity (TA).

a positive correlation to the weight and therefore to the calcification is not unexpected (see chapter 4.5.2.3). HCO_3^- remains on a rather high level even during MIS 5.5, which possibly maintains the heavy Noelaerhabdaceae mean weight during MIS 5.5. Further, there is a correlation between the abundance of large Gephyrocapsa and the concentration of HCO_3^-, TA and DIC. This is in agreement with the study of Rickaby et al. (2010) who reported about increasing growth rates of *G. oceanica* at higher DIC. At the Florida Straits it is very likely that the increase in Noelaerhabdaceae coccolith weight is connected to the changing parameters of the carbonate system which affects the Noelaerhabdaceae mean weight in two ways: altering coccolith calcification and changing species abundance.

4.5.4 Comparison with previous results from Termination I

In contrast to the Florida Strait, the coccolith weigh response of the Rockall Plateau to changing seawater conditions is more connected to the strong shifts within the assemblage induced by the harsh seawater conditions during H11. As assemblage compositions change with different ocean regions (McIntyre and Bé, 1967) it is likely that the response of an assemblage to changing seawater conditions within the same ocean region is rather similar. To compare the coccolith weight response in Termination I and II we therefore focus in the following on similar conditions related to the ocean region, i.e. on our results from the tropics of Termination II (Florida Strait) in comparison to the tropical stack of Termination I from Beaufort et al. (2011).

As mentioned above, our results are in conflict with the findings of Beaufort et al. (2011) who reported a decrease in Noelaerhabdaceae mean coccolith weight during the conditions of the glacial interglacial change of Termination I. The authors noted a correlation of the weight to CO_3^{2-} and an anti-correlation to HCO_3^- with the best accordance in the tropical stack and thus suggested the oceanic carbonate system to play a key role in coccolithophore calcification. Interestingly, in the authors results abundance changes of species and morphotypes within Noelaerhabdaceae were responsible for the decrease in Noelaerhabdaceae mean coccolith weight to the same extent as the decrease in single coccolith weights. Our results from the Florida Strait support the assertion of Beaufort et al. (2011) that the carbonate system plays a key role in coccolith calcification, but our results show opposing trends to the findings of Beaufort et al. (2011). As Termination I and II basically underlie the same mechanism related to increasing atmospheric CO_2, there might be some differences in the carbonate system which seem to have an important influence on coccolith calcification. At both Terminations CO_2 increased around 80 - 90 ppmv (Monnin et al., 2001; Petit et al., 1999) at a comparable time interval of approximately 10 ka (Kukla et al., 2002) (Fig. 4.4). The increase in atmospheric CO_2 generally leads to decreasing pH and CO_3^{2-} and increasing DIC, H^+ and HCO_3^-. However, the strength of CO_2 uptake into the ocean and the resulting changes in the seawater carbonate system depend on parameters as e.g. SST and salinity, which results in regional differences of the oceans chemistry with various ion concentrations (Zeebe and Wolf-Gladrow, 2001). Distinct differences in the parameters of the reconstructed seawater carbonate system of Termination I and II are detectable in concentrations of CO_3^{2-}, total alkalinity, DIC and the calcite saturation state, whereas HCO_3^- and pH show a similar trend or range. In the Florida Strait the reconstructed concentrations of CO_3^{2-} during Termination II are higher and fluctuate stronger than in the results of Beaufort et al. (2011) during Termination I (Fig. 4.11b). The observed increase in Noelaerhabdaceae weight during Termination II can not be explained by CO_3^{2-} since there is no clear coupling, but a potential positive effect on the coccolith calcification due to higher ion concentration is possible. Further, the calcite saturation

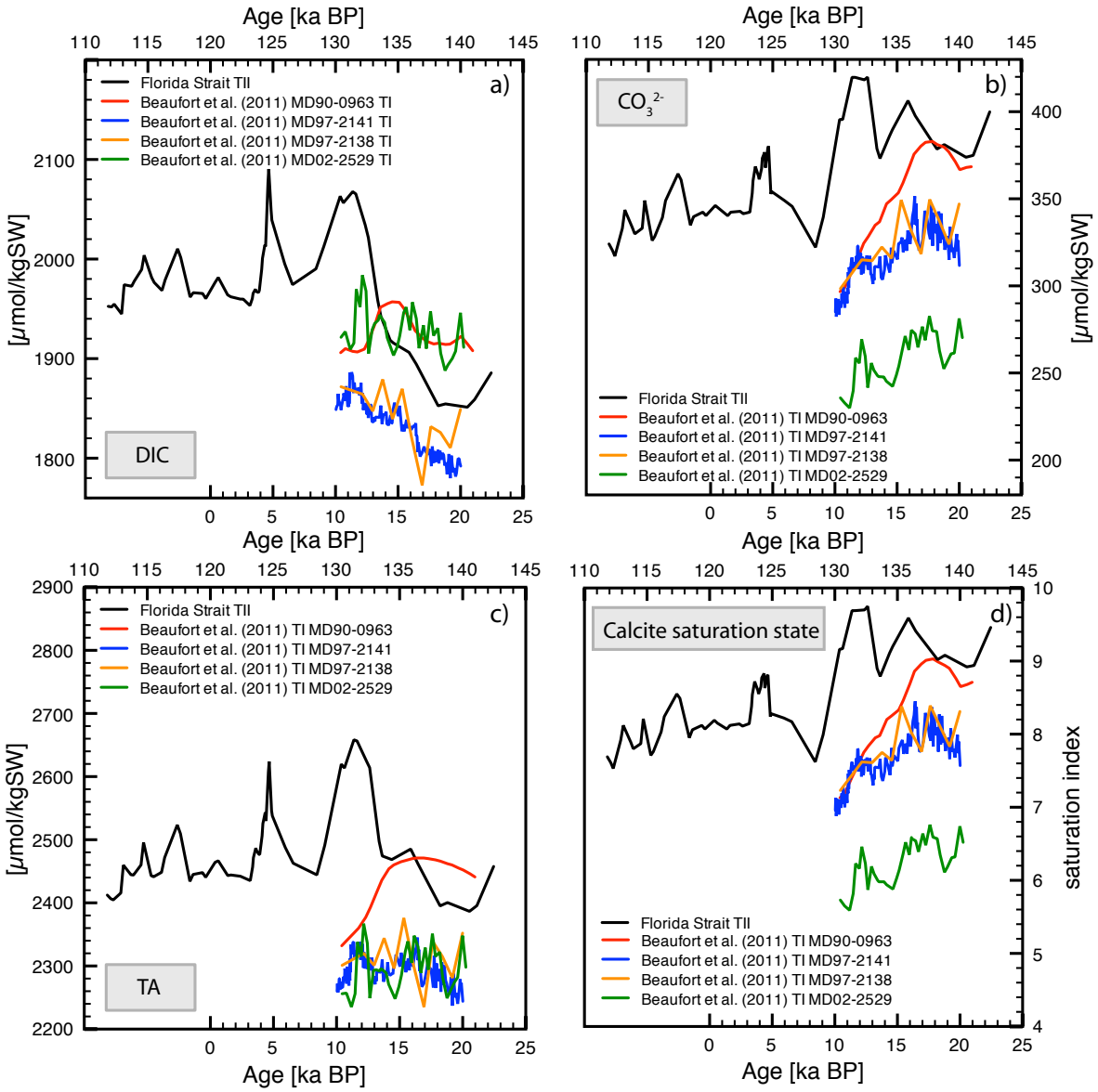

Figure 4.11. Comparison of selected parameters from the tropical carbonate system during the CO_2 increase of Termination I (Beaufort et al., 2011) and Termination II: a) Dissolved inorganic carbon (DIC); b) Carbonate ion concentration (CO32-); c) Total Alkalinity (TA); d) Calcite saturation state (Ω).

state in the Florida Strait during Termination I is higher than in the results of Beaufort et al. (2011) from Termination I (Fig. 4.11d). The concentrations of DIC and TA in the Florida Strait strongly increase during the CO_2 rise of Termination II followed by high fluctuations but within high concentration levels, in the results of Beaufort et al. (2011) the changes of DIC and TA are comparably minor (Fig. 4.11a, c). Interestingly, in a previous study of Beaufort et al. (2008) coccolith weight increased with rising alkalinity (excluding the highly calcifying *E. huxleyi* R-Type), and suggested a likely fundamental importance of alkalinity on coccolith calcification. Certainly, the high total alkalinity and saturation state in Termination II offers favourable conditions for calcification, but overall it is difficult to entangle which factor of the carbonate system induced the opposing Noelaerhabdaceae weight response in Termination I

and II. Since there is no clear key factor responsible for the different weight trends it can not be ruled out that the calcification of coccoliths is not constrained to a specific seawater ion concentration but rather various combinations of ion concentration can offer favourable conditions for coccolithophore calcification. The calcification response to changing carbonate chemistry is likely to underly the same mechanisms in all coccolithophores (Krug et al., 2011). This is reflected in an optimum curve response with species and strain specific optimum concentrations to different carbonate chemistry conditions rather than various intracellular calcification mechanisms between species and strains (Krug et al., 2011; Bach et al., 2011). Proposed by Bach et al. (2011), coccolith calcification is influenced by different parameters of the carbonate system at both sides of their optimum. The differences in the composition of the carbonate system between Termination I and II show that two disparate carbonate systems are considered. Probably, the combination of the carbonate system parameters during Termination II at the Florida Strait is more favourable for coccolith calcification than during Termination I. Possibly, the moderate CO_2 increase during Termination II in the highly supersaturated waters of the Florida Strait is too weak to cause a decline in coccolithophore calcification. Instead, the rise in DIC and HCO_3^- caused by the CO_2 rise may favour coccolithophore calcification above a threshold in calcite super-saturation.

4.6 Conclusion

We show that despite increasing atmospheric CO_2 and the resulting changes in the oceans carbonate system during a glacial interglacial change, the Noelaerhabdaceae mean weight can strongly increase. This is caused by different mechanisms at each site. At the Rockall Plateau the increase in Noelaerhabdaceae coccolith mean weight is in strong connection to a shift within the assemblage induced by a combination of several factors from the harsh seawater conditions around Heinrich event 11. At the Florida Strait, the concentration of carbonate-system-related ions is favourable for calcification and stimulates an increase in Noelaerhabdaceae coccolith mean weight. Additionally, the increase in Noelaerhabdaceae weight is intensified by an increase in the relative abundance of *E. huxleyi* and *Gephyrocapsa* large. The influence of other environmental factors at the Florida Strait as coccolithophore productivity or temperature are exceeded by the strong changes in the carbonate system. Our results illustrate that regional coccolithophore assemblage compositions have a variable response to changing seawater conditions and therefore have a major influence on the total amount of $CaCO_3$ production from coccolithophores. The calcification of a coccolithophore assemblage can be quite sensitive to the relative concentration of carbonate-system-related ions in the ocean, but shifts in the assemblage due to other environmental factors can have the same effects on the coccolithophore mean weight. The individual re-

sponse of a coccolithophore assemblage enhances the difficulty to make general statements about the total amount of coccolithophore calcite production in past, present and future oceans.

Acknowledgements

We thank K. Stolz and J. Schönfeld for providing us sample material of ODP Site 980 and SO164-17-2 and for the helpful discussions. We thank R. Warwas for carrying out SEM counts. T. Oberließen and S. Häuser are thanked for their help with the sample preparation and the images. This study was funded by the Federal Ministry of Education and Research (Bundesministerium für Bildung und Forschung; 03F0608A) within the Biological Impacts of Ocean Acidification (BIOACID) project.

5. Ocean eutrophication versus acidification: anthropogenic influence on coccolithophore calcification over the last 200 years in the Gulf of Taranto

C. Bauke[1], K.J.S. Meier[1], H. Kinkel[2,]

[1]Christian-Albrechts-Universität zu Kiel, Institute of Geosciences, Ludewig-Meyn-Str. 10, 24118 Kiel, Germany

[2]University of Southern Denmark, Campusvej 55, 5230 Odense, Denmark

in preparation for submission to Ocean Acidification

5.1 Abstract

Rising coccolithophore productivity due to favourable nutrient conditions can increase coccolith weight, in contrast to the possible negative effects on coccolith weight due to the ongoing ocean acidification. In coastal areas, both processes are influenced by human activity over the past 200 years. We studied a record from the Gulf of Taranto, central Mediterranean Sea, a region which is affected by enhanced nutrient loads from the Po River due to the increased use of fertilizers since 1800 AD. At the same time, ocean pH has decreased due to rising atmospheric CO_2 and the concomitant changes in the seawater carbonate system. Neither of these two processes is directly reflected in Noelaerhabdaceae coccolith weight records of the past 200 years. Coccolith weight increases during times of a negative North Atlantic Oscillation index, when the nutrient rich Po River discharge is strongest, and the coccolith coccolithophore productivity season is prolonged. The continuous ocean acidification is so far not reflected in the coccolith weight. Therefore, the increase of nutrient availability leads to more coccolithophore productivity which has so far reduced the negative effect of ocean acidification on coccolithophore calcification.

5.2 Introduction

With the beginning of the industrial revolution the emission of anthropogenic CO_2 started increasing due to deforestation and burning of fossil fuels. Since 1800 AD, the atmospheric CO_2 concentration has risen more than 100 ppmv (Sabine et al., 2004). The absorption of atmospheric CO_2 by the oceans has altered the seawater carbonate system towards increasing dissolved inorganic carbon (DIC) bicarbonate ion concentration (HCO_3^-), and a reduction of carbonate ion concentration (CO_3^{2-}) and seawater pH. This ongoing shift to higher acidity

is known as ocean acidification (Feely et al. 2004; Raven et al., 2005; IPCC, 2007). Since the industrial revolution, about half of the CO_2 emission has been stored in the oceans, which led to a decrease in pH of 0.1 units compared with preindustrial levels (Orr et al., 2005). By the end of the century the pH is predicted to decrease by another 0.4 units (Caldeira and Wickett, 2003). The changing seawater carbonate system will have impacts on marine organisms, in particular on marine calcifiers such as coccolithophores. Coccolithophores are known to be sensitive to changing seawater carbonate chemistry (e.g. Riebesell et al., 2000; Beaufort et al., 2011) but the response of their calcification is different between species and strains under future CO_2 scenarios (Langer et al., 2009; Krug et al., 2011). Under the influence of other environmental parameters (temperature, nutrients, salinity) the complexity of the response to changing carbonate chemistry is even higher (Zondervan et al., 2002; Feng et al., 2008; De Bodt et al., 2010; Müller et al., 2012; Rouco et al; 2013).

Beside the changes in the seawater carbonate system due to increasing atmospheric CO_2, the anthropogenic activity of the last 200 years is observable in e.g. the rising use of fertilizer in agriculture and discharge of wasted water which has significant consequences for the marine environment as well. Especially coastal areas are under influence of the rising delivery of nutrients from river discharge which affects the primary production in the ocean by e.g. stimulating their productivity (Spatharis et al., 2007; Rabalais et al., 2009; Zonneveld et al., 2012). In the coastal environments of the Adriatic Sea and the Gulf of Taranto in the central Mediterranean Sea, primary producers are under strong influence of the Po River discharge, representing a primary source of nutrients (Degobbis & Gilmartin, 1990; Pušcarić et al., 1990; Penna et al., 2004). The rising nutrient load of the Po River is reflected in e.g. a rising total abundance of dinoflagellate cysts and coccolithophores (Sangiorgi and Donders, 2004; Pušcarić et al., 1990; Zonneveld et al., 2012). Coccolithophores are one of the dominant phytoplankton groups in the Mediterranean Sea, and their coccoliths dominate the carbonate flux (Ziveri et al., 1995, 2000; Mozetič et al., 1998; Malinverno et al., 2003). Thus, changes in coccolith calcification affect the carbonate flux to depth. It has been reported that coccoliths are heavier during enhanced coccolithophore productivity (Beaufort et al., 2007). As coccolith weight can be used as an indicator for coccolithophore calcification rates (Bach et al., 2012), variations in the primary production are likely to be reflected in the coccolith weight. However, it is unclear if a possible positive effect of enhanced nutrient load from the Po River on coccolithophore calcification is counteracting the consequences of the changing seawater carbonate system.

To obtain insights into coccolithophore calcification during human induced environmental changes of the past 200 years, we reconstructed the calcification response of the dominant coccolithophore family Noelaerhabdaceae. Mean Noelaerhabdaceae coccolith weights of a sediment core from the Gulf of Taranto were measured between 1830 - 2006 AD. We com-

pared the weights with possible environmental factors which are known to affect coccolith calcification (e.g. temperature, nutrients, carbonate system, Po River discharge) in order to gain insights into the response of coccolithophores to the recent environmental changes. The main questions are to which extent coccolith weight changes and whether changes in coccolith weight are referable to the carbonate system or rather to other environmental factors i.e. the elevated nutrient load from the Po River.

5.3 Material and Methods

5.3.1 Material and age models

Sediment core GeoB 10709-5 (39°45.39´N; 17°53.57´E, 172.3 m water depth) was retrieved with a multicoring device during the POSEIDON cruise "CAPPUCCINO" in June 2006 from the Gulf of Taranto (Zonneveld et al., 2008) (Fig. 5.1). The age model bases on ^{210}Pb/^{137}Cs-dating via gamma spectroscopy from 9 sediment slices from depths between 0.5 - 34.75 cm (Elshanawany, 2010).

5.3.2 Sample preparation and weight measurements

Smear slides were prepared by taking a few milligram of sediment with a toothpick, mixing it with a drop of water on a glass microscope slide and smearing it homogeneously on the slide. After drying quickly on a hot plate the sediment was fixed with 3 - 4 drops of the resin EUKITT and a cover slip. After drying, the smear slides were scanned with a polarised light microscope (Leica DM6000B,1000x magnification), which was equipped with a SPOT Insight black and white camera. Between 200 and 400 pictures of every sample were taken. The light of the microscope bulb was continuously controlled to avoid a decrease in light intensity over time. Consistently after the imaging of 10 smear slides, each 200 pictures of two control-slides were taken and the brightness was checked with the program ImageJ and compared with the previous results. In addition a weekly control with the highest possible light conditions of the microscope was conducted. Both methods revealed brightness changes of less than 2 % and are negligible.

The automated recognition software for coccolithophores SYRACO (Beaufort and Dollfus, 2004) was used to identify and measure coccoliths. The software identifies and classifies coccoliths in the image files and returns output files containing coccoliths of a single species. In the output files, coccolith length and the grey level of every component pixel were measured. The sum of grey levels of a coccolith image was used to estimate coccolith weight. The brightness of coccolith calcite depends on its thickness, which can be expressed in an equa-

tion. After calibration to a known calcite standard (method after Beaufort et al., 2005, with a calcite particle size of 1-2 μm) the summation of grey level of every single coccolith can be converted with an equation (weight = grey level * 0.0016) into the estimated weight of the coccolith in picogram. Depending on coccolith content in the sediment sample, preparation of the smear slide and state of preservation of the coccoliths, roughly between 150 and 2300 Noelaerhabdaceae coccoliths were measured in each sample, in total 42,842 single coccoliths. Error bars are shown in Fig. 2 and 3 to assess the statistical significance of each data point. For a more detailed description of SYRACO see Beaufort et al. (2004 and 2005). SEM samples for assemblage counts were processed following standard protocols (Andruleit, 1996).

5.3.3 Carbonate chemistry, temperature, and salinity

Sea surface temperature (SST) reconstructions are available from Grauel et al. (2013) and base on alkenone measurements of sediment core GeoB10709-4. The alkenone temperatures from the Gulf of Taranto reflect winter/spring conditions when alkenone production of coccolithophores is highest (Leider et al., 2010; Grauel et al., 2013). The reconstruction of the carbonate system largely bases on these temperatures and consequently reflects winter/spring conditions as well. Parameters of the surface ocean carbonate system were reconstructed with the program CO2Sys (Lewis and Wallace, 1998). As input parameters salinity, temperature, total alkalinity and pCO_2 are required. Atmospheric CO_2 data are available from Law Dome DE08 and DSS ice cores measurements (Etheridge et al., 1998), total alkalinity was calculated using the equation of Lee et al. (2006) for the zone 3 (North Atlantic). Salinity was derived from $\Delta\delta^{18}O$, using the equation of Duplessy et al. (1991). For the calculation of $\Delta\delta^{18}O$, $\Delta\delta^{18}O_{seawater}$ was calculated after Bemis et al. (1998) and corrected with the global sea level effect ($\delta^{18}O_{ice\ volume}$) after Waelbroeck et al. (2002) using sea level data of Jevrejeva et al. (2008). $\delta^{18}O$ is available from the planktic foraminifera *Globigerinoides ruber* (white) of the adjacent core NU04 (Grauel et al., 2012).

The solubility of CO_2 in seawater is dependent on parameters such as SST, salinity, alkalinity and productivity, which can lead to strong geographical and seasonal differences (Feely et al., 2001; Zeebe & Wolf-Gladrow, 2001). Reconstructions of the carbonate system at our coring site do not include influences of the biological productivity. Enhanced productivity strengthens the biological pump, leading to a decrease in CO_2 of surface waters and to changes in the oceanic carbonate system (Sigman and Haug, 2003). High productivity at the coring site could therefore weaken the decrease in pH and CO_3^{2-} as well as the increase in HCO_3^- and DIC. On the contrary it should be mentioned that the Mediterranean is a sensitive system, the reaction to environmental changes are faster compared to the open ocean (Be-

thoux et al., 1999). Especially in the coastal zones, the CO_2 uptake is higher than e.g. in the Atlantic Ocean (Goyet and Touratier, 2008).

5.4 Oceanographic settings

Site GeoB 10709-5 is located in the Gulf of Taranto in the northwestern Ionian Sea between Calabria and Apulia (Fig. 5.1). Its hydrography is influenced by the ocean circulation of the Adriatic Sea and the Ionian Sea. In the Adriatic Sea the surface waters are strongly influenced by the discharge of the Po-river, the so called “Po-discharge plume“, which is the primary source of nutrients to the Adriatic Sea (e.g. Penna et al., 2004).

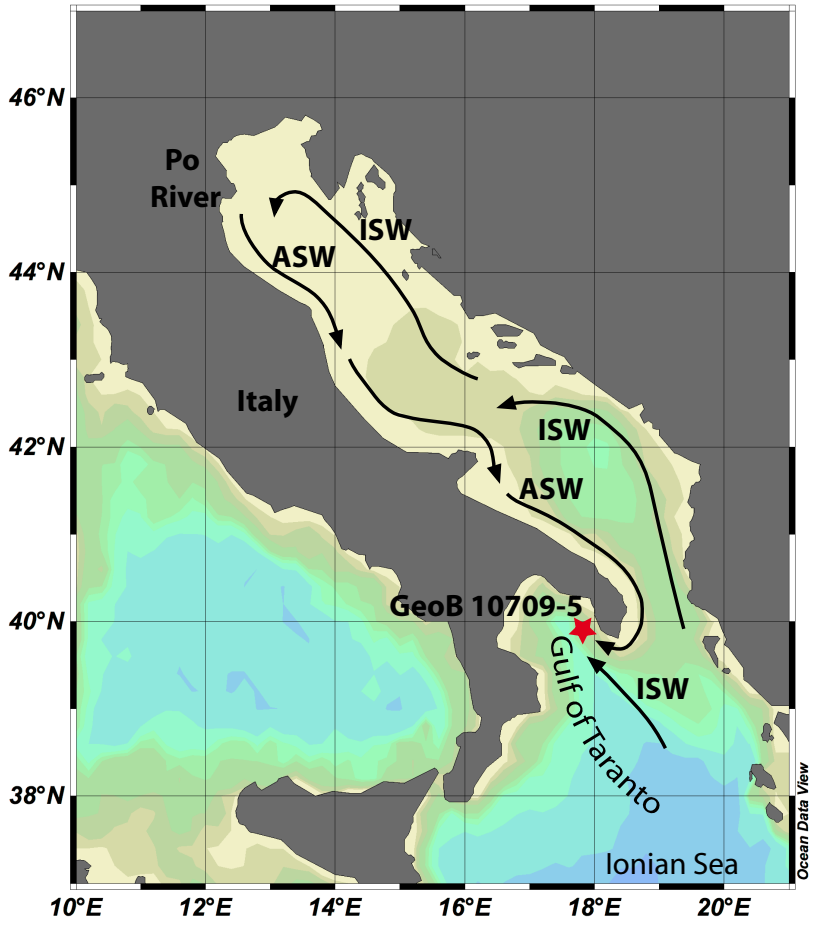

Figure 5.1. Position of Site GeoB 10709-5 (red star) and main oceanographic features. Black arrows show major ocean surface currents: Adriatic Surface Water (ASW), Ionian Surface Water (ISW).

An anti-clockwise surface water circulation transports the fresh, nutrient rich and low salinity waters along the southwest Adriatic coast and in the Gulf of Taranto (Lee et al., 2007). These waters, called Adriatic Surface Water (ASW), lead to a nutrient rich belt with enhanced pro-

ductivity along the western Italian coast (Turchetto et al., 2007). Within the Golf of Taranto, water masses of the ASW mix with the warmer and more saline Ionian Surface Water (ISW), coming from Eastern Mediterranean (Socal et al., 1999; Poulain, 2001; Turchetto et al., 2007). The distribution of the water masses is characterised by a high seasonal variability with stronger ASW during winter/spring and weaker ASW during summer as a result of reduced Po River discharge (Poulain, 2001; Milligan and Cattaneo, 2007).

5.5 Results and discussion

There is considerable short term variability in the Noelaerhabdaceae mean weight record, that is most probably due to the sampling resolution of 0.5 cm, sporadically 0.25 cm. As sedimentation rates are more than 1 cm y^{-1}, it is likely that the coccolith weight record displays seasonal variations in, e.g. nutrient content or CO_2 uptake. To observe the overall development of the Noelaerhabdaceae mean coccolith weight of the past 200 years we focus on the long term trend.

Around 1860 and 1960 the Noelaerhabdaceae mean coccolith weight trend shows elevated values of around 9.8 pg while otherwise there is no strong trend (Fig. 5.2a). *E. huxleyi* is the dominant species of the coccolithophore and the Noelaerhabdaceae assemblage, contributing up to 90 % of the Noelaerhabdaceae assemblage. Other members of the Noelaerhabdaceae are *Gephyrocapsa oceanica*, *Gephyrocapsa muellerae*, and *Gephyrocapsa ericsonii* but with relatively low relative abundances. The relative abundance of the species within Noelaerhabdaceae is rather constant, changes are less than 8 % (Fig. 5.2b). The assemblage composition is therefore unlikely to have a strong influence on the Noelaerhabdaceae mean weight, especially after 1900 AD. Between 1830 and 1900 the decrease in abundance of large *Gephyrocapsa* could point to a decrease in Noelaerhabdaceae mean weight but the increase in weight after 1900 can not be explained by an abundance shift of any of the species (Fig. 5.2b). This suggests that Noelaerhabdaceae weight changes at the coring site are primarily induced by variations in the coccolith calcification of the single species.

The atmospheric CO_2 concentration has risen by more than 100 ppmv over the last 200 years**,** leading to a decrease in surface pH by 0,1 unit, and in CO_3^{2-} by around 57 μmol/kgSW (Fig. 5.2c, d, e). This increase is rather comparable to the rising CO_2 conditions of the last two deglaciations but on a completely different time scale (Pelejero et al., 2010; Hönisch et al., 2012; Zeebe et al., 2012). During the last two deglaciations, the CO_2 increase took place

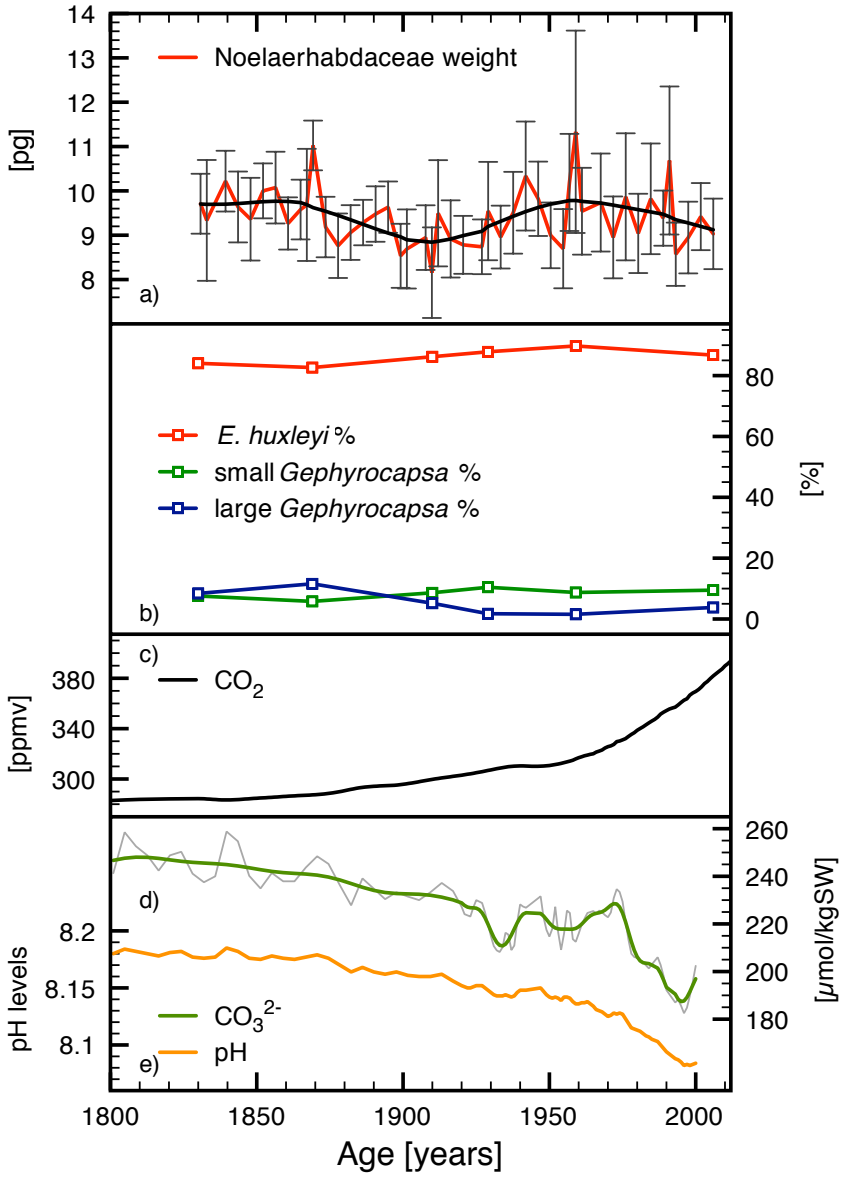

Figure 5.2. a) Noelaerhabdaceae mean coccolith weight (red line: original data, black line: smoothed data), error bars indicate 95 % confidence intervals of the mean weight; b) Relative abundance of Noelaerhabdaceae species: *E. huxleyi* (red line), small *Gephyrocapsa* (green line), large *Gephyrocapsa* (blue line); c) Atmospheric CO_2 from Law Dome DE08 and DSS (black line); d) CO_3^{2-} concentration (green line: smoothed data, grey thin lines: original data; e) pH levels (orange line).

over approximately 10000 years, and factors as assemblage shifts and environmental change have lead to a non-uniform response of Noelaerhabdaceae assemblages to this CO_2 increase (Beaufort et al., 2011; Bauke et al., submitted). The relatively quick increase in atmospheric CO_2 over the last 200 years is, however, not reflected in the Noelaerhabdaceae mean coccolith weight (Fig. 5.2a, c). This is surprising, as different field studies have shown a decrease of coccolith calcification even at slower rates of CO_2 decrease, if assemblages are stable (e.g. Beaufort et al. 2011). Other studies also have shown the potential influence

of other environmental parameters that may lead to an increase in coccolithophore calcification and therefore potentially could counteract the ocean acidification effect (e.g. Beaufort et al., 2007).

The effect of SST on coccolith calcification has been investigated in previous studies and has shown different results (e.g. Langer et al., 2007; de Bodt et al., 2010). Beaufort et al. (2007) concluded the absence of a global relationship between SST and the calcification of *E. huxleyi* coccoliths and further noticed no strong correlation between SST and Noelaerhabdaceae weight (Beaufort et al., 2011). The alkenone-based SST ($U^{K'}_{37}$) at the coring site mainly reflects winter/spring conditions because alkenone production in coccolithophores is highest during the colder seasons when vertical mixing and nutrient transport from the ASW are strongest (Leider et al., 2010). SST of the last 200 years (Fig. 5.3b) is in agreement with present SST in the Gulf of Taranto which varies from 13 - 18 °C between late autumn and late spring (Grauel et al., 2013). The general decreasing alkenone SST trend over the last 200 years is not reflected in the mean Noelaerhabdaceae coccolith weight, indicating no influence of the SST on the weight.

Previous studies show correlations between salinity and the size of *E. huxleyi* in plankton and culture studies (Bollmann et al., 2009; Fielding et al., 2009), while coccolith weight generally shows no strong correlation with salinity (Beaufort et al., 2011; Bauke et al., 2013). There is also no correlation between Noelaerhabdaceae mean coccolith weight in our results and the reconstructed palaeo-salinity (not shown).

Alkenone concentrations at the coring site (Grauel et al., 2013) document an increase in Noelaerhabdaceae productivity from 1800 that has intensified in the early 20th century (Fig. 5.3c). This is an anthropogenic effect due to the increasing use of fertilizers. From 1800 AD the population in Italy strongly increased, leading to enhanced agricultural productivity and high input of nutrients in major rivers (Lotze et al., 2011). The Adriatic Sea and the Gulf of Taranto are under influence of discharge waters from the Po River (Degobbis & Gilmartin, 1990; Pušcarić et al., 1990; Penna et al., 2004). Variations in the river runoff influence the strength of the ASW and thus the nutrient input into the Adriatic Sea and the Gulf of Taranto (Poulain, 2001; Milligan and Cattaneo, 2007; Zonneveld et al., 2012). The enhanced anthropogenic nutrient supply stimulates primary productivity in the Adriatic Sea and in the Gulf of Taranto, as indicated by e.g. a rising total abundance of dinoflagellate cysts (Sangiorgi and Donders, 2004; Zonneveld et al., 2012) or increasing abundance of coccolithophores (Pušcarić et al., 1990). The high nutrient supply in the Gulf of Taranto is further reflected in $\delta^{13}C$ values, rising marine lipid biomarker concentrations and an increase in TOC (Grauel et al., 2013).

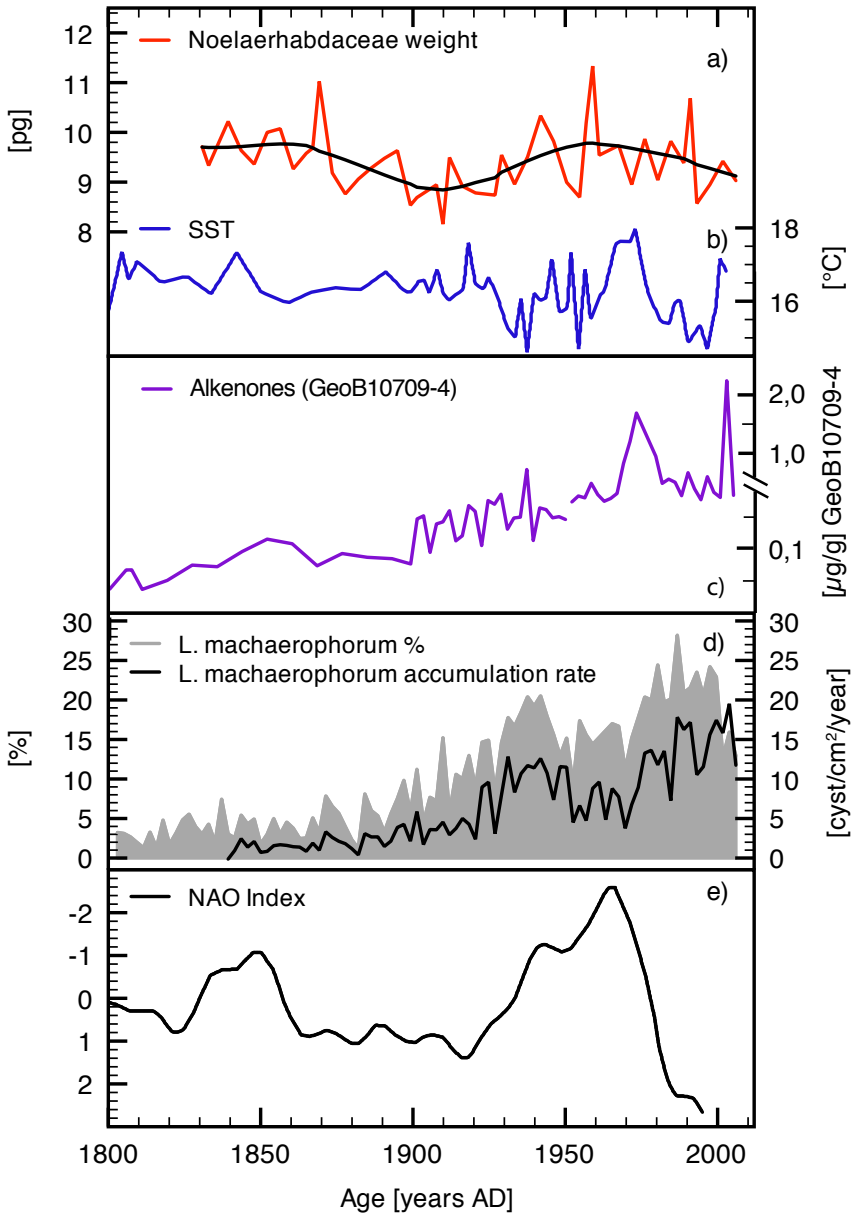

Figure 5.3. a) Noelaerhabdaceae mean coccolith weight (red line: original data, black line: smoothed data); b) Alkenone SST from Grauel et al. (2013) (blue line); c) Alkenone concentration from site GeoB10709-4, note the axis break (Grauel et al., 2013) (purple line) d) Relative abundance (grey shaded) and accumulation rate (black line) of the dinoflagellate cyst species *L. machaerophorum* from Zonneveld et al. (2012); e) NAO index (black line, note the reversed scale)

Furthermore, a change in the dinoflagellate assemblage with an increase of *Lingulodinium machaerophorum* documents the effect of increased fertilizer use in agriculture and resulting eutrophication at the coring site (Fig. 5.3d) (Zonneveld et al., 2012).

It has been shown that enhanced productivity of coccolithophores due to rising nutrient content can increase coccolith calcification (Beaufort et al., 2007; Engel et al., 2005). At the coring site this seems not to be the case as the coccolithophore weight trend does not follow the

coccolithophore productivity increase. Alkenone concentration reflects the overall increasing nutrient content at the coring site, but the coccolithophore production is additionally under the influence of the NAO index (Grauel et al., 2013). The Po River discharge as well as the entire Mediterranean region is strongly influenced by the North Atlantic Oscillation (NAO), especially in cold seasons (Dünkeloh and Jacobeit, 2003; Xoplaki et al., 2004). During periods of negative NAO index, North Atlantic storm tracks shift southwards into the Mediterranean region, leading to enhanced precipitation and higher river discharge of i.e. the Po River (Quadrelli et al., 2001; Brunetti et al., 2004; Struglia et al., 2004; Zanchettin et al., 2008). Grauel et al. (2013) suggested that the higher river discharge and nutrient load during times of a negative NAO index lead to enhanced ASW strength. As a result, more nutrients are brought into the photic zone due to ASW transport and due to increased vertical mixing at the coring site (Poulain, 2001; Leider et al., 2010; Grauel et al., 2013). This results in an extension of the alkenone production period to late spring, which can also be seen in the warmer alkenone SSTs during these periods (Fig. 5.3b, e). The NAO therefore has a strong influence on the seasonality of the Noelaerhabdaceae production at the coring site, as these coccolithophores are the main alkenone producers. The Noelaerhabdaceae weight trend coincides with the reverse trend of the NAO index, i.e. coccolith weight is highest when the NAO index is negative (Fig. 5.3a, e). Noelaerhabdaceae mean weight seems to be higher when the coccolithophore productivity season is extended during times of negative NAO. Increased productivity during negative NAO index phases is not reflected in the dinoflagellates and alkenone concentration, likely due to the lower nutrient concentration during the first period of a negative NAO index (~1820 - 1870).

Although the trends of productivity and ocean acidification are not reflected in the mean coccolith weight, there might be a connection or probably a compensation between these processes. Enhanced biological productivity at the coring site is likely to strengthen the biological pump. This could result in a decrease of surface CO_2 in the ocean and therefore change the seawater carbonate system, which leads to a higher pH in the surface waters (Sigman and Haug, 2003; Doney et al., 2012). The rising nutrient load during winter/spring due to stronger ASW could therefore lead to more favourable carbonate system for calcification than during other seasons with comparably higher CO_2 concentration in the surface ocean. Ocean eutrophication and ocean acidification are happening at exactly the same time in the Gulf of Taranto. Both processes are known to have a considerable impact on coccolithophore calcification, but neither the increasing coccolithophore productivity nor the changes in the carbonate system over the last 200 years are reflected in the long term trend of the Noelaerhabdaceae coccolith weight. We therefore propose that the increasing nutrient content is able to counterbalance the negative influence of the seawater carbonate system, leading to a relatively stable mean Noelaerhabdaceae coccolith weight. Only during times of a negative

NAO index, when the coccolithophore growth seasons extends into late spring, the mean coccolith weight in the Gulf of Taranto is increased. Our results suggest that a possible negative effect of the rising ocean acidification on coccolith calcification can be at least temporarily outcompeted by enhanced nutrient content. However, this is likely to be a local effect due to the specific environmental setting in the Gulf of Taranto. If eutrophication and acidification will proceed at the same rates than during the last years, the balance between the two processes will likely not be sustained. Future work should therefore focus on sedimentary records that are not under the influence of eutrophication.

Acknowledgements

We thank K.-H. Baumann and K. Zonneveld for providing us sample material of GeoB10709-5. T. Oberließen and S. Häuser are thanked for their help with the sample preparation and the images. This study was funded by the Federal Ministry of Education and Research (Bundesministerium für Bildung und Forschung; 03F0608A) within the Biological Impacts of Ocean Acidification (BIOACID) project.

6. Influence of changing carbonate chemistry on morphology and weight of coccoliths formed by *Emiliania huxleyi*

L. T. Bach[1], C. Bauke[2], K. J. S. Meier[2], U. Riebesell[1], K. G. Schulz[1]

[1]Helmholtz-Zentrum für Ozeanforschung Kiel (GEOMAR), Düsternbrooker Weg 20, 24105 Kiel, Germany

[2]Christian-Albrechts-Universität zu Kiel, Institute of Geosciences, Ludewig-Meyn-Str. 10, 24118 Kiel, Germany

Published in Biogeosciences

6.1 Abstract

The coccolithophore *Emiliania huxleyi* is a marine phytoplankton species capable of forming small calcium carbonate scales (coccoliths) which cover the organic part of the cell. Calcification rates of *E. huxleyi* are known to be sensitive to changes in seawater carbonate chemistry. It has, however, not yet been clearly determined how these changes are reflected in size and weight of individual coccoliths and which specific parameter(s) of the carbonate chemistry drive morphological modifications. Here, we compare data on coccolith size, weight, and malformation from a set of five experiments with a large diversity of carbonate chemistry conditions. This diversity allows distinguishing the influence of individual carbonate chemistry parameters such as carbon dioxide (CO_2), bicarbonate (HCO_3^-), carbonate (CO_3^{2-}), and protons (H^+) on the measured parameters. Measurements of fine-scale morphological structures reveal an increase of coccolith malformation with decreasing pH suggesting that H^+ is the major factor causing malformations. Coccolith distal shield area varies from about 5 to 11 μm^2. Changes in size seem to be mainly induced by varying [HCO_3^-] and [H^+] although influence of [CO_3^{2-}] cannot be entirely ruled out. Changes in coccolith weight were proportional to changes in size. Increasing $CaCO_3$ production rates are reflected in an increase in coccolith weight and an increase of the number of coccoliths formed per unit time. The combined investigation of morphological features and coccolith production rates presented in this study may help to interpret data derived from sediment cores, where coccolith morphology is used to reconstruct calcification rates in the water column.

6.2 Introduction

Coccolithophores are unicellular photoautotrophic organisms, able to form blooms in all major ocean basins (Moore et al., 2012). Their unique feature is the intracellular formation of small scales (coccoliths) made of calcium carbonate ($CaCO_3$) covering the organic surface of the cell. Coccolithophores appeared for the first time about 220 million years ago in the fossil record and are found ever since in marine sediments although their abundance was highly variable (Bown et al., 2004). They are important components in the marine carbon cycle because the $CaCO_3$ in their coccoliths serves as ballasting material accelerating the organic carbon flux from the surface into the deep ocean (e.g. Honjo, 1976; Ploug et al., 2008). In modern oceans, *Emiliania huxleyi* is the most abundant species (Paasche, 2002). It evolved from *Gephyrocapsa* spec. about 291-270 ky ago and dominates the coccolithophore community for the last ~82-63 ky (Thierstein et al., 1977; Raffi et al., 2006). *E. huxleyi* frequently forms large blooms that can cover up to a million km^2 and can be seen from space (Holligan et al., 1993; Tyrell and Young, 2009). These blooms are typically found in stratified waters during later stages of the phytoplankton spring succession (Tyrell and Merico, 2004), although, recently, high *E. huxleyi* abundance has also been reported in turbulent regimes when cell numbers are integrated over the whole water column (Schiebel et al., 2011).

The invasion of anthropogenic CO_2 into the ocean currently changes the marine carbonate chemistry by increasing [CO_2] and decreasing seawater pH – a process known as ocean acidification (Raven et al., 2005). Although these changes in carbonate chemistry are known to influence calcification rates of *E. huxleyi* (Riebesell and Tortell, 2011), it is still not understood how changing calcification rates are reflected in coccolith size, weight, and exocytosis rate (i.e. the number of coccoliths formed and egested per day). Such knowledge is, however, urgently needed in case morphometric data originating for example from sediment cores is used to reconstruct calcification rates within the water column. The influence of changing carbonate chemistry on the appearance of coccolith malformations in *E. huxleyi* is better understood (Langer et al., 2010; 2011) but key questions such as for example which carbonate chemistry parameter is actually causing malformations are still unknown.

The study presented here aims to improve our understanding on the following three research questions. 1) Does morphology (size and weight) of *E. huxleyi* coccoliths change in response to changing carbonate chemistry conditions? 2) Are potential changes in morphology reflected in calcium carbonate production rates? 3) Which particular carbonate chemistry parameter(s) drive potential changes in *E. huxleyi* coccolith morphology? In order to address these questions, we evaluated samples for *E. huxleyi* coccolith size, weight and malformation from five culture experiments with a large diversity of carbonate chemistry conditions. This

diversity allowed us to disentangle the carbonate system and assess which of the carbonate system parameters that can directly influence the cell physiology (i.e. CO_2, HCO_3^-, CO_3^{2-} and H^+) are responsible for possible changes in the morphology of coccoliths formed by *E. huxleyi*.

6.3 Material and methods

6.3.1 Basic experimental settings

Five experiments were conducted with monospecific cultures of the coccolithophore *Emiliania huxleyi* strain PML B92/11 (morphotype A), isolated in 1992 at the field station of the University of Bergen (Raunefjorden; 60°18' N, 05°15'E). At this site, *E. huxleyi* usually blooms during late spring at typical surface water temperatures between 10-12°C (e.g. Schulz et al., 2008). All experiments are generally similar in their design. Differences between them are exclusively manifested in the carbonate chemistry parameters of the culture medium (see section 6.3.2).

All experiments were conducted with dilute batch cultures (LaRoche et al., 2010) at 15 °C and 150 μmol photons m^{-2} sec^{-1} incident photon flux density in a 16/8 light/dark cycle. The growth medium was artificial seawater, prepared as described in Kester et al. (1967) but without the addition of $NaHCO_3$. The artificial seawater medium (free of dissolved inorganic carbon (DIC) and total alkalinity (TA)) was enriched with ~64 μmol/kg nitrate, 4 μmol/kg phosphate, f/8 concentrations for trace metals and vitamins (Guillard and Ryther, 1962), 2 ml kg^{-1} of natural North Sea water and 10 nmol kg^{-1} of SeO_2 to avoid nutrient limitation in the course of the experiments. Samples for nitrate and phosphate were 0.7 μm filtered at the beginning and the end of the experiments and measured according to Hansen and Koroleff (1999). The nutrient-enriched medium was sterile-filtered (0.2 μm) into sterile polycarbonate bottles where the carbonate system was adjusted (see following section). Samples for carbonate chemistry measurements (~500 mL) were taken from these bottles after adjustment. The remaining medium was gently transferred into sterile 2 L polycarbonate bottles. The headspace in the 2 L bottles was kept below 5 mL. The culture medium was acclimated to 15 °C overnight to avoid a thermal shock when transferring the cells from the pre-cultures to bottles in which the main experiments were performed. Cells were acclimated to the carbonate chemistry conditions of the main experiment for at least 7 generations prior to inoculation.

6.3.2 Carbonate chemistry manipulations

The experiments only differed with respect to the carbonate chemistry manipulation of the culture medium. In the first experiment, cells were cultured at constant total alkalinity (2320 ±22 μmol kg^{-1}) and varying fCO_2 levels, ranging from ~20 to ~5960 μatm. Here, DIC and TA levels were adjusted by adding calculated amounts of Na_2CO_3 and hydrochloric acid (3.571 mol L^{-1}, certified by Merck) (Gattuso et al., 2010). In the second, third and fourth experiment, pH was kept constant at pH_f (free scale) 7.74 (±0.004), 8 (±0.01), and 8.34 (±0.008), while fCO_2 was increased from ~100 to ~3600, from ~40 to 3650, and from ~21 to ~1163 μatm, respectively. Carbonate chemistry in the constant pH approaches was adjusted by adding 2 mmol kg^{-1} of 2-[-4-(2-Hydroxyethyl)-1-piperazinyl]-ethanesulfonic acid (HEPES) to the culture medium which was adjusted to the target pH_f levels. DIC was added as $NaHCO_3$. The small change in pH in the HEPES buffered seawater medium due to $NaHCO_3$ addition was compensated by adding small amounts of strong NaOH or HCl. In the fifth experiment, fCO_2 was kept constant (430 ±47 μatm), while DIC ranged from ~500 to 4100 μmol kg^{-1}. DIC and fCO_2 were adjusted by adding calculated amounts of Na_2CO_3 and hydrochloric acid (Gattuso et al., 2010). For an overview of carbonate chemistry conditions in all treatments see Fig. 6.1 and table 6.1. Note that each culture bottle is considered as individual treatment in our data analysis and the error given in Fig. 6.1 and table 6.1 denotes the change of the carbonate chemistry within the culture bottle from the beginning to the end of the experiment.

6.3.3 Carbonate chemistry sampling and measurements

Samples for TA measurements were filtered (0.7 μm), poisoned with a saturated $HgCl_2$ solution (0.5‰ final concentration) and stored at 4°C until measurements. TA was measured in duplicate applying a two-stage potentiometric open cell titration (Dickson et al., 2003) and corrected with certified reference material (Prof. A. Dickson, La Jolla, CA). Some TA samples of the constant CO_2 experiment were higher than ~4700 μmol kg^{-1} and had to be diluted in order to get reliable results. Therefore, these TA samples were mixed with double de-ionised water, containing no alkalinity. The ratio of double de-ionised water relative to the TA sample was determined on a balance (Sartorius) with a precision of +- 0.01 g. (2001). In most treatments of the constant pH experiments, DIC was either too high or too low to be measured according to Stoll et al. (2001). To solve this problem, sample medium was mixed with artificial seawater of known DIC concentration. The ratio of the mixing solvent to the original DIC sample was determined by first weighing the mixing solvent alone and in a second step the mixing solvent plus the original DIC sample on a balance with a precision of ±0.01 mg (Sartorius).

	DIC	213	169	217	315	347	339	913	900	920	2027	2028	2023	4071	4048	4058	7376	7364	7356
	fCO_2	104	83	106	152	167	162	445	439	451	1002	1004	1004	1956	1949	1953	3601	3616	3591
	pH_f	7,74	7,74	7,74	7,75	7,75	7,75	7,74	7,74	7,74	7,74	7,74	7,74	7,75	7,75	7,75	7,74	7,74	7,74
	HCO_3^-	201	160	205	298	329	321	865	852	871	1920	1920	1916	3853	3832	3841	6983	6972	6964
	CO_3^{2-}	7	6	8	11	12	12	32	31	32	70	70	70	145	143	144	258	256	257
	$\Omega_{calcite}$	0,18	0,14	0,18	0,27	0,29	0,29	0,76	0,75	0,76	1,67	1,66	1,66	3,45	3,42	3,43	6,15	6,1	6,13
	weight	**	**	**	**	**	**	1.43 (1.03)	1.20 (0.48)	1.46 (1.06)	1.80 (1.26)	1.52 (0.83)	1.69 (1.28)	2.96 (2.18)	3.47 (3.05)	2.86 (1.85)	1.57 (1.10)	1.65 (0.77)	1.87 (1.60)
	DSA	*	*	*	*	*	*	8.1 (1.68)			9.32 (1.92)			10.05 (2.13)			9.54 (2.20)		
pH= 7.7 constant	malformation							0.44 (0.09)			0.41 (0.20)			0.35 (0.09)			0.45 (0.16)		
	DIC	148	300	351	486	705	808	1430	1817	2283	2879	3417	4025	5249	5624	7360	8994	12360	14085
	fCO_2	41	79	95	129	190	221	388	494	608	788	912	1061	1401	1511	1940	2380	3230	3657
	pH_f	7,98	8	7,99	8	7,99	7,98	7,99	7,99	8	7,98	8	8	8	7,99	8	8	8	8,01
	HCO_3^-	138	274	326	451	655	751	1329	1689	2120	2677	3173	3735	4874	5224	6830	8348	11466	13061
	CO_3^{2-}	9	18	21	30	43	48	87	110	141	173	210	250	322	343	457	557	774	887
	$\Omega_{calcite}$	0,21	0,43	0,51	0,71	1,03	1,16	2,06	2,62	3,35	4,12	5	5,96	7,69	8,19	10,9	13,27	18,44	21,14
	weight	**	**	**	1.34 (0.90)	1.47 (1.30)	1.71 (1.85)	2.13 (1.54)	2.05 (1.81)	1.95 (1.50)	2.23 (1.15)	2.17 (1.54)	2.30 (1.67)	2.27 (1.45)	2.29 (1.41)	2.30 (1.87)			
	DSA	*	*	*	5.46 (1.12)	6.81 (1.19)	9.11 (1.75)		10.76 (2.25)		10.77 (2.45)		10.69 (2.40)		11.51 (2.54)		11.14 (2.22)		10.00 (2.30)
pH= 8 constant	malformation				****	0.39 (0.13)	0.34 (0.12)		0.30 (0.12)		0.29 (0.06)		0.31 (0.10)		0.34 (0.12)		0.34 (0.12)		0.37 (0.17)
	DIC	199	179	194	894	899	898	2247	2250	2252	3922	3925	3934	6684	6681	6674	9917	9938	9962
	fCO_2	24	21	22	103	102	102	257	257	256	442	443	444	741	741	738	1155	1160	1163
	pH_f	8,32	8,33	8,33	8,33	8,34	8,34	8,34	8,34	8,34	8,34	8,34	8,34	8,35	8,35	8,35	8,33	8,33	8,33
	HCO_3^-	173	155	168	778	781	781	1955	1957	1957	3406	3410	3418	5794	5792	5784	8643	8663	8685
	CO_3^{2-}	24	22	24	112	114	113	283	284	285	499	499	500	862	861	862	1231	1231	1234
	$\Omega_{calcite}$	0,58	0,53	0,58	2,67	2,71	2,7	6,75	6,76	6,79	11,9	11,89	11,92	20,54	20,53	20,54	29,34	29,35	29,42
	weight	**	**	**	1.57 (0.40)	2.08 (1.22)	1.72 (0.59)	2.24 (0.57)	2.35 (0.56)	2.09 (0.30)	2.44 (0.60)	2.59 (0.62)	1.91 (0.47)	2.57 (0.56)	2.28 (0.57)	2.14 (0.47)	4.23 (1.31)	3.05 (0.77)	3.47 (0.85)
	DSA	***	***	***	6.42 (1.17)			10.14 (2.02)			9.83 (2.06)			9.93 (2.10)			10.10 (2.02)		
pH= 8.3 constant	malformation				0.36 (0.10)			0.34 (0.10)			0.30 (0.07)			0.31 (0.12)			0.37 (0.13)		
	DIC	545	535	520	822	828	829	1159	1184	1181	1913	1910	1912	4117	4107	4112			
	fCO_2	451	382	321	481	481	492	465	474	463	407	404	407	415	407	408			
	pH_f	8	8	8	8	8	8	8	8	8	8	8	8	8	8	8			
	HCO_3^-	517	508	494	780	785	787	1093	1116	1112	1754	1750	1753	3531	3515	3519			
	CO_3^{2-}	11	13	14	24	24	24	49	50	51	144	144	144	571	577	577			
	$\Omega_{calcite}$	0	0	0	1	1	1	1	1	1	3	3	3	14	14	14			
	weight	**	**	**	1.07 (0.60)	**	**	1.65 (1.42)	2.41 (1.56)	1.35 (1.07)	1.84 (1.20)	1.78 (1.38)	1.74 (0.87)	1.85 (1.10)	2.09 (1.44)	1.91 (1.47)			
	DSA	*	*	4.59 (0.98)	7.49 (1.73)			8.32 (1.76)			9.61 (1.78)			10.62 (2.27)					
CO_2 constant	malformation			****	0.46 (0.15)			0.34 (0.19)			0.30 (0.12)			0.29 (0.10)					
	DIC	1421	1612	1749	1854	1942	1996	2064	2105	2131	2175	2192	2227	2236	2283	2328	2375	2459	2514
	fCO_2	20	50	89	140	209	288	398	492	621	745	891	1004	1165	1791	2441	3075	4787	5494
	pH_f	9,06	8,81	8,63	8,49	8,36	8,24	8,13	8,05	7,96	7,89	7,82	7,78	7,72	7,54	7,41	7,32	7,13	7,08
	HCO_3^-	804	1125	1355	1531	1678	1776	1880	1940	1986	2040	2068	2105	2119	2166	2199	2229	2260	2290
	CO_3^{2-}	617	485	390	318	256	209	169	146	122	107	91	84	74	50	38	31	20	18
	$\Omega_{calcite}$	14,69	11,56	9,3	7,57	6,11	4,98	4,03	3,49	2,91	2,54	2,18	2,01	1,76	1,19	0,9	0,74	0,49	0,43
	weight	0.90 (0.36)	1.36 (0.59)	1.66 (0.74)	1.80 (0.78)	1.94 (0.87)	2.07 (0.98)	1.93 (0.87)	1.85 (0.98)	1.74 (0.78)	1.67 (0.71)	1.58 (0.76)	1.60 (0.71)	1.49 (0.67)	1.25 (0.50)	1.28 (0.60)	1.28 (0.50)	1.21 (0.53)	**
	DSA	5.94 (1.07)	6.77 (1.28)	8.93 (1.86)			9.32 (2.00)			9.93 (2.47)			9.74 (2.06)			8.00 (1.63)	7.25 (1.55)	7.07 (1.50)	
TA constant	malformation	0.25 (0.09)	0.24 (0.07)	0.24 (0.06)			0.27 (0.08)			0.37 (0.16)			0.46 (0.10)			0.49 (0.14)	0.44 (0.12)	0.61 (0.15)	

Table 6.1. Overview on investigated samples. DIC, HCO_3^-, CO_3^{2-} in μmol kg^{-1}; fCO_2 in μatm; $\Omega_{calcite}$ dimensionless; weight (of coccoliths) in pg $CaCO_3$; DSA in μm^2; malformation dimensionless. The error values shown in brackets represent the standard deviation of all measured coccoliths within a treatment. Empty fields indicate that data was not collected for these treatments.

* no coccoliths found by scanning electron microscopy

** coccoliths not detectable in cross-polarized light

*** coccoliths incomplete

**** no slit present in between adjacent distal shield elements so that malformation could not be determined with the applied method

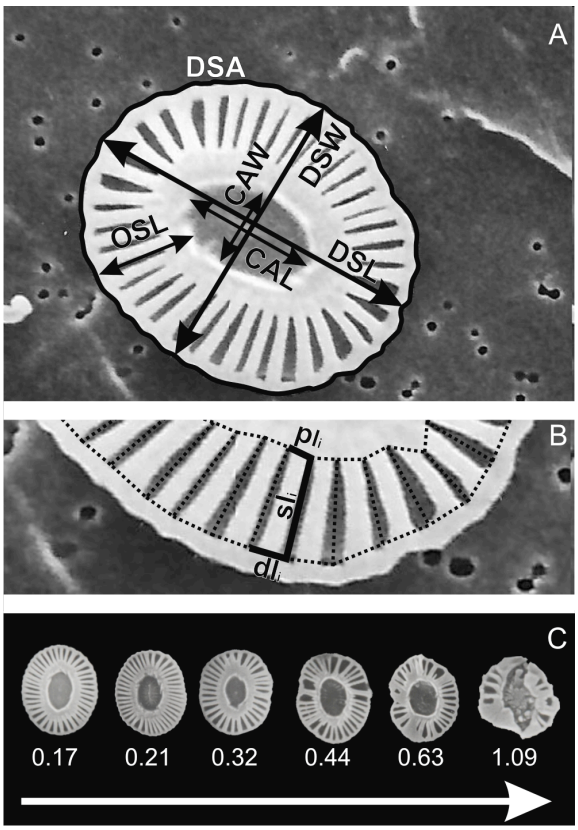

Figure 6.1. Morphological quantities measured by SEM. (A) Measured size attributes, distal shield area (DSA), distal shield length (DSL), distal shield width (DSW), central area length (CAL), central area width (CAW), and outer shield length (OSL). (B) Measurements for calculation of malformation index, proximal distance between two adjacent slits (pl), length of slit (sl), and distal distance between two adjacent slits (dl). pl, sl, and dl were measured for each slit of the investigated coccolith and then processed with eq. 6.8. (C) Examples of coccoliths with corresponding malformation calculated from eq. 6.8. The arrow indicates increasing malformation.

Samples for DIC were sterile filtered (0.2 μm) with gentle pressure and stored bubble-free at 4 °C in 4 ml borosilicate bottles. All DIC samples were measured according to Stoll et al., The

mixture was carefully rotated in a 50 mL tube with ~1 mL headspace. The ratio of sample to mixing solvent was adjusted to result in a final DIC concentration of approximately 1800 – 2200 μmol kg^{-1}. After the mixing procedure, DIC samples were processed identical to undiluted samples (see above).

Samples for pH_f were measured potentiometrically at 15°C with separate glass and reference electrodes (Metrohm) which were calibrated with reference material certified for TA and DIC with a salinity of 33.3 (Prof. A. Dickson, La Jolla, CA). pH_f of the reference material was calculated from certified TA and DIC applying the constants of Roy et al. (1993). Measured electromotive force (E) of the samples and standards were used to calculate the pH_f of the sample as

$$\mathrm{pH_f} = \mathrm{pH_{f\_ref}} + \frac{E_s - E_x}{\mathrm{R} \times \mathrm{T} \times \frac{\ln 10}{\mathrm{F}}} \tag{6.1}$$

where, pH_{f_ref} is the calculated pH_f of the certified reference material, T is the temperature of the sample in Kelvin, R is the universal gas constant, F the Farady constant and E_s and E_x are the measured electromotive forces in Volts of the standard and the sample, respectively, (Dickson et al., 2007).

6.3.4 DIC estimations

Unfortunately, we lost all DIC measurements of the constant TA experiment and the DIC measurements from the beginning of constant pH_f 8 experiment due to storage problems. The estimation of DIC of these samples is shown in detail in Bach et al. (2011) and shall be outlined only briefly in the following. DIC concentrations from the beginning of the constant pH_f 8 experiment were estimated by adding the total particulate carbon build-up which was produced during the experiment to the final DIC concentrations. Initial DIC concentrations from the constant TA experiment were calculated as:

$$\mathrm{DIC} = \frac{\mathrm{TA_{measured}} + \left(\mathrm{Volume_{acid}} \times 3.571\right)}{2} \tag{6.2}$$

where $TA_{measured}$ is the measured TA in μmol kg^{-1} at the beginning of the experiment, $Volume_{acid}$ is the volume of acid that was added in μl kg^{-1} and 3.571 is the molarity of the acid

(certified by Merck) in mol l^{-1}. This estimate has an uncertainty of approximately 40-50 μmol kg^{-1} which is small compared to the large DIC range in this experiment (Bach et al., 2011). DIC concentrations at the end of the constant TA experiment were calculated by subtracting the measured total particulate carbon build-up from the initial DIC concentrations.

6.3.5 Carbonate chemistry calculations

Carbonate chemistry conditions within experiments were calculated from temperature, salinity, inorganic phosphate concentrations and two measured (or estimated) carbonate system parameters, applying the equilibrium constants of Roy et al. (1993) and the program CO2Sys (Lewis and Wallace, 1998). Measured (or estimated) carbonate system parameters were: TA and DIC in the constant TA experiment; pH_f and DIC in the constant pH experiments; TA and pH_f in the constant CO_2 experiment. The biological response data are plotted to the mean of initial and final carbonate chemistry conditions.

6.3.6 Sampling and calculation of coccolith exocytosis rate

Sampling started two hours after the onset of the light period and lasted no longer than two and a half hours. Two samples for particulate organic carbon (POC) and two for total particulate carbon (TPC) were filtered (200 mbar) onto precombusted (5 hours, 500°C) GF/F filters and stored in the dark at -20°C. POC and TPC samples from constant pH experiments were rinsed with artificial seawater after filtration (supersaturated with respect to calcite) in order to wash off HEPES buffer which otherwise would have contributed ~40 pg of carbon to every TPC and POC measurement. POC samples were stored for two hours in a desiccator containing fuming HCl to remove all inorganic carbon and subsequently dried for ~6 hours at 60°C. TPC filters were dried in the same way as the POC filters, but in a separate oven and without prior acid treatment. Carbon concentrations of POC and TPC filters were measured using an isotope ratio mass spectrometer (Finnigan) combined with an elemental analyzer (EuroEA, Hekatech GmbH). Particulate inorganic carbon (PIC) was calculated as the difference between TPC and POC. Four POC samples from the constant pH_f 8 experiment were lost during measurements.

Cell numbers were measured at the beginning and the end of the experiment with a Coulter Counter (Beckmann). The growth rate (μ) was calculated from initial and final cell numbers as

$$\mu = \frac{\ln(t_{fin}) - \ln(t_0)}{d} \qquad (6.3)$$

where t_0 and t_{fin} is the cell number at beginning and the end of the experiment, respectively and d is the number of days the cell culture was growing. PIC production rates were calculated by multiplying μ and PIC cell^{-1}. $CaCO_3$ production rates were calculated by multiplying PIC production rates (in μmol C cell^{-1} d^{-1}) with the molecular weight of $CaCO_3$. The number of egested coccoliths per day was subsequently determined as

$$\text{coccolith exocytosis rate} = \frac{\text{CaCO}_3 \text{ production}}{\text{coccolith weight}} \tag{6.4}$$

where coccolith weight was measured as described in section 6.3.8.

6.3.7 Scanning electron microscopy (SEM)

5-10 mL of sample were filtered by gravity on a polycarbonate filters (0.2 μm pore size). Samples taken from the constant TA and the constant pH_f 8 experiment were dehydrated with ethanol and bis(trimethylsilyl)amine solution, to conserve the organic part of the cell, and subsequently dried in a desiccator (Bach et al., 2011). Samples for the other three experiments were not dehydrated and dried for 2 hours at 60°C directly after filtration. All samples were kept in the desiccator until they were sputtered with gold-palladium and processed with the scanning electron microscope.

SEM pictures were taken with a CamScan CS 44 scanning electron microscope and evaluated using the software imageJ. Measured lengths or areas on the pictures were calibrated with the size bar given on each SEM picture. Manually measured parameters on coccoliths were the surface area of the distal shield (DSA), the length of the distal shield (DSL), the width of the distal shield (DSW), the length of the central area (CAL) and the width of the central area (CAW) (compare Fig. 6.1A). CAL and CAW could not be determined in case the coccolith was lying upside down on the filter. In average, 82 coccoliths per sample were investigated for DSA, DSL and DSW and 36 for CAL and CAW. Note that not all treatments could be investigated with SEM due to the extremely elaborate manual evaluation. Evaluated treatments are shown in table 1.

Measured DSA was compared to an estimated value calculated from DSL and DSW as

$$calculated\ DSA = \pi \times \frac{DSL \times DSW}{4} \tag{6.5}$$

assuming an elliptical shape of the coccolith. The outer shield length (OSL) was calculated as

$$OSL = \frac{DSL - CAL + DSW - CAW}{4} \tag{6.6}$$

6.3.8 Determination of coccolith weight by birefringence

5-10 ml of sample were filtered with ~100 mbar on a cellulose nitrate filter (0.45 μm pore size). Filters were dried for 2 hours at 60°C and subsequently embedded with Acrifix 192 (Roehm) on microscope slides. Acrifix makes cellulose nitrate filters transparent without damaging the coccoliths and has a refraction index of 1.44 so that it does not interfere with the optical analysis.

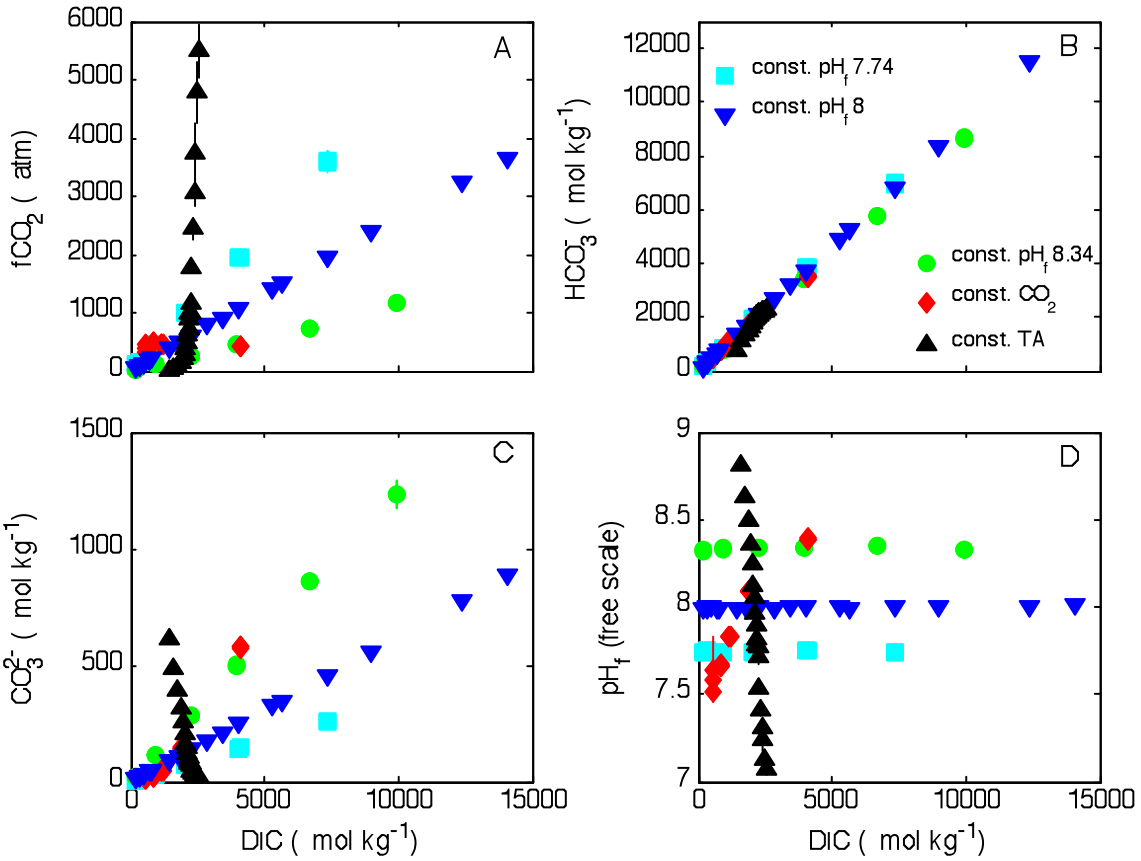

Figure 6.2. Carbonate chemistry speciation in relation to DIC. Error bars denote the change in carbonate chemistry from the beginning to the end of the experiment. Note that error bars are in most cases masked by symbol size. (A) fCO_2 (B) HCO_3^- (C) CO_3^{2-} (D) pH_f. Symbol and colour coding is shown in panel B.

Images of coccoliths were taken with a Leica DM6000B light microscope equipped with a SPOT Insight b/w camera. Under cross-polarized light only the birefringent calcite of the coccoliths is illuminated. 200 images were randomly taken per sample and analyzed with the software SYRACO (Beaufort and Dollfus, 2004). The software identifies *E. huxleyi* coccoliths and measures the grey level for each pixel. Coccolith weight was subsequently calculated from measured grey level following Beaufort et al., (2008). On average, ~500 coccoliths were evaluated for each sample.

6.3.9 Calculation of malformation

Coccolith malformation has been defined as 'irregular coccolith formation as a result of departure from the normal growth process' and is commonly expressed in reduced symmetry or altered shape of individual elements (Young and Westbroek, 1991). In order to meet the demands given in this definition, fine-scale morphological structures of individual coccoliths were measured and subsequently used in an algorithm to quantify the degree of malformation. The measured morphological quantities comprised vectors associated to the openings between distal shield elements (slits). These were: (1) the distances between the distal ends of two adjacent slits (dl). 2) the distances between the proximal ends of two adjacent slits (pl). 3) The length of each slit (sl) (compare Fig. 6.1B). Incomplete coccoliths were not measured.

In general, regular and repetitive structures like the individual elements composing a coccolith appear to be malformed in case these adjacent structures differ in an irregular manner. Malformations are therefore characterized in the evaluation procedure as the degree of asymmetry of adjacent slits.

The algorithm to calculate the malformation index makes use of the average deviation. It is defined as:

$$\text{Average deviation} = \frac{1}{n}\sum_{i=1}^{n}\left|x_i - mean(x)_n\right| \tag{6.7}$$

where n is the number of all measured elements, x_i is a measured element and $mean(x)_n$ is the mean value of all measured elements. Using the *average deviation* has the advantage that it is not influenced by the number of measured elements. Hence, the malformation index is not sensitive to the number of distal shield elements of the investigated coccolith. Applying the *average deviation* the degree of malformation is calculated as:

$$Malformation = \frac{1}{n}\sum_{i=1}^{n}\left|\frac{|dl_i - dl_{i+1}|}{\frac{1}{2}(dl_i + dl_{i+1})} - mean\left(\frac{|dl_i - dl_{i+1}|}{\frac{1}{2}(dl_i + dl_{i+1})}\right)_n\right| + \frac{1}{n}\sum_{i=1}^{n}\left|\frac{|sl_i - sl_{i+1}|}{\frac{1}{2}(sl_i + sl_{i+1})} - mean\left(\frac{|sl_i - sl_{i+1}|}{\frac{1}{2}(sl_i + sl_{i+1})}\right)_n\right| \ldots$$

$$+ \frac{1}{n}\sum_{i=1}^{n}\left|\frac{|pl_i - pl_{i+1}|}{\frac{1}{2}(pl_i + pl_{i+1})} - mean\left(\frac{|pl_i - pl_{i+1}|}{\frac{1}{2}(pl_i + pl_{i+1})}\right)_n\right| \quad (6.8)$$

where *dl*, *sl* and *pl* are the measured quantities of the distal shield elements (see above) and *n* is the total number of slits. In this way, higher values calculated from eq. 6.8 reflect increased malformation (Fig. 6.1C). In average, 27 coccoliths were evaluated per sample with eq. 6.8.

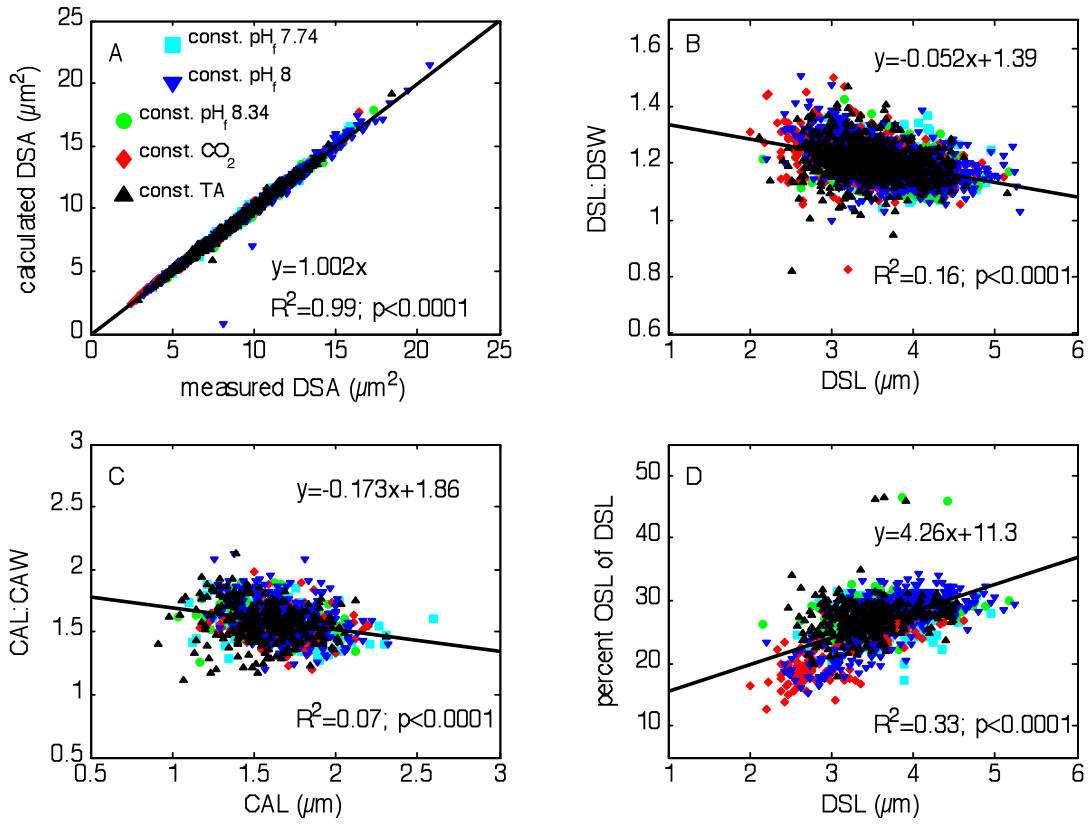

Figure 6.3. Morphology of coccoliths. Each data point represents an individual coccolith. (A) Correlation between measured DSA and DSA calculated from DSL and DSW using eq. 6.4. (B) Aspect ratio of distal shield with increasing DSL. (C) Aspect ratio of central area with increasing CAL. (D) Percentage of OSL that contributes to the total DSL. Symbol size and colour coding is shown in panel A.

6.4 Results

6.4.1 Carbonate chemistry

A large diversity of carbonate chemistry conditions was set up in the five experiments presented in this study. In each one of the five experiments, one particular carbonate system parameter was kept constant while all the others changed with increasing DIC (Fig. 6.2). In the constant TA experiment, fCO_2 and $[HCO_3^-]$ increased, while pH and $[CO_3^{2-}]$ decreased with increasing DIC. The carbonate system manipulation of this experiment is similar to the way seawater carbonate chemistry is currently changing due to anthropogenic CO_2 invasion. In the three constant pH experiments, all carbonate system parameters except for pH_f were increasing linearly with increasing DIC. pH_f remained constant in all of these experiments but at different levels. In the constant CO_2 experiment, all carbonate system parameters except for CO_2 were increasing with DIC.

6.4.2 General morphological features

Measured and calculated DSA are in excellent agreement to each other. The slope of the linear regression is close to one which shows that DSA can reliably derived from DSL and DSW (Fig. 6.3A). The aspect ratio of the coccolith (i.e. DSL:DSW) gets closer to one with increasing coccolith length, indicating that larger coccoliths are rounder than smaller ones (Fig. 6.3B). The same trend was found for the aspect ratio of the central area. The larger the central area became, the rounder it was (Fig. 6.3C) which is in good agreement with results obtained by Young and Westbroek (1991). The relative contribution of OSL to total DSL increased with increasing DSL (Fig. 6.3D).

6.4.3 Malformation

Malformations of coccoliths correlated best to seawater pH_f, indicating a key influence of H^+. Malformations remained relatively stable above a pH_f of about 8 whereas they increased with decreasing pH_f in the range from ~8 down to 7.1 (Fig. 6.4). $CaCO_3$ production rates did not correlate with malformations (data not shown) suggesting that the appearance of malformations is not coupled to calcification rates in *E. huxleyi*.

6.4.4 Coccolith size

Changes in DSA, DSL and DSW in response to varying carbonate chemistry conditions were largely identical to each other. All three parameters increased most pronounced in the range

from low to intermediate [HCO_3^-] or fCO_2 whereas changes were minor above this threshold in all except the constant TA experiment where a decreasing trend above ~1000 μatm was observed (Fig. 6.5A-D; data for DSW not shown).

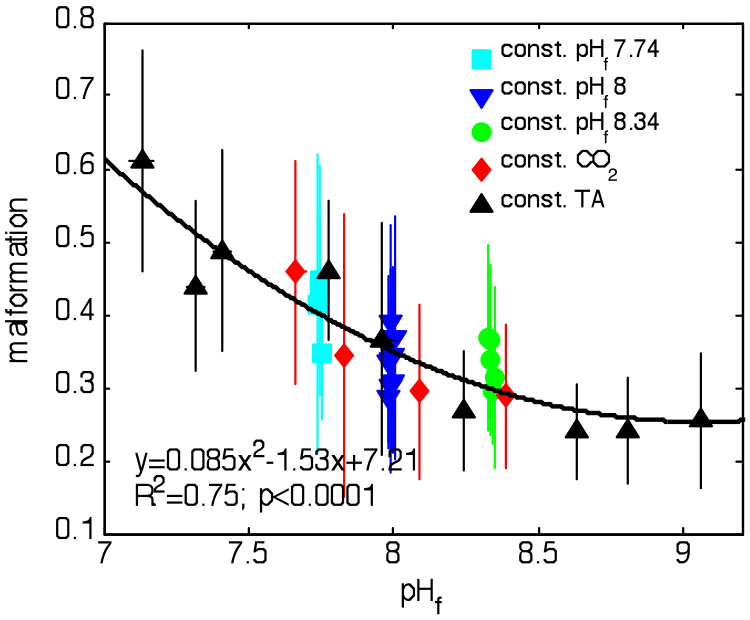

Figure 6.4. Malformation of coccoliths calculated with eq. 6.8. Error bars denote the standard deviation from measured mean malformation of all coccoliths of a treatment.

The smallest coccoliths were measured at very low HCO_3^- of ~500 μmol kg^{-1} (Fig. 6.5; Table 6.1). These carbonate chemistry conditions are unrealistically low and most likely rarely existed in the natural habitat of *E. huxleyi* since its appearance about 270 ky ago. Hence, sizes determined in these particular treatments should be considered as physiological potentials rather than realistic representations of naturally occuring *E. huxleyi* coccolith sizes. Variations in size were minor within a realistic DIC and fCO_2 range of the last 270 kyears (i.e. from present conditions down to about 1800 μmol kg^{-1} and 180 μatm, respectively). DSA for example, varied from about 8 to 9 μm^2 and showed no clear trend within that range if all experiments are considered. Note, however, that DSA increases in the constant TA experiment which simulates ocean acidification, from ~180 to 650 μatm by about 10% and starts to decrease slightly above this threshold.

CAL and CAW remained largely unaffected by changing carbonate chemistry except for the very lowest fCO_2 levels in the constant TA experiment (below ~100 μatm) where they showed a decreasing tendency (Fig. 6.5E and F).

6.4.5 Coccolith weight and production

The mean weight of coccoliths increased by approximately 100% from lowest to highest $CaCO_3$ production rates (estimated from linear fit). Measured mean weight ranged from ~1 to 4 pg (Fig. 6.6A) which is in reasonable agreement with previous estimates of ~2 pg for the same *E. huxleyi* morphotype (Fagerbakke et al., 1994; Young and Ziveri, 2000). The coccolith exocytosis rate also increased with $CaCO_3$ production by an estimated 100%, similar as for coccolith weight. Minimum and maximum calculated coccolith exocytosis rates were ~12 and 45 coccoliths $cell^{-1}$ d^{-1}, respectively (Fig. 6.6B). Changes in coccolith weight correlate with changes in coccolith size (Fig. 6.6C).

In the three highest DIC treatments of the constant pH 8 experiment, mean coccolith weight was up to 8 pg which seems unrealistically high. After careful re-evaluation of SEM samples we occasionally found coccoliths that were associated with cubic crystals of unknown material. This might have caused interference with the coccolith weight estimation. Since we could not find a concomitant increase in the $CaCO_3$ content per cell we expect these values to be the result of non-biological processes.

6.5 Discussion

6.5.1 Comparison of different evaluation methods of malformations

Malformations of coccoliths in response to changing carbonate chemistry conditions have been observed in several coccolithophore species (e.g. Riebesell et al. 2000; Langer et al. 2006; Müller et al. 2010). In case these malformations were quantified, it was done by visual comparisons of individual coccoliths and subsequent classifications to fixed categories like for example ‘normal’, ‘slightly malformed’, ‘strongly malformed’, and ‘incomplete (Langer et al. 2006; Kaffes et al., 2010; Langer et al., 2011; Bach et al. 2011). Here, we propose an alternative method to approximate malformations of *E. huxleyi* which aims to quantify malformations by direct measurements of fine-scale morphological structures (see section 6.3.9). A direct comparison of both methods shows that they both lead to similar conclusions. Bach et al. (2011) have visually evaluated the same samples of the constant TA and the constant pH_f 8 experiment as used in this study and concluded ‘that malformations are mainly induced by seawater pH_f below ~8. This is largely confirmed by the results from the evaluation of malformation by eq. 6.8 (Fig. 6.4) indicating that both methods seem to be equally appropriate to evaluate malformations of *E. huxleyi*. The application of these two methods reveals distinct advantages of each one of them. Visual evaluations can be done ‘online‘ during scanning of the sample by electron microscopy whereas measurements of

morphological structures require a time-intensive analysis of pictures taken by the microscope after having scanned the sample.

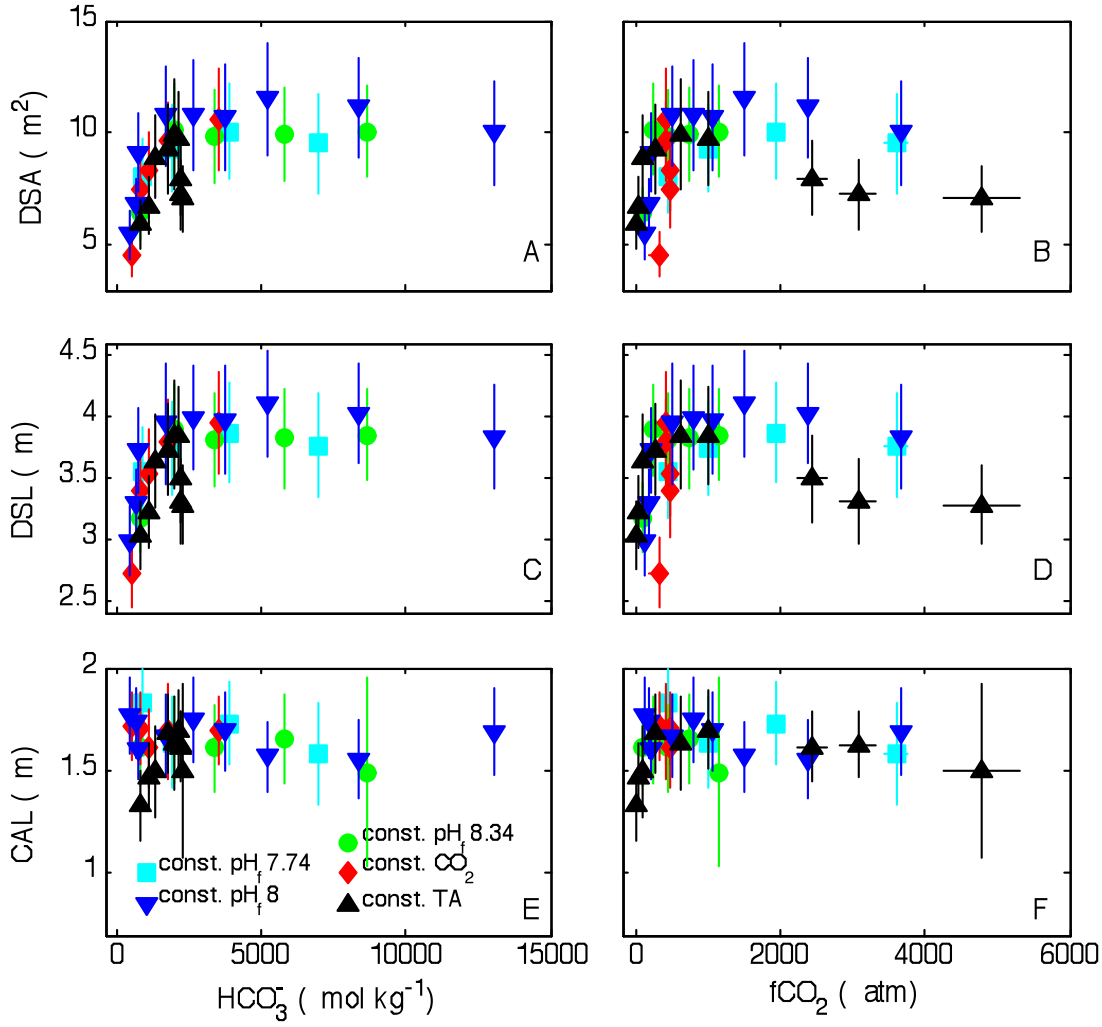

Figure 6.5. Coccolith size (DSA, DSL, and DSW) as a function of carbonate chemistry speciation. (A, C, E) in relation to HCO_3^-. (B, D, F) in relation to fCO_2. Symbol size and color coding shown in panel E. Error bars denote the standard deviation from measured mean size of all coccoliths of a treatment.

Hence, visual evaluations facilitate analysis of high number of coccoliths per treatment and therefore usually lead to an investigation of a more representative sample size. (Typically 350 evaluated coccoliths per sample with visual evaluations (e.g. Langer et al., 2011) in contrast to 27 evaluated coccoliths with the new method presented in our study.) Furthermore, visual evaluations are easy to adapt to all coccolithophore species whereas quantification of malformations by direct measurements of morphological structures can so far only be applied to complete coccoliths from *E. huxleyi* morphotype A (including var. corona), B, C, and O while it cannot be applied to morphotype R since there are

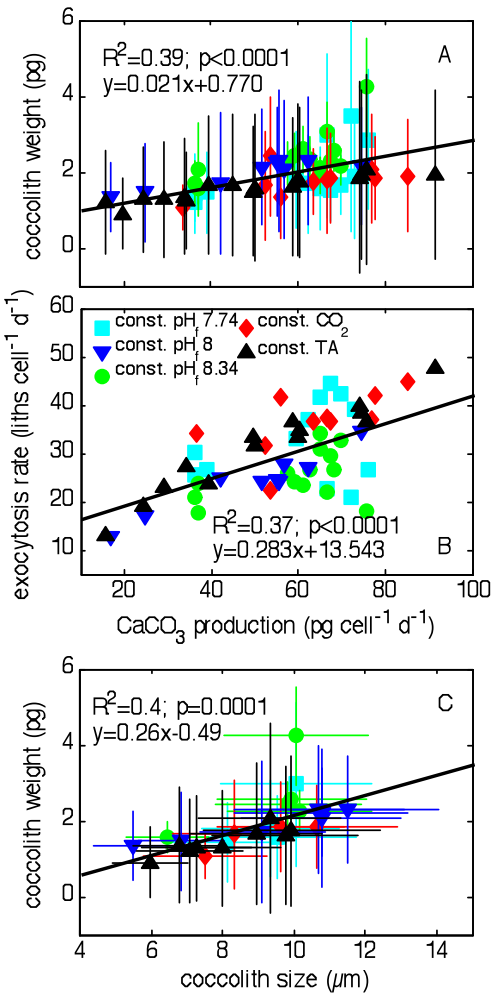

Figure 6.6. Coccolith weight, production and size. (A) Correlation between cellular $CaCO_3$ production rate and mean coccolith weight. (B) Correlation between cellular $CaCO_3$ production rate and the number of coccoliths formed per day. (C) Correlation between coccolith size and weight. Error bars denote the standard deviation from measured mean weight or size of all coccoliths of a treatment. Regression line shows a fit through data from all experiments with fit equation and significance given in the figure. Note that the correlation does not apply equally well for individual experiments.

usually no slits between two adjacent distal shield elements in the latter (for morphotype taxonomy see Young et al., 2003; Hagino et al., 2011). Although adaption of eq. 6.8 to other species or morphotype R is generally possible, it would require measurements of other fine scale structures than the ones used in *E. huxleyi*. The major advantage of the new method is the reduction of subjectivity. A direct measurement of morphological structures reduces human influence on the measurement and makes it easier to compare with results of other studies. Furthermore, eq. 6.8 could be implemented in an evaluation software which would analyze malformations automatically. This would be the most efficient and the most reproducible way to quantify malformations.

6.5.2 Cause of malformations

Malformations of *E. huxleyi* coccoliths are most likely induced by high concentrations of H^+ (Fig. 6.4). In order to understand how excess seawater [H^+] could interfere with coccolith formation, it may be helpful to consider the development of a coccolith on a cellular basis. The formation takes place in a Golgi-derived vesicle (coccolith vesicle or 'CV') which is closely associated with a labyrinthine membrane system (reticular body). Coccolith formation is initiated inside the CV with the production of an organic base plate which serves as template (van der Wal et al., 1983; Westbroek et al., 1984; 1989; Young et al., 1999). Nucleation of calcite occurs subsequently on the rim of the organic base plate from where the initial crystals start to grow in a radial direction until coccolith formation is completed (Westbroek et al., 1984, 1989; Young et al., 1992). Crystal growth is tightly controlled by the cellular machinery. The inner side of the CV membrane always remains in close contact with the coccolith and is actively expanded from the outside by the cytoskeleton located within the cytosol so that the growing calcite crystals fill the space defined by the expanding vesicle (Westbroek et al., 1984; 1989; Didymus et al., 1994, Marsh et al., 1994 Young et al., 2009). Inside the CV, coccolith-associated polysaccharides (CAPs) bound to the inner side of the membrane, have a crucial role in controlling $CaCO_3$ precipitation due to their potential to bind Ca^{2+} (De Jong et al., 1976) and inhibit precipitation at places where they cover the calcite (Borman et al., 1982; Henriksen et al., 2004).

Considering the pathway described above, the cytoskeleton and CAPs seem to be two major cellular components controlling the correct growth of calcite crystals within *E. huxleyi* (Young et al., 1999; Langer et al., 2006). Langer et al., (2010) examined in detail the consequences of a malfunctioning of the cytoskeleton on coccolith formation by applying chemical inhibitors for microtubules and actin filaments. They found an increasing degree of coccolith malformation, the more these cytoskeleton structures and therefore the active expansion of the CV was disturbed by these inhibitors. Possibly, malformations found in our study are also resulting from a malfunctioning of the cytoskeleton, in our case with the chemical driving force being H^+. This explanation seems plausible since H+ is known to easily enter into the cytosol of *E. huxleyi* (Suffrian et al., 2011). Here, a change in [H^+] could disturb the correct functioning of cytoskeleton elements or the enzymes associated with them so that the controlled expansion of the CV is handicapped (Langer et al., 2006).

The second possible option of a negative effect of H^+ on crystal growth is a disturbance of CAPs inside the CV (Langer et al., 2006; 2011). Henriksen and Stipp (2009) demonstrated that the capability of CAPs to bind onto calcite crystals depends on the ion composition of the solution in which CAPs are dissolved. A change of the ion composition inside the CV may therefore disturb controlled crystal growth. Such a change could be the direct consequence

of a change in [H^+] inside the CV in case H^+ can somehow enter this compartment. Ion composition inside the CV could, however, also indirectly be altered by changing [H^+] in the cytosol assuming that H^+ gradients between the cytosol and the CV potentially drive numerous transport processes of major ions such as Ca^{2+} or Mg^{2+} (Langer et al., 2006; Mackinder et al., 2010; 2011).

The prominent influence of [H^+] on malformations observed in the investigated *E. huxleyi* strain raises the question whether this particular carbonate chemistry parameter is also responsible for observed malformations in other coccolithophore species and *E. huxleyi* strains. Langer and Bode (2011) examined coccolith malformation of *Calcidiscus leptoporus* in response to various carbonate system parameters. In contrast to our findings, they identified CO_2 as the key carbonate chemistry parameter causing malformations which suggests that the control mechanisms of coccolith formation are affected by different carbonate system parameters on a species level. A comparison on the strain level is not possible because there is no such data on different strains of the same species available so far. The only information available at the moment is that the carbonate chemistry conditions at which malformations start to appear differ between different strains of *E. huxleyi* (Langer et al., 2011). Clearly, this does not mean that the key carbonate chemistry parameter causing malformations differs between *E. huxleyi* strains but it shows that sensitivities to changes in carbonate chemistry do.

6.5.3 Influence of individual carbonate chemistry parameters on coccolith size

There is experimental evidence that HCO_3^- is the principal inorganic carbon source utilised for calcification (Sikes et al., 1980; Buitenhuis et al., 1999). The dependence of calcification on HCO_3^- seems to be reflected in DSA, DSL, and DSW which increased comparably in all experiments from low to high [HCO_3^-] up to ~2000 μmol HCO_3^- kg^{-1}. The close correlation to [HCO_3^-] makes this ion a key candidate responsible for at least some of the pronounced increase in DSA, DSL, and DSW observed within that range (Fig. 6.5A-D; data for DSW not shown). Next to HCO_3^-, H^+ is another factor with potential influence. H^+ might be particularly important in the high fCO_2 range of the constant TA experiment. Here, the observed decrease in size cannot be explained by [HCO_3^-] since the concentration of this ion is still increasing whereas DSA, DSL, and DSW are already decreasing (Fig. 6.5D). A potential negative effect of very high [H^+] seems possible since H^+ has already been shown to be detrimental to calcification rates above certain thresholds (Bach et al., 2011). In contrast to HCO_3^- and H^+, the influence of CO_2 is of minor importance (Fig. 6.5A-D; data for DSW not shown). DSA, DSL, and DSW clearly decreased in the constant CO_2 experiment. If CO_2 was of primary importance in determining these morphological parameters, then DSA, DSL, and

DSW would have remained constant in the constant CO_2 experiment. The fourth parameter with possible influence is CO_3^{2-}. CO_3^{2-} is of high importance for the dissolution of calcite due to its influence on the calcium carbonate saturation state of seawater. Whether it is of direct physiological influence on coccolith formation is more difficult to assess because relatively little is known about the possibilities of cells to transport CO_3^{2-} across membranes. Such transporters have so far not been identified (Mackinder et al., 2010). In our study, a differentiation between HCO_3^- and CO_3^{2-} is only possible in the constant TA experiment because they positively correlate in all others (Fig.6.1). In the constant TA experiment, DSA, DSL and DSW correlate with [HCO_3^-] and not [CO_3^{2-}] in the low fCO_2 range. This indicates that increasing [CO_3^{2-}] is not likely to be responsible for increasing DSA, DSL and DSW.

CAL and CAW displayed no clear change in response to changing carbonate chemistry except for the very low fCO_2 range in the constant TA experiment where they tended to decrease (Fig. 6.5F, data for CAW not shown). As discussed in section 4.2, coccolith formation starts with the construction of an organic base plate on which calcite crystals start to grow in a radial direction. The dimensions of the central area of the coccolith largely reflect the dimensions of the organic base plate (Westbroek et al., 1984; Young, 1994). Hence, if the dimensions of the central area are affected to a lesser extent by changing carbonate chemistry, so are the dimensions of the organic base plate. Accordingly, we hypothesize that changing carbonate chemistry primarily influences crystal growth and not so much formation and size of the organic base plate.

6.5.4 Correlation between calcification rates and coccolith weight

Changes in cellular calcification rates can be expressed in three different ways. 1) A change in coccolith weight at constant coccolith exocytosis rate. 2) A change in coccolith exocytosis rate at constant coccolith weight. 3) A simultaneous change in coccolith weight and exocytosis rate. Results presented in Fig. 6.6A and B support the third option, indicating that a correlation between calcification rates and coccolith weight exists in the investigated *E. huxleyi* strain. This suggests that measurements of coccolith weight could potentially be useful to reconstruct calcification rates. Nevertheless, this correlation bears uncertainties which should be considered before extrapolating these results to the field. There is the high genetic variability between different coccolithophore species and even strains of the same species (e.g., Brand et al., 1982; Westbroek and Young, 1991; Iglesias-Rodriguez et al., 2006). It has been demonstrated that this variability translates in species- and strain-specific sensitivities of calcification rates to simulated ocean acidification (Langer et al., 2006, 2009). Genetically based differences in sensitivities to changes in carbonate chemistry could also be reflected in strain- and species-specific coupling between $CaCO_3$ production and coccolith

weight. On the other hand, differences in sensitivities within a certain fCO_2 range do not necessarily result in a fundamentally different response if the whole fCO_2 range at which the strain is able to calcify is considered. It has been speculated that the general response of presumably all *E. huxleyi* strains to a very broad fCO_2 range is similar (resembling an optimum curve), even though there are strain-specific differences within distinct parts of the whole optimum curve (Bach et al., 2011). Therefore, it seems feasible that the positive physiological correlation between $CaCO_3$ production rates and coccolith weight that has been found for the investigated *E. huxleyi* strain also emerges in other strains and possibly even in other coccolithophore species at least when a very wide range of carbonate chemistry conditions is investigated.

Another factor to consider is the driving force that causes changes in $CaCO_3$ production rates and coccolith weight. Aside from carbonate chemistry, temperature can influence $CaCO_3$ production. A temperature rise from 10 to 20°C increases $CaCO_3$ production rates in *E. huxleyi* by more than 40% under ambient carbonate chemistry conditions (Langer et al., 2007) whereas it influences coccolith size (and therefore most likely also coccolith weight) only marginally (Watabe and Wilbur, 1966; Fielding et al., 2009). Under this consideration it seems possible that the physiological coupling between $CaCO_3$ production and coccolith weight is not universal but rather specific for changes induced by the carbonate chemistry conditions.

Furthermore, it is important to keep in mind that the correlation between coccolith weight and $CaCO_3$ production rates given in Fig. 6.6A is derived from monoclonal culture experiments which exclude ecological processes. This is a limitation of the correlation because in a natural *E. huxleyi* assemblage, changing carbonate chemistry could not only directly affect the cell physiology but also induce a shift in the dominant strain. A strain shift in a natural assemblage can change both, mean calcification rate and mean coccolith weight but these two factors do not necessarily have to be correlated to each other as implied in Fig. 6.6A. The unknown role of ecological processes should therefore clearly be considered before using the correlation between calcification rates and coccolith weight to interpret field data.

6.5.5 Environmental control of coccolith size and weight

There are two different mechanisms how an environmental change in the habitat of an *E. huxleyi* assemblage can induce a change of mean coccolith size and/or weight:

1) The changing environmental factor (e.g. temperature) induces a dominance shift in the assemblage towards an *E. huxleyi* strain or morphotype which forms coccoliths of different size and weight than the one dominant initially. Here, the influence is indirect and in the following termed '*ecologically*' driven change in coccolith size and/or weight. Morphotype-

specific size and weight variations range from 2.5 – 5 μm and 0.6 – 4.6 pg, respectively (Young and Ziveri, 2000). Coccoliths of morphotye R or over-calcified coccoliths of morphotype A are usually relatively heavy, whereas the delicate coccoliths of morphotype B (pujosiae) are particularly large (Young and Ziveri, 2000; Young et al., 2003).

2) A change in some environmental factor directly affects the physiology of the dominant *E. huxleyi* strain or morphotype present in the assemblage thereby directly causing a change in mean size and weight (in the following termed '*physiologically*' driven change in coccolith size and/or weight'). Environmental factors known to modify size and/or weight are salinity (Green et al., 1998; Bollmann and Herrle, 2007; Fielding et al., 2009), temperature (Watabe and Wilbur, 1966), nutrient availability (Batvik et al., 1997; Paasche, 1998), growth stage (Westbroek and Young, 1991), seasonality (Triantaphyllou et al., 2010) and carbonate chemistry (Iglesias-Rodriguez et al., 2008; Halloran et al., 2008; Beaufort et al., 2011; this study). In the following we discuss the potential of some of these environmental factors (salinity, temperature and carbonate chemistry) to induce either *ecologically* or *physiologically* driven change in coccolith size and/or weight of *E.huxleyi*.

Increasing salinity was shown to positively influence the size of *E. huxleyi* coccoliths (e.g. Green et al., 1998). Fielding et al. (2009) reported a 30% increase in DSW in a salinity gradient ranging from 26 to 41 under constant culture conditions indicating that salinity has a relatively high *physiological* influence on coccolith size. However, whether changing salinity also has the potential to cause a shift in the dominant morphotype in a natural *E. huxleyi* assemblage is unknown. An *ecophysiological* influence seems conceivable in coastal environments with comparatively large salinity variations while it is less likely in the more stable conditions found in the open ocean.

Temperature seems to have a small *physiological* influence on *E. huxleyi* coccolith size. Watabe and Wilbur (1966) observed no change in DSL from 7 to 18°C and only a minor decrease of about 10% from 18 to 27°C. This is largely in line with results by Fielding et al., (2009) who found no detectable influence between 10 and 20°C. In contrast to that, the *ecological* influence of temperature on coccolith size could be considerably larger. It is likely that coccolithophores are adapted to the mean temperature of their natural habitat (Buitenhuis et al., 2008). In case the mean temperature in a given area changes, another strain or morphotype (potentially having a different coccolith size and/or weight) could take over. A possible example where this might have been observed is given by Triantaphyllou et al. (2010) who investigated changes in *E. huxleyi* coccolith size in a seasonal cycle in the Aegean Sea (Eastern Mediterranean Sea). They reported a shift towards larger coccoliths during cooler winter/spring periods with one possible explanation being the dominance of another *E. huxleyi* strain during that time of the year.

The results presented in our study demonstrate a negligible *physiological* influence of carbonate chemistry on *E. huxleyi* coccolith size and weight within a realistic range (DIC ~1800 – 2400 and fCO_2 ~180 – 1000 (Sarmiento and Gruber, 2006). However, there seems to be a high potential of changing carbonate chemistry to cause *ecologically* driven change in coccolith size and/or weight. In a recent investigation, Beaufort et al. (2011) concluded that carbonate chemistry conditions regulate the relative abundance of different species and morphotypes in the oceans and that species and morphotypes which form heavier coccoliths are predominantly found at sites with supposedly more favourable carbonate chemistry conditions. According to the interpretations by Beaufort et al. (2011), the carbonate chemistry has a particularly large *ecological* influence on coccolith weight.

Currently, the *physiological* influence of the environmental factors mentioned above is understood better than the *ecological* influence. This is probably due to the fact that *physiological* experiments are in most cases easier to perform and easier to evaluate than ecological data sets. However, in order to improve our understanding of what drives changes in coccolith size and weight in the oceans, it is essential to focus particularly on the *ecological* component since this seems to be of larger influence.

Acknowledgments

We thank Andrea Ludwig for her support on DIC measurements, Ute Schuldt and Arno Lettmann from the SEM laboratory at the Institute of Geosciences for their support during scanning electron microscopy and Luke Mackinder for interesting discussions on the dataset. This research was funded by the Federal Ministry of Education and Research (Bundesministerium für Bildung und Forschung; 03F0608A) in the framework of the Biological Impacts of Ocean Acidification (BIOACID) project (subproject 3.1.1 in collaboration with subproject 3.5.3).

7. Conclusions and outlook

7.1 Conclusions

The results of this thesis emphasise the complex response of natural Noelaerhabdaceae assemblages to changing environmental conditions. Mean coccolith weights from the coccolithophore family Noelaerhabdaceae show a high intrinsic variability under the rather stable atmospheric CO_2 conditions of the Holocene, reflecting the strong influence of other environmental factors. Main factors controlling mean Noelaerhabdaceae coccolith weight in the absence of strong CO_2 variability are the coccolithophore assemblage composition and coccolithophore productivity. Increasing coccolithophore productivity generally accompanies an increase in Noelaerhabdaceae coccolith weight, when the assemblage is stable. Changes in the assemblage composition can have a strong influence on the total $CaCO_3$ produced by Noelaerhabdaceae. Abundance shifts of the assemblage are ecologically driven during times of strong environmental change or on longer timescales due to evolutionary shifts within species, e.g. adaptation to a better adjusted morphotype. The variable assemblage compositions in different regions of the ocean and the various response of the species to changing seawater conditions enhance the difficulty to make a general statement about the total coccolithophore calcification with the results from single locations. More advantageous are comparisons from assemblages of the same ocean region, e.g. from the tropics where the composition of the species, and likely its response to changing environmental conditions, is rather similar.

The recently debated negative influence of increasing atmospheric CO_2 and the concomitant ocean acidification on coccolithophore calcification could not be detected on shorter (past 200 years) and longer time scales (Termination II). In contrast, coccolith weight strongly increased (Termination II) or was driven by other environmental factors (past 200 years). As well as in the Holocene record, the assemblage composition has a large influence on the mean weight over longer time scales. Species shifts which are induced by other environmental factors beside the acidifying ocean, are able to mask a possible negative influence of the changing carbonate system. In regions as the tropics which are far from strong environmental changes and have a high calcite saturation state, shifts in the assemblage are minor. These conditions allow a strong increase in coccolith weight on long term scales, even under rising atmospheric CO_2 conditions and despite constant coccolithophore productivity.

The coccolith weight response to ocean acidification on shorter time scales (past 200 years) of a stable assemblage can be so far counteracted by the rising ocean eutrophication. As a result, neither the ocean acidification nor the eutrophication is reflected in the weight trend, but the duration of the growth season of the coccolithophores is mirrored in the mean Noelaerhabdaceae coccolith weight.

The results of this thesis show that in non of the studied time intervals changes in the carbonate system have a significant negative influence on the total Noelaerhabdaceae coccolith weight. Even during the increasing atmospheric CO_2 conditions of Termination II the seawater carbonate system can offer favourable conditions for calcification. However, the conditions of the moderate CO_2 increase during Termination II (~100 ppmv in 10000) years can not be used as an analogue for the recent rising CO_2 conditions (~100 ppmv in 200 years). Further, assemblage shifts and evolutionary adaptation play a major role over larger time scales and can have a strong influence on the mean weight. But the results of the past 200 years suggest that up to now a possible negative effect of the rising ocean acidification on coccolith calcification may be compensated by enhanced nutrient availability. Despite these results, it is difficult to predict the total response of Noelaerhabdaceae calcification in the future on a global scale due to the different factors which should be taken into account such as the assemblage composition and its various response in different regions as well as the strong influence of the coccolithophore productivity. Additionally, adaptations of coccolithophores to changing seawater conditions should be taken into account, especially over long-term scales.

7.2 Outlook

The present study provides new information on the total calcification of the coccolithophore family Noelaerhabdaceae which dominates the coccolithophore assemblage in most regions and contributes a major part to the calcite production. To gain insights into the entire calcite production of a complete coccolithophore assemblage, studies on coccolith weights beside Noelaerhabdaceae are required. Especially weight measurements on large species such as *Calcidiscus leptopoturs* and *Coccolithus pelagicus* which produce heavy coccoliths with large amounts of calcite will complete the results. An improvement of SYRACO which allows the identification and weight assessment of more species beyond Noelaerhabdaceae would be beneficial. Recently, a new method to measure coccolith weights in cross polarised light with the application of a circular polariser has been introduced, which eliminates the extinction pattern and thus displays complete coccoliths (Bollmann et al., 2013). This method will simplify the identification of coccoliths in light microscope. Beside different species, an additional recognition of morphotypes would further advance the record. Differently calcified morphotypes of the same species have other coccolith weights and can influence the mean coccolith weight of a species when e.g. the abundance of this morphotype changes. As it is rather difficult to distinguish morphotypes with the light microscope, coccolith weight measurements of SYRACO combined with SEM counts which focus on morphotypes in more detail will be ad-

vantageous. In any case, SEM samples will improve the understanding of morphotype evolution and adaptation as well as their influence on the total calcite production of coccolithophores. With a quantitative analysis which includes coccolith abundance and weight of single species and morphotypes, a more accurate calculation of the $CaCO_3$ production from coccolithophores would be possible.

The results of this study further reveal the variable response of different coccolithophore assemblages in various regions of the ocean. Even in the Holocene North Atlantic the response of the mean Noelaerhabdaceae coccolith weight changed in three investigated locations. Due to the ecological differences, studies on heterogeneous natural coccolithophore assemblages are of great importance but more complicated than laboratory experiments with single species or strains and should be considered more frequently. To give an improved statement on a global scale about the calcification from different coccolithophore assemblages in past or present oceans, more observations which equally cover all biogeographic areas will be valuable and facilitate predictions about calcification in the future.

The local results of the tropics from Termination II show that despite rising atmospheric CO_2 concentration an increase in coccolith weight is possible. Although the rates of the recent and the CO_2 increase during Termination II strongly differs, the question arises if the calcite production of coccolithophores in some regions of the ocean probably benefits at least temporarily from the changing seawater carbonate chemistry. Indeed, in some regions of the ocean e.g. in the coastal areas, the enhanced nutrient supply is likely to outcompete the recent rising ocean acidification up to a certain degree. For the future it is possible that despite the counterbalance between changing seawater carbonate chemistry and enhanced nutrient supply the rising ocean acidification reaches a tipping point below which coccolithophore calcification is probably impeded. In the worst-case scenario, coccolithophores could stop calcification or completely disappear in some regions of the ocean. As coccolithophores form an important part of the food chain, this is likely to have strong influences on the entire ecosystem (Fabry et al., 2008).

Danksagung

Ein großer Dank geht an Prof. Dr. Priska Schäfer für die Ermöglichung dieser Arbeit an der Uni Kiel und für die Übernahme des Erstgutachtens. Prof. Dr. Birgit Schneider danke ich für die fachlichen Diskussionen und für die Übernahme des Zweitgutachtens.

Ein riesengroßes Dankeschön geht an Dr. Sebastian Meier und Dr. Hanno Kinkel für die kompetente Betreuung, sowie für die konstruktiven Diskussionen, zahlreichen Anregungen und kritischen Betrachtungen meiner Arbeit, besonders in den letzten Wochen.

Weiterhin geht mein Dank an alle Mitarbeiter der Arbeitsgruppe Paläontologie - Historische Geologie für die Unterstützung und das herzliche Arbeitsklima.

Meiner Kollegin und Freundin Dr. Anke Regenberg danke ich außerordentlich für ihre Unterstützung durch wertvolle Diskussionen in allen Bereichen, Problemlösungsstrategien und Motivationsschübe sowie für ehrliche Kritik.

Für das kritische Korrekturlesen von Teilen meiner Arbeit bedanke ich mich ganz herzlich bei Dr. Marcus Regenberg und Dr. Katharina Stolz.

Ein besonderes Dankeschön geht an Thea Oberließen und Steffen Häuser für ihren Einsatz bei der Erstellung von Smear Slides und den Cocco Fotos am Lichtmikroskop. Ebenso danke ich Boyke Prädel für die Erstellung der REM Fotos und Rick Warwas für die Bereitstellung der REM Daten aus seiner Bachelorarbeit. Birgit Mohr danke ich für das Bearbeiten der REM Fotos, sowie für die Verbreitung von guter Laune am REM.

Dr. Christian Schwab danke ich herzlich für seine Hilfe bei der Cocco Bestimmung am REM, sowie für fachliche Diskussionen. Weiterhin danke ich Janne Repschläger für Ratschläge und Diskussionen.

Ein ganz dickes Dankeschön geht an Dirk Ruge für seine Unterstützung und die Opferung seiner Samstage.

Ebenso danke ich meinen Freunden und meiner Familie, die mir zur Seite standen und so zum Gelingen dieser Arbeit beigetragen haben.

Ein ganz besonderer Dank geht an Papa und Anneke die mir den Rücken frei gehalten und mich bedingungslos unterstützt haben. Ohne euch wäre diese Arbeit nicht möglich gewesen!

Am allermeisten danke ich Christoph für seinen uneingeschränkten Glauben an mich, sein unermüdliches Cocco-Interesse, sowie für den Rückhalt und die emotionale Unterstützung, vor allem in der Endphase dieser Arbeit. Endlich Nichtschwimmer. Dankeschön!

References

Andersson, C., Pausata, F. S. R., Jansen, E., Risebrobakken, B., and Telford, R. J.: Holocene trends in the foraminifer record from the Norwegian Sea and the North Atlantic Ocean, Clim. Past, 6, 179–193, doi:10.5194/cp-6-179-2010, 2010.

Andruleit, H.: Coccolithophoriden im Europäischen Nordmeer: Sedimentation und Akkumulation; sowie ihre Entwicklung während der letzten 15 000 Jahre, Berichte aus dem Sonderforschungsbereich, 313, Christian-Albrechts-Universität, Kiel, 59, 1995.

Andruleit, H.: A filtration technique for quantitative studies of coccoliths. Micropaleontology 42, 403– 406, 1996.

Andruleit, H. A. and Baumann, K.-H.: History of the Last Deglaciation and Holocene in the Nordic Seas as revealed by coccolithophore assemblages, Mar. Micropaleontol., 35, 179–201, 1998.

Antonov, J. I., Locarnini, R. A., Boyer, T. P., Mishonov, A. V. and Garcia, H. E.: World Ocean Atlas 2005, Volume 2: Salinity, in NOAA Atlas NESDIS 62, edited by S. Levitus, p. 182, U.S. Government Printing Office, Washington, D.C., 2006.

Archer, D., Winguth, A., Lea, D. and Mahowald, N.: What caused the glacial/interglacial atmospheric pCO_2 cycles, Rev. Geophys, 2000.

Bach, L. T., Riebesell, U. and Georg Schulz, K.: Distinguishing between the effects of ocean acidification and ocean carbonation in the coccolithophore *Emiliania huxleyi*, Limnol Oceanogr 56(6), 2040–2050, doi:10.4319/lo.2011.56.6.2040, 2011.

Bach, L. T., Bauke, C., Meier, K. J. S., Riebesell, U., and Schulz, K. G.: Influence of changing carbonate chemistry on morphology and weight of coccoliths formed by *Emiliania huxleyi*, Biogeosciences, 9, 3449–3463, doi:10.5194/bg-9-3449-2012, 2012.

Bach, L. T., Mackinder, L. C. M., Schulz, K. G., Wheeler, G., Schroeder, D. C., Brownlee, C. and Riebesell, U.: Dissecting the impact of CO_2 and pH on the mechanisms of photosynthesis and calcification in the coccolithophore *Emiliania huxleyi*, New Phytol., doi:10.1111/nph.12225, 2013.

Bahr, A., Nürnberg, D., Schönfeld, J. and Garbe-Schönberg, D.: Hydrological variability in Florida Straits during Marine Isotope Stage 5 cold events, Paleoceanography 26(4), PA2214, doi:10.1029/2011PA002157, 2011.

Balch, W. M., Kilpatrick, K.A., Holligan, P.M., Cucci, T.: Coccolith production and detachment by Emiliania huxleyi (Prymnesiophyceae). J. Phycol. 29: 566–575, doi:10.1111/j.0022-3646.1993.00566.x, 1993.

Bauke, C., Meier, K.J.S., Kinkel, H. and Baumann, K.-H.: Changes in coccolith calcification under stable atmospheric CO_2, Biogeosciences Discuss. 10, 9415-9450, doi:10.5194/bgd-10-9415-2013, 2013.

Bauke, C., Meier, K.J.S., Kinkel, H.: Increasing coccolith calcification during CO_2 rise of the penultimate deglaciation (Termination II), submitted to Marine Micropaleontology, 2013.

Baumann,K.H.,Cepek,M.,Kinkel,H.: Coccolithophores as indicators of ocean water masses, surface-water temperature, and paleoproductivity-examples from the South Atlantic. In: Fischer, G., Wefer, G. (Eds.), Use of Proxies in Paleoceanography: Examples from the South Atlantic,Springer-Verlag, Berlin, pp. 117, 1999.

Baumann, K.-H., Meggers, H. and Henrich, R.: 30. Variations in surface water mass conditions in the Norwegian-Greenland Sea: Evidence from Pliocene/Pleistocene calcareous plankton Records (Sites 644,907,909), Proceedings of the Ocean Drilling Program, Scientific Results, Vol. 151, 1993.

Baumann, K., Andruleit, H., Böckel, B., Geisen, M. and Kinkel, H.: The significance of extant coccolithophores as indicators of ocean water masses, surface water temperature, and palaeoproductivity: a review, Paläontologische Zeitschrift, 79(1), 93–112, 2005.

Bassinot, F. C. and Labeyrie, L. D.: Shipboard Scientific Party (1996): IMAGES MD101 Brest- Marseille 29/05/95–11/07/95 – A coring cruise of the R/V Marion Dufresne in the North Atlantic Ocean and Norwegian Sea, Les rapports de campagnes à la mer, Institut Français pour la Recherche et la Technologie Polaires, Technopole de Brest-Iroise, BP75–29280 Plouzane, Francee de Brest-Iroise, BP75–29280 Plouzane, France, 96–1, 217 pp., 1996.

Batvik, H., Heimdal, B. R., Fagerbakke, K. M. and Green, J. C.: Effects of unbalanced nutrient regime on coccolith morphology and size in *Emiliania huxleyi* (Prymnesiophyceae), Eur. J. Phycol., 32, 155–165, 1997.

Beaufort, L. and Heussner, S.: Seasonal dynamics of calcareous nannoplankton on a West European continental margin: the Bay of Biscay, Mar. Micropaleontol., 43, 27–55, 2001.

Beaufort, L. and Dollfus, D.: Automatic recognition of coccoliths by dynamical neural networks, Mar. Micropaleontol., 51, 57–73, doi:10.1016/j.marmicro.2003.09.003, 2004.

Beaufort, L.: Weight estimates of coccoliths using the optical properties (birefringence) of calcite, Micropaleontology, 51, 289–297, 2005.

Beaufort, L., Probert, I., and Buchet, N.: Effects of acidification and primary production on coccolith weight: implications for carbonate transfer from the surface to the deep ocean, Geochem. Geophy. Geosy., 8, Q08011, doi:10.1029/2006GC001493, 2007.

Beaufort, L., Couapel, M., Buchet, N., Claustre, H., and Goyet, C.: Calcite production by coccolithophores in the south east Pacific Ocean, Biogeosciences, 5, 1101–1117, 2008.

Beaufort, L., Probert, I., de Garidel-Thoron, T., Bendif, E. M., Ruiz-Pino, D., Metzl, N., Goyet, C., Buchet, N., Coupel, P., Grelaud, M., Rost, B., Rickaby, R. E. M., and de Vargas, C.: Sensitivity of coccolithophores to carbonate chemistry and ocean acidification, Nature, 476, 80–83, doi:10.1038/nature10295, 2011.

Bemis, B., Spero, H. and Bijma, J.: Reevaluation of the oxygen isotopic composition of planktonic foraminifera: Experimental results and revised paleotemperature equations, Paleoceanography 13(2), 150-160, 1998.

Berner, K., Koç, N., Godtliebsen, F., and Divine, D.: Holocene climate variability of the Norwegian Atlantic Current during high and low solar insolation forcing, Paleoceanography, 26, PA2220, doi:10.1029/2010PA002002, 2011.

Birks, C. and Koç, N.: A high-resolution diatom record of late-Quaternary sea-surface temperatures and oceanographic conditions from the eastern Norwegian Sea, Boreas, 31, 323–344, 2002.

Blackburn, S. I. and Cresswell, G.: A Coccolithophorid bloom in Jervis Bay, Australia. Aust. J. Mar. Freshw. Res., 44, 253–60, 1993.

Blindheim, J. and Østerhus, S.: The Nordic Seas, main oceanographic features, in: The Nordic Seas, An Integrated Perspective, edited by: Drange, H., Dokken, T., Furevik, T., Gerdes, R., and Berger, W., Geophysical Monograph Series 158, American Geophysical Union, Washington DC, 11–38, 2005.

Boeckel, B., Baumann, K.-H., Henrich, R., and Kinkel, H.: Coccolith distribution patterns in South Atlantic and southern Ocean surface sediments in relation to environmental gradients, Deep-Sea Res. Pt. I, 53, 1073–1099, doi:10.1016/j.dsr.2005.11.006, 2006.

Bollmann, J.: Morphology and biogeography of Gephyrocapsa coccoliths in Holocene sediments, Mar. Micropaleontol., 29, 319–350, 1997.

Bollmann, J. and Herrle, J.: Morphological variation of *Emiliania huxleyi* and sea surface salinity, Earth Planet. Sc. Lett., 255, 273–288, doi:10.1016/j.epsl.2006.12.029, 2007.

Bollmann, J., Herrle, J. O., Cortés, M. Y., Fielding, S. R.: The effect of sea water salinity on the morphology of *Emiliania huxleyi* in plankton and sediment samples, Earth and Planetary

Science Letters, 284, 320 – 328, doi:10.1016/j.epsl.2009.05.003, 2009.

Bollmann, J.: Technical Note: Weight approximation of single coccoliths inferred from retardation estimates using a light microscope equipped with a circular polariser - (the CPR Method), Biogeosciences Discuss., 10(7), 11155–11179, doi:10.5194/bgd-10-11155-2013, 2013.

Borchard, C., Borges, A. V., Haendel, N. and Engel, A.: Biogeochemical response of *Emiliania huxleyi* (PML B92/11) to elevated CO_2 and temperature under phosphorous limitation: A chemostat study, J Exp Mar Biol Ecol, 410, 61–71, doi:10.1016/j.jembe.2011.10.004, 2011.

Borman, A. H., De Jong, E. W., Huizinga, M., Kok, D. J., Westbroek, P. and Bosch, L.: The role in $CaCO_3$ crystallization of an acid Ca^{2+}-binding polysaccharide associated with coccoliths of *Emiliania huxleyi*, Eur. J. Biochem., 129, 179–83, 1982.

Bown, P.R.: Calcareous nannofossils biostratigraphy, Kluwer Academic Press, 315 pp, 1998.

Bown. P. R., Lees. J. A. and Young, J. R.: Calcareous nannoplankton evolution and diversity through time, in: Coccolithophores – From Molecular Processes to Global Impact, Thierstein, H. R. and Young, J. R. (Eds.), Springer, Heidelberg, 481–508, 2004.

Bethoux, J. P., Gentili, B., Morin, P., Nicolas, E., Pierre, C., Ruiz-Pino, D.: The Mediterranean Sea: a miniature ocean for climatic and environmental studies and a key for the climatic functioning of the North Atlantic, Progress in Oceanography, 44, 131-146, 1999.

Brand, L. E., and Guillard, R.R.L.:The effects of continuous light and light intensity on the reproduction rates of twenty-two species of marine phytoplankton. J. Exp. Mar. Biol. Ecol. 50: 119–132, 1981.

Brand, L. E.: Genetic variability and spatial patterns of genetic differentiation in the reproductive rates of the marine coccolithophores *Emiliania huxleyi* and *Gephyrocapsa oceanica*, Limnol. Oceanogr., 27, 236–245, 1982.

Brand L.E. (1994) Physiological ecology of marine coccolithophores. In: Winter A and Siesser WG (editors) "Coccolithophores". Cambridge University Press, Cambridge, UK, pp. 39-49.

Broerse, A., Brummer, G. and Hinte, J.: Coccolithophore export production in response to monsoonal upwelling off Somalia (northwestern Indian Ocean), Deep-Sea Research Part II, 2000a.

Broerse, A., Ziveri, P. and Honjo, S.: Coccolithophore (–CaCO 3) flux in the Sea of Okhotsk: seasonality, settling and alteration processes, Mar Micropaleontol, 39(1), 179–200, 2000b.

Brown C.W. and Yoder J.A.: Coccolithophorid blooms in the global ocean. J. Geophys. Res., 99(C): 7467-7482, 1994.

Bown, P.R. and Young, J.R.: Introduction. In: P.R. Bown (ed.), Calcareous nannofossil biostratigraphy, pp. 1-15, 1998.

Brunetti, M., Buffoni, L., Mangianti, F., Maugeri, M., Nanni, T.: Temperature, precipitation and extreme events during the last century in Italy, Global and Planetary Change, 40, 141-149, 2004.

Buitenhuis, E. T., de Baar, H. J. W. and Veldhuis, M. J. W.: Photosynthesis and calcification by *Emiliania huxleyi* (Prymnesiophyceae) as a function of inorganic carbon species, J. Phycol., 35, 949–959, 1999.

Buitenhuis, E. T., Van der Wal., P., de Baar, H. J. W.: Blooms of *Emiliania huxleyi* are Sinks of atmospheric Carbon Dioxide: A Field and Mesocosm Study derived Simulation, Global Biogeochemical Cycles, 15(3), 577-587, 2011.

Buitenhuis, E. T., Pangerc, T., Franklin, D. J., Le Quéré, C. and Malin, G.: Growth rates of six coccolithophorid strains as a function of temperature, Limnol. Oceanogr 53, 1181-1185, 2008.

Brownlee, C. and Taylor, A.: Calcification in coccolithophores: A cellular perspective, Coccolithophores—From Molecular Processes to Global Impact, 31–49, 2004.

Burns, D. A.: Phenotypes and dissolution morphotypes of the genus *Gephyrocapsa kamptner* and *Emiliania huxleyi* (Lohmann), New Zealand Journal of Geology and Geophysics, 20(1), 143–155, doi:10.1080/00288306.1977.10431596, 1977.

Caldeira, K. and Wickett, M. E.: Oceanography: anthropogenic carbon and ocean pH, Nature, 425(6956), 365, doi:10.1038/425365a, 2003.

Calvo, E., Grimalt, J., and Jansen, E.: High resolution U37K sea surface temperature reconstruction in the Norwegian Sea during the Holocene, Quaternary Sci. Rev., 21, 1385–1394, 2002.

Colmenero-Hidalgo, E., Flores, J. A., and Sierro, F. J.: Biometry of *Emiliania huxleyi* and its biostratigraphic significance in the eastern North Atlantic Ocean and western Mediterranean Sea in the last 20 000 years, Mar. Micropaleontol., 46, 247–263, 2002.

Comeau, S., Gorsky, G., Jeffree, R., Teyssié, J. L. and Gattuso, J. P.: Impact of ocean acidification on a key Arctic pelagic mollusc (Limacina helicina), Biogeosciences, 6(9), 1877–1882, doi:10.5194/bg-6-1877-2009, 2009.

Cook, S. S., Whittock, L., Wright, S. W. and Hallegraeff, G. M.: Photosynthetic pigment and genetic differences between two southern ocean morphotypes of *Emiliania huxleyi* (haptophyta), J Phycol, 47(3), 615–626, doi:10.1111/j.1529-8817.2011.00992.x, 2011.

Cortes M. Y., Bollmann J., and Thierstein H. R.: Coccolithophore ecology at the HOT station ALOHA, Hawaii. *Deep-sea Research II* **48**, 1957-1981, 2001.

Cros, L. and Fortuño, J.: Atlas of northwestern Mediterranean coccolithophores, Scientia Marina, 66(S1), 2002.

Cubillos, J. C., Wright, S. W., Nash, G., De Salas, M. F., Griffiths, B., Tilbrook, B., Poisson, A. and Hallegraeff, G. M.: Calcification morphotypes of the coccolithophorid *Emiliania huxleyi* in the Southern Ocean: changes in 2001 to 2006 compared to historical data, Marine ecology progress series. Oldendorf, 348, 47–54, doi:10.3354/meps07058, 2007.

De Bodt, C., Van Oostende, N., Harlay, J., Sabbe, K., and Chou, L.: Individual and interacting effects of pCO_2 and temperature on *Emiliania huxleyi* calcification: study of the calcite production, the coccolith morphology and the coccosphere size, Biogeosciences, 7, 1401–1412, doi:10.5194/bg-7-1401-2010, 2010.

De Jong, E. W., Bosch, L. and Westbroek, P.: Isolation and characterization of a Ca^{2+}-binding polysaccharide associated with coccoliths of *Emiliania huxleyi* (Lohmann) Kamptner, Eur. J. Biochem., 70, 611-621, 1976.

Degobbis, D. and Gilmartin, M.: Nitrogen, phosphorus, and biogenic silicon budgets for the northern Adriatic Sea, Oceanologica Acta, 13(1), 31–45, 1990.

De Vargas, C., Aubry, M., Probert, I. and Young, J.: Origin and evolution of coccolithophores: From coastal hunters to oceanic farmers, 2007.

Decoursey, T. E.: Voltage-Gated Proton Channels: Molecular Biology, Physiology, and Pathophysiology of the HV Family, Physiol. Rev., 93(2), 599–652, doi:10.1152/physrev.00011.2012, 2013.

Dickson, A. G.: An exact definition of total alkalinity and a procedure for the estimation of alkalinity and total inorganic carbon from titration data, Deep Sea Research, 28A(6), 609-623, 1981.

Dickson, A. G., Afghan, J. D. and Anderson, G. C.: Reference materials for oceanic CO_2 analysis: A method for the certification of total alkalinity, Mar. Chem., 80, 185–197, 2003.

Dickson, A. G., Sabine, C. L. and Christian, J. R.: Guide to best practices for ocean CO_2 Measurements, PICES Special Publication, Sidney, 2007.

Didymus, J. M., Young, J. R. and Mann, S.: Construction and morphogenesis of the chiral ultrastructure of coccoliths from the marine alga *Emiliania huxleyi*, Proc. R. Soc. London B, 258, 237–245, 1994.

Doo, S. S., Dworjanyn, S. A., Foo, S. A., Soars, N. A. and Byrne, M.: Impacts of ocean acidification on development of the meroplanktonic larval stage of the sea urchin Centrostephanus rodgersii, ICES Journal of Marine Science, 69(3), 460–464, doi:10.1093/icesjms/fsr123, 2012.

Doney, S., Fabry, V., Feely, R., and Kleypas, J.: Ocean acidification: the other CO_2 problem, Annual Review of Marine Science, 1, 169–192, 2009.

Duplessy, J. C., Labeyrie, L., Juillet-Leclerc, A., Maitre, F., Duprat, J., and Sarnthein, M.: Surface salinity reconstruction of the North Atlantic Ocean during the last glacial maximum, Oceanol. Acta, 14, 311–324, 1991.

Duplessy, J. C., Cortijo, E., and Kallel, N.: Marine records of Holocene climatic variations, C. R. Geosci., 337, 87–95, doi:10.1016/j.crte.2004.08.007, 2005.

Dünkeloh, A. and Jacobeit, J.: Circulation dynamics of Mediterranean precipitation variability 1948–98 - Dünkeloh - 2003 - International Journal of Climatology - Wiley Online Library, International Journal of Climatology, 2003.

Edvardsen, B., Eikrem, W., Green, J., Andersen, R., van der Staay, S. and MEDLIN, L.: Phylogenetic reconstructions of the Haptophyta inferred from 18S ribosomal DNA sequences and available morphological data, Phycologia, 2000.

Edvardsen, B., and Medlin, L.K.: Molecular systemat- ics of Haptophyta. In *Unravelling the Algae: The past, Present and Future of Algal Systematics*. Brodie, J., and Lewis, J. (eds). Oxford, UK: CRC Press, Taylor and Francis Group, pp. 183–196, 2007.

Elshanawany, R.: Microfossil Assemblages as Proxies to Reconstruct Anthropogenic Induced Eutrophication of Two Marginal Eastern Mediterranean Basins, Dissertation, 2010.

Engel, A., Zondervan, I., Aerts, K., Beaufort, L., Benthien, A., Chou, L., Delille, B., Gattuso, J. P., Harlay, J., Heemann, C., Hoffmann, L., Jacquet, S., Nejstgaard, J., Pizay, M. D., Rochelle-Newall, E., Schneider, U., Terbrueggen, A., Riebesell, U.: Testing the direct effect of CO2 concentration on a bloom of the coccolithophorid *Emiliania huxleyi* in mesocosm experiments, Limnol. Oceanogr., 50, 493–507, 2005.

Etheridge, D. M., Steele, L. P., Langenfelds, R. L., Francey, R. J., Barnola, J. - M., and Morgan, V. I.: Historical CO_2 records from the Law Dome DE08, DE08-2, and DSS ice cores. In Trends: A Compendium of Data on Global Change. Carbon Dioxide Information Analysis

Center, Oak Ridge National Laboratory, U.S. Department of Energy, Oak Ridge, Tenn., U.S.A, 1998.

Fabry, V. J., Seibel, B. A., Feely, R. A., and Orr, J. C.: Impacts of ocean acidification on marine fauna and ecosystem processes, ICES J. Mar. Sci., 65, 414–432, doi:10.1093/icesjms/fsn048, 2008.

Feely, R., Doney, S. and Cooley, S.: Ocean acidification: Present conditions and future changes in a high-CO2 world, Oceanography, 2009.

Fagerbakke, K., M., Heldal, M., Norland, S., Heimdal, B., R. and Batvik, H.: *Emiliania huxleyi*. Chemical composition and size of coccoliths from enclosure experiments and a Norwegian fjord, Sarsia, 79, 349-355, 1994.

Feely, R., Sabine, C., Takahashi, T. and Wanninkhof, R.: Uptake and storage of carbon dioxide in the ocean, Oceanography, 2001.

Feely RA, Sabine CL, Kitack L, Berelson W, Kleypas J, Fabry VJ and Millero F.J.: Impact of anthropogenic CO_2 on the $CaCO_3$ system in the ocean. Science 305: 362–366, 2004.

Feng, Y., Warner, M. E., Zhang, Y., Sun, J., Fu, F.-X., Rose, J. M. and Hutchins, D. A.: Interactive effects of increased pCO 2, temperature and irradiance on the marine coccolithophore *Emiliania huxleyi* (Prymnesiophyceae), European J. of Phycology, 43(1), 87–98, doi:10.1080/09670260701664674, 2008.

Fielding, S. R., Herrle, J. O., Bollmann, J., Worden, R. H., Montagnes, D. J. S.: Assessing the application of *Emiliania huxleyi* coccolith morphology as a sea-surface salinity proxy, Limnol. Oceanogr., 54, 5, 1475 – 1480, 2009.

Fiorini, S., Middelburg, J. and Gattuso, J.: Effects of elevated CO_2 partial pressure and temperature on the coccolithophore *Syracosphaera pulchra*, Aquat. Microb. Ecol. 64(3), 221–232, doi:10.3354/ame01520, 2011.

Findlay, C.S., Giraudeau, J.: Extant calcareous nannoplankton in the Australian Sector of the Southern Ocean (austral summers 1994 and 1995) Mar Micropaleontol 40: 417–439, 2000.

Findlay, C. S., and Giraudeau, J.:, Movement of oceanic fronts south of Australia during the last 10 ka: Interpretation of calcareous nanno- plankton in surface sediments from the Southern Ocean, Mar. Micropaleontol., 46, 431–444, 2002.

Flores, J. A., Colmenero-Hidalgo, E., Mejía-Molina, A. E., Baumann, K.-H., Henderiks, J., Lars- son, K., Prabhu, C. N., Sierro, F. J., and Rodrigues, T.: Distribution of large *Emiliania huxleyi* in the Central and Northeast Atlantic as a tracer of surface ocean dynamics during the last 25 000 years, Mar. Micropaleontol., 76, 53–66, doi:10.1016/j.marmicro.2010.05.001,

2010.

Flores, J.-A., Filippelli, G. M., Sierro, F. J., and Latimer, J.: The “white ocean” hypothesis: a late pleistocene southern ocean governed by coccolithophores and driven by phosphorus, Front. Microbiol., 3, 233, doi:10.3389/fmicb.2012.00233, 2012.

Gattuso, J., Frankignoulle, M., Bourge, I., Romaine, S., and Buddemeier, R.: Effect of calcium carbonate saturation of seawater on coral calcification, Global Planet. Change, 18, 37–46, 1998.

Gattuso, J. P., Gao, K., Lee, K., Rost, B. and Schulz, K. G.: Approaches and tools to manipulate the carbonate chemistry, in: Guide for best practices for ocean acidification research and data reporting, Riebesell, U., Fabry, V., Hansson, L. and Gattuso, J. P. (Eds.), Publications Office of the European Union, 41–52, 2010.

Gianguzza, F., Ragusa, M.A., Roccheri, M.C., Di Liegro, I., Rinaldi, A.M.: Isolation and characterization of a Paracentrotus lividus cDNA encoding a stress-inducible chaperonin. Cell Stress Chaperones, 5, 87–89.1466-1268, 2000.

Giraudeau, J., Monteiro, P. and Nikodemus, K.: Distribution and malformation of living coccolithophores in the northern Benguela upwelling system off Namibia. Marine Micropaleontology 22, 93–110, 1993

Giraudeau, J., Grelaud, M., Solignac, S., Andrews, J., Moros, M., and Jansen, E.: Millennial-scale variability in Atlantic water advection to the Nordic Seas derived from Holocene coccolith concentration records, Quaternary Sci. Rev., 29, 1276–1287, doi:10.1016/j.quascirev.2010.02.014, 2010.

Gordon, A. L.: Circulation of the Caribbean Sea. J. Geophys. Res. 72(24) 6207-6223, 1967.

Goyet, C. and Touratier, F.: Temporal variations of anthropogenic CO_2 concentrations in the Mediterranean Sea, In: Briand, F.: CIESM, 2008. Impacts of acidification on biological, chemical and physical systems in the Mediterranean and Black Seas. N° 36, CIESM Workshop Monographs, 124 pages, Monaco, 2008

Grauel, A.: Calibration of the ‘clumped isotope’ Thermometer on Foraminifera and its Application to High-resolution Climate Reconstruction of the past 2500yr in the Gulf of Taranto (Eastern Mediterranean Sea), Dissertation, 2012.

Grauel, A. L., Goudeau, M. L. S., De Lange, G. J. and Bernasconi, S. M.: Climate of the past 2500 years in the Gulf of Taranto, central Mediterranean Sea: A high-resolution climate reconstruction based on 18O and 13C of Globigerinoides ruber (white), The Holocene, doi:10.1177/0959683613493937, 2013a.

Grauel, A.-L., Leider, A., Goudeau, M.-L. S., Müller, I. A., Bernasconi, S. M., Hinrichs, K.-U., de Lange, G. J., Zonneveld, K. A. and Versteegh, G. J.: What do SST proxies really tell us? A high-resolution multiproxy (U K′ 37, TEX H 86 and foraminifera δ 18 O) study in the Gulf of Taranto, central Mediterranean Sea, Quaternary Science Reviews, 73, 115–131, 2013b.

Green, J. C., Heimdal, B. R., Paasche, E. and Moate, R.: Changes in calcification and the dimensions of coccoliths of *Emiliania huxleyi* (Haptophyta) grown at reduced salinities, Phycologia 37, 121–131, 1998.

Grelaud, M., Beaufort, L., Cuven, S. and Buchet, N.: Glacial to interglacial primary production and El Niño–Southern Oscillation dynamics inferred from coccolithophores of the Santa Barbara Basin, Paleoceanography, 2009a.

Grelaud, M., Schimmelmann, A. and Beaufort, L.: Coccolithophore response to climate and surface hydrography in Santa Barbara Basin, California, AD 1917–2004, Biogeosciences, 2009b. Guillard, R. R. and Ryther J. H.: Studies of marine planktonic diatoms. I. Cyclotella nana Hustedt, and Detonula confervacea (cleve) Gran, Can. J. Microbiol., 8, 229–239, 1962.

Hagino, K., Okada, H., and Matsuoka, H.: Coccolithophore assemblages and morphotypes of *Emiliania huxleyi* in the boundary zone between the cold Oyashio and warm Kuroshio currents off the coast of Japan, Mar. Micropaleontol., 55, 19–47, 2005.

Hagino, K., Bendif, E. M., Young, J. R., Kogame, K., Probert, I., Takano, Y., Horiguchi, T., de Vargas, C., and Okada, H.: New evidence for morphological and genetic variation in the cosmopolotan coccolithophore *Emiliania huxleyi* (Prymnesiophyceae) from the COX1b-ATP4 GENES1, J. Phycol., 47, 1164–1176, doi:10.1111/j.1529-8817.2011.01053.x, 2011.

Halloran, P. R., Hall, I. R., Colmenero-Hidalgo, E., and Rickaby, R. E. M.: Evidence for a multi-species coccolith volume change over the past two centuries: understanding a potential ocean acidification response, Biogeosciences, 5, 1651–1655, 2008.

Hansen, H. P. and Koroleff, F.: Determination of nutrients, in: Methods of seawater analysis, in: Grasshoff, K., Kremling, K. and Ehrhardt, M. (Eds.), Wiley-VCH, 159–228, 1999.

Hansen, B. and Østerhus, S.: North Atlantic-nordic seas exchanges, Prog. Oceanogr., 45, 109– 208, 2000.

Harlay, J., Borges, A. V., Van Der Zee, C., Delille, B., Godoi, R.H.M., Schiettecatte, L.-S., Roevros, N., Aerts, K., Lapernat, P.-E-, Rebreanu, L., Groom, S., Daro, M.-H., Van Grieken, R., Chou, L.: Biogeochemical study of a coccolithophore bloom in the northern Bay of Biscay (NE Atlantic Ocean) in June 2004, Progress in Oceanography 86, 317-336, 2010.

Henderiks, J., Winter, A., Elbrächter, M., Feistel, R., Plas, der, A., Nausch, G., and Barlow,

R.: Environmental controls on *Emiliania huxleyi* morphotypes in the Benguela coastal upwelling system (SE Atlantic), Mar. Ecol.-Prog. Ser., 448, 51–66, doi:10.3354/meps09535, 2012.

Henriksen, K., Stipp, S. L. S., Young, J. R. and Marsh, M. E.: Biologic control on calcite crystallization: AFM investigation of coccolith polysaccharide function, Am. Mineralogist 89, 1586–96, 2004.

Henriksen, K. and Stipp, S., L., S.: Controlling Biomineralization: The Effect of Solution Composition on Coccolith Polysaccharide Functionality, Cryst. Growth Des., 9, 2088–2097, 2009.

Herfort, L., Thake, B. and Roberts, J.: Acquisition and use of bicarbonate by *Emiliania huxleyi,* New Phytologist 156, 427-436, 2002.

Herfort, L., Loste, E., Meldrum, F. and Thake, B.: Structural and physiological effects of calcium and magnesium in *Emiliania huxleyi* (Lohmann) Hay and Mohler, J. Struct. Biol., 2004.

Hönisch, B., Ridgwell, A., Schmidt, D., Thomas, E., Gibbs, S., Sluijs, A., Zeebe, R., Kump, L., Martindale, R., Greene, S., Kiessling, W., Ries, J., Zachos, J., Royer, D., Barker, S., Marchitto , T. Jr., Moyer, R., Pelejero, C., Ziveri, P., Foster, G., Williams, B.: The Geological Record of Ocean Acidification, Science 335, doi: 10.1126/science.12082771058, 2012.

Holligan, P. M., Fernandez, E., Aiken, J., Balch, W. M., Boyd, P., Burkill, P. H., Finch, M., Groom, S. B., Malin, G., Muller, K., Purdie, D. A., Robinson, C., Trees, C. C., Turner, S. M. and van der Wal, P.: A biogeochemical study of the coccolithophore, *Emiliania huxleyi,* in the North Atlantic, Global Biogeochem. Cy., 7, 879–900, 1993.

Honjo, S.: Coccoliths: Production, transportation and sedimentation, Mar. Micropaleontol., 1, 65-79, 1976.

Houghton, S. D.: Coccolith sedimentation and transport in the North Sea, Marine Geology, 99(1-2), 267–274, doi:10.1016/0025-3227(91)90097-N, 1991.

Hulburt, E. M.: Distribution of Phytoplankton in Coastal Waters of Venezuela. Ecology 44:169–171, 1963.

Iglesias-Rodriguez, M. D., Schofield, O. M., Batley, J., Medlin, L. K. and Hayes, P. K.: Intraspecific genetic diversity in the marine coccolithohore *Emiliania huxleyi* (Prymnesiophyceae): The use of microsatellite analysis in marine phytoplankton population studies, J. Phycol., 42, 526–536, 2006.

Iglesias-Rodriguez, M. D., Halloran, P. R., Rickaby, R. E. M., Hall, I., Colmenero-Hidalgo, E., Gittins, J., Green, D., Tyrell, T., Gibbs, S., Dassow, von, P., Rehm, E., Armbrust, E. and Boessenkool, K.: Phytoplankton calcification in a high-CO_2 world, Science 320 (336), 2008a.

Iglesias-Rodriguez, M. D., Buitenhuis, E. T., Raven, J. A., Schofield, O., Poulton, A. J., Gibbs, S., Halloran, P. R. and De Baar, H. J. W.: Response to Comment on "Phytoplankton Calcification in a High-CO2 World," Science, 322(5907), 1466c–1466c, doi:10.1126/science.1161501, 2008a.

Indermühle, A., Stocker, T. F., Joos, F., Fischer, H., Smith, J., Wahlen, M., DeCk, B., Mastroianni, D., Tschumi, J., and Blunier, T.: Holocene carbon-cycle dynamics based on CO_2 trapped in ice at Taylor Dome, Antarctica, Nature, 398, 121–126, 1999.

IPCC (Intergovernmental Panel on Climate Change). 2007. Global Climate Projections. In: S Solomon, D Qin, M Manning, Z Chen, M Marquis, KB Averyt, M Tignor and HL Miller (eds), Climate Change 2007: The Physical Science Basis. Contribution of Working Group I to the Fourth Assessment of the Intergovernmental Panel on Climate Change. Cambridge and New York: Cambridge University. pp. 747–845, 2007

IPCC (Intergovernmental Panel on Climate Change), Contribution of Working Group to the fifth assesment report "Climate Change 2013: The Physical Science Basis", 2013.

Jansen, E., Raymo, M. E., Blum, P., Anderson, E. S., Austin, W. E. N., Baumann, K-H., Bout-Roumazeilles, V., Carter, S. J., Channell, J. E. T., Cullen, J. L., Flower, B., Higgins, S., Hodell, D. A., Hood, J.A., Hyun, S., Ikehara, M., King, T., Larter, R., Lehman, B., Locker, S., Mclntyre, K., McManus, J., Meng, L. B., O'Commell, S., Ortiz, J.D., Rack, F. R., Solheim, A., Wei, W.: Proceedings of the ODP Initial Reports, 162; College Station, TX (Ocean Drilling Program), 1182 pp, 1996.

Jansen, E., Raymo, M. E., Blum, P., Anderson, E. S., Austin, W. E. N., Baumann, K- H., Bout-Roumazeilles, V., Carter, S. J., Channell, J. E. T., Cullen, J. L., Flower, B., Higgins, S., Hodell, D. A., Hood, J. A., Hyun, S., Ikehara, M., King, T., Larter, R., Lehman, B., Locker, S., Mclntyre, K., McManus, J., Meng, L. B., O'Commell, S., Ortiz, J. D., Rack, F. R., Solheim, A., and Wei, W.: Proceedings of the ODP Initial Reports, 162, College Station, TX (Ocean Drilling Program), 1182 pp., 1996. Jansen, E., Blum, P., and Party, S. S.: Gamma-ray attenuation measurements of bulk density using whole-core multi-sensing track on Hole 162-980B, doi:10.1594/PANGAEA.259998, 2005.

Jevrejeva, S., Moore, J. C., Grinsted, A., Woodworth, P. L.: Recent global sea level acceleration started over 200 years ago?, Geophysical Research Letters, 35, L08715, doi:10.1029/2008GL033611, 2008.

Jones, B. M., Iglesias-Rodriguez, M. D., Skipp, P. J., Edwards, R. J., Greaves, M. J., Young, J. R., Elderfield, H. and O'Connor, C. D.: Responses of the *Emiliania huxleyi* Proteome to Ocean Acidification, PLoS ONE 8(4), e61868, doi:10.1371/journal.pone.0061868, 2013.

Jouzel, J., Masson-Delmotte, V., Cattani, O., Dreyfus, G., Falourd, S., Hoffmann, G., Minster, B., Nouet, J., Barnola, J.-M., Chappellaz, J., Fischer, H., Gallet, J. C., Johnsen, S., Leuenberger, M., Loulergue, L., Luethi, D., Oerter, H., Parrenin, F., Raisbeck, G., Raynaud, D., Schilt, A., Schwander, J., Selmo, E., Souchez, R., Spahni, R., Stauffer, B., Steffensen, J. P., Stenni, B., Stocker, T. F., Tison, J. L., Werner, M. and Wolff, E. W.: Orbital and millennial Antarctic climate variability over the past 800,000 years. Science 317(5839), 793–796, doi:10.1126/science.1141038, 2007.

Kaffes, A., Thoms, S., Trimborn, S., Rost, B., Langer, G., Richter, K.-U., Köhler, A., Norici, A. and Giordano, M.: Carbon and nitrogen fluxes in the marine coccolithophore *Emiliania huxleyi* grown under different nitrate concentrations. J. Exp. Mar. Biol. Ecol., 393, 1–8, 2010.

Kester, D., Duedall, I. W., Connors, D. N. and Pytkowicz, R. M.: Preparation of artificial seawater, Limnol. Oceanogr., 1, 176–179, 1967.

Kissel, C., Kleiven, K., and Morin, X.: Les rapports de champagnes à la mer – MD 168/ AMOCINT IMAGES XVII on board R/V Marion Dufresne, Inst. Polaire Fr., Plouzané, France, 1–104, 2009.

Klaas, C. (1999): Morphological and growth characteristics of Gephyrocapsa as a function of temperature conditions , CODENET 2nd annual Workshop. Chateau de Blagnac, France.

Klaas, C., Archer, D. E.: Association of sinking organic matter with various types of mineral ballast in the deep sea: Implications for the rain ratio, Global Biogeochemical cycles, 16, 4, 1116, doi:10.1029/2001GB001765, 2002.

Klaveness, D.: *Emiliania huxleyi* (Lohmann) Hay and Mohler. III. Mineral deposition and the origin of the matrix during coccolith formation, Protistologica, 12, 217–24, 1976.

Kleijne, A., Kroon, D., and Zevenboom, W.: Phytoplankton and foraminiferal frequencies in northern Indian Ocean and Red Sea surface waters, Neth. J. Sea Res., 24, 531–539, doi:10.1016/0077-7579(89)90131-2, 1989.

Klein, B. and Siedler, G.: On the Origin of the Azores Current, J. Geophys. Res., 94, 6159–6168, 1989.

Kleypas, J. and Langdon, C.: Coral reefs and changing seawater carbonate chemistry, Coral reefs and Climate Change: Science and Management, Coastal and Estuarine Studies, 61, 2006.

Krug, S. A., Schulz, K. G., and Riebesell, U.: Effects of changes in carbonate chemistry speciation on *Coccolithus braarudii*: a discussion of coccolithophorid sensitivities, Biogeosciences, 8, 771–777, doi:10.5194/bg-8-771-2011, 2011.

Kukla, G. J., Bender, M. L., de Beaulieu, J.-L., Bond, G., Broecker, W. S., Cleveringa, P., Gavin, J. E., Herbert, T. D., Imbrie, J. and Jouzel, J.: Last interglacial climates, Quaternary Research 58(1), 2–13, 2002.

Kump, L. R., Bralower, T. J. and Ridgwell, A.: Ocean acidification in deep time, Oceanography, 22(34), 94–107, 2009.

Langer, G., Geisen, M., Baumann, K.-H., Kläs, J., Riebesell, U., Thoms, S., and Young, J. R.: Species-specific responses of calcifying algae to changing seawater carbonate chemistry, Geochem. Geophy. Geosy., 7, Q09006, doi:10.1029/2005GC001227, 2006.

Langer, G., Gussone, N., Nehrke, G., Riebesell, U., Eisenhauer, A., and Thoms, S.: Calcium isotope fractionation during coccolith formation in *Emiliania huxleyi*: independence of growth and calcification rate, Geochem. Geophys. Geosys., 8, Q05007, doi:10.1029/2006GC001422, 2007.

Langer, G., Nehrke, G., Probert, I., Ly, J. and Ziveri, P.: Strain-specific responses of *Emiliania huxleyi* to changing seawater carbonate chemistry, Biogeosciences 6(11), 2637–2646, 2009.

Langer, G., Probert, I., Nehrke, G. and Ziveri, P.: The morphological response of *Emiliania huxleyi* to seawater carbonate chemistry changes: an inter-strain comparison, J. Nannoplankton Res., 32 , 2011, 29-34, 2011.

Langer, G. and Bode, M.: CO_2 mediation of adverse effects of seawater acidification in *Calcidiscus leptoporus*, Geochem. Geophy. Geosy., 12, Q05001, doi: 10.1029/2010GC003393, 2011.

Langer, G., De Nooijer, L. J. and Oetjen, K. : On the role of the cytoskeleton in coccolith morphogenesis: the effect of cytoskeleton inhibitors. J. Phycol., 46, 1252-1256, 2010.

LaRoche, J., Rost, B. and Engel, A.: Bioassay, batch culture and chemostat experimentation, in: Guide for best practices for ocean acidification research and data reporting, Riebesell, U., Fabry, V., Hansson, L. and Gattuso, J.-P. (Eds.). Publications Office of the European Union, 81-94, 2010.

Lea, D. W., Martin, P. A., Pak, D. K. and Spero, H. J.: Reconstructing a 350 ky history of sea level using planktonic Mg/Ca and oxygen isotope records from a Cocos Ridge core, Quaternary Science Reviews 21: 283-293, 2002.

Lee, K., Tong, L. T., Millero, F. J., Sabine, C. L., Dickson, A. G., Goyet, C., Park, G. H., Wan-

ninkhof, R., Feely, R. A., and Key, R. M.: Global relationships of total alkalinity with salinity and temperature in surface waters of the world's oceans, Geophys. Res. Lett., 33, L19605, doi:10.1029/2006GL027207, 2006.

Lee, C. M., Orlic, M., Poulain, P.- M. and Cushman-Roisin, B.: Introduction to special section: Recent advances in oceanography and marine meteorology of the Adriatic Sea, J Geophysical Research, 112, C03S01, doi:10.1029/2007JC004115, 2007.

Leider, A., Hinrichs, K.-U., Mollenhauer, G. and Versteegh, G. J. M.: Core-top calibration of the lipid-based UK37' and TEX86 temperature proxies on the southern Italian shelf (SW Adriatic Sea, Gulf of Taranto), Earth Planet Sc Lett, 300(1-2), 112–124, doi:10.1016/j.epsl.2010.09.042, 2010.

Leonardos, N., Read, B., Thake, B., and Young, J. R.: No mechanistic dependence of photosynthesis on calcification in the coccolithophorid *Emiliania huxleyi* (Haptophyta), J. Phycol., 45, 1046– 1051, 2009.

Lewis, E. and Wallace, D.W. R.: Program Developed for CO_2 System Calculations ORNL/ CDIAC-105, Carbon Dioxide Information Analysis Centre, Oak Ridge National Laboratory, US Department of Energy, 1998.

Lewis, E. and Wallace, D. W. R.: Program Developed for CO_2 System Calculations, ORNL/ CDIAC-105, Carbon Dioxide Information Analysis Center, Oak Ridge National Lab- oratory, US Department of Energy, Oak Ridge, Tennessee 37831-6290, USA, 1998.

Locarnini, R. A., Mishonov, A. V., Antonov, J. I., Boyer, T. P. and Garcia, H. E.: World Ocean Atlas 2005, Volume 1: Temperature, in NOAA Atlas NESDIS 61, edited by S. Levitus, p. 182, U.S. Government Printing Office, Washington, D.C., 2006.

Lohbeck, K. T., Riebesell, U., and Reusch, T. B. H.: Adaptive evolution of a key phytoplankton species to ocean acidification, Nat. Geosci., 5, 346–351, doi:10.1038/ngeo1441, 2012.

Lototskaya, A., Ziveri, P., Ganssen, G. M., and van Hinte, J. E.: Calcareous nannofloral response to Termination II at 45○ N, 25○ W (northeast Atlantic), Mar. Micropaleontol., 34, 47–70, 1998.

Lotze, H. K., Coll, M. and Dunne, J. A.: Historical Changes in Marine Resources, Food-web Structure and Ecosystem Functioning in the Adriatic Sea, Mediterranean, Ecosystems, 14(2), 198–222, doi:10.1007/s10021-010-9404-8, 2011.

Lüthi, D.: Fast Antarctic temperature variations imprint in the CO_2 concentration? A high-resolution CO_2 record over the last glacial period,, 2008.

Lüthi, D., Le Floch, M., Bereiter, B., Blunier, T., Barnola, J.-M., Siegenthaler, U., Raynaud, D., Jouzel, J., Fischer, H., Kawamura, K. and Stocker, T. F.: High-resolution carbon dioxide concentration record 650,000-800,000 years before present, Nature, 453(7193), 379–382, doi:10.1038/nature06949, 2008.

Lynch-Stieglitz, J., Curry, W. B. and Slowey, N.: Weaker Gulf Stream in the Florida straits during the last glacial maximum, Nature 402, 644-648, 1999.

Mackinder, L. C. M., Wheeler, G., Schroeder, D., Riebesell, U., Brownlee, C.: Molecular mechanisms underlying calcification in coccolithophores, Geomicrobiol. J., 27, 585–595, 2010.

Mackinder, L. C. M., Wheeler, G., Schroeder, D., von Dassow, P., Riebesell, U., Brownlee, C.: Expression of biomineralization-related ion transport genes in *Emiliania huxleyi*, Environ. Microbiol., 2011.

Malinverno, E., Ziveri, P., Corselli, C.: Coccolithophorid distribution in the Ionian Sea and its relationship to eastern Mediterranean circulation during late fall to early winter 1997, J. Geophys. Res, 108(C9), 8115, doi:10.1029/2002JC001346, 2003.

Marchal, O., Cacho, I., Stocker, T. F., Grimalt, J. O., Calvo, E., Martrat, B., Shackleton, N., Vautravers, M., Cortijo, E., van Kreveld, S., Andersson, C., Koç, N., Chapman, M., Sbaffi, L., Duplessy, J. C., Sarnthein, M., Turon, J. L., Duprat, J., and Jansen, E.: Apparent long-term cooling of the sea surface in the northeast Atlantic and Mediterranean during the Holocene, Quaternary Sci. Rev., 21, 455–483, 2002.

Marlowe, I. T., Brassell, S. C., Eglinton, G. and Green, J. C.: Long-chain alkenones and alkyl alkenoates and the fossil coccolith record of marine sediments, Chemical Geology, 88(3), 349–375, 1990.

Marsh, M. E.: Polyanion-mediated mineralization – assembly and reorganization of acidic polysaccharides in the Golgi system of a coccolithophorid alga during mineral deposition, Protoplasma, 177, 108–22, 1994.

Marsh, M. E.: Regulation of $CaCO_3$ formation in coccolithophores, Comparative Biochemistry and Physiology [online] Available from: http://www.sciencedirect.com/science/article/pii/S1096495903001805, 2003.

Matthiessen, B., Eggers, S. L. and Krug, S. A.: High nitrate to phosphorus regime attenuates negative effects of rising pCO_2 on total population carbon accumulation, Biogeosciences 9(3), 1195–1203, doi:10.5194/bg-9-1195-2012, 2012.

McIntyre, A. and Bé, A.: Modern coccolithophoridae of the atlantic ocean -I. Placoliths and cyrtoliths, Deep Sea Research and Oceanographic Abstracts 14, 561-597, 1967.

McIntyre, A.: *Gephyrocapsa protohuxleyi* sp. n. a possible phyletic link and index fossil for the Pleistocene, Deep Sea Research and Oceanographic Abstracts, 17(1), 187–190, doi:10.1016/0011-7471(70)90097-5, 1970.

Medlin, L. K., Barker, G., Campbell, L., Green, J. C., Hayes, P. K., Marie, D., Wrieden, S., and Vaulot, D.: Genetic characterisation of *Emiliania huxleyi* (Haptophyta), J. Marine Syst., 9, 13– 31, 1996.

Milligan, T. G. and Cattaneo, A.: Sediment Dynamics in the Western Adriatic Sea: from transport to stratigraphy, Cont. Shelf Res., 27, 287-295, 2007.

Milliman, J. D.: Production and accumulation of calcium carbonate in the ocean: Budget of a nonsteady state, Global Biogeochemical Cycles, 7(4), 927–957, 1993.

Mohan, R., Mergulhao, L. P., Guptha, M. V. S., Rajakumar, A., Thamban, M., AnilKumar, N., Sudhakar, M. and Ravindra, R.: Ecology of coccolithophores in the Indian sector of the Southern Ocean, Mar Micropaleontol, 67(1-2), 30–45, doi:10.1016/j.marmicro.2007.08.005, 2008.

Molinari, R. L. and Morrison, J.: The separation of the Yucatan Current from the Campeche Bank and the intrusion of the Loop Current into the Gulf of Mexico. J. Geophys. Res 93(C9), 10645, doi:10.1029/JC093iC09p10645, 1988.

Monnin, E., Indermühle, A., Dällenbach, A., Flückiger, J., Stauffer, B., Stocker, T. F., Raynaud, D., Barnola, J.-M.: Atmospheric CO_2 Concentrations over the Last Glacial Termination. Science 291(5501), 112–114, doi:10.1126/science.291.5501.112, 2001.

Moore, T. S., Dowell, M. D. and Franz, B. A.: Detection of coccolithophore blooms in ocean color satellite imagery: A generalized approach for use with multiple sensors, Remote Sens. Environ., 117, 249-263, 2012.

Mozetiĉ, P., Umani, S. F., Cataletto, B. and Malej, A.: Seasonal and inter-annual plankton variability in the Gulf of Trieste (northern Adriatic), ICES Journal of Marine Science, 55, 711-722, 1998.

Müller, P. J., Cepek, M., Ruhland, G. and Schneider, R. R.: Alkenone and coccolithophoridspecies changes in late Quaternary sediments from the Walvis Ridge: Implications for the alkenone Abstract paleotemperature method, Palaeogeography, 1997.

Müller, M., Antia, A. and LaRoche, J.: Influence of cell cycle phase on calcification in the coccolithophore *Emiliania huxleyi*, Limnol Oceanogr, 53(2), 2008.

Müller, M. N., Schulz, K. G. and Riebesell, U.: Effects of long-term high CO_2 exposure on two species of coccolithophores, Biogeosciences, 7, 1109–1116, 2010.

Müller, M. N., Beaufort, L., Bernard, O., Pedrotti, M. L., Talec, A., Sciandra, A.: Influence of CO_2 and nitrogen limitation on the coccolith volume of *Emiliania huxleyi* (Haptophyta), Biogeosciences 9, 4155-4167, doi:10.5194/bg-9-4155-2012, 2012.

Nanninga, H. J. and Tyrrell, T.: Importance of light for the formation of algal blooms by *Emiliania huxleyi*, Marine Ecology Progress Series, 136, 195–203, doi:10.3354/meps136195, 1996.

Nielsen, J. E. Ø.: Variability at Ocean Weather Station M in the Norwegian Sea, ICES Marine Science Symposia, 219, 371 – 374, 2003.

Nimer, N. and Merrett, M.: Calcification rate in *Emiliania huxleyi* Lohmann in response to light, nitrate and availability of inorganic carbon, New phytologist, 123(4), 673–677, 1993.

Nimer, N. A. and Merrett, M. J.: The development of a CO_2-concentrating mechanism in *Emiliania huxleyi*., New Phytol., 133, 387–389, 1996.

Nishida, T.:The social structure of chimpanzees of the Mahale mountains. In Hamburg, D. A., and McCown, E. R. (eds.), The Great Apes, Benjamin/Cummings, Menlo Park, CA, pp. 73–122, 1979.

Nürnberg, D., J. Schönfeld, W. C. Dullo, and Rühlemann, C.: RV Sonne Cruise report, Rep. SO164(RASTA), 151 pp., GEOMAR, Kiel, Germany, 2003.

Okabe, K: hange in fishing methods and conditions caused by bloom of *Gephyrocapsa oceanica*. Bull Kanagawa Prefect Fish Res Inst 2: 49–54, 1997.

Okada, H. and Honjo, S.:The distribution of oceanic coccolithophorids in the Pacific, Deep Sea Research, 20, 355-374, 1973.

Okada, H. & McIntyre, A.: Modern coccolithophores of the Pacific and North Atlantic Oceans. Micropaleontology 23: 1-55, 1977.

Okada, H. and McIntyre, A.: Seasonal distribution of modern coccolithophores in the western North Atlantic Ocean. Marine Biology 54, 319–328, 1979.

Okada, H. and Wells, P.: Late Quaternary nannofossil indicators of climate change in two deep-sea cores associated with the Leeuwin Current off Western Australia, Palaeogeogr. Palaeocl., 131, 413–432, 1997.

Oppo, D., McManus, J., and Cullen, J.: Evolution and demise of the last inter- glacial warmth in the subpolar North Atlantic, Quaternary Sci. Rev., 25, 3268–3277, doi:10.1016/j.quascirev.2006.07.006, 2006.

Orr, J. C., Fabry, V. J., Aumont, O., Bopp, L., Doney, S. C., Feely, R. A., Gnanadesikan, A., Gruber, N., Ishida, A., Joos, F., Key, R. M., Lindsay, K., Maier-Reimer, E., Matear, R., Monfray, P., Mouchet, A., Najjar, R. G., Plattner, G.-K., Rodgers, K. B., Sabine, C. L., Sarmiento, J. L., Schlitzer, R., Slater, R. D., Totterdell, I. J., Weirig, M.-F., Yamanaka, Y. and Yool, A.: Anthropogenic ocean acidification over the twenty-first century and its impact on calcifying organisms, Nature, 437(7059), 681–686, doi:10.1038/nature04095, 2005.

Paasche, E., Brubak, S. Skattebol, S. Young, J.R. and J.C. Green: Growth and calcification in the coccolithophorid *Emiliania huxleyi* (Haptophyceae) at low salinities. Phycologia 35: 394–403, 1996.

Paasche, E.: Roles of nitrogen and phosphorus in coccolith formation in *Emiliania huxleyi* (Prymnesiophyceae), Eur. J. of Phycol., 33, 33–42, 1998.

Paasche, E.: A review of the coccolithophorid *Emiliania huxleyi* (Prymnesiophyceae), with particular reference to growth, coccolith formation, and calcification-photosynthesis interactions., Phycologia, 40, 503–529, 2002.

Paillard, D., Labeyrie, L., and Yiou, P.: Macintosh program performs time-series analysis, EOS 77, 379 pp., Transactions of the American Geophysical Union, USA, 1996.

Pelejero, C., Calco, E., Hoegh-Guldberg, O.: Paleo-perspectives on ocean acidification, Trends in Ecology and Evolution,25(6), doi:10.1016/j.tree.2010.02.002, 2010.

Penna, N., Capellacci, S. and Ricci, F.: The influence of the Po River discharge on phytoplankton bloom dynamics along the coastline of Pesaro (Italy) in the Adriatic Sea, Marine Pollution Bulletin, 48(3-4), 321–326, doi:10.1016/j.marpolbul.2003.08.007, 2004.

Petit, J. R., Jouzel, J., Raynaud, D., Barkov, N. I. and Barnola, J.-M.: Climate and atmospheric history of the past 420,000 years from the Vostok ice core, Antarctica. Nature 399, 429-436, 1999.

Ploug, H., Hvitfeldt Iversen, H., Koski, M., and Buitenhuis, E. T.: Production, oxygen respiration rates, and sinking velocity of copepod fecal pellets: direct measurements of ballasting by opal and calcite, Limnol. Oceanogr., 53, 469–476, 2008.

Pollard, R. T., Read, J. F., Holliday, N. P., and Leach, H.: Water masses and circulation pathways through the Iceland Basin during Vivaldi 1996, J. Geophys. Res, 109, C04004, doi:10.1029/2003JC002067, 2004.

Poulain, P. M.: Adriatic Sea surface circulation as derived from drifter data between 1990 and 1999, Journal of Marine Systems, 29, 3-32, 2001.

Prahl, F., Herbert, T., Brassell, S. C. and Ohkouchi, N.: Status of alkenone paleothermometer calibration: Report from Working Group 3 - Prahl - 2000 - Geochemistry, Geophysics, Geosystems - Wiley Online Library, Geochemistry, 2000.

Pujos, A.: Late Eocene to Pleistocene medium-sized and small-sized ´Reticulofenestrids`, Abh. Geol. B.-A., 39, 239-277, 1987.

Purdie, D.A. and Finch, M.S.: Impact of a coccolithophorid on dissolved carbon-dioxide in seawater enclosures in a Norwegian fiord, Sarsia, 79, 379-387, 1993.

Pušcarić, S., Berger, G. W. and Jorissen, F. J.: Successive appearance of subfossil phytoplankton species in holocene sediments of the northern adriatic and its relation to the increased eutrophication pressure, Estuarine, Coastal and Shelf Science, 31, 177-187, 1990.

Quadrelli, R., Pavan, V. and Molteni, F.: Wintertime variability of Mediterranean precipitation and its links with large-scale circulation anomalies, Climate Dynamics, 17(5-6), 457–466, doi:10.1007/s003820000121, 2001.

Rabalais, N. N., Turner, R. E., Díaz, R. J. and Justić, D.: Global change and eutrophication of coastal waters, ICES Journal of Marine Science, 66, 1528-1537, 2009.

Raffi, I., Backman, J., Fornaciari, E., Pälike, H., Rio, D., Lourens, L., Hilgen, F.: A review of calcareous nannofossil astrobiochronology encompassing the past 25 million years. Quaternary Sci. Rev., 25, 3113-3137, 2006.

Raven, J., Caldeira, K., Elderfield, H., Hoegh-Guldberg, O., Liss, P., Riebesell, U., Shepherd, J., Turley, C., and Watson, A.: Ocean acidification due to increasing atmospheric carbon dioxide, The Royal Society, Policy Document 12/05, p. 60, 2005.

Raven, J. A. and Crawfurd, K.: Environmental controls on coccolithophore calcification, Marine Ecology Progress Series, 470, 137–166, doi:10.3354/meps09993, 2012.

Read, J. F.: CONVEX-91: water masses and circulation of the Northeast Atlantic subpolar gyre, Prog. Oceanogr., 48, 461–510, 2001.

Richardson, W. S., Schmitz, W. J. Jr., and Niiler, P. P.: The velocity structure of the Florida Current from the Straits of Florida to Cape Fear, Deep-Sea Res., Suppl. to 16, 225-231, 1969.

Rhodes, L. L., Peake, B. M., MacKenzie, A. L. and Marwick, S.: Coccolithophores Gephyrocapsa oceanica and *Emiliania huxleyi* (Prymnesiophyceae = Haptophyceae) in New Zealand's coastal waters: Characteristics of blooms and growth in laboratory culture, New Zealand Journal of Marine and Freshwater Research, 29(3), 345–357, doi:10.1080/00288330.1995.9516669, 1995.

Richter, T.: Sedimentary fluxes at the Mid-Atlantic Ridge: sediment sources, accumulation rates, and geochemical characterization, GEOMAR Rep. 73, GEOMAR Res. Cent. for Mar. Geosci., Christian Albrechts Univ., Kiel, Germany, 1998.

Rickaby, R., Bard, E., Sonzogni, C., Rostek, F., Beaufort, L., Barker, S., Rees, G., and Schrag, D. P.: Coccolith chemistry reveals secular variations in the global ocean carbon cycle?, Earth Planet. Sc. Lett., 253, 83–95, doi:10.1016/j.epsl.2006.10.016, 2007.

Ridgwell, A., Schmidt, D. N., Turley, C., Brownlee, C., Maldonado, M. T., Tortell, P. and Young, J.,: From laboratory manipulations to Earth system models: scaling calcification impacts of ocean acidification, Biogeosciences (BG) 6, 2611–2623, 2009.

Riebesell, U., Zondervan, I., Rost, B. È., Tortell, P. D., Zeebe, R. E., and Morel, F. M. M.: Reduced calcification of marine plankton in response to increased atmospheric CO_2, Nature, 407, 364–367, 2000.

Riebesell, U., Koertzinger, A. and Oschlies, A.: Sensitivities of marine carbon fluxes to ocean change, P Natl Acad Sci Usa, 106(49), 20602–20609, doi:10.1073/pnas.0813291106, 2009.

Riebesell, U., Fabry, V. J., Hansson, L. and Gattuso, J. P.: Guide to best practices for ocean acidification research and data reporting,, 1–263, 2010.

Riebesell, U. and Tortell, P. D.: Effects of ocean acidification on pelagic organisms and ecosystems, in: ocean acidification, Gattuso, J.-P., Hansson, L. (Eds.), Oxford University Press, Oxford, 99-121, 2011.

Rios, A. F., Pérez, F. F., Álvarez, M., Mintrop, L., González-Dávila, M., Santana Casiano, J. M., Lefèvre, N., Watson, A. J.: Seasonal sea-surface carbon dioxide in the Azores area, Marine Chemistry, 96, 35 – 51, doi10.1016/j.marchem.2004.11.001, 2005.

Risebrobakken, B., Jansen, E., Andersson, C., Mjelde, E., and Hevrøy, K.: A high-resolution study of Holocene paleoclimatic and paleoceanographic changes in the Nordic Seas, Paleoceanography, 18, 1017, doi:10.1029/2002PA000764, 2003.

Robertson, J.E., Robinson, C., Turner, D.R., Watson, A.J., Boyd, P., Fernandez, E., Finch, M.: The impact of a coccolithophore bloom on oceanic carbon uptake in the Northeast Atlantic during summer 1991. Deep-Sea Re- search Part I 41, 297–314, 1994.

Rogers, A., Ainsworth, E. A. and Leakey, A. D. B.: Will Elevated Carbon Dioxide Concentration Amplify the Benefits of Nitrogen Fixation in Legumes

Rogerson, M., Rohling, E. J., Weaver, P., and Murray, J. W.: The Azores front since the last glacial maximum, Earth Planet. Sc. Lett., 222, 779–789, doi:10.1016/j.epsl.2004.03.039, 2004.

Rost, B., Riebesell, U., Burkhardt, S. and Sültemeyer, D.: Carbon acquisition of bloom-forming marine phytoplankton, Limnol. Oceanogr. 48, 55-67, 2003.

Rost, B. and Riebesell, U.: Coccolithophores and the biological pump: responses to environmental changes, Coccolithophores—From Molecular Processes to Global Impact, 76–99, 2004.

Rouco, M., Branson, O., Lebrato, M. and Iglesias-Rodriguez, M. D.: The effect of nitrate and phosphate availability on *Emiliania huxleyi* (NZEH) physiology under different CO_2 scenarios, Front Microbiol, 4, 155, doi:10.3389/fmicb.2013.00155, 2013.

Roy, R. N., Roy, L. N., Vogel, K. M., Porter-Moore, C., Pearson, T., Good, C. E., Millero, F. J. and Campbell, D. C.: Thermodynamics of the dissociation of boric acid in seawater at S 5 35 from 0 degrees C to 55 degrees C, Mar. Chem., 44, 243–248, 1993.

Rowson, J. D., Leadbeater, B.S.C. and Green, J.C.: Calcium carbonate deposition in the motile (Crystallolithus) phase of Coccolithus pelagicus (Prymnesiophyceae), Br. Phycol. J., 21, 359-379, 1986.

Sabine, C. L., Feely, R. A., Gruber, N., Key, R. M.; Lee, K., Bullister, J. L., Wanninkhof, R., Wong, C. S., Wallace, D. W. R., Tilbrook, B., Millero, F. J., Peng, T. - H., Kozyr, A., Ono, T. and Rios, A. F.: The oceanic sink for anthropogenic CO_2, Science, 305(367), doi:10.1126/science.1097403, 2004.

Samtleben, C.: Die Evolution der Coccolithophoriden-Gattung *Gephyrocapsa* nach Befunden im Atlantik, Paläont. Z. 54, 1/2, 91-127, 1980.

Sangiorgi, F. and Donders, T. H.: Reconstructing 150 years of eutrophication in the north-western Adriatic Sea (Italy) using dinoflagellate cysts, pollen and spores, Estuarine, Coastal and Shelf Science, 60(1), 69–79, doi:10.1016/j.ecss.2003.12.001, 2004.

Sarmiento, J. L., Gruber, N. (Eds.): Ocean biogeochemical dynamics, Cambridge University Press, Cambridge, United States of America, 2006.

Schiebel, R., Brupbacher, U., Schmidko, S., Nausch, G., Waniek, J. J., and Thierstein, H.-R.: Spring coccolithophore production and dispersion in the temperate eastern North Atlantic Ocean, J. Geophys. Res., 116, C08030, doi:10.1029/2010JC006841, 2011.

Schnellnhuber, H.-J., Buchmann, N., Epiney, A., Grießhammer, R., Kulessa, M., Messner, M., Rahmstorf, S., Schmid, J.: Warming Up, Rising High, Turning Sour, German Advisory Council on Global Change (WBGU), Special Report, 2006.

Schroeder D, Biggi G, Hall M, Davy J and others: A genetic marker to separate *Emiliania huxleyi* (Prymne- siophyceae) morphotypes. J Phycol 41:874–879, 2005.

Schulz, K. G., Rost, B., Burkhardt, S., Riebesell, U., Thoms, S. & Wolf-Gladrow, D. A.: The effect of iron availability on the regulation of inorganic carbon acquisition in the coccolithophore *Emiliania huxleyi* and the significance of cellular compartmentation for stable carbon isotope fractionation. Geochim. Cosmochim. Ac. 71:5301–12, 2007.

Schulz, K. G., Riebesell, U., Bellerby, R. G. J., Biswas, H., Meyerhöfer, M., Müller, M. N., Egge, J. K., Nejstgaard, J. C., Neill, C., Wohlers, J., and Zöllner, E.: Build-up and decline of organic matter during PeECE III, Biogeosciences, 5, 707–718, 2008.

Schwab, C., Kinkel, H., Weinelt, M., and Repschläger, J.: Coccolithophore paleoproductivity and ecology response to deglacial and Holocene changes in the Azores Current System, Paleoceanography, 27, PA3210, doi:10.1029/2012PA002281, 2012.

Schwarz, J. and Rendle-Bühring, R.: Controls on modern carbonate preservation in the southern Florida Straits, Sedimentary Geology 175, 153-167, doi:10.1016/j.sedgeo.2004.12.024, 2005.

Sciandra, A., Harlay, J., Lefèbvre, D. et al.: Response of coccolithophorid *Emiliania huxleyi* to elevated partial pressure of CO_2 under nitrogen limitation. Mar. Ecol. Prog. Ser., 261, 111–122, 2003.

Shackleton, N.: The 100,000-year ice-age cycle identified and found to lag temperature, carbon dioxide, and orbital eccentricity, Science, 2000.

Shackleton, N. J., Hall, M. A. and Vincent, E.: Phase relationships between millennial-scale events 64,000-24,000 years ago, Paleoceanography, 15(6), 565–569, doi:10.1029/2000PA000513, 2000.

Shi, D., Xu, Y. and Morel, F.: Effects of the pH/pCO2 control method on medium chemistry and phytoplankton growth, Biogeosciences, 2009.

Shiraiwa, Y.: Physiological regulation of carbon fixation in the photosynthesis and calcification of coccolithophorids, Comp. Biochem. Physiol. B, Biochem. Mol. Biol., 136(4), 775–783, 2003.

Siegenthaler, U., Stocker, T. F., Monnin, E., Lüthi, D., Schwander, J., Stauffer, B., Raynaud, D., Barnola, J.-M., Fischer, H., Masson-Delmotte, V. and Jouzel, J.: Stable carbon cycle-climate relationship during the Late Pleistocene, Science, 310(5752), 1313–1317, doi:10.1126/science.1120130, 2005.

Sigman, D. M. & Haug, G. H.: The Biological Pump in the Past, Treatise on Geochemistry, 6, 491 – 528, ISBN: 0-08-044341-9, 2003

Sikes, C. S., Reef, R. D. and Wilbur, K. M.: Photosynthesis and coccolith formation: inorganic carbon sources and net inorganic reaction of deposition, Limnol. Oceanogr. 25: 248-261, 1980.

Smith, H. E. K., Tyrrell, T., Charalampopoulou, A., Dumousseaud, C., Legge, O. J., Birchenough, S., Pettit, L. R., Garley, R., Hartman, S. E., Hartman, M. C., Sagoo, N., Daniels, C. J., Achterberg, E. P., and Hydes, D. J.: Predominance of heavily calcified coccolithophores at low $CaCO_3$ saturation during winter in the Bay of Biscay, P. Natl. Acad. Sci. USA, 109, 8845–8849, doi:10.1073/pnas.1117508109, 2012.

Stoll, M. H. C., Bakker, K., Nobbe, G. H. and Haese, R. R.: Continuous-flow analysis of dissolved inorganic carbon content in seawater, Anal. Chem., 73, 4111–4116, 2001.

Stoll, H. M. and Ziveri, P.: Coccolithophorid-based geochemical paleoproxies, Coccolithophores—From Molecular Processes to Global Impact, 1–35, 2004.

Socal, G., Boldrin, A., Bianchi, F., Civitarese, G., De Lazzari, A., Rabitti, S., Totti, C. and Turchetto, M. M.: Nutrient, particulate matter and phytoplankton variability in the photic layer of the Otranto strait, Journal of Marine Systems, 20(1-4), 381–398, doi:10.1016/S0924-7963(98)00075-X, 1999.

Solignac, S., Grelaud, M., de Vernal, A., Giraudeau, J., Moros, M., McCave, I. N., and Hoogakker, B.: Reorganization of the upper ocean circulation in the mid-Holocene in the northeastern Atlantic, Can. J. Earth Sci., 45, 1417–1433, doi:10.1139/E08-061, 2008.

Spatharis, S., Tsirtsis, G., Danielidis, D. B., Chi, T. D. and Mouillot, D.: Effects of pulsed nutrient inputs on phytoplankton assemblage structure and blooms in an enclosed coastal area, Estuarine, Coastal and Shelf Science, 73, 801-815, 2007.

Stolz, K. and Baumann, K-H., Changes in palaeoceanography and palaeoecology during Ma-

rine Isotope Stage (MIS) 5 in the eastern North Atlantic (ODP Site 980) deduced from calcareous nannoplankton observations, Palaeogeography, Palaeoclimatology, Palaeoecology, 292, 295-305, doi:10.1016/j.palaeo.2010.04.002, 2010.

Struglia, M. V., Mariotti, A. and Filograsso, A.: River discharge into the Mediterranean Sea: climatology and aspects of the observed variability, Journal of climate, 17(24), 4740–4751, 2004.

Suffrian K., Schulz, K. G., Gutowska, M., Riebesell, U. and Bleich, M.: Cellular pH measurements in *Emiliania huxleyi* reveal pronounced membrane proton permeability, New Phytol., 190, 595–608, 2011.

Swift, J.H.: The Arctic waters, In: Hurdle, B.G. (Ed.), The Nordic Seas, Springer-Verlag, New York, pp. 129–153, 1986.

Takahashi, T. Sutherland, S. C., Sweeney, C., Poisson, A., Metzl, N., Tilbrook, B., Bates, N., Wanninkhof, R., Feely, R. A., Sabine, C., Olafsson, J., Nojiri, Y.: Global sea-air CO_2 flux based on climatological surface ocean pCO_2, and seasonal biological temperature effects. Deep-Sea Research II, 49, 1601 – 1622, 2002.

Tans, P. P. and Conway, T.J.: Monthly Atmospheric CO_2 Mixing Ratios from the NOAA CMDL Carbon Cycle Cooperative Global Air Sampling Network, 1968-2002. In Trends: A Compendium of Data on Global Change. Carbon Dioxide Information Analysis Center, Oak Ridge National Laboratory, U.S. Department of Energy, Oak Ridge, Tenn., U.S.A, 2005.

Trans, P. and Keeling, R. CO_2 record from Mauna Loa, 2012 (www.esrl.noaa.gov/gmd/ccgg/trends/)

Thierstein, H. R., Geitzenauer, K., R., Molfino, B. and Shackleton, N. J.: Global synchroneity of late quaternary coccolith datum levels: validation by oxygen isotopes, Geology, 5, 400–404, 1977.

Triantaphyllou, M., Dimiza, M., Krasakopoulou, E., Malinverno, E., Lianou, V. and Souvermezoglou, E: Seasonal variation in *Emiliania huxleyi* coccolith morphology and calcification in the Aegean Sea (Eastern Mediterranean), Geobios 43(1), 99–110, doi:10.1016/j.geobios.2009.09.002, 2010.

Trimborn, S., Langer, G. and Rost, B.: Effect of varying calcium concentrations and light intensities on calcification and photosynthesis in *Emiliania huxleyi*, Limnol Oceanogr, 2007.

Turchetto, M., Boldrin, A., Langone, L., Miserocchi, S., Tesi, T. and Foglini, F.: Particle transport in the Bari Canyon (southern Adriatic Sea), Marine Geology, 246, 231-247, 2007.

Tyrell, T. and Merico, A.: *Emiliania huxleyi*: bloom observations and the conditions that induce them, in: Coccolithophores from molecular processes to global impact, Thierstein, H.-R. and Young, J. R. (Eds.), Springer, Heidelberg, 2004.

Tyrrell, T. and Young, J. R.: Coccolithophores, in: Encyclopedia of Ocean Sciences, Steele, J. H., Turekian, K. K. and Thorpe, S. A. (Eds.), Academic Press, San Diego, 3568-3576, 2009.

Van Bleijswijk, J. van der Wal, P., Kempers, R., Veldhuis, M.: Distribution of two types of *Emiliania huxleyi* (Prymnesiophyceae) in the northeast atlantic region as determined by immunoflourescence and coccolith morphology, J. Phycol., 27, 566-570, 1991.

van der Wal, P., De Jong, E. W., Westbroek, P., De Bruijn, W. C. and Mulder-Stapel, A. A.: Ultrastructural polysaccharide localization in calcifying and naked cells of the coccolithophorid *Emiliania huxleyi*. Protoplasma 118, 157–68, 1983.

Van Kreveld, S., Knappertsbusch, M., Ottens, J., Ganssen, G. M., and Van Hinte, J. E.: Biogenic carbonate and ice-rafted debris (Heinrich layers) accumulation in deep-sea sediments from a Northeast Atlantic piston core, Mar. Geol., 131, 21–46, 1996.

Watabe, N. and Wilbur, K. M.: Effects of temperature on growth, calcification and coccolith form in *Coccolithus huxleyi* (Coccolithineae), Limnol. Oceanogr., 11, 567-575, 1966.

Waelbroeck, C., Labeyrie, L., Michel, E., Duplessy, J., McManus, J., Lambeck, K., Balbon, E., and Labracherie, M.: Sea-level and deep water temperature changes derived from benthic foraminifera isotopic records, Quaternary Sci. Rev., 21, 295–305, 2002.

Weaver, P. P. E. and Pujol, C.: History of the last deglaciation in the alboran sea (western Mediterranean) and adjacent north Atlantic as revealed by coccolith floras, Palaeogeogr. Palaeocl., 64, 35–42, doi:10.1016/0031-0182(88)90140-X, 1988.

Wennekens, M. P.: Water Mass Properties of the Straits of Florida and Related Waters, Bulletin of Marine Science 9(1), 1-52, 1959.

Westbroek, P., De Jong, E. W., Van Der Wal, P., Borman, A. H., De Vrind, J. P. M., Kok, D., De Bruijn, W. C. and Parker, S. B.: Mechanism of calcification in the marine alga *Emiliania huxleyi*. Philos. Trans. R. Soc. Lond. B, 304, 435–44, 1984.

Westbroek, P., Young, J. R., and Linschooten, K.: Coccolith production (biomineralisation) in the marine alga *Emiliania huxleyi*, J. Protozool., 36, 368–373, 1989.

Westbroek, P., Brown, C. W., Bleijswijk, J., Brownlee, C., Brummer, G. J., Conte, M., Egge, J., Fernández, E., Jordan, R., Knappertsbusch, M., Stefels, J., Veldhuis, M., van der Wal, P., and Young, J.: A model system approach to biological climate forcing, The example of *Emiliania huxleyi*, Global Planet. Change, 8, 27–46, 1993.

Winter, A. and Siesser, W. G.: Coccolithophores, Coccolithophores, Edited by Amos Winter and William G. Siesser, pp. 252. ISBN 0521380502. Cambridge, UK: Cambridge University Press, July 1994., -1, 1994.

Xoplaki, E., Gonzalez-Rouco, J. F., Luterbacher, J. and Wanner, H.: Wet season Mediterranean precipitation variability: influence of large-scale dynamics and trends, Climate Dynamics, 23, 63-78, doi:10.1007/s00382-004-0422-0, 2004.

Young, J. R. and Westbroek, P.: Genotypic variation in the coccolithophorid species *Emiliania huxleyi*, Mar. Micropaleontol., 18, 5-23, 1991.

Young, J. R., Didymus, J. M., Bown, P. R., Prins, B. and Mann, S.: Crystal assembly and evolution in heterococcoliths, Nature, 356, 516–518, 1992.

Young, J. R.: Variation in *Emiliania huxleyi* coccolith morphology in samples from the Norwegian EHUX mesocosm experiment, 1992, Sarsia, 79, 417–25, 1994.

Young, J. R., Davis, S. A., Bown, P. R. and Mann, S.: Coccolith ultrastructure and biomineralisation, J. Struct. Biol., 126, 195–215, 1999.

Young, J., and Ziveri, P.: Calculation of coccolith volume and its use in calibration of carbonate flux estimates, Deep Sea Res., 47, 1679-1700, 2000.

Young, J., Geisen, M., Cros, L., Kleijne, A., Sprengel, C., Probert, I., and Østergaard, J.: A guide to extant coccolithophore taxonomy, Journal of Nannoplankton Research, 1, 1–125, 2003.

Young, J.: Function of coccoliths. In: Winter, A., Siesser, W.G. (Eds.), Coccolithophores. Cambridge University Press, Cambridge, pp. 63-82, 1994.

Young, J., Geisen, M. and Probert, I.: Review of selected aspects of coccolithophore biology with implications for paleobiodiversity estimation, Micropaleontology, 51(4), 267–288, 2005.

Young, J. R., Andruleit, H. and Probert, I.: Coccolith function and morphogenesis: insights from appendage-bearing coccolithophores of the family Syracosphaeraceae (Haptophyta), J. Phycol., 45, 213–26, 2009.

Zanchettin, D., Traverso, P. and Tomasino, M.: Po River discharges: a preliminary analysis of a 200-year time series, Climatic Change, 89(3-4), 411–433, doi:10.1007/s10584-008-9395-z, 2008.

Zeebe, R. E. and Wolf-Gladrow, D.: CO_2 in Seawater: Equilibrium, Kinetics, Isotopes: Equilibrium, Kinetics, Isotopes, Elsevier Science, Amsterdam, 2001.

Zeebe, R.E., Marchitto, T.M.: Glacial cycles: atmosphere and ocean chemistry. Nat. Geosci. 3, 386–387, 2010.

Zeebe, R. E.: Where are you heading Earth? Nature Geoscience, 4(7), 416–417, doi:10.1038/ngeo1196, 2011.

Zeebe, R. E., 2012: History of Seawater Carbonate Chemistry, Atmospheric CO_2, and Ocean Acidification, Annu Rev Earth Pl Sc 40(1), 141–165, doi:10.1146/annurev-earth-042711-105521, 2012.

Ziveri, P., Grandi, C., Stefanetti, A. and Cita, M. B.: Biogenic fluxes in Bannock Basin: first results from a sediment trap study (November 1991 - May 1992), Rend. Fis. Acc. Lincei, 6(2), 131–145, doi:10.1007/BF03001662, 1995.

Ziveri, P. and Thunell, R.: Coccolithophore export production in Guaymas Basin, Gulf of California: response to climate forcing. Deep Sea Research Part II: Topical Studies in Oceanography 47, 2073–2100, 2000.

Ziveri, P., Baumann, K., Böckel, B., Bollmann, J., and Young, J.: Biogeography of selected Holocene coccoliths in the Atlantic Ocean, Coccolithophores – from Molecular Processes to Global Impact, Springer, Berlin, 403 pp., 2004.

Ziveri, P., de Bernardi, B., Baumann, K.-H., Stoll, H., and Mortyn, P.: Sinking of coccolith carbonate and potential contribution to organic carbon ballasting in the deep ocean, Deep-Sea Res. Pt. II, 54, 659–675, doi:10.1016/j.dsr2.2007.01.006, 2007.

Zondervan, I., Zeebe, E., Rost, B., Riebesell., U.: Decreasing marine biogenic calcification: A negative feedback on rising atmospheric pCO_2, Global Biogeochemical Cycles, 15, 507 – 516, 2001.

Zondervan, I., Rost, B., and Riebesell, U.: Effect of CO_2 concentration on the PIC/POC ratio in the coccolithophore *Emiliania huxleyi* grown under light-limiting conditions and different daylengths, J. Exp. Mar. Biol. Ecol., 272, 55–70, 2002.

Zondervan, I., 2007, The effects of light, macronutrients, trace metals and CO_2 on the production of calcium carbonate and organic carbon in coccolithophores-A review, Deep-Sea Research Part II 54, 521-537, 2007.

Zonneveld, K.A.F., Emeis, K.C., Holzwarth, U., Kniebel, N., Kuhnt, T., Möbius, J., Ní Fhlaithearta, S., Schmiedl, G., Versteegh, G., Welti, R.: Report and preliminary results of R/V POSEIDON Cruise P339, Piräus – Messina, 16 June – 2 July 2006. CAPPUCCINO – Calabrian and Adriatic palaeoproductivity and climatic variability in the last two millennia. Ber. Fachber. Geowiss. Univ. Bremen. 268, pp. 1–61, 2008.

Zonneveld, K. A. F., Chen, L., Elshanawany, R., Fischer, H. W., Hoins, M., Ibrahim, M. I., Pittauerova, D. and Versteegh, G. J. M.: The use of dinoflagellate cysts to separate human-induced from natural variability in the trophic state of the Po River discharge plume over the last two centuries, Marine Pollution Bulletin, 64(1), 114–132, doi:10.1016/j.marpolbul.2011.10.012, 2012.

Appendix

I) Reconstructions of the carbonate system

Site	Age (yrs BP)	TA (µmol/ kgSW)	HCO3 (µmol/ kgSW)	CO3 (µmol/ kgSW)	CO2 (µmol/ kgSW)	DIC	pH	ΩCa
Geofar KF 16	1362.40	2383.71	1800.80	231.28	7.55	2039.63	8.48	5.50
Geofar KF 16	1572.00	2382.82	1796.05	232.82	7.46	2036.33	8.48	5.54
Geofar KF 16	1696.66	2383.47	1800.16	231.44	7.54	2039.14	8.48	5.51
Geofar KF 16	1821.31	2378.79	1796.14	231.15	7.51	2034.80	8.48	5.50
Geofar KF 16	1945.97	2380.95	1796.06	232.05	7.49	2035.60	8.48	5.52
Geofar KF 16	2070.63	2380.79	1795.51	232.21	7.48	2035.20	8.48	5.53
Geofar KF 16	2195.28	2387.03	1796.47	234.35	7.43	2038.24	8.49	5.58
Geofar KF 16	2319.94	2391.47	1801.39	234.18	7.48	2043.05	8.48	5.57
Geofar KF 16	2444.59	2392.21	1797.91	235.87	7.40	2041.18	8.49	5.61
Geofar KF 16	2569.25	2390.28	1791.82	237.52	7.30	2036.63	8.49	5.65
Geofar KF 16	2693.91	2390.91	1791.37	237.96	7.28	2036.61	8.49	5.66
Geofar KF 16	2818.56	2394.71	1790.11	240.00	7.21	2037.32	8.50	5.71
Geofar KF 16	2943.22	2390.54	1792.23	237.46	7.30	2036.99	8.49	5.65
Geofar KF 16	3067.88	2375.91	1788.93	232.87	7.39	2029.19	8.49	5.55
Geofar KF 16	3192.53	2367.81	1785.41	231.00	7.41	2023.82	8.48	5.51
Geofar KF 16	3317.19	2364.43	1787.46	228.82	7.49	2023.76	8.48	5.46
Geofar KF 16	3441.84	2369.25	1789.10	230.11	7.47	2026.68	8.48	5.48
Geofar KF 16	3566.50	2375.70	1794.22	230.67	7.50	2032.40	8.48	5.49
Geofar KF 16	3706.07	2379.53	1796.56	231.29	7.51	2035.36	8.48	5.51
Geofar KF 16	3845.64	2381.12	1796.15	232.09	7.48	2035.73	8.48	5.53
Geofar KF 16	3985.21	2388.60	1796.80	234.86	7.41	2039.08	8.49	5.59
Geofar KF 16	4124.78	2398.06	1801.80	236.69	7.42	2045.91	8.49	5.63
Geofar KF 16	4264.35	2404.42	1802.80	238.87	7.37	2049.04	8.49	5.68
Geofar KF 16	4473.70	2401.90	1798.28	239.65	7.30	2045.24	8.49	5.69
Geofar KF 16	4822.62	2380.48	1781.51	237.68	7.19	2026.38	8.50	5.66
Geofar KF 16	5101.76	2381.96	1785.73	236.59	7.26	2029.58	8.49	5.63
Geofar KF 16	5799.61	2391.77	1791.12	238.42	7.26	2036.80	8.49	5.67
Geofar KF 16	5993.23	2394.33	1790.57	239.67	7.23	2037.46	8.50	5.70
Geofar KF 16	6108.67	2401.58	1793.02	241.63	7.20	2041.85	8.50	5.74
Geofar KF 16	6397.27	2443.07	1811.84	250.95	7.15	2069.94	8.50	5.94
Geofar KF 16	6570.43	2403.63	1788.42	244.30	7.09	2039.81	8.50	5.80

Geofar KF 16	6685.87	2408.73	1788.15	246.47	7.03	2041.66	8.51	5.85
Geofar KF 16	6974.46	2406.67	1780.40	248.73	6.91	2036.04	8.51	5.91
Geofar KF 16	7147.62	2393.40	1775.46	245.33	6.94	2027.73	8.51	5.83
Geofar KF 16	7263.06	2386.90	1772.76	243.78	6.95	2023.50	8.51	5.80
Geofar KF 16	7551.66	2383.11	1771.55	242.73	6.97	2021.25	8.51	5.78
Geofar KF 16	7724.82	2392.39	1775.53	244.90	6.95	2027.38	8.51	5.82
Geofar KF 16	7840.26	2395.59	1776.47	245.82	6.94	2029.23	8.51	5.84
Geofar KF 16	8112.50	2366.06	1773.64	235.01	7.18	2015.83	8.50	5.60
Geofar KF 16	8187.50	2360.08	1774.49	232.26	7.26	2014.01	8.49	5.54
Geofar KF 16	8237.50	2362.53	1776.96	232.26	7.29	2016.51	8.49	5.54
Geofar KF 16	8421.89	2432.60	1779.18	259.75	6.64	2045.58	8.53	6.16
Geofar KF 16	8568.15	2429.13	1777.25	259.11	6.64	2043.01	8.53	6.14
Geofar KF 16	8665.66	2436.92	1780.24	261.09	6.62	2047.95	8.53	6.19
Geofar KF 16	8958.19	2452.76	1789.44	263.85	6.65	2059.93	8.53	6.24
Geofar KF 16	9055.70	2448.85	1787.53	263.02	6.65	2057.20	8.53	6.22
Geofar KF 16	9153.21	2450.59	1788.31	263.42	6.65	2058.37	8.53	6.23
Geofar KF 16	9396.99	2442.91	1786.12	261.17	6.67	2053.97	8.53	6.18
Site	**Age [yrs]**	**TA (µmol/ kgSW)**	**HCO3 (mmol/ kgSW)**	**CO3 (mmol/ kgSW)**	**CO2 (mmol/ kgSW)**	**DIC**	**pH**	**ΩCa**
ODP 980	539.10	2375.17	1900.37	188.15	10.31	2098.82	8.37	4.48
ODP 980	937.50	2374.47	1906.91	185.26	10.54	2102.70	8.36	4.42
ODP 980	1142.10	2372.71	1901.84	186.57	10.40	2098.81	8.36	4.45
ODP 980	1657.50	2377.96	1904.48	187.63	10.39	2102.50	8.37	4.47
ODP 980	2124.50	2381.26	1910.38	186.61	10.52	2107.51	8.36	4.44
ODP 980	2854.40	2372.11	1898.41	187.69	10.30	2096.41	8.37	4.47
ODP 980	3602.17	2383.47	1901.90	190.88	10.20	2102.97	8.37	4.55
ODP 980	4265.70	2382.97	1896.80	192.71	10.04	2099.55	8.38	4.59
ODP 980	4750.30	2394.55	1900.41	195.94	9.94	2106.30	8.38	4.66
ODP 980	5103.20	2391.56	1895.76	196.59	9.86	2102.20	8.39	4.68
ODP 980	5279.80	2386.27	1897.45	193.78	10.00	2101.24	8.38	4.61
ODP 980	6041.80	2376.65	1882.10	196.03	9.71	2087.83	8.39	4.67
ODP 980	6575.20	2390.67	1882.90	201.36	9.49	2093.75	8.40	4.79
ODP 980	7087.30	2377.17	1874.97	199.08	9.49	2083.54	8.40	4.74
ODP 980	7624.40	2376.02	1865.88	202.24	9.25	2077.37	8.41	4.82
ODP 980	8046.50	2376.06	1868.45	201.24	9.32	2079.00	8.40	4.80
ODP 980	8595.38	2363.22	1862.87	198.29	9.37	2070.53	8.40	4.73

ODP 980	9202.10	2370.32	1869.60	198.47	9.45	2077.51	8.40	4.73
ODP 980	9602.88	2369.94	1860.60	201.90	9.20	2071.70	8.41	4.81
ODP 980	9854.46	2374.73	1870.02	200.07	9.38	2079.48	8.40	4.77
Site	**Age [yrs]**	**TA (µmol/ kgSW)**	**HCO3 (mmol/ kgSW)**	**CO3 (mmol/ kgSW)**	**CO2 (mmol/ kgSW)**	**DIC**	**pH**	**ΩCa**
MD08-3192	533.00	2455.08	1946.04	202.20	10.25	2158.48	8.38	4.79
MD08-3192	540.00	2420.94	1927.91	195.63	10.31	2133.85	8.37	4.64
MD08-3192	551.00	2377.41	1902.79	188.08	10.34	2101.22	8.37	4.48
MD08-3192	558.00	2370.21	1898.39	186.94	10.34	2095.67	8.37	4.46
MD08-3192	570.00	2350.10	1890.56	181.97	10.48	2083.01	8.36	4.35
MD08-3192	577.00	2374.91	1901.79	187.48	10.36	2099.62	8.37	4.47
MD08-3192	595.00	2379.76	1903.41	188.78	10.32	2102.51	8.37	4.50
MD08-3192	607.00	2353.62	1890.20	183.53	10.40	2084.12	8.36	4.38
MD08-3192	614.00	2382.09	1906.42	188.52	10.37	2105.31	8.37	4.49
MD08-3192	633.00	2368.90	1897.86	186.62	10.35	2094.83	8.37	4.45
MD08-3192	644.00	2365.28	1897.36	185.36	10.40	2093.12	8.36	4.42
MD08-3192	651.00	2390.75	1907.67	191.51	10.24	2109.42	8.37	4.56
MD08-3192	663.00	2366.75	1895.72	186.61	10.32	2092.65	8.37	4.45
MD08-3192	670.00	2387.15	1903.12	191.87	10.17	2105.16	8.37	4.57
MD08-3192	681.00	2351.08	1893.00	181.39	10.54	2084.94	8.36	4.33
MD08-3192	685.00	2379.77	1901.18	189.68	10.24	2101.10	8.37	4.52
MD08-3192	728.00	2373.24	1910.81	183.21	10.69	2104.71	8.35	4.37
MD08-3192	754.00	2408.11	1918.77	194.09	10.27	2123.12	8.37	4.61
MD08-3192	793.00	2348.76	1890.78	181.34	10.51	2082.63	8.36	4.33
MD08-3192	832.00	2382.90	1913.04	186.20	10.57	2109.82	8.36	4.43
MD08-3192	870.00	2408.76	1929.84	189.94	10.61	2130.39	8.36	4.51
MD08-3192	922.00	2343.82	1893.57	178.25	10.71	2082.53	8.35	4.26
MD08-3192	948.00	2358.91	1899.91	181.79	10.62	2092.31	8.36	4.34
MD08-3192	1032.00	2378.99	1912.53	184.84	10.63	2108.00	8.36	4.40
MD08-3192	1050.00	2410.07	1924.60	192.56	10.42	2127.57	8.37	4.57
MD08-3192	1078.00	2401.13	1922.31	189.86	10.52	2122.68	8.36	4.51
MD08-3192	1123.00	2375.01	1915.64	181.99	10.83	2108.46	8.35	4.34
MD08-3192	1141.00	2364.21	1911.06	179.47	10.90	2101.43	8.35	4.28
MD08-3192	1171.00	2381.02	1918.53	183.26	10.80	2112.59	8.35	4.37
MD08-3192	1195.00	2391.84	1922.39	186.08	10.71	2119.18	8.36	4.43
MD08-3192	1231.00	2398.98	1929.59	186.09	10.80	2126.49	8.35	4.43

MD08-3192	1255.00	2366.05	1909.02	181.03	10.78	2100.83	8.35	4.32
MD08-3192	1292.00	2351.92	1900.50	178.74	10.79	2090.02	8.35	4.27
MD08-3192	1316.00	2404.51	1929.00	188.55	10.67	2128.23	8.36	4.48
MD08-3192	1352.00	2383.35	1913.52	186.20	10.58	2110.30	8.36	4.43
MD08-3192	1376.00	2332.26	1881.65	178.35	10.54	2070.54	8.36	4.27
MD08-3192	1412.00	2371.09	1903.26	185.35	10.48	2099.09	8.36	4.42
MD08-3192	1424.00	2394.23	1916.27	189.49	10.45	2116.21	8.36	4.51
MD08-3192	1496.00	2415.56	1927.59	193.58	10.41	2131.57	8.37	4.60
MD08-3192	1532.00	2361.07	1897.86	183.47	10.50	2091.83	8.36	4.38
MD08-3192	1593.00	2350.60	1893.20	181.12	10.56	2084.88	8.36	4.33
MD08-3192	1617.00	2360.72	1897.57	183.45	10.50	2091.51	8.36	4.38
MD08-3192	1665.00	2344.42	1887.43	180.94	10.49	2078.85	8.36	4.32
MD08-3192	1713.00	2358.06	1899.86	181.46	10.63	2091.96	8.36	4.33
MD08-3192	1749.00	2372.19	1906.32	184.57	10.56	2101.45	8.36	4.40
MD08-3192	1785.00	2358.50	1899.62	181.74	10.62	2091.97	8.36	4.34
MD08-3192	1834.00	2353.05	1894.29	181.67	10.55	2086.50	8.36	4.34
MD08-3192	1858.00	2355.68	1890.86	184.09	10.38	2085.33	8.36	4.39
MD08-3192	1894.00	2312.13	1871.84	174.19	10.62	2056.66	8.35	4.18
MD08-3192	1942.00	2342.72	1888.34	179.89	10.56	2078.79	8.36	4.30
MD08-3192	2011.00	2342.85	1884.56	181.44	10.42	2076.43	8.36	4.34
MD08-3192	2080.00	2338.46	1880.72	181.21	10.38	2072.32	8.36	4.33
MD08-3192	2126.00	2338.62	1880.34	181.43	10.37	2072.14	8.36	4.34
MD08-3192	2194.00	2384.79	1904.24	190.48	10.25	2104.96	8.37	4.54
MD08-3192	2240.00	2359.59	1895.41	183.85	10.45	2089.71	8.36	4.39
MD08-3192	2309.00	2360.33	1906.15	179.87	10.80	2096.83	8.35	4.29
MD08-3192	2338.00	2387.00	1914.10	187.44	10.53	2112.06	8.36	4.46
MD08-3192	2412.00	2374.88	1908.85	184.65	10.59	2104.10	8.36	4.40
MD08-3192	2456.00	2309.03	1870.62	173.43	10.65	2054.70	8.35	4.16
MD08-3192	2485.00	2344.67	1886.20	181.52	10.44	2078.17	8.36	4.34
MD08-3192	2529.00	2301.66	1864.77	172.81	10.60	2048.18	8.35	4.15
MD08-3192	2588.00	2292.26	1859.62	171.10	10.61	2041.34	8.35	4.11
MD08-3192	2647.00	2417.59	1922.97	196.24	10.22	2129.44	8.37	4.66
MD08-3192	2691.00	2458.27	1946.32	203.38	10.20	2159.89	8.38	4.81
MD08-3192	2750.00	2409.03	1914.70	196.09	10.12	2120.91	8.38	4.66
MD08-3192	2823.00	2505.85	1962.01	216.43	9.84	2188.28	8.40	5.10
MD08-3192	2896.00	2393.08	1902.77	194.41	10.04	2107.22	8.38	4.63

MD08-3192	2970.00	2419.63	1916.67	199.58	9.99	2126.24	8.38	4.74
MD08-3192	3043.00	2360.82	1884.06	188.87	10.06	2082.98	8.38	4.51
MD08-3192	3117.00	2354.93	1884.91	186.16	10.20	2081.27	8.37	4.44
MD08-3192	3190.00	2402.47	1904.66	197.44	9.93	2112.03	8.38	4.69
MD08-3192	3264.00	2401.41	1906.46	196.30	10.01	2112.76	8.38	4.67
MD08-3192	3337.00	2384.35	1901.86	191.25	10.18	2103.28	8.37	4.55
MD08-3192	3411.00	2393.24	1900.41	195.41	9.97	2105.79	8.38	4.65
MD08-3192	3484.00	2421.50	1916.92	200.24	9.96	2127.12	8.38	4.75
MD08-3192	3557.00	2439.64	1930.91	201.99	10.06	2142.96	8.38	4.79
MD08-3192	3631.00	2462.44	1941.91	206.83	9.99	2158.73	8.39	4.89
MD08-3192	3704.00	2449.42	1927.86	207.17	9.80	2144.83	8.39	4.91
MD08-3192	3776.00	2450.65	1933.31	205.49	9.94	2148.75	8.39	4.87
MD08-3192	3842.00	2504.61	1955.67	218.45	9.68	2183.81	8.40	5.15
MD08-3192	3908.00	2476.57	1943.51	211.93	9.80	2165.24	8.39	5.01
MD08-3192	3974.00	2477.90	1946.18	211.40	9.85	2167.43	8.39	4.99
MD08-3192	4039.00	2441.85	1920.61	207.00	9.72	2137.33	8.39	4.90
MD08-3192	4105.00	2464.40	1939.77	208.49	9.89	2158.15	8.39	4.93
MD08-3192	4237.00	2483.86	1947.10	213.45	9.78	2170.33	8.40	5.04
MD08-3192	4289.00	2452.58	1930.14	207.54	9.82	2147.50	8.39	4.91
MD08-3192	4368.00	2442.05	1922.36	206.39	9.77	2138.51	8.39	4.89
MD08-3192	4597.00	2417.61	1909.98	201.44	9.82	2121.24	8.39	4.78
MD08-3192	4760.00	2438.19	1923.25	204.47	9.86	2137.57	8.39	4.85
MD08-3192	4842.00	2443.51	1921.42	207.35	9.72	2138.48	8.39	4.91
MD08-3192	4923.00	2442.13	1919.64	207.50	9.69	2136.83	8.40	4.92
MD08-3192	5005.00	2444.65	1925.28	206.27	9.81	2141.36	8.39	4.89
MD08-3192	5087.00	2471.65	1935.73	213.04	9.66	2158.43	8.40	5.04
MD08-3192	5168.00	2459.32	1929.26	210.63	9.68	2149.56	8.40	4.98
MD08-3192	5331.00	2429.39	1917.21	203.31	9.83	2130.36	8.39	4.82
MD08-3192	5413.00	2406.89	1905.06	199.07	9.86	2113.99	8.39	4.73
MD08-3192	5494.00	2395.55	1900.37	196.36	9.92	2106.65	8.38	4.67
MD08-3192	5576.00	2432.36	1917.81	204.28	9.80	2131.89	8.39	4.84
MD08-3192	5658.00	2450.85	1924.36	209.15	9.68	2143.19	8.40	4.95
MD08-3192	5739.00	2446.92	1919.55	209.48	9.61	2138.63	8.40	4.96
MD08-3192	5821.00	2468.75	1920.68	217.88	9.29	2147.85	8.41	5.15
MD08-3192	5902.00	2437.62	1912.17	208.66	9.55	2130.38	8.40	4.95
MD08-3192	6017.00	2455.14	1912.98	215.43	9.29	2137.71	8.41	5.10

MD08-3192	6066.00	2460.67	1918.38	215.52	9.35	2143.25	8.41	5.10
MD08-3192	6310.00	2468.94	1914.85	220.29	9.14	2144.28	8.42	5.21
MD08-3192	6555.00	2489.37	1932.20	221.65	9.28	2163.14	8.41	5.23
MD08-3192	6718.00	2462.91	1915.00	217.78	9.23	2142.01	8.41	5.15
MD08-3192	6800.00	2499.28	1934.07	224.94	9.19	2168.19	8.42	5.30
MD08-3192	6881.00	2481.64	1922.20	222.51	9.14	2153.85	8.42	5.25
MD08-3192	6963.00	2483.42	1924.14	222.46	9.16	2155.76	8.42	5.25
MD08-3192	7044.00	2516.33	1941.42	228.94	9.13	2179.48	8.42	5.39
MD08-3192	7126.00	2491.35	1925.61	225.09	9.08	2159.79	8.42	5.31
MD08-3192	7208.00	2461.51	1910.07	219.18	9.12	2138.38	8.42	5.18
MD08-3192	7289.00	2471.23	1920.48	218.97	9.25	2148.70	8.41	5.18
MD08-3192	7371.00	2481.17	1927.94	220.03	9.30	2157.26	8.41	5.20
MD08-3192	7452.00	2443.92	1905.24	213.98	9.26	2128.48	8.41	5.07
MD08-3192	7534.00	2464.55	1916.59	217.82	9.25	2143.65	8.41	5.15
MD08-3192	7615.00	2430.56	1899.87	210.72	9.32	2119.90	8.41	5.00
MD08-3192	7697.00	2419.62	1892.07	209.40	9.28	2110.75	8.41	4.97
MD08-3192	7963.00	2486.54	1928.64	221.93	9.23	2159.80	8.42	5.24
MD08-3192	8095.00	2496.54	1929.06	225.83	9.10	2163.98	8.42	5.33
MD08-3192	8228.00	2515.09	1929.69	233.13	8.85	2171.67	8.43	5.49
MD08-3192	8361.00	2487.96	1915.92	227.60	8.89	2152.40	8.43	5.37
MD08-3192	8494.00	2505.93	1930.73	228.98	9.01	2168.72	8.43	5.40
Site	**Age [yrs]**	**TA (μmol/ kgSW)**	**HCO3 (mmol/ kgSW)**	**CO3 (mmol/ kgSW)**	**CO2 (mmol/ kgSW)**	**DIC**	**pH**	**ΩCa**
ODP 980	110180	2451.62	1882.87	229.77	9.99	2122.63	8.22	5.37
ODP 980	110180	2448.63	1883.06	228.44	10.02	2121.53	8.22	5.34
ODP 980	110410	2431.04	1875.26	224.38	10.08	2109.72	8.22	5.26
ODP 980	110530	2421.79	1871.14	222.25	10.11	2103.50	8.22	5.21
ODP 980	111000	2409.38	1867.50	218.64	10.21	2096.35	8.21	5.13
ODP 980	111120	2401.38	1870.01	214.26	10.37	2094.63	8.21	5.03
ODP 980	111940	2469.47	1913.40	224.65	10.52	2148.56	8.21	5.24
ODP 980	112180	2428.24	1892.80	216.07	10.61	2119.49	8.20	5.06
ODP 980	112650	2419.44	1892.94	212.40	10.77	2116.11	8.20	4.98
ODP 980	113120	2433.68	1893.60	218.03	10.57	2122.20	8.20	5.11
ODP 980	113710	2451.37	1912.97	217.36	10.80	2141.14	8.20	5.08
ODP 980	113940	2429.36	1901.74	212.97	10.90	2125.61	8.19	4.99
ODP 980	114530	2407.94	1892.74	207.84	11.01	2111.59	8.19	4.88

ODP 980	115000	2419.23	1895.97	211.15	10.90	2118.03	8.19	4.95
ODP 980	115470	2446.05	1907.48	217.47	10.77	2135.71	8.20	5.09
ODP 980	115710	2434.59	1897.55	216.80	10.67	2125.03	8.20	5.08
ODP 980	116180	2398.44	1879.08	209.38	10.69	2099.15	8.20	4.92
ODP 980	116650	2408.62	1881.36	212.71	10.63	2104.70	8.20	4.99
ODP 980	117080	2418.75	1891.84	212.58	10.75	2115.17	8.20	4.99
ODP 980	117170	2423.73	1884.62	217.70	10.54	2112.85	8.20	5.10
ODP 980	117380	2387.95	1877.28	205.85	10.85	2093.98	8.19	4.84
ODP 980	117640	2460.71	1885.13	233.00	10.14	2128.28	8.20	5.44
ODP 980	117810	2439.18	1894.76	219.97	10.60	2125.33	8.20	5.15
ODP 980	117980	2491.44	1889.22	244.22	9.92	2143.37	8.20	5.68
ODP 980	118150	2464.72	1883.35	235.51	10.11	2128.96	8.19	5.50
ODP 980	118360	2490.92	1910.80	235.01	10.37	2156.17	8.20	5.47
ODP 980	118440	2492.31	1892.71	243.19	10.01	2145.91	8.19	5.66
ODP 980	118660	2366.54	1845.33	210.44	10.49	2066.26	8.18	4.96
ODP 980	118780	2447.94	1878.55	230.50	10.21	2119.27	8.19	5.39
ODP 980	118950	2446.88	1876.59	230.88	10.18	2117.65	8.19	5.40
ODP 980	119170	2465.96	1890.93	232.85	10.24	2134.02	8.19	5.43
ODP 980	119340	2457.18	1879.00	234.16	10.10	2123.25	8.19	5.47
ODP 980	119630	2479.23	1891.20	238.23	10.06	2139.49	8.20	5.55
ODP 980	119720	2433.35	1876.14	225.31	10.26	2111.71	8.20	5.28
ODP 980	119890	2412.33	1866.88	220.37	10.30	2097.55	8.20	5.17
ODP 980	120060	2407.18	1865.95	218.61	10.34	2094.90	8.20	5.13
ODP 980	120270	2462.66	1868.41	240.87	9.83	2119.11	8.20	5.62
ODP 980	120360	2400.60	1865.93	215.99	10.49	2092.41	8.19	5.07
ODP 980	120530	2419.98	1858.16	227.40	10.15	2095.71	8.19	5.33
ODP 980	120690	2435.72	1875.43	226.79	10.34	2112.55	8.18	5.31
ODP 980	120820	2427.27	1881.34	220.77	10.55	2112.65	8.18	5.17
ODP 980	120990	2439.31	1870.52	230.32	10.18	2111.03	8.19	5.39
ODP 980	121200	2423.71	1874.19	222.24	10.43	2106.86	8.19	5.21
ODP 980	121540	2483.51	1878.25	245.56	9.84	2133.65	8.19	5.72
ODP 980	121630	2442.48	1866.16	233.43	10.03	2109.62	8.19	5.46
ODP 980	121800	2413.64	1861.35	223.37	10.25	2094.97	8.19	5.24
ODP 980	121970	2438.06	1859.60	234.30	9.94	2103.84	8.19	5.48
ODP 980	122180	2458.21	1863.79	241.01	9.83	2114.62	8.19	5.63
ODP 980	122270	2452.03	1874.84	233.80	10.11	2118.74	8.19	5.46

ODP 980	122480	2474.16	1877.83	241.85	9.95	2129.62	8.19	5.64
ODP 980	122820	2502.03	1876.69	254.01	9.65	2140.35	8.19	5.90
ODP 980	122900	2481.79	1880.99	243.70	9.91	2134.61	8.19	5.68
ODP 980	123070	2480.95	1887.06	240.78	10.02	2137.86	8.19	5.61
ODP 980	123240	2485.66	1884.27	243.91	9.91	2138.09	8.20	5.68
ODP 980	123460	2498.69	1871.15	254.85	9.53	2135.54	8.20	5.93
ODP 980	123540	2488.92	1876.91	248.32	9.72	2134.95	8.20	5.78
ODP 980	123750	2511.67	1885.72	254.16	9.64	2149.52	8.20	5.90
ODP 980	124010	2491.12	1869.37	252.33	9.52	2131.22	8.20	5.87
ODP 980	124180	2508.35	1871.16	258.81	9.39	2139.37	8.21	6.01
ODP 980	124350	2479.42	1868.62	247.78	9.64	2126.04	8.20	5.77
ODP 980	124690	2483.62	1887.31	241.90	10.06	2139.27	8.19	5.63
ODP 980	124810	2451.08	1882.99	230.05	10.32	2123.36	8.19	5.38
ODP 980	125030	2408.47	1872.36	216.66	10.59	2099.61	8.18	5.09
ODP 980	125280	2448.21	1880.96	229.66	10.28	2120.90	8.19	5.37
ODP 980	125450	2433.76	1875.66	225.82	10.33	2111.81	8.19	5.29
ODP 980	125710	2465.69	1873.79	239.96	9.94	2123.68	8.19	5.60
ODP 980	126000	2373.55	1847.23	212.46	10.37	2070.06	8.19	5.01
ODP 980	126090	2416.59	1845.59	231.08	9.83	2086.50	8.20	5.42
ODP 980	126260	2454.78	1861.70	240.27	9.72	2111.69	8.20	5.61
ODP 980	126430	2421.49	1855.16	229.05	9.92	2094.13	8.20	5.37
ODP 980	126640	2406.67	1843.35	227.80	9.85	2081.00	8.20	5.35
ODP 980	126730	2456.73	1854.92	243.89	9.55	2108.36	8.21	5.70
ODP 980	126900	2484.01	1859.75	253.33	9.40	2122.49	8.21	5.90
ODP 980	127070	2458.44	1867.56	239.41	9.83	2116.80	8.20	5.59
ODP 980	127280	2352.53	1855.04	200.52	10.87	2066.43	8.18	4.74
ODP 980	127360	2388.96	1855.94	215.34	10.44	2081.73	8.18	5.07
ODP 980	127580	2426.98	1871.77	224.62	10.34	2106.72	8.19	5.26
ODP 980	127920	2309.51	1919.38	155.76	13.56	2088.69	8.18	3.70
ODP 980	127920	2303.53	1919.24	153.35	13.69	2086.28	8.17	3.65
ODP 980	128000	2285.23	1914.80	147.64	13.98	2076.42	8.17	3.52
ODP 980	128210	2294.94	1917.02	150.72	13.82	2081.55	8.17	3.59
ODP 980	128430	2298.56	1939.75	142.93	14.80	2097.48	8.16	3.40
ODP 980	128690	2378.47	1977.33	160.32	14.18	2151.83	8.17	3.78
ODP 980	128800	2363.37	1979.93	152.94	14.65	2147.51	8.17	3.62
ODP 980	129490	2469.61	1941.86	212.81	11.18	2165.85	8.21	4.97

ODP 980	129600	2476.35	1975.72	201.39	11.91	2189.03	8.21	4.70
ODP 980	129820	2425.97	1953.70	189.55	12.14	2155.40	8.21	4.45
ODP 980	129895	2436.66	1941.84	198.98	11.64	2152.47	8.21	4.66
ODP 980	130055	2554.69	2005.49	221.68	11.44	2238.61	8.22	5.14
ODP 980	130349	2532.01	1974.89	224.95	11.01	2210.84	8.23	5.22
ODP 980	130589	2540.28	1961.51	234.00	10.59	2206.09	8.23	5.42
ODP 980	130669	2538.05	1956.17	235.29	10.49	2201.95	8.23	5.45
ODP 980	130803	2367.91	1866.74	201.60	10.69	2079.03	8.21	4.75
ODP 980	131043	2496.28	1937.03	225.68	10.54	2173.25	8.23	5.25
ODP 980	131230	2499.70	1934.01	228.34	10.41	2172.76	8.24	5.31
ODP 980	131417	2500.14	1930.54	229.93	10.31	2170.78	8.24	5.35
ODP 980	131657	2534.64	1945.64	238.00	10.18	2193.83	8.25	5.52
ODP 980	131844	2526.31	1938.85	237.31	10.12	2186.27	8.25	5.51
ODP 980	131977	2464.42	1904.23	225.86	10.12	2140.21	8.24	5.27
ODP 980	132217	2492.51	1916.11	232.58	10.00	2158.69	8.25	5.42
ODP 980	132404	2513.55	1924.56	237.81	9.91	2172.28	8.26	5.53
ODP 980	132591	2473.53	1901.19	230.79	9.87	2141.85	8.25	5.39
ODP 980	132778	2477.87	1900.81	232.72	9.79	2143.32	8.26	5.43
ODP 980	132911	2455.98	1886.78	229.41	9.74	2125.93	8.26	5.36
ODP 980	133018	2586.41	1951.52	256.95	9.57	2218.04	8.27	5.93
ODP 980	133205	2505.16	1903.85	242.77	9.50	2156.12	8.27	5.65
ODP 980	133392	2521.55	1909.78	247.09	9.42	2166.29	8.27	5.74
ODP 980	133579	2464.93	1878.06	236.59	9.37	2124.02	8.27	5.53
ODP 980	133765	2433.02	1859.85	230.79	9.33	2099.97	8.27	5.41
ODP 980	133952	2386.27	1833.18	222.40	9.28	2064.85	8.28	5.24
ODP 980	134139	2507.99	1887.59	250.36	9.00	2146.95	8.29	5.82
ODP 980	134459	2399.73	1819.27	233.68	8.81	2061.77	8.29	5.49
ODP 980	134833	2359.00	1785.83	230.70	8.59	2025.12	8.28	5.45
ODP 980	135229	2383.77	1786.45	240.66	8.34	2035.45	8.29	5.67
ODP 980	135683	2365.25	1774.47	237.85	8.25	2020.58	8.30	5.61
ODP 980	136136	2410.73	1808.86	242.49	8.47	2059.82	8.30	5.69
ODP 980	136589	2451.58	1837.53	247.37	8.52	2093.42	8.31	5.79
ODP 980	137883	2398.63	1867.21	212.64	9.56	2089.41	8.32	5.01
ODP 980	139437	2385.96	1860.41	210.22	9.57	2080.20	8.31	4.96
ODP 980	140343	2387.49	1848.61	215.87	9.33	2073.81	8.31	5.09
ODP 980	141314	2470.05	1876.26	238.79	9.00	2124.05	8.31	5.58

ODP 980	142155	2548.52	1857.15	279.62	7.96	2144.74	8.33	6.48
ODP 980	142285	2535.42	1850.10	277.06	7.95	2135.10	8.33	6.42
Site	**Age Samples Florida**	**TA (µmol/ kgSW)**	**HCO3 (mmol/ kgSW)**	**CO3 (mmol/ kgSW)**	**CO2 (mmol/ kgSW)**	**DIC**	**pH**	**ΩCa**
SO164-17-2	111827.5	2412.28	1621.66	324.08	6.72	1952.46	8.19	7.69
SO164-17-2	112100	2406.54	1624.72	320.42	6.80	1951.94	8.18	7.61
SO164-17-2	112300	2404.62	1630.68	317.08	6.89	1954.66	8.18	7.53
SO164-17-2	112900	2415.59	1605.19	333.02	6.59	1944.79	8.18	7.92
SO164-17-2	113100	2459.75	1624.02	343.56	6.58	1974.16	8.18	8.12
SO164-17-2	113700	2444.54	1632.43	333.52	6.75	1972.70	8.18	7.89
SO164-17-2	113900	2443.99	1640.82	329.85	6.88	1977.56	8.17	7.80
SO164-17-2	114500	2460.00	1649.49	333.08	6.93	1989.50	8.17	7.87
SO164-17-2	114700	2495.63	1648.04	349.00	6.76	2003.80	8.17	8.21
SO164-17-2	115300	2443.10	1648.42	326.04	6.95	1981.41	8.18	7.71
SO164-17-2	115500	2441.30	1641.41	328.26	6.87	1976.54	8.18	7.76
SO164-17-2	116125	2448.30	1622.58	339.25	6.61	1968.44	8.18	8.03
SO164-17-2	116375	2471.77	1623.60	348.89	6.53	1979.02	8.18	8.24
SO164-17-2	117375	2523.43	1639.45	364.35	6.51	2010.31	8.18	8.55
SO164-17-2	117625	2509.63	1634.08	360.87	6.52	2001.47	8.18	8.49
SO164-17-2	118375	2433.95	1620.18	334.84	6.75	1961.77	8.17	7.95
SO164-17-2	118625	2444.93	1619.81	339.70	6.70	1966.21	8.17	8.06
SO164-17-2	119375	2447.91	1616.40	342.34	6.63	1965.37	8.17	8.12
SO164-17-2	119625	2440.49	1613.41	340.33	6.61	1960.35	8.17	8.07
SO164-17-2	120375	2464.21	1623.81	346.15	6.65	1976.61	8.17	8.19
SO164-17-2	120625	2466.54	1630.10	344.68	6.75	1981.52	8.16	8.15
SO164-17-2	121375	2443.23	1617.05	340.28	6.70	1964.02	8.17	8.07
SO164-17-2	121625	2444.11	1613.17	342.31	6.64	1962.12	8.17	8.12
SO164-17-2	122375	2442.13	1610.36	342.80	6.64	1959.80	8.16	8.14
SO164-17-2	122625	2439.94	1611.56	341.42	6.67	1959.65	8.16	8.11
SO164-17-2	123097.5	2435.73	1605.17	342.24	6.60	1954.02	8.17	8.14
SO164-17-2	123160	2435.18	1604.32	342.36	6.59	1953.27	8.17	8.14
SO164-17-2	123347.5	2456.83	1600.54	353.26	6.46	1960.26	8.17	8.38
SO164-17-2	123410	2471.49	1598.87	360.29	6.39	1965.54	8.17	8.54
SO164-17-2	123597.5	2486.71	1594.90	368.52	6.29	1969.71	8.17	8.72
SO164-17-2	123660	2482.72	1593.94	367.20	6.29	1967.43	8.17	8.69
SO164-17-2	123847.5	2476.80	1597.05	363.08	6.31	1966.44	8.17	8.60

SO164-17-2	123910	2476.66	1601.12	361.17	6.34	1968.63	8.18	8.55
SO164-17-2	124097.5	2506.08	1615.99	367.22	6.36	1989.57	8.18	8.65
SO164-17-2	124160	2525.48	1621.11	373.30	6.33	2000.75	8.18	8.77
SO164-17-2	124347.5	2543.25	1631.07	376.69	6.38	2014.13	8.18	8.83
SO164-17-2	124410	2529.64	1638.26	367.85	6.52	2012.64	8.18	8.63
SO164-17-2	124597.5	2607.68	1690.63	378.89	6.77	2076.29	8.17	8.80
SO164-17-2	124660	2623.80	1703.32	380.22	6.81	2090.36	8.18	8.81
SO164-17-2	124847.5	2546.09	1689.32	352.77	6.98	2049.07	8.17	8.24
SO164-17-2	124910	2537.76	1678.02	354.13	6.91	2039.06	8.17	8.28
SO164-17-2	125937.5	2487.54	1639.58	348.99	6.67	1995.24	8.18	8.22
SO164-17-2	126562.5	2462.73	1622.15	345.61	6.54	1974.30	8.18	8.17
SO164-17-2	128437.5	2444.28	1660.82	322.10	7.26	1990.18	8.15	7.62
SO164-17-2	129062.5	2491.06	1666.06	339.49	7.02	2012.58	8.17	7.99
SO164-17-2	130375	2619.74	1661.37	395.48	6.25	2063.09	8.20	9.16
SO164-17-2	130625	2613.50	1654.69	395.53	6.18	2056.40	8.21	9.17
SO164-17-2	131375	2658.26	1642.17	419.71	5.86	2067.75	8.22	9.69
SO164-17-2	131625	2656.39	1639.89	419.70	5.82	2065.41	8.22	9.69
SO164-17-2	132375	2624.40	1610.34	418.27	5.62	2034.23	8.23	9.70
SO164-17-2	132625	2614.10	1596.16	419.85	5.52	2021.53	8.23	9.75
SO164-17-2	133375	2497.23	1574.12	378.80	5.61	1958.54	8.24	8.90
SO164-17-2	133625	2474.23	1563.92	373.14	5.56	1942.62	8.24	8.79
SO164-17-2	134375	2468.54	1527.44	385.79	5.19	1918.42	8.26	9.11
SO164-17-2	134625	2471.26	1520.93	389.67	5.12	1915.73	8.26	9.20
SO164-17-2	135877.5	2485.20	1495.17	406.33	4.85	1906.35	8.27	9.59
SO164-17-2	136460	2461.48	1491.90	397.64	4.89	1894.42	8.27	9.41
SO164-17-2	138207.5	2395.12	1469.27	378.53	4.80	1852.60	8.28	9.02
SO164-17-2	138792.5	2400.38	1468.65	381.09	4.79	1854.53	8.28	9.08
SO164-17-2	140540	2386.51	1472.49	373.84	4.89	1851.22	8.27	8.92
SO164-17-2	141122.5	2395.53	1479.02	374.92	4.93	1858.87	8.27	8.94
SO164-17-2	142451.2712	2457.62	1481.08	399.91	4.73	1885.72	8.28	9.46
Site	**Age [AD]**	**TA (µmol/ kgSW)**	**HCO3 (mmol/ kgSW)**	**CO3 (mmol/ kgSW)**	**CO2 (mmol/ kgSW)**	**DIC**	**pH out**	**ΩCa**
GeoB10709-5	1800.98	2474.08	1879.32	241.33	10.06	2130.71	8.18	5.63
GeoB10709-5	1804.85	2520.24	1884.59	258.51	9.71	2152.80	8.18	6.00
GeoB10709-5	1808.72	2503.71	1882.08	252.62	9.82	2144.52	8.18	5.87

GeoB10709-5	1812.59	2488.45	1875.93	248.79	9.87	2134.58	8.18	5.79
GeoB10709-5	1816.46	2467.55	1870.21	242.42	9.97	2122.60	8.18	5.66
GeoB10709-5	1820.33	2499.19	1886.64	248.82	9.95	2145.41	8.18	5.79
GeoB10709-5	1824.20	2503.54	1887.48	250.29	9.93	2147.70	8.18	5.82
GeoB10709-5	1828.07	2462.98	1868.83	241.09	10.00	2119.92	8.18	5.63
GeoB10709-5	1831.94	2452.50	1867.03	237.45	10.07	2114.55	8.18	5.55
GeoB10709-5	1835.81	2457.94	1866.40	239.99	10.00	2116.38	8.18	5.60
GeoB10709-5	1839.68	2530.96	1894.59	258.83	9.78	2163.19	8.19	6.00
GeoB10709-5	1843.55	2507.63	1881.00	254.72	9.77	2145.49	8.18	5.92
GeoB10709-5	1847.42	2455.50	1863.38	240.24	9.97	2113.59	8.18	5.61
GeoB10709-5	1851.29	2444.88	1865.42	234.95	10.13	2110.50	8.17	5.49
GeoB10709-5	1855.16	2482.61	1887.82	241.39	10.16	2139.36	8.18	5.62
GeoB10709-5	1859.03	2471.08	1884.57	237.92	10.23	2132.72	8.18	5.55
GeoB10709-5	1862.90	2466.92	1880.59	237.86	10.20	2128.65	8.18	5.55
GeoB10709-5	1866.77	2492.25	1891.97	243.72	10.15	2145.84	8.18	5.67
GeoB10709-5	1870.64	2514.67	1903.32	248.39	10.14	2161.85	8.18	5.77
GeoB10709-5	1874.51	2499.24	1895.55	245.18	10.17	2150.90	8.18	5.70
GeoB10709-5	1878.38	2459.59	1877.22	236.26	10.25	2123.73	8.17	5.52
GeoB10709-5	1882.25	2423.44	1861.37	227.80	10.36	2099.53	8.16	5.34
GeoB10709-5	1886.12	2476.93	1887.85	239.13	10.31	2137.29	8.17	5.57
GeoB10709-5	1889.99	2449.63	1871.00	234.77	10.29	2116.06	8.16	5.49
GeoB10709-5	1893.86	2435.04	1866.88	230.39	10.38	2107.64	8.16	5.39
GeoB10709-5	1897.73	2460.45	1885.34	233.30	10.46	2129.11	8.16	5.45
GeoB10709-5	1901.60	2446.20	1875.47	231.49	10.44	2117.40	8.16	5.41
GeoB10709-5	1905.47	2451.04	1883.96	229.99	10.57	2124.52	8.16	5.38
GeoB10709-5	1909.34	2467.28	1892.39	233.28	10.58	2136.25	8.16	5.44
GeoB10709-5	1913.21	2499.01	1914.92	237.18	10.68	2162.78	8.16	5.51
GeoB10709-5	1917.08	2464.47	1888.48	233.79	10.56	2132.83	8.16	5.46
GeoB10709-5	1920.00	2434.19	1873.89	227.24	10.62	2111.75	8.15	5.32
GeoB10709-5	1921.00	2428.05	1875.30	224.08	10.73	2110.11	8.15	5.25

GeoB10709-5	1922.00	2427.98	1876.45	223.58	10.76	2110.79	8.15	5.24
GeoB10709-5	1923.00	2427.79	1877.41	223.10	10.78	2111.30	8.15	5.23
GeoB10709-5	1924.00	2442.54	1883.21	226.85	10.73	2120.80	8.15	5.31
GeoB10709-5	1925.00	2455.23	1888.49	229.96	10.70	2129.15	8.15	5.37
GeoB10709-5	1926.00	2459.46	1894.13	229.38	10.77	2134.28	8.15	5.36
GeoB10709-5	1927.00	2463.72	1899.79	228.80	10.84	2139.43	8.15	5.34
GeoB10709-5	1928.00	2450.93	1896.43	224.86	10.93	2132.22	8.15	5.26
GeoB10709-5	1929.00	2435.73	1893.20	219.85	11.05	2124.11	8.15	5.15
GeoB10709-5	1930.00	2419.31	1888.71	214.87	11.17	2114.75	8.15	5.04
GeoB10709-5	1931.00	2406.24	1885.73	210.67	11.28	2107.68	8.14	4.95
GeoB10709-5	1932.00	2402.44	1886.17	208.90	11.35	2106.42	8.14	4.91
GeoB10709-5	1933.00	2402.13	1887.47	208.24	11.39	2107.09	8.14	4.89
GeoB10709-5	1934.00	2407.83	1888.38	210.25	11.33	2109.96	8.14	4.94
GeoB10709-5	1935.00	2423.04	1889.00	216.35	11.15	2116.50	8.14	5.07
GeoB10709-5	1936.00	2423.04	1890.98	215.53	11.20	2117.71	8.14	5.05
GeoB10709-5	1937.00	2413.16	1896.79	208.96	11.47	2117.22	8.14	4.90
GeoB10709-5	1938.00	2424.60	1903.49	210.94	11.47	2125.90	8.14	4.94
GeoB10709-5	1939.00	2452.66	1908.28	220.68	11.21	2140.17	8.15	5.16
GeoB10709-5	1940.00	2472.62	1910.39	228.17	11.01	2149.56	8.15	5.32
GeoB10709-5	1941.00	2471.84	1911.77	227.26	11.04	2150.08	8.15	5.30
GeoB10709-5	1942.00	2472.32	1913.24	226.84	11.07	2151.15	8.15	5.29
GeoB10709-5	1947.00	2489.47	1919.17	231.55	10.99	2161.71	8.15	5.39
GeoB10709-5	1948.00	2459.32	1909.76	222.85	11.16	2143.77	8.15	5.20
GeoB10709-5	1949.00	2434.12	1897.40	217.48	11.21	2126.09	8.14	5.09
GeoB10709-5	1950.00	2418.32	1888.23	214.72	11.21	2114.16	8.14	5.04
GeoB10709-5	1951.00	2416.65	1878.77	217.99	11.03	2107.78	8.14	5.11
GeoB10709-5	1952.00	2439.31	1879.53	227.15	10.78	2117.46	8.14	5.32
GeoB10709-5	1953.00	2422.87	1888.70	216.44	11.18	2116.32	8.14	5.07
GeoB10709-5	1954.00	2413.89	1897.35	209.07	11.50	2117.92	8.14	4.91
GeoB10709-5	1955.00	2440.51	1907.64	215.91	11.38	2134.92	8.14	5.05

GeoB10709-5	1956.00	2460.10	1904.17	225.58	11.07	2140.81	8.14	5.27
GeoB10709-5	1957.00	2454.24	1900.71	224.58	11.07	2136.36	8.14	5.25
GeoB10709-5	1958.00	2426.45	1899.21	213.58	11.40	2124.19	8.14	5.01
GeoB10709-5	1959.00	2421.89	1897.38	212.46	11.43	2121.27	8.14	4.98
GeoB10709-5	1960.00	2435.43	1902.66	215.92	11.38	2129.97	8.14	5.06
GeoB10709-5	1961.00	2448.93	1907.65	219.50	11.33	2138.48	8.14	5.13
GeoB10709-5	1962.00	2460.59	1912.97	222.17	11.30	2146.44	8.14	5.19
GeoB10709-5	1963.00	2470.51	1917.04	224.63	11.27	2152.94	8.14	5.24
GeoB10709-5	1964.00	2462.53	1908.25	224.98	11.19	2144.42	8.14	5.25
GeoB10709-5	1965.00	2454.80	1899.41	225.45	11.10	2135.96	8.13	5.27
GeoB10709-5	1966.00	2441.64	1888.70	224.44	11.06	2124.19	8.13	5.25
GeoB10709-5	1967.00	2440.03	1884.26	225.64	10.99	2120.89	8.13	5.28
GeoB10709-5	1968.00	2438.18	1884.17	224.91	11.02	2120.10	8.13	5.27
GeoB10709-5	1969.00	2435.68	1884.54	223.73	11.08	2119.35	8.13	5.24
GeoB10709-5	1970.00	2433.55	1884.75	222.77	11.12	2118.64	8.13	5.22
GeoB10709-5	1971.00	2446.05	1892.32	224.84	11.14	2128.30	8.13	5.26
GeoB10709-5	1972.00	2473.12	1904.93	230.92	11.09	2146.94	8.13	5.39
GeoB10709-5	1973.00	2493.23	1916.30	234.63	11.11	2162.04	8.13	5.46
GeoB10709-5	1974.00	2503.28	1929.22	233.45	11.26	2173.93	8.13	5.43
GeoB10709-5	1975.00	2495.87	1931.42	229.43	11.41	2172.25	8.13	5.34
GeoB10709-5	1976.00	2470.68	1925.66	221.28	11.61	2158.56	8.12	5.16
GeoB10709-5	1977.00	2444.96	1918.65	213.47	11.82	2143.94	8.12	4.99
GeoB10709-5	1978.00	2425.72	1913.70	207.51	11.99	2133.21	8.11	4.86
GeoB10709-5	1979.00	2426.97	1918.42	206.08	12.10	2136.60	8.11	4.83
GeoB10709-5	1980.00	2434.83	1927.31	205.67	12.23	2145.21	8.11	4.82
GeoB10709-5	1981.00	2439.59	1933.99	204.88	12.34	2151.21	8.11	4.79
GeoB10709-5	1982.00	2440.04	1937.09	203.79	12.43	2153.30	8.11	4.77
GeoB10709-5	1983.00	2437.61	1937.61	202.58	12.50	2152.68	8.11	4.74
GeoB10709-5	1984.00	2434.84	1937.98	201.28	12.57	2151.83	8.11	4.71
GeoB10709-5	1985.00	2439.28	1938.29	203.03	12.52	2153.84	8.11	4.75

GeoB10709-5	1987.00	2448.37	1940.51	205.95	12.48	2158.94	8.10	4.81
GeoB10709-5	1988.00	2442.57	1942.32	202.79	12.64	2157.76	8.10	4.74
GeoB10709-5	1989.00	2432.34	1943.22	198.16	12.85	2154.22	8.10	4.64
GeoB10709-5	1990.00	2414.24	1939.37	192.22	13.06	2144.64	8.09	4.51
GeoB10709-5	1993.00	2386.08	1923.75	187.04	13.14	2123.92	8.09	4.40
GeoB10709-5	1994.00	2392.17	1927.10	188.19	13.15	2128.45	8.09	4.43
GeoB10709-5	1995.00	2388.94	1930.05	185.63	13.32	2129.00	8.08	4.37
GeoB10709-5	1996.00	2384.05	1932.76	182.48	13.51	2128.75	8.08	4.30
GeoB10709-5	1997.00	2397.67	1940.92	184.76	13.51	2139.19	8.08	4.34
GeoB10709-5	1998.00	2418.75	1950.02	189.80	13.43	2153.24	8.08	4.45
GeoB10709-5	1999.00	2441.79	1959.07	195.67	13.30	2168.04	8.08	4.58
GeoB10709-5	2000.00	2458.65	1959.85	202.42	13.05	2175.32	8.08	4.73

II) Coccolith data from SYRACO

Sample Geo-far KF16 (A-zores)	Sample depth [cm]	Age [yrs]	Number of coccoliths	Noelaerhabdaceae mean coccolith weight (pg)	
1000	000-001	104.80	3072	6.49	
1001	002-003	524.00	191	4.79	
1002	003-004	733.60	1043	5.56	
1003	004-005	943.20	1098	6.35	
1004	005-006	1152.80	133	5.63	
1005	006-007	1362.40	886	5.48	
1006	007-008	1572.00	872	5.49	
1007	008-009	1696.66	1011	6.21	
1008	009-010	1821.31	811	5.30	
1009	010-011	1945.97	939	6.73	
1010	011-012	2070.63	1074	6.22	
1011	012-013	2195.28	448	5.81	
1012	013-014	2319.94	147	6.13	
1013	014-015	2444.59	372	6.71	
1014	015-016	2569.25	431	5.83	
1015	016-017	2693.91	2471	6.40	
1016	017-018	2818.56	569	6.23	

1017	018-019	2943.22	798	6.39	
1018	019-020	3067.88	293	6.48	
1019	020-021	3192.53	812	6.54	
1020	021-022	3317.19	493	6.42	
1021	022-023	3441.84	585	5.89	
1022	023-024	3566.50	237	6.45	
1023	024-025	3706.07	207	6.92	
1024	025-026	3845.64	571	7.09	
1025	026-027	3985.21	533	7.67	
1026	027-028	4124.78	1341	7.77	
1027	028-029	4264.35	667	5.88	
1028	029-031	4473.70	1602	7.25	
1029	032-033	4822.62	1730	7.13	
1030	034-035	5101.76	952	6.14	
1031	039-040	5799.61	172	7.72	
1032	042-043	5993.23	3249	8.04	
1033	044-045	6108.67	1580	7.54	
1034	049-050	6397.27	402	7.32	
1035	052-053	6570.43	279	6.91	
1036	054-055	6685.87	196	7.12	
1037	059-060	6974.46	180	6.36	
1038	062-063	7147.62	153	8.83	
1039	064-065	7263.06	255	6.18	
1040	069-070	7551.66	859	6.70	
1041	072-073	7724.82	221	7.33	
1042	074-075	7840.26	470	7.62	
1043	079-080	8112.50	596	6.70	
1044	082-083	8187.50	420	7.14	
1045	084-085	8237.50	866	8.06	
1046	089-090	8421.89	182	6.22	
1047	092-093	8568.15	140	7.46	
1048	094-095	8665.66	622	6.72	
1049	100-101	8958.19	325	6.95	
1050	102-103	9055.70	188	6.64	
1051	104-105	9153.21	143	7.61	
1052	109-110	9396.99	744	6.57	

Sample MD08-3192 (Vøring Plateau)	Sample depth [cm]	Age [yrs]	Number of coccoliths	Noelaerhabdaceae mean coccolith weight (pg)	
1001	000-001	0.00	489	10.83	
1002	012-013	911.36	850	8.56	
1003	036-037	1290.10	824	8.69	
1004	048-049	1479.47	792	8.12	
1005	072-073	1895.29	1431	7.52	
1006	084-085	2128.93	1134	7.73	
1007	108-109	2596.23	1084	7.84	
1008	120-121	2829.87	457	7.60	
1009	144-145	3297.16	601	6.53	
1010	156-157	3521.01	692	6.78	
1011	180-181	3929.45	657	7.44	
1012	192-193	4133.68	387	7.40	
1013	216-217	4542.13	424	7.32	
1014	228-229	4746.35	319	7.23	
1015	252-253	5154.80	456	7.73	
1016	264-265	5359.02	902	6.75	
1017	288-289	5767.47	505	6.89	
1018	300-301	5971.69	489	6.43	
1019	324-325	6380.14	446	7.50	
1020	336-337	6584.36	368	7.17	
1021	360-361	6992.81	654	7.77	
1022	372-373	7197.04	839	6.84	
1023	396-397	7605.48	553	6.78	
1024	408-409	7815.34	731	7.44	
1025	432-433	8363.56	640	6.57	
1026	444-445	8637.67	1187	6.88	
1027	468-469	9185.90	730	6.39	
1028	480-481	9460.01	806	7.02	
1029	504-505	10008.23	921	6.24	
1030	516-517	10282.34	982	6.30	
1031	540-541	10830.57	1021	6.65	
1032	552-553	11104.68	504	7.56	
1033	576-577	11652.90	1092	7.79	
1034	588-589	11927.01	1176	8.47	
1035	612-613	12475.23	826	7.99	
1036	624-625	12749.35	373	7.17	
1037	648-649	13297.57	740	8.23	

1038	660-661	13571.68	588	8.00	
1039	684-685	14119.90	392	8.21	
1040	696-697	14394.01	440	7.67	
1041	720-721	14942.24	331	7.70	
1042	732-733	15216.35	917	8.01	
Sample ODP Site 980 (Rockall Plateau) Holocene	**depth**	**Sample depth [cm]**	**Age [yrs]**	**Number of coccoliths**	**Noelaerhabdaceae mean coccolith weight (pg)**
1001	B1H1 2 - 4 cm	2.50	539.10	279	7.96
1002	B1H1 20 - 22 cm	21.00	937.50	728	7.77
1003	B1H1 30 - 32 cm	30.50	1142.10	907	7.96
1004	B1H1 44 - 46 cm	44.50	1657.50	583	6.96
1005	B1H1 54 - 56 cm	54.50	2124.50	287	6.49
1006	B1H1 68 - 70 cm	69.50	2854.40	477	6.67
1007	B1H1 85 - 87 cm	86.50	3602.17	562	5.65
1008	B1H1 97 - 99 cm	97.50	4265.70	760	5.94
1009	B1H1 105 - 107 cm	106.00	4750.30	281	6.00
1010	B1H1 111 - 113 cm	114.50	5103.20	626	6.08
1011	B1H1 117 - 119 cm	117.50	5279.80	320	6.21
1012	B1H1 127 - 129 cm	127.50	6041.80	405	5.48
1013	B1H1 134 - 136 cm	134.50	6575.20	1001	6.03
1014	B1H1 145 - 147 cm	146.00	7087.30	810	5.94
1015	B1H2 9 - 11 cm	159.50	7624.40	569	5.58
1016	B1H2 22.5 - 25 cm	171.00	8046.50	1096	5.66
1017	B1H2 30 - 32 cm	180.50	8595.38	1211	5.58
1018	B1H2 40 - 42 cm	191.00	9202.10	494	6.15
1019	B1H2 50 - 52 cm	200.00	9602.88	933	6.20
1020	B1H2 59 - 60 cm	209.00	9854.46	2025	6.01
1021	B1H2 95 - 97 cm	246.00	10929.10	711	5.96
1022	B1H2 127 - 129 cm	278.00	11909.51	1305	5.82

1023	B1H2 133 - 135 cm	284.00	12093.33	1008	5.52
1024	B1H2 137 - 139 cm	288.00	12215.90	919	5.49
1025	B1H2 141 - 143 cm	292.00	12338.48	625	5.93
1026	B1H3 0 - 2 cm	301.00	12662.40	312	7.27
1027	B1H3 5 - 7 cm	306.00	12863.80	531	6.16
1028	B1H3 13 - 15 cm	314.00	13186.04	319	7.37
1029	B1H3 27 - 29 cm	328.00	13749.96	148	6.36
1030	B1H3 43 - 45 cm	344.00	14394.44	547	6.50
Sample MD08-3192 (Vøring Plateau)	**Sample depth [cm]**	**Age [yrs]**	**Number of coccoliths**	**Noelaerhabdaceae mean coccolith weight (pg)**	
1001	000-001	0.00	489	10.83	
1002	012-013	911.36	850	8.56	
1003	036-037	1290.10	824	8.69	
1004	048-049	1479.47	792	8.12	
1005	072-073	1895.29	1431	7.52	
1006	084-085	2128.93	1134	7.73	
1007	108-109	2596.23	1084	7.84	
1008	120-121	2829.87	457	7.60	
1009	144-145	3297.16	601	6.53	
1010	156-157	3521.01	692	6.78	
1011	180-181	3929.45	657	7.44	
1012	192-193	4133.68	387	7.40	
1013	216-217	4542.13	424	7.32	
1014	228-229	4746.35	319	7.23	
1015	252-253	5154.80	456	7.73	
1016	264-265	5359.02	902	6.75	
1017	288-289	5767.47	505	6.89	
1018	300-301	5971.69	489	6.43	
1019	324-325	6380.14	446	7.50	
1020	336-337	6584.36	368	7.17	
1021	360-361	6992.81	654	7.77	
1022	372-373	7197.04	839	6.84	
1023	396-397	7605.48	553	6.78	
1024	408-409	7815.34	731	7.44	
1025	432-433	8363.56	640	6.57	

1026	444-445	8637.67	1187	6.88	
1027	468-469	9185.90	730	6.39	
1028	480-481	9460.01	806	7.02	
1029	504-505	10008.23	921	6.24	
1030	516-517	10282.34	982	6.30	
1031	540-541	10830.57	1021	6.65	
1032	552-553	11104.68	504	7.56	
1033	576-577	11652.90	1092	7.79	
1034	588-589	11927.01	1176	8.47	
1035	612-613	12475.23	826	7.99	
1036	624-625	12749.35	373	7.17	
1037	648-649	13297.57	740	8.23	
1038	660-661	13571.68	588	8.00	
1039	684-685	14119.90	392	8.21	
1040	696-697	14394.01	440	7.67	
1041	720-721	14942.24	331	7.70	
1042	732-733	15216.35	917	8.01	
Sample ODP Site 980 (Rockall Plateau) Termination II	**depth**	**Sample depth [m]**	**Age [yrs]**	**Number of coccoliths**	**Noelaerhabdaceae mean coccolith weight (pg)**
1001	980C 3-1-97	14.86	116861.29	1899	5.17
1002	980C 3-1-110	14.99	117509.50	1289	5.12
1003	980C 3-1-149	15.38	119166.00	1235	5.25
1004	980C 3-2-10	15.49	119633.00	2004	5.00
1005	980C 3-2-40	15.79	120907.00	2113	5.25
1006	980C 3-2-55	15.94	121544.00	3017	5.32
1007	980C 3-2-80	16.19	122606.27	2395	5.30
1008	980C 3-2-100	16.39	123456.00	3882	5.33
1009	980C 3-2-110	16.49	123880.40	2876	5.58
1010	980C 3-2-139	16.78	125112.00	1693	5.47
1011	980C 3-2-149	16.88	125536.25	1655	5.52
1012	980C 3-3-10	16.99	126004.00	1594	5.44
1013	980C 3-3-29	17.18	126811.17	1177	5.81
1014	980C 3-3-40	17.29	127278.00	564	6.19
1015	980C 3-3-49.5	17.39	127681.46	1640	5.70
1016	980C 3-3-55	17.44	127915.00	156	7.71
1017	980C 3-3-62.5	17.52	128293.50	326	6.04
1018	980C 3-3-74	17.64	128939.35	162	7.45

1019	980C 3-3-80	17.70	129260.11	49	6.25
1020	980C 3-3-85	17.75	129532.24	392	6.00
1021	980C 3-3-89	17.78	129708.10	165	7.58
1022	980C 3-3-101	17.90	130349.00	191	6.24
1023	980C 3-3-110	17.99	130829.67	286	6.24
1024	980C 3-3-121	18.10	131417.00	320	5.32
1025	980C 3-3-129A	18.18	131844.00	374	5.58
1026	980C 3-3-143	18.32	132591.00	704	5.18
Sample SO164-17-2 (Florida Strait) Termination II	**Sample depth [cm]**	**Age [yrs]**	**Number of coccoliths**	**Noelaerhabdaceae mean coccolith weight (pg)**	
1001	350.50	111827.50	105	12.77	
1002	352.50	112100.00	111	10.74	
1003	353.50	112300.00	233	10.95	
1004	356.50	112900.00	148	11.65	
1005	357.50	113100.00	228	11.68	
1006	360.50	113700.00	91	12.87	
1007	361.50	113900.00	82	13.04	
1008	364.50	114500.00	192	11.60	
1009	365.50	114700.00	217	10.57	
1010	368.50	115300.00	236	11.93	
1011	369.50	115500.00	174	11.06	
1012	372.50	116125.00	214	10.83	
1013	373.50	116375.00	325	10.44	
1014	377.50	117375.00	216	10.43	
1015	378.50	117625.00	237	10.76	
1016	381.50	118375.00	210	10.08	
1017	382.50	118625.00	170	9.81	
1018	385.50	119375.00	165	11.54	
1019	386.50	119625.00	148	11.31	
1020	389.50	120375.00	197	11.92	
1021	390.50	120625.00	123	11.76	
1022	393.50	121375.00	184	11.18	
1023	394.50	121625.00	256	9.25	
1024	397.50	122375.00	137	12.03	
1025	398.50	122625.00	347	10.77	
1026	401.50	123097.50	152	10.48	

1027	402.50	123160.00	352	10.13	
1028	405.50	123347.50	258	10.54	
1029	406.50	123410.00	376	10.96	
1030	409.50	123597.50	172	11.18	
1031	410.50	123660.00	331	10.88	
1032	413.50	123847.50	273	9.61	
1033	414.50	123910.00	272	9.80	
1034	417.50	124097.50	314	10.29	
1035	418.50	124160.00	214	9.18	
1036	421.50	124347.50	559	10.30	
1037	422.50	124410.00	617	9.97	
1038	425.50	124597.50	518	10.49	
1039	426.50	124660.00	613	10.82	
1040	429.50	124847.50	759	11.94	
1041	430.50	124910.00	634	11.79	
1042	433.50	125937.50	410	11.92	
1043	434.50	126562.50	427	9.42	
1044	437.50	128437.50	230	11.08	
1045	438.50	129062.50	356	8.86	
1046	441.50	130375.00	149	9.38	
1047	442.50	130625.00	291	9.72	
1048	445.50	131375.00	365	7.50	
1049	446.50	131625.00	251	8.47	
1050	449.50	132375.00	506	6.89	
1051	450.50	132625.00	334	7.66	
1052	453.50	133375.00	345	7.38	
1053	454.50	133625.00	372	6.42	
1054	457.50	134375.00	348	6.38	
1055	458.50	134625.00	347	5.63	
1056	461.50	135877.50	479	5.33	
1057	462.50	136460.00	603	5.33	
1058	465.50	138207.50	420	5.26	
1059	466.50	138792.50	870	5.12	
1060	469.50	140540.00	780	5.27	
1061	470.50	141122.50	422	5.39	
1062	473.50	142451.27	1155	5.55	
1063	474.50	142752.12	682	5.72	

Sample GeoB 10709-5 (Gulf of Taranto) past 200 years	Sample depth (mm)	Age AD	Number of coccoliths	Noelaerhabdaceae mean coccolith weight (pg)	
1001	0.00	2006.00	850	9.03	
1002	5.00	2001.73	942	9.42	
1003	10.00	1997.45	633	8.95	
1004	15.00	1993.18	738	8.57	
1005	17.50	1991.04	278	10.69	
1006	20.00	1988.91	1219	9.38	
1007	25.00	1984.63	449	9.82	
1008	30.00	1980.36	691	9.04	
1009	35.00	1976.09	356	9.87	
1010	40.00	1971.81	506	8.95	
1011	45.00	1967.54	517	9.74	
1012	52.50	1961.13	643	9.54	
1013	55.00	1958.99	155	11.33	
1014	57.50	1956.85	584	10.19	
1015	60.00	1954.72	598	8.70	
1016	65.00	1950.44	799	9.00	
1017	70.00	1946.17	899	9.82	
1018	75.00	1941.90	560	10.33	
1019	80.00	1937.62	802	9.51	
1020	85.00	1933.35	807	8.96	
1021	90.00	1929.08	482	9.54	
1022	92.50	1926.94	1080	8.74	
1023	100.00	1920.53	995	8.78	
1024	105.00	1916.26	757	8.92	
1025	110.00	1911.98	453	9.49	
1026	112.50	1909.85	202	8.15	
1027	115.00	1907.71	1219	8.95	
1028	122.50	1901.30	541	8.69	
1029	125.00	1899.16	925	8.54	
1030	130.00	1894.89	1786	9.63	
1031	135.00	1890.62	1356	9.48	
1032	140.00	1886.34	1758	9.29	
1033	145.00	1882.07	1140	9.06	
1034	150.00	1877.79	928	8.76	
1035	155.00	1873.52	1191	9.18	
1036	160.00	1869.25	2321	11.02	

1037	162.50	1867.11	331	9.68	
1038	165.00	1864.97	1172	9.58	
1039	170.00	1860.70	1417	9.27	
1040	175.00	1856.43	1107	10.07	
1041	180.00	1852.15	1764	10.00	
1042	185.00	1847.88	884	9.36	
1043	190.00	1843.61	1095	9.64	
1044	195.00	1839.33	1490	10.22	
1045	202.50	1832.92	347	9.33	
1046	205.00	1830.79	1437	9.71	

III) Established age model of site MD08-3192

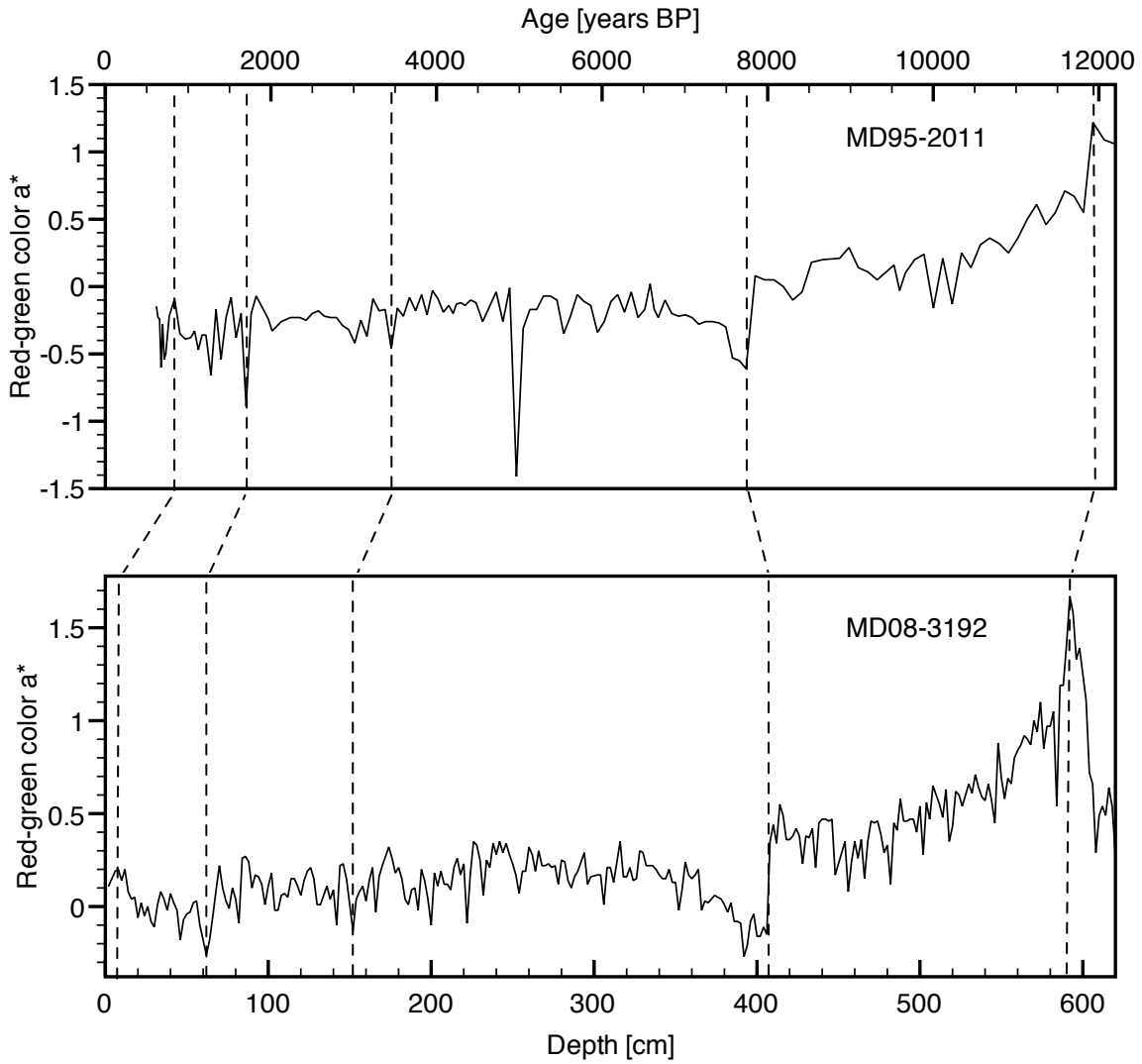

Age BP 2000 [yrs](a* MD95-2011)	depth (cm)(a* MD08-3192)
839,4316364	7,441944483
1699,601536	61,9494667
3452,986754	152,0032242
7793,246626	407,0328065
11874,68953	585,7094699

IV) Brightness controll of the microscope bulb